The impact and underlying molecular mechanisms of cell adhesion molecules integrins and syndecans in the cisplatin chemoresistance of melanoma cells

Dissertation

zur Erlangung des Doktorgrades (Dr. rer. nat.)
der Mathematisch-Naturwissenschaftlichen Fakultät
der Rheinischen Friedrich-Wilhelms-Universität Bonn

vorgelegt von

Maria Bethania Rossi Piva

aus Campinas, Brasil

Bonn, Juni 2019

Angefertigt mit Genehmigung der Mathematisch-Naturwissenschaftlichen Fakultät der
Rheinischen Friedrich-Wilhelms-Universität Bonn

Erstgutachter: Prof. Dr. Gerd Bendas

Zweitgutachter: Prof. Dr. Ulrich Jaehde

Tag der mündlichen Prüfung: 16.09.2019

Erscheinungsjahr: 2019

Home is where the heart is

To family and friends who I have left in Brasil, thank you for supporting my decision to move to Germany even when it is hard on our relationship, and loving me all the same.

To my German family of friends, it is because of you that I can call Germany my home.

I could not have done it without you all.

Acknowledgments

I would like to thank all the members of the Examination Board for taking the time to evaluate this work, specially my advisor Prof. Dr. Gerd Bendas.

He gave me a chance to work in his lab, first in 2011 without even knowing me, and then again in 2014. Prof. Bendas is not only an advisor; he does his best to ensure that we are happy and there is harmony in the group. Gerd, I would like to express my deepest gratitude for all the support you gave me when I moved to Germany, inviting me to spend time with your family and making me feel welcome.

I would also like to thank Prof. Dr. Ulrich Jaehde for being the co-advisor of this project, taking the time to carefully read it, and for the friendly communication between us, and the members of your group. Prof. Jaehde has also supported this work by allowing us to use his laboratory facilities, for which I am very grateful.

Prof. Dr. Christa E. Müller and Dr. Anke Schiedel, I would like to show my appreciation for all the support provided in the viral transfection, allowing us to use the S2 laboratory facilities and helping us with the safety requirements documentation.

I would like to thank Conselho Nacional de Desenvolvimento Ciêntifico e Tecnológico - CNPq and the Coordenação de Aperfeiçoamento de Pessoal de Nível Superior – CAPES for providing the doctoral scholarship Ciência Sem Fronteiras Doutorado no Exterior – GDE, which provided the financial support for almost the totality of my doctorate.

I would also like to extend my sincere thanks the Bonn International Graduate School of Drug Sciences for its financial support, which enabled me to participate in the CESAR Annual Meeting in Munich, on September 2016, within the framework of the program International PhD in Germany - for all.

I would also like to thank Prof. Dr. Christa E. Müller, Dr. Ralf Mayer and all assistants involved in the organization and work for the 7. Semester Arzneimittelanalytik. Thank you for having the patience to show me the ropes and for the friendly atmosphere.

I also wish to thank all the members of the Jaehde and Wiese work groups, for sharing their labs, work space and kitchen with us. The friendly atmosphere, conversations and laughs made the time at work even more enjoyable.

I would also like to show my appreciation to the technical assistants whose help can never be overestimated. They were always ready to help and make sure we got the best out of our experiments: Iris, Dieter, Svenja, Angelika, Hilde and Dagmar. Dr. Mathias Weigt, thank you for taking care of our computers, email and servers.

I am deeply indebted to all the members of the Bendas work group for all the coffee, laughs, help and beers. Despite German winter, frustrations and bad moods, each of you, in your own way, made coming to the institute every day worthwhile. It is great to you know there will be someone there that can take 10 minutes to have coffee and just talk; or that knows exactly what are going through, because they are in the same boat; or someone who has a great idea that can help you get out of a tight corner. So, thank you! Five years is a long time and I would not have been able to endure it all without a great work environment such as this. But I want to thank three members of the group in particular:

Sebastian; I think it is only appropriate that we met in my first days, over a couple of beers. You quickly became my best friend and later office partner. Thank you for all the good and bad moments we shared. I am immensely gratefully to have you in my live, you are like a brother to me. Thank you for bringing Wiebke into our lives, I love you both.

Basti, thank you for your friendship, for all the talks, great ideas, great work together, chilli con carne and beers. I am so glad I had the privilege to work so closely with one of my best friends. This work was only possible because of you, go dream team!!! I am especially thankful for the chance to share my culture with Rita and you, this made the trip to Brasil very special. You and Sebastian were pillars throughout all the frustrations of the past five years, I cannot thank you guys enough!

Kathleen, you came into the group later and quickly became very special to me. Many thanks for your unbreakable optimism and willingness to help, always. I have cherished every coffee we have shared in your office and will miss these moments very much. You are a true friend and I am fortunate to have had the opportunity to get to know you.

I would also like to thank all the very special people from work and other friends that have come to be my "German family". I know I can always count on you and you are the reason I feel happy living in this country.

Katharina, for having this wonderful energy that you bring into everything you do. You are so much fun, yet so knowledgeable. I have learned a lot from you and your culture in our amazing trip, about architecture, science, gin; you name it, so thank you. Thank you for being there for the fun as much as you were there for the hard bits and the work. You are a true friend.

Philipp, thank you not only for being an amazing friend, but for giving me the gift of two other wonderful friends: Daniela and Flo. Each one has helped me in many ways in countless different situations. Thank you for all the support, game and movie nights and getting me into bouldering. I am especially grateful to Daniela and the Südekum family for always opening their house to me and treating me as family, especially when I could not fly home. I have nothing but gratitude for you.

Volker, thank you for being my friend and my partner especially through the stressful times of the article submission and writing of this work. I am thankful for the times you did not let me settle for self-pity and always pushed me to do what I should, because you know that I can achieve everything I set my mind to and you have faith in me, even when I doubt myself. I am so grateful for you in my life.

Pioio, I miss you dearly. We have known each other for over 11 years now and I cannot express how grateful I am for everything. You are my lab partner, my roommate, my co-worker, my best friend, my sister. Even miles apart, we still help each other in the lab, sharing so many happy moments, frustrations, sadness, confidences, all of which make our friendship so especial.

Finally, the biggest thank you of all to my family who has loved and supported me my whole life, even when my decision to live in Germany brought them pain. To my mother Denise and my father José for all the sacrifices you have made for João and I, because you made them all with love and joy. Thank you all for providing me with a wonderful home. João, having a sibling is the best gift someone could receive, it is a bond unlike any other, and I am so blessed to have you in my life. Thank you for being my friend, foe and accomplice all at the same time. I am also grateful to my grandparents Dora, Rossi, Isabel and Vitório, for loving and looking after me, each in their own way. I love and miss you all very much.

Table of Contents

Figure Table

Formula Table

Table Index

Abbreviations

Abbreviations that are part of product names, legal forms and companies, as well as well-known chemical formulas, Greek and Roman numerals were not taken into account.

% (m/v)	Mass concentration in percent
% (v/v)	Volume in percent
µm	Micrometre
ADAM9	Disintegrin and metalloproteinase domain-containing protein 9
AKT	Protein kinase B
AMP	Adenosine monophosphate
ANOVA	Analysis of variance
ATP	Adenosine triphosphate
ATP7A	Copper-transporting ATPase 1
ATP7B	Copper-transporting ATPase 2
AXL	Tyrosine-protein kinase receptor UFO
BAK	BCL-2 homologous antagonist/killer
BAX	BCL-2 associated X, apoptosis regulator
BCA	Bicinchoninic acid
BCL-2	Apoptosis regulator BCL-2
BCL-2A1	BCL-2-related protein A1
BCL-X	Apoptosis regulator BCL-X
BCL-XL	BCL-2-like protein 1
BER	Base excision repair
BEZ235	Dual mTOR / PI3K inhibitor, Dactolisib
Bim	BCL-2-like protein 11
BIRC-7	Baculoviral IAP repeat-containing protein 7
BRAF	Rapidly Accelerated Fibrosarcoma protein B
BRCA	Breast cancer susceptibility protein
BSA	Bovine serum albumin
CAM-DR	Cell adhesion-mediated drug resistance
Caspase	Cysteine aspartate-specific protease
CBP	CREB-binding protein

CD44	Cluster of differentiation 44
CD47	Cluster of differentiation 47
CDDP	Cisplantin [cis-diamminedichloridoplatinum]
CDK4	Cyclin-dependent kinase 4
CDKN	Cyclin-dependent kinase inhibitor
Coll	Collagen
CTC	Circulating tumour cells
CTLA-4	Cytotoxic T-lymphocyte-associated protein 4, CD152
CTR1	High affinity copper uptake protein 1
CXCR	CXC chemokine receptors
DAPI	4’,6-Diamidin-2-phenylindol-dihydrochlorid
DDR	Discoidin domain receptors
DMEM	Dulbecco’s Modified Eagle Medium
DMF	Dimethylfuran
DMSO	Dimethylsulfoxid
DPBS	Dulbecco’s Phosphate Buffered Saline
DTP	Drug-tolerant persister
ECM	Extra cellular matrix
EDTA	Ethylenediaminetetraacetic acid
EGF	Epidermal growth fact
EM-DR	Environment-mediated drug resistance
EMT	Epithelial–mesenchymal transition
EPO Berlin	Experimental Pharmacology and Oncology Berlin-Buch
ER	Endoplasmic reticulum
ERCC1	Endonucleases complementation group 1
ERK	Extracellular signal–regulated kinases
FACIT	Fibril-associated Collagens with interrupted triple-helices
FACS	Fluorescence-activated cell sorting
FAK	Focal adhesion kinase
FAT	C-terminal focal adhesion-targeting domain
FBS	Foetal bovine serum
FDA	US Food and Drug Administration

FERM domain	4.1 protein, ezrin, radixin, moesin domain
FGF	Fibroblast growth factor
FITC	Fluorescein isothiocyanate
FKS	Foetal Calf Serum
FN	Fibronectin
FOXO	Subgroup of the Forkhead family of transcription factors
FSC	Forward scattered light
GAG	Glycosaminoglycan
GAPDH	Glycerinaldehyd-3-phosphat-Dehydrogenase
GFR	Growth factor receptors
GLOBOCAN	Global Cancer Incidence, Mortality and Prevalence
Gly	Glycine
GPCR	G-protein coupled receptor
GSK3	Glycogen synthase Kinase-3
Hep	Heparin
HEPES	4-(2-hydroxyethyl)-1-piperazineethanesulfonic acid
HER-2	Human epidermal growth factor receptor 2, ERBB2, CD340
HRP	Horseradish peroxidase
HRR	Homologous recombination repair
HS	Heparan sulfate
HSPG	Heparan sulfate proteoglycans
Hyp	Hydroxyproline
IC_{50}	Half maximal inhibitory concentration
IDTC	Called induced drug-tolerant cells
IgG	Immunglobulin G
IL-2	Interleukin 2
IL-8	Interleukin-8
ILK	Integrin linked kinase
Kd	Knock-down
LM	Laminin
LMWH	Low Molecular Weight Heparin
LRRC8	Leucine-rich repeat-containing 8 protein family

MAPK	Mitogen-activated protein kinase
MC1R	Melanocortin receptor 1
MCL-1	Induced myeloid leukaemia cell differentiation protein
MDM	E3 ubiquitin-protein ligase
MEK	Mitogen-activated protein kinase or MAP2K
MIDAS	Metal ion-dependent adhesion site
MITF	Microphthalmia-associated transcription factor
MLH1	Mutl homolog 1
Mmps	Matrix metalloproteinases
MMR	Mismatch repair
MR	Mortality rate
MRD	Minimal residual disease
MRP2	Multidrug resistance-associated protein 2, cMOAT or ABCC2
MSH	Melanocyte stimulating hormone
MSH2	DNA mismatch repair protein or mutS homolog 2
mTOR	Mammalian target of rapamycin
mTORC	Mammalian target of rapamycin complex
MTT	3-(4,5-Dimethylthiazol-2-yl)-2,5-diphenyltetrazolium bromide
MV3 Syn-4 kd	MV3 Syn-4 knockdown cell line
MV3 β1-integrin kd	MV3 β1-integrin knockdown line
NCAM1	Neural cell adhesion molecule 1
NCSC	Neutral crest stem cells
NER	Nucleotide excision repair
NRAS	Rat sarcoma protein or p21 N
ON	Over night
OPN	Osteopontin
P21	Cyclin-dependent kinase inhibitor 1
P53	Tumour suppressor p53
P5D2	Blocking anti-body against human β1 Integrin
PAC	Puromycin N-acetyltransferase
PARP	Poly-(ADP-Ribose) Polymerase
PD-1	Programmed cell death protein 1, CD279 or PD-L1

PDGF	Platelet-derived growth factor
PDK1	3 – phosphoinositide-dependent protein kinase 1
Pen / Strep	Penicillin / Streptomycin Solution
PFA	Paraformaldehyde
PI3K	Phosphoinositide-3-kinase
pIC_{50}	Negative log of the half maximal inhibitory concentration (IC_{50})
PIP	Phosphoinositide lipids
PIP2	Phosphatidylinositol-3,4,5-diphosphate [ptdins(3,4,5)P2]
PIP3	Phosphatidylinositol-3,4,5-trisphosphat
PKC	Protein kinase C
PMEL	Premelanosome protein or gp100
PMSF	Phenylmethylsulfonylfluorid
POLH	DNA polymerase eta
POMC	Pro-opiomelanocortin
PRIMA-1	P53 Reactivation of Massive Apoptosis
Pro	Proline
PSI	Plexin/semaphorin/integrin domain
PTEN	Phosphatase and tensin homolog
PVDF	Polyvinylidene fluoride
QC	Quality controls
RAD51	DNA repair protein RAD51
RAF	Rapidly Accelerated Fibrosarcoma protein
RAS	Rat sarcoma protein or p21
RB1	Retinoblastoma associated protein 1
REV3	DNA polymerase zeta catalytic subunit
REV7	DNA polymerase delta catalytic subunit
RF	Resistance Factor
RGD	Arginine, Glycine and Aspartate
Rhoa	RAS homolog gene family, member A
RISC	RNA-induced silencing complex
RNA	Ribonucleic acid
RPMI	Roswell Park Memorial Institute

RT	Room temperature
RTK	Receptor tyrosine kinase
SD	Standard deviation
SDS	Sodium dodecyl sulfate
SEM	Standard Error
SH2	P85 Src-homology 2 domain
shRNA	Small hairpin RNA
SLNB	Sentinel lymph node biopsy
Src	Proto-oncogene tyrosine-protein kinase
SSC	Side scattered light
Syn	Syndecan
TBS	TRIS buffered saline
TBS-T	TRIS buffered saline with Tween 20
TCGA	Cancer Genome Atlas Program
Tinz	Tinzaparin
TLS	Translesion synthesis
TN	Tenascin
TSP	Thrombospondin
UFH	Unfractionated heparin
UV	Ultraviolet
VCAM-1	vascular cell adhesion molecule 1 or CD106
VDAC	Voltage-dependent anion-selective channel protein
VEGF	Vascular endothelial growth factor
VRAC	Volume-regulated anion channel family
VTN	Vitronectin
WHO	World Health Organization
wt	Wild Type
XPA	Xeroderma pigmentosum group A
XPF or ERCC4	Xeroderma pigmentosum group F
βTD	Cysteine-rich membrane proximal-β tail

Abstract

Cancer is a complex, but also devastating disease, which today, more than ever, is present in our lives and society. Practically every person has a close relative or friend, or has been themselves affected by this disease. Although the incidence of cancer has been increasing rapidly, it is not a modern illness. Cancer has been detected in several archaeological findings, from dinosaurs to mummies (1–3). Most recently, in February 2019, a report was published about the oldest indication of cancer ever found in vertebrates. It describes the finding of osteosarcoma in a Middle Triassic stem-turtle (1). As discussed in the article, the reason why this disease can be found virtually from the beginning of life, is because it is an unfortunate side effect of cell development during life and evolution (1). The authors of the paper put it most adequately, in my opinion, as they say: "Cancer is not a modern physiological defect but rather a vulnerability that is deeply rooted in vertebrate evolutionary history" (1).

Cells are constantly renewing, dividing and adapting themselves to survive. These adaptations can provide an evolutionary advantage and, sometimes, be passed on and change the species. However, sometimes mistakes occur that lead cells to lose replication control and cancer arises. The fact that cancer arises from errors or changes during cell development makes it very complex, adaptable and difficult to understand and treat. This complexity can be observed in the different tissues, types and sub-types of the disease, which often manifest themselves as almost completely different entities, with different causes, development and outcomes. Moreover, the fact that it is your body attacking itself, and not a foreign organism, makes it difficult to detect and treat, but also hard for patients and society to understand and accept it. Curiously, cancer findings in fossils are a rare discovery, one of the reasons for this is the degradation of soft tissue in time, which makes detection in these tissues impossible (1). Other reasons are environmental and genetic changes.

As constant technological developments have, on one hand, increased our lifespan allowing for more cell replication and stress exposure, which increases the chances of mutation. On the other hand, they put us in contact with carcinogens such as growth hormones, pesticides, pollution and radiation that contribute for an increased incidence of cancer. Moreover, better understanding and diagnostics tools allow cancer patients to be identified more often and rapidly than ever.

One of the environmental causes for cancer is radiation, such as, for example, solar UV light, which is one of the main causes of malignant melanoma, one of the most aggressive malignancies in humans (4). It has a high incidence worldwide, which is unfortunately expected to increase, with a global mortality rate of 20% (5). Case numbers can be correlated with tropical, sunny regions and ozone layer holes, as is the case of Australia, as well as phenotypic features such as pale white skin, blond or red hair and blue eyes, and familial history (4,6,7). Since skin cells are designed to have a protective role, they are very adaptable and resistant to apoptosis induced by DNA mutation, characteristics which are preserved in and often used by malignant cells for their survival (6). Therefore, the malignant transformation, metastasis and drug-resistance development that follows are all complex, multifactorial processes dependent on many variables, which present tremendous challenges for the development of curative therapy. Although there have been many therapeutic improvements, most drugs only interfere with the growth of primary tumours (8–10). As a result, patients develop metastatic melanoma, which is one of the most aggressive and drug resistant neoplasm that sadly leads to death in the majority of cases, usually due to resistance to treatment (4).

Resistance development is a complex, multipart process, not yet fully understood. In this work our main interest is the environment-mediated drug resistance (EM-DR), which is an innate, transient protective effect that the microenvironment provides to cells. It is an important phenomenon because it allows for the development of acquired drug resistance, i.e. genetic adaptations in response to prolonged therapy.

One type of EM-DR is cell adhesion-mediated drug resistance (CAM-DR), which is mediated by the attachment of cell membrane proteins, such as integrins and syndecans, to components of the extracellular matrix (ECM), which triggers survival cell-signalling pathways. The mitogen-activated protein kinase (MAPK) pathway has been associated with melanoma development, progression and resistance and intensively studied (11,12). For this reason, we decided to focus this work in the study of an associated but less studied pathway in melanoma, the FAK/PI3K/AKT signalling pathway, which is also known to lead to cell survival.

With this purpose, we have investigated the sensitivity of melanoma cells to cisplatin treatment under different integrin-activating experimental conditions. Cells were seeded on surfaces coated with ECM components - fibronectin and collagen - and treated with Mn^{2+}; a known integrin activator, previously to cisplatin addition. A PI3K/mTOR inhibitor was also used, in order to interfere in cell signalling. After the treatments, cell sensitivity to cisplatin was evaluated using a colorimetric cytotoxicity test. Moreover, β1 integrin-deficient cells were generated and tested, together with syndecan-4 knockdown cells, with the purpose of assessing the importance of these adhesion molecules for the cells in the context of cisplatin resistance. Finally, the activation of the FAK/PI3K/AKT signalling pathway was observed under these experimental conditions through flow cytometry.

This work provides a view into one of the CAM-DR mechanisms used by melanoma cells to protect themselves from cisplatin stress. It shows the importance of integrins, syndecans and the ECM in this context, as well as in cell plasticity and the complexities of resistance formation.

Melanoma

The last report from the International Agency for Research on Cancer (GLOBOCAN – WHO), on September 2018, showed over 18 million new cases of cancer worldwide, more than half leading to death; this number is expected to rise to 29.5 million by 2040 (5). In Germany and Brazil there were 608,742 and 559,371 new cases (this number is expected to duplicate by 2040); and 247,462 and 243,588 deaths by cancer in 2018, respectively (5).

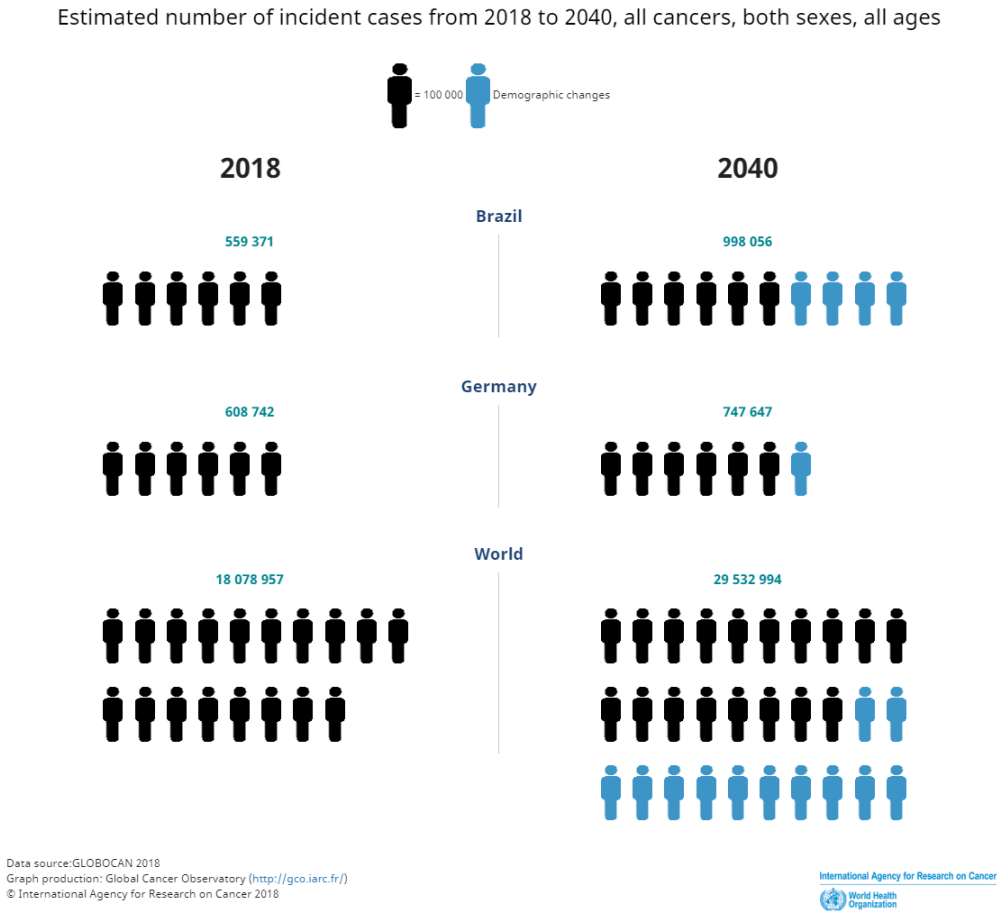

Figure 1. Cancer incidence in the world in 2018 and 2040 projection according to report released by the World Health Organization (5).

Malignant melanoma, specifically, has an incidence of 287,723 new cases worldwide with a mortality rate (MR) of about 20% (5). In Germany, 31,432 (MR 11,5%) people are affected and in Brazil 7,407 (MR 28%), unfortunately these numbers are expected to increase in the next two decades (5).

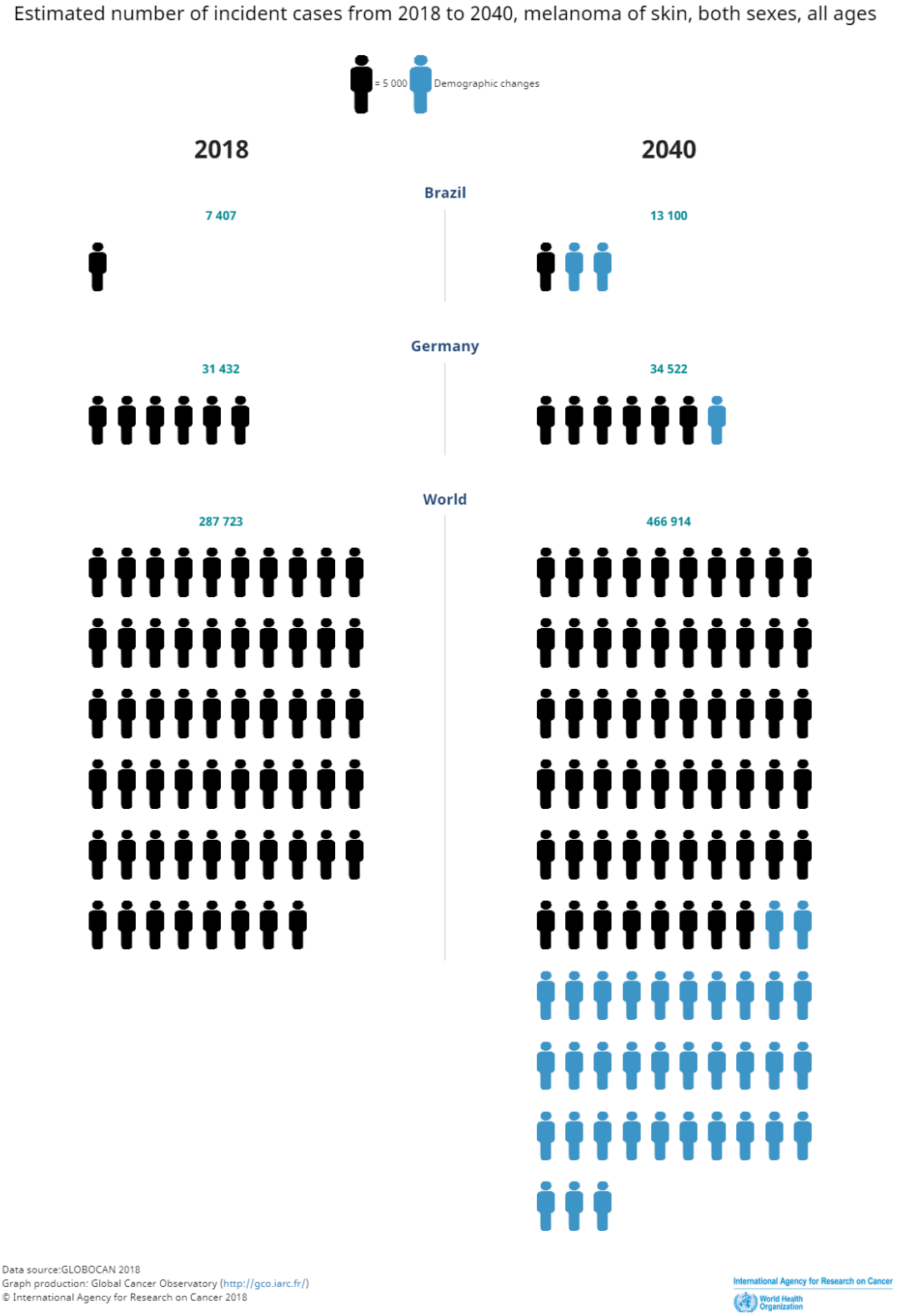

Figure 2. Melanoma incidence in the world in 2018 and 2040 projection according to report released by the World Health Organization (5).

The 5-year survival rate of melanoma is low, only 14% of patients survive (4). Malignant melanoma is one of the most aggressive malignancies in humans and is responsible for 60–80% of deaths from skin cancer (4). This results from the lack of deeper understanding of the genetic alterations and signalling pathways of malignant transformation events, metastasis process, and chemotherapy and radiotherapy resistance mechanisms.

Normal melanocytes originate from the neural crest as pluripotent cells that suffer induction through bone morphogenic protein signalling; induction causes neural crest stem cells to undergo epithelial–mesenchymal transition (EMT), lose adhesion to neighbouring cells and gain migrative capacities (4,6,7). Mature melanocytes produce pigment through very complex cell machinery in vesicles called melanosomes. The pigment produced has been classified as eumelanin (brown/black) and pheomelanin (red/blond), which have been associated with an innate higher oxidative stress in the skin, independent of UV radiation; but also have shown to carry a non-functional polymorphic variant of the melanocortin receptor 1 (MC1R) that is involved in melanin production as protective response to UV radiation (4,6,13). Moreover, skin pigmentation can also be constitutive or adaptive. The former refers to the amount and type of pigment synthesized, as well as the maturation process of the melanosomes, while the latter refers to melanin production as a protection mechanism triggered by UV radiation (6). UV exposure can cause DNA damage (usually C → T) to the most superficial skin layers, this leads to p53 stabilization and upregulation of pro-opiomelanocortin (POMC) (6,14). POMC is cleaved forming various derivates including β-endorphin, which is responsible for sun-seeking behaviour; and melanocyte stimulating hormone (MSH) (14). MSH is secreted in order to activate its receptor, MC1R, in other underlying melanocytes (6). This leads to cAMP induction and consequent upregulation of microphthalmia-associated transcription factor (MITF), which regulates the melanocyte lineage. This protective role of the melanocytes renders them innately programmed to adapt to DNA damage and stress; this is known as melanocyte plasticity and is preserved in and often used by malignant cells for their survival.

Malignant transformation and drug-resistance development of melanocytes is a complex process, which involves interactions of environmental and genetic factors leading to loss of regulation of cell proliferation, apoptosis and cell-cell interactions.

Thus, the risk for melanoma depends on various factors, such as genetic and environmental influences, some risk factors include UV exposure, pale white skin, blond or red hair and blue eyes phenotypes, as mentioned above, but also large and irregular atypical or dysplastic nevi, and family history (10% of cases) (4,6,7). The many genetic alterations that occur in the melanocytes during malignant transformation have been thoroughly analysed and reviewed by the melanoma Cancer Genome Atlas Program (TCGA), and only a few examples will be discussed in this work (15).

One of the familial melanoma mutations is in the CDKN2A gene, which regulates cell cycle and p53, a known cancer related protein (4,16,17). Other melanoma-susceptibility genes include CDK4, RB1 and MITF. As previously mentioned, MITF is a melanocyte-specific transcription factor involved in melanin production, thus melanocytes are highly dependent on MITF for their UV protective function (6). However, MITF is involved in many other essential cell processes, such as differentiation, proliferation and survival (6,18). Interestingly, MITF dependence is retained in malignant transformation of melanocytes, where this gene is mutated (2-8% of amelanotic tumours), overexpressed or upregulated (18,19). Several mechanisms are involved in the regulation of MITF expression and/or activity in cancer, including epigenetic and microenvironmental signals, as well as transcription factors and signalling pathways; for example, MITF deregulation can often be observed with BRAF mutation, which is consistent with the role of MITF as an oncogene in melanoma cells, highly dependent on and as a factor for familial melanoma (6,20–23). Moreover, ERK mutations can also cause MITF deregulation (18).

The abovementioned BRAF and ERK are known components of the MAPK signalling pathway, which is upregulated in melanoma, and one of the most important malignancy drivers. It is initiated by tyrosine kinase (RTK) or G-protein coupled receptors (GPCR), which recruit and activate the protein RAS (H-, K- or N- isoforms). Activated RAS then binds to RAF (A-, B- or C- isoforms), inducing RAF dimerization and activation. RAF is then able to phosphorylate and activate MEK, which then phosphorylates and activates its downstream effector ERK that, in turn, is able to regulate cell cycle progression. Therefore, this signalling pathway is often mutated in melanoma cells. BRAF-activating mutation is usually a cytosine to tyrosine exchange, usually associated with UV-radiation (6,24). It is the most common of such mutations, present in 40–50% of melanomas (16,17,24–26). Found in another 15–30% of cases are NRAS

mutations, which can also be connected to UV-radiation damage (16,17,24,27,28). Interestingly, NRAS and BRAF mutations seem to be mutually exclusive. On the other hand, BRAF-activation mutation correlates with ERK mutation, overexpression and constitutive activation (4,29).

The high prevalence of BRAF and NRAS mutations in malignant melanoma has drawn therapeutic and research efforts upon this signalling pathway, while the PI3K/AKT pathway has been considered secondary. However, this is a major regulator of cell behaviour and its mutation and deregulation is an essential part of cancer cell transformation and the maintenance of the malignant phenotype (30). The PI3K/AKT pathway is one of the most studied in cancer and has been shown to be one of the most affected by genetic alterations caused by tumour development, growth, resistance and metastasis (31). Also, in melanoma, the effectors of this pathway have been shown to be mutated or genetically altered. The most common PI3K/AKT activating mutations in melanoma are NRAS (15 - 20%) and the loss or mutation of the PI3K regulator, PTEN (up to 30%) (15,31,32). These two mutations are concomitantly exclusive, probably because of their redundant role as PI3K/AKT activators. Furthermore, PTEN mutation is usually accompanied by BRAF mutation, thereby concomitant de-regulation of MAPK pathway, results in concurrent activation of both pathways (16,31,33–36).

Moreover, PI3K and AKT can be found to be mutated or overexpressed in other cases (6,24,37). For example, 40% of melanomas present upregulation of AKT due to mutations, upregulation of upstream kinases or loss of function of regulating proteins (15,31). TCGA has shown an association between AKT overexpression and NRAS mutated phenotype (40%), although some studies have shown higher AKT activation in cells with PTEN loss (15,38). AKT point mutations are considered rare (1-2%), but can be observed in melanoma, often associated to PI3K mutations (15,31). Curiously, although point mutations in AKT subtype 1 could be observed in all cancer types, AKT isoform 3 is only mutated in melanoma cells, which could be used as a specific drug target in patients that carry this mutation (31,37,39–41). Additionally, point mutations of the PI3K gene can be found in 2% to 6% of melanomas (15,31,42,43).

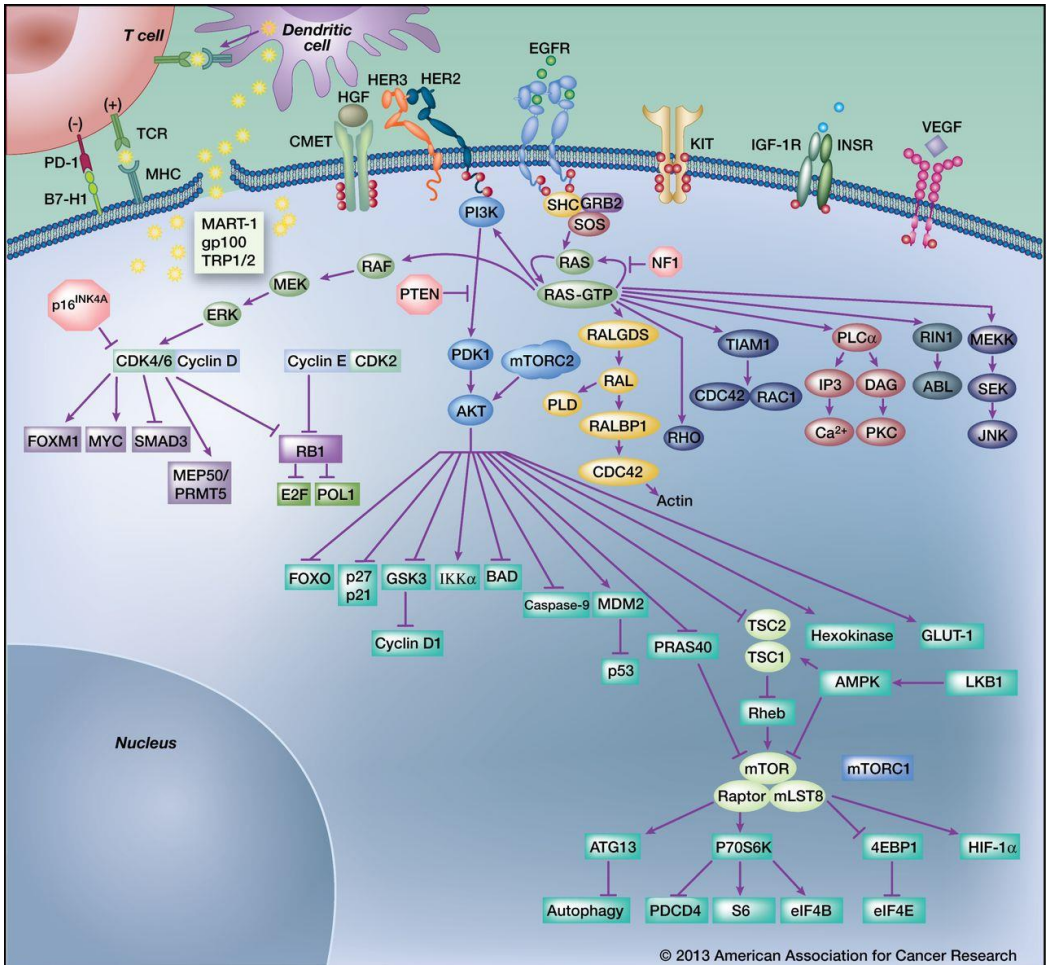

Figure 3. Molecular and immunologic signalling in melanoma. Depicted summary of the complex and intertwined signalling present in melanoma cells. Adapted from Sullivan et al. (16).

The primary therapeutic treatment option is the surgical removal of the malignant melanoma tissue with a sentinel lymph node biopsy (SLNB) in order to evaluate the presence of cancer cells on the lymph node(s) where the melanoma is most likely to disperse. Early surgical removal of primary tumours and lymph node resection is an effective treatment, but up to 20% of patients may go on to develop metastatic disease, which has a very poor prognosis (44–46). This occurs because standard chemotherapeutics, that display a proven success record against many different cancers, are ineffective on metastatic melanoma (44–46). The plasticity of skin cells to adapt and protect themselves from UV stress gives them an almost innate metastatic potential. Thus, melanoma recurrence is often manifested in a metastatic spread of the primary tumour. Until 2010, dacarbazine was the only treatment for melanoma, sometimes administrated with interleukin 2 (IL-2) as an adjuvant (only approved in the USA) (6,17). In the last decade, however, therapy for metastatic melanoma has advanced significantly. The new therapeutic approaches can be divided into immunomodulation,

as for example, IL-2 itself or more relevant, monoclonal antibodies blocking CTLA-4, PD-1 or PD-L1, which have been shown to decrease immune tolerance, consequently inducing tumour regression by intensifying T-cell attack (16,17). Other approaches target mutated signalling pathway components, that make use of the abovementioned mutations to select adequate targeted therapy in the form of inhibitors. Two BRAF inhibitors, for instance, have shown promising clinical results and have been approved for treatment of patients with BRAF-mutant melanomas (16,17,25,47,48). Inhibitors have also been developed against other MAPK pathway proteins, which are often mutated or over-expressed/activated in melanoma, such as the MEK inhibitor AS703026 (NCT01693068); MEK inhibitor MEK162 (NCT01763164, NCT01320085, NCT01337765); MEK inhibitor AZD6244 (NCT00866177, NCT00338130) and ERK inhibitor LTT462 (NCT02711345) (49–51). Inhibitors of members of the PI3K/AKT signalling pathway have also been developed: PI3K inhibitor BEZ235 (NCT01343498, NCT01195376, NCT01337765, NCT01337765, NCT01285466, NCT00620594, NCT01508104), AKT inhibitor GSK2110183 (NCT01653912, NCT01531894, NCT01476137), AKT inhibitor AZD5363 (NCT02465060, NCT03310541, NCT01226316), AKT inhibitor GDC0068 (NCT01562275, NCT02536391, NCT02536391), AKT inhibitor MK2206 (NCT01519427, NCT01480154).

Despite all the treatment advances listed above, the American cancer society still recognizes chemotherapy as a non-usual treatment for melanoma in palliative setting, to relieve symptoms and extend patient survival in extreme cases where other treatments have failed (52). Especially, by using direct infusion of the drug into the tumour or electrochemotherapy, which consists of applying an electric field to the cell membrane to increase its permeability (53–55). Electrochemotherapy is well-established in the treatment of superficial neoplastic lesions such as melanomas, usually in cases if unresectable tumours as a palliative measure (53–55). The chemotherapeutic arsenal of agents includes cisplatin, carboplatin, paclitaxel, and dacarbazine (4). Moreover, metastatic development and treatment resistance is still a big issue which prevents permanent curative results. Sadly the majority of metastatic melanoma patients still dies within a few years of metastasis development (6,56). For this reason, even though the response to chemotherapeutic drugs is only moderated, studies have been made to try to combine these older treatment options to the newer inhibitors and overcome drug resistance (45,57–59).

Cisplatin

As mentioned above, the global incidence of melanoma has been increasing. New therapies offer exciting prospects for improved survival and have supplanted the role of chemotherapy as first- and second-line therapy in melanoma treatment. However, the development of resistance against such therapies is a major problem and the need for additional effective melanoma therapy remains. Cytostatic compounds, such as cisplatin are still used in extreme cases and can be combined with the newer agents to enhance their effect (52). Platinum compounds, such as cisplatin, are the most effective chemotherapeutics for a number of major cancers, but have been considered ineffective on metastatic melanoma, even though they show a similar average response rate as dacarbazine (about 14%), which has been considered standard treatment for melanoma for three decades (44,46).

Cisplatin was synthesized for the first time by Michele Peyrone in the 19th century, but it was not until 1960 that its cytostatic effect was identified (60,61). The effect of the compound was attributed to two active platinum complexes: [Pt IV $(NH_3)_2Cl_4$] and its *cis* isomer [Pt II $(NH_3)_2Cl_2$], which became known as *cis*platin. Shortly thereafter the first *in vivo* assays was conducted, where cancer infected mice were treated with cisplatin showing tumour reduction (62). Already in 1971, the first clinical trials were performed and, in 1978, the FDA approved cisplatin as a cancer therapy drug (63,64). Due to the severe effects of cisplatin, such as neuro-, oto- and nephrotoxicity, some less toxic analogues, such as carboplatin, have since been synthesized (65–67).

The structure of *cis*- diamminedichloridoplatinum(II) is formed by a square planar coordination complex with platinum in the middle and two ammines and chlorides in a cis-position (shown in 1) (68,69). The neutral charge of the structure, caused by the balance between the two negatively charged chlorides and the two positive platinum atoms, makes cisplatin hard to dissolve in water (64). In contact with water the parent species, depicted in 1, is hydrolysed into five dissociation products: chlorido-aqua (2), diaqua (3), chlorido-hydroxido (4), hydroxido-aqua (5), and dihydroxido (6) (68,70).

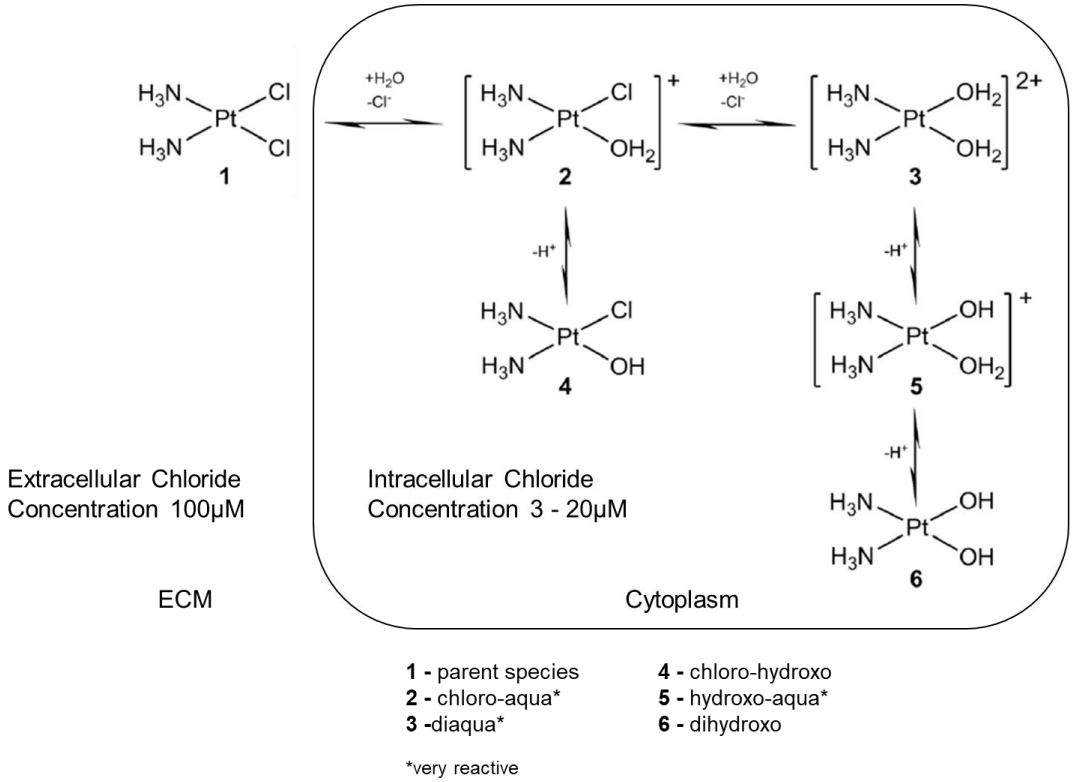

Figure 4. Hydrolysis of cisplatin. In aqueous environments, cisplatin **(1)** hydrolyses into chlorido-aqua **(2)**, diaqua **(3)**, chlorido-hydroxido **(4)**, hydroxido-aqua **(5)**, and dihydroxido **(6)**. Adapted from Khateeb et al. (70).

This dissociation process is dependent on the total drug and chloride concentration and pH, and influences the amount of reactive species that can actually induce cytotoxicity (68). For this reason, the final intravenous formula to be injected in patients is stabilized with saline solution (NaCl 0.9 % (w/v)) that preserves the dichloride parental species at 89 - 97% of the solution, conditions similar to the blood and extracellular situations (85%) (68,69). Upon arrival at the cells, cisplatin complexes infiltrate the cell through different mechanisms, which are still under debate. Passive diffusion has been accepted as the main cisplatin absorption mechanism for decades (71). Cisplatin absorption is slow and dependent on many parameters, such as pH and intracellular ion concentration (63). However, other uptake mechanisms such as transporters and ion channels have also been associated with cisplatin absorption (72). The most important of which, is the copper-transporter CTR1, which has been shown to be downregulated in cisplatin resistant cells (73).

Once inside the cell, intracellular conditions lead to hydrolysis of about 50% of the dichloride form, from 85% to 44%, leading to a rapid increase in the mono- and diaqua complexes (hydroxido-aqua (2%), chlorido-aqua (24%) diaqua (less than 1%) (68). These aqua complexes are very reactive electrophile species, hence, they display high affinity for structures with nucleophilic cores such as DNA (71). Cisplatin causes DNA adducts by binding to the N7-position of the imidazole ring of the DNA purine bases adenine and guanine, thereby resulting in DNA-protein crosslinks, interstrand crosslinks, as well as the more toxic intrastrand crosslinks (69). These adducts lead to abnormal bending of the DNA molecule, which can be detected by cell repair machinery, which activates apoptotic signals leading to cell death (74).

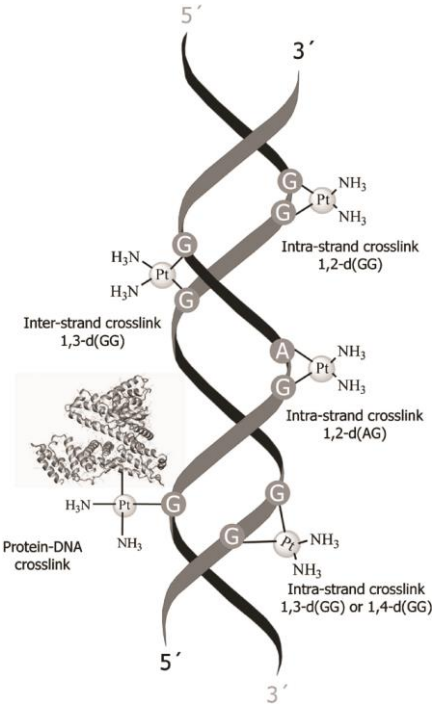

Figure 5. Cisplatin DNA adducts. Cisplatin binds to the DNA leading to abnormal bending and apoptosis (75).

However, cisplatin cell uptake, DNA damage and cytotoxic effect mechanisms are often deregulated in cancer cells that develop treatment resistance. Chemoresistance is a complex and important obstacle for patient treatment. Therefore, understanding the mechanism and effects of such events is imperative to improve clinical approaches and will be discussed below.

Chemoresistance

Although there have been many developments in cancer pharmacotherapy, which mostly interfere with the growth and development of primary tumours, drug resistance still presents itself as one of the major obstacles to the complete cure of most cancers (8–10). The lower sensitivity of tumour cells to chemotherapeutic treatment is a grave limitation, in light of the restricted dose escalation due to unwanted cytotoxic side-effects in patients.

Constant therapeutic advances increase the chance of cancer patients achieving complete remission status. Unfortunately, this often does not mean the patient is a hundred percent disease free, but it refers to the absence of detectable tumours. This means that a small group of cells, usually 10^9 - 10^{11} cells, which could potentially form a new tumour, can remain undetected in the body (76–78). These cells are called minimal residual disease (MRD) and can endure treatment stress through innate survival mechanisms, such as quiescence, which enable the development of drug resistant cell expansion (8,10,79). This leads to treatment resistant disease relapse and usually the death of the patient. This presents a major challenge for physicians trying to ensure patient survival. Although melanoma can be treated by surgical resection, metastatic melanoma is one of the most aggressive and drug resistant neoplasm with poor overall survival. The new BRAF inhibitors, combination therapies and immunotherapies offer exciting prospects for improving survival, but not all patients respond positively and the development of resistance is a major problem (80,81), hence the need for effective additional melanoma therapy. In order to overcome this problem, we need more efficient diagnostic tools that are able to identify this small number of cells and also new therapies to specifically target MRD resistant cells.

Many efforts have been made to understand this phenomena, first identified in hematopoietic cancers, and that consists of a three-step process: first there is tumour cell homing to the bone marrow, which bears fibroblasts and extracellular matrix components that act as a sanctuary that facilitates survival (78). This microenvironment protection leads to transient environment-mediated drug resistance (EM-DR) and finally, the development of microenvironment-independent resistance or acquired drug resistance, through which tumour cells suffer genetic modifications in response to prolonged therapy, leading to insensibility to treatment (77,78,82).

The exact harbouring location for epithelial tumours is still uncertain, MRD population is not uniform; it features cellular and geographic heterogeneity, they can allocate in the bone marrow but do not necessarily do so (10,79). The cells disassociate from the main tumour and become circulating tumour cells (CTC) that travel through the blood stream in a process denominated leukemic phase (76,83). Efforts have been made to effectively use the detection of these few CTC in the blood to prevent metastasis, MRD and resistance. This has been called liquid biopsy (76,83).

However, not all CTC are treatment resistant, not all of them have the potential to form MRD niches, or initiate new tumours (8,79). Only a small subpopulation of CTC with stem-like properties is inherently refractory to treatment (8,9,79,84). These cells have been consistently identified in several different tumours. For example, in melanoma, Rambow et al. called them neutral crest stem cells (NCSC), Menon et al. had already observed similar melanoma cells that they called induced drug-tolerant cells (IDTCs), and Sharma et al. studied drug-tolerant persister (DTP) cells in lung cancer (8,9,79). The most interesting fact about these cells is that the resistance mechanisms are transient and mutation independent; this means that these are quick responses to environmental stress, such as anti-cancer treatment, but also pH changes, starvation and hypoxia, mediated by epigenetics and/or interactions with the extracellular matrix and its compounds (9,78). Since these adaptations do not interfere in the genetic code of the cell, that is, there are no mutations, this transient resistant state can be reverted after a so-called "drug – holiday" period (8,9). This consists of suspending treatment for a specific amount of time until the resistance mechanisms are turned off. Then, the drug regime can be reinstated and previously resistant cells will die (8,9). The exact amount of time needed as "holiday" is tumour, treatment, and it seems patient/host, dependent. However, the previously discussed liquid biopsy could be a powerful tool to analyse resistance development, in real-time, in a non-invasive way, and help decide the best moment to reinstate treatment and which treatment protocol to use (8,9,76,83).

Resistance is a natural adaptation process used by living beings to survive environmental changes/stress. Thus, it is not surprising that tumour cells make use of a number of potential molecular mechanisms to adapt and circumvent chemotherapeutic treatment. There is a vast array of different adaptations used by cancer cells to try to avoid the cytotoxic effects of cisplatin, which are very complex and often intertwined, some of these adaptations will be explained in the section below. Even though cellular

events are often dependent and associated with each other, cisplatin resistance mechanisms are classically divided into:

- Pre-target
- On-target
- Post-target
- Off-target.

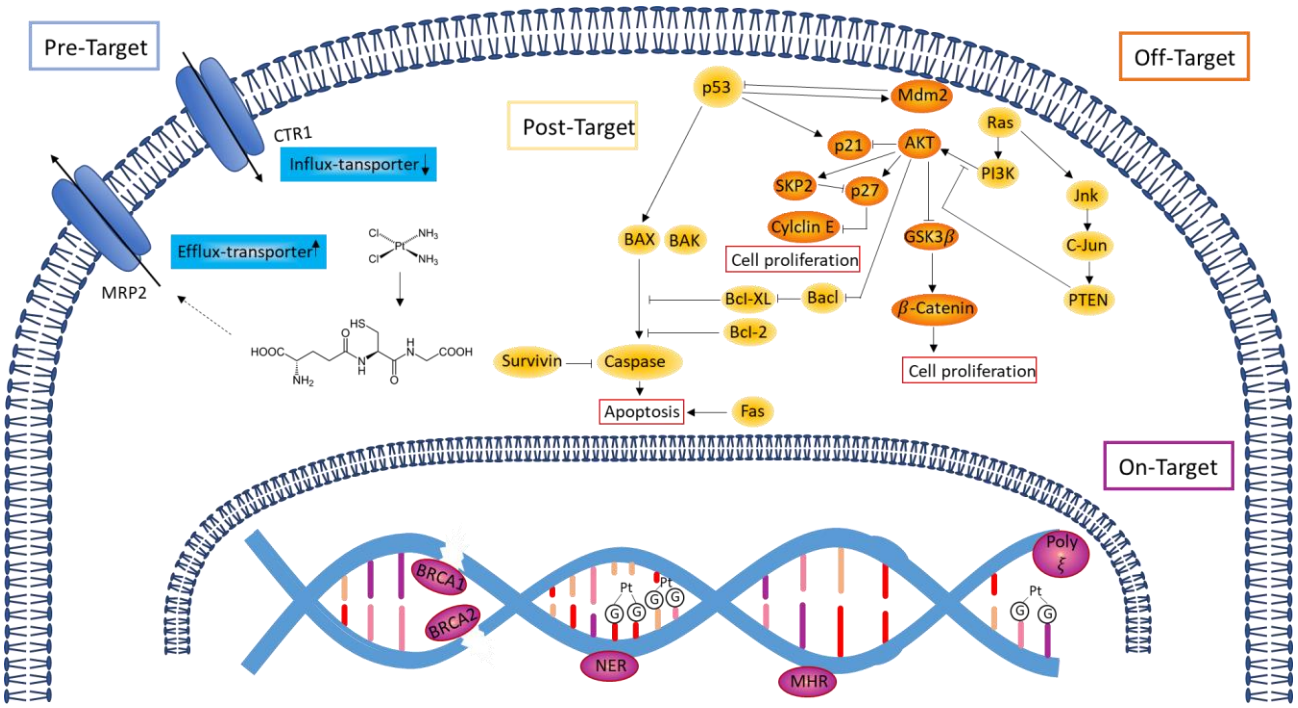

Figure 6. Cisplatin resistance mechanisms. Summarized depiction of tumour cells numerous cisplatin circumventing molecular mechanisms, that are typically divided into: pre-target (blue), post-target (yellow), off-target (orange), on-target (purple). Adapted from Wantoch von Rekowski (85).

Pre-Target Resistance

Pre-target resistance consists of cell protective mechanisms used by tumour cells to avoid cisplatin binding to DNA. They involve (i) decreasing drug uptake; (ii) cisplatin sequestration and facilitated extrusion; and (iii) increased efflux rate.

Reduced cisplatin uptake is usually achieved by cancer cells through downregulation of the copper influx-transporter CTR1 and/or reduction of LRRC8 protein expression, which reduces the activity of the VRCA complex.

CTR1 is formed by three monomers, each containing three trans-membrane domains with cytosolic C-terminals (73,86,87). It is usually involved in copper ions influx into the cytoplasm but can be used by cisplatin to enter the cell. It has been shown that, after being internalized, cisplatin interacts with the CTR1 transporter in two different residues (Y103 and C189) responsible for transporter endocytosis and membrane placement, respectively, thereby cisplatin uptake itself automatically induces downregulation of CTR1, and therefore resistance (73,86,87).

VRAC or volume-regulated anion channel family is responsible for, but not restricted to, cell volume restauration under osmotic cell swelling conditions, and therefore, its activity is pH dependent and can be influenced by cisplatin chloride anions. Alkaline conditions, for example, have been shown to increase its activity, which is regulated by the leucine-rich repeat-containing 8 (LRRC8) protein family (88). It seems possible that the acidic conditions innate from tumour milieu might be associated with downregulation of VRAC. Osmotic cell swelling, as well as ROS, have been shown to increase cisplatin accumulation in the cell, which shows that the LRRC8 – VRCA complex is involved in the influx of cisplatin (87). Thus, the downregulation of both LRRC8 proteins expression and VRAC activity have been associated with cisplatin resistance. This complex also affects cell cycle progression, apoptosis and proliferation. In fact, VRAC activity has been shown to affect cell cycle in a chloride concentration dependent manner (89). LRRC8 downregulation is also involved in post-target cisplatin resistance by preventing activation of apoptotic signals, through p53, MDM2, p21 and CBP 9 and 3, following cisplatin treatment (87).

Another pre-target resistance mechanism makes use of the extrusion mechanisms of the cell which consist of tagging substances to suffer exocytose. For example, nucleophilic species, such as glutathione, can be conjugated to cisplatin by glutathione S-transferase (73,86). The expression of both glutathione and its conjugating enzyme have been shown to be upregulated in cisplatin resistant cancers (90). With respect to melanoma, organelles that synthesize, store, and transport melanin in melanocytes, known as melanosomes, have been shown to sequester and extrude cytotoxic drugs, thereby decreasing drug concentration and damage to the cell (91,92). Examples of some melanosome proteins that have been shown to be overexpressed and assist in cisplatin resistance in melanoma cells are the premelanosome protein (gp100/PMEL), G-protein

coupled receptor 143 (GPR143) and, of course, MITF, which is also involved in cisplatin off-target resistance (see below) (91,92).

An additional mechanism of cisplatin pre-target resistance consists of increasing the efflux rate of the drug by upregulating the expression and activity of efflux transporters. As mentioned above, copper transporters play a role in cisplatin influx, logically copper transporters are also involved in the cisplatin outflow. ATP7A and B are ATPases responsible for copper and platinum ATP-dependent transport through the cell membrane (73,86,87). Interestingly, the effect of ATP7A/ATP7B in cisplatin resistance not only depends on its overexpression, but also seems to be location specific. For example, Kalayda et al. have shown that these enzymes concentrate on the trans-Golgi network in sensitive ovarian cancer cells (A2780) and translocate to peripheral vesicles in the resistant cell-sub type (93). Similar to CTR1 copper influx transporters, the accumulation of cisplatin in the cell leads to ATP7A/ATP7B overexpression and recruitment to the plasma membrane, and therefore resistance.

Multidrug resistance-associated protein 2 (MRP2) also called cMOAT or ABCC2, is another ATP-dependent efflux transporter that has been shown to be overexpressed in cisplatin-resistant cancers, including melanoma (73,94). This effect is specific to platinum-derived drugs and allows resistant cells to evade G2 cycle arrest and apoptosis due to lower concentration of cisplatin adducts in the cell (94).

On-Target Resistance

There are three main modes of action of on-target resistance, (i) increased DNA repair rate; (ii) cells become able to tolerate DNA lesions; or (iii) impaired recognition of DNA damage.

One of the main downstream effectors of increased DNA repair is the polymerase family PARP. They play an important role in various cellular processes, including modulation of chromatin structure, transcription, replication, recombination, and DNA repair, especially in the G2 cell cycle phase (95). PARP is part of some of the main DNA repair machinery involved in cisplatin resistance, such as base excision repair (BER), nucleotide excision repair (NER) and the homologous recombination repair (HRR). Interestingly, PARP has been shown to be generally upregulated in melanomas, including naïve tumours, which suggests that this is not an adaptation to DNA

damaging agents, but a part of the malignant transformation, likely used to tolerate other mutations (96). For this reason, PARP inhibitors have been developed and used in tumour therapies alone or in combination with DNA damaging agents, such as cisplatin (95).

NER is formed by several different proteins that recognize, extract and repair monofunctional adducts and intrastrand crosslinks. One of such proteins is the xeroderma pigmentosum group A (XPA), a key protein in the NER pathway, which has been shown to be overexpressed and promote resistance of melanoma tumour cells to cisplatin-based drugs by facilitating the DNA repair process (97,98). Moreover, increased XPA can induce off-target cisplatin resistance by activating PARP1 (97). The endonucleases complementation group 1 (ERCC1) and xeroderma pigmentosum group F (XPF or ERCC4) are also members of the NER system and have been shown to be upregulated in melanoma cells in response to exposure to cisplatin (98–101). ERCC1-XPF complex inactivation or inhibition renders melanoma cells sensitive to cisplatin (102).

A different cisplatin-DNA-damage repair system is the homologous recombination repair (HRR), which is mostly active in the S phase of the cell cycle and can fix double-strand breaks. Inhibition or mutation of HRR proteins sensitize cells to cisplatin (73). Some proteins that belong to the HRR system are BRCA1, BRCA2 and RAD51, which are frequently mutated in breast, ovarian and skin cancers (73,98). BRCA mutation and lack of function confers synthetic lethality in response to PARP inhibition (103). The PARP inhibitor Olaparib traps PARP onto DNA repair intermediates, causing obstruction of replication forks, which is normally resolved by BRCA (103). However, when BRCA is mutated, it loses its function, and this obstruction leads to cell death (103).

On the other hand, the RAD51 inhibition mechanism involves a different mode of action called replicative bypass, which enables cells to tolerate DNA lesions and move forward with the cell cycle. Upon encountering interstrand crosslinks during replication, following cisplatin treatment, melanoma cells downregulate RAD51 and increase the activity of translesion synthesis (TLS) DNA polymerase zeta (REV3) (98). Translesion synthesis polymerases are able to insert bases on a damaged template to

allow replication to proceed. Other TLS polymerases involved in the recognition of GpG abducts and replicative bypass are POLH and REV7 (73).

The MMR DNA damage detection system is able to recognize, but not repair DNA. Once a lesion is detected apoptotic signals are initiated. Two proteins from this system, MSH2 and MLH1, which recognize GpG interstrand adducts, are often mutated or downregulated in cisplatin resistant tumours, including melanoma (73,104–106). Similarly to other mechanism mentioned above, it has been observed that naïve tumours present normal MSH2 expression levels, and that the downregulation of this protein is an adaptive response subsequent to cisplatin treatment (73). In the case of MLH1, mutations in this protein have also been associated with replicative bypass (107).

Post-Target Resistance

Cisplatin post-target resistance involves many different cell alterations that are deeply intertwined and involve (i) defects in the apoptotic signalling pathway and (ii) faulty cell death machinery. In this context, different protein alterations can affect cells distinctively.

There are two main signalling pathways, which are responsible for sending messages from the cell membrane to the nucleus and dictate cell fate. The famous MAPK and PI3K/AKT signalling pathways emit pro- or anti-apoptotic signals, through the BCL-2 protein family, depending on a variety of different factors, such as cell type, cell confluence, stress conditions, etc. (108). Moreover, these pathways regulate each other in order to keep a healthy balance in the cell (108). Thus, the deregulation of one or both pathways is a complex, though recurrent, phenomenon in tumour cell resistance (108).

As mentioned above, the PI3K/AKT pathway is one of the most deregulated in all cancer types, over 50% of cancers present upregulation of AKT due to mutations, upregulation of upstream kinases or loss of function of regulating proteins (30). In melanoma, several genetic and epigenetic activating modifications could be identified in the members of this cascade as part of treatment resistance development (31). For example, Survivin, a caspase-inhibitory protein, has been shown to be upregulated following cisplatin treatment in different tumour entities, in a PI3K/AKT dependent manner (73,109). Moreover, clinical studies using Survivin or PI3K inhibitors (YM155

and BEZ235 respectively) alone or combined to platinum-based chemotherapy, have shown good results (NCT01009775, NCT00281541, NCT00818480, NCT01343498, NCT01195376, NCT01337765, NCT01285466, NCT00620594, NCT01508104).

As discussed above, the MAPK pathway is often overexpressed and upregulated in melanoma. This is associated with a worse prognosis, and usually generated by point mutations, such as BRAF and NRAS mutations, that cause the pathway to be constitutively active (16,17,110,111). This pathway has been targeted directly by many specific inhibitors, however, it is also involved in the resistance mechanisms of cytostatic drugs, such as cisplatin. ERK phosphorylation, for example, has been shown to be increased in response to cisplatin treatment (51). Additionally, the signals transmitted by MAPK and PI3K/AKT pathways often converge into the BCL-2 protein family, that has been reported to be deregulated in cisplatin resistant tumours, including melanoma, causing faulty cell-death machinery (17,73,104,112). Its pro-apoptotic members, such as BAX and BAK are often downregulated, while their counterparts, BCL-2, BCL-X_L and MCL-1 are overexpressed (16,73,108).

The expression of anti-apoptotic genes from the BCL-2 family can also be increased by MITF. As mentioned above, MITF is overexpressed or upregulated in 2-8% of amelanotic tumours, as part of malignant transformation of melanocytes (18,19). Once activated, MITF can activate the expression of almost one hundred genes and regulate multiple biological processes in melanoma cells, such as differentiation, proliferation, migration, senescence, metabolism and plasticity, as well as survival (113–117). The latter is achieved by increasing the expression of anti-apoptotic genes including BCL-2A1, BCL-2 and BIRC-7 and could influence cell chemoresistance (115).

Finally, one of the best studied proteins of the cell-death machinery, the tumour-suppressive protein (p53), which is responsible for DNA repair and apoptosis initiation followed by cellular stress. It has been broadly studied *in vitro* and in clinical settings and its mutation and inactivation is classically associated with drug-resistance, including cisplatin (118–122). The mutation and inactivation of p53 is present in several tumour types, including melanoma, where it has been shown to be inactivated in approximately 90% of patients (118–122). p53 mutations are often observed concomitantly to NRAS mutation (15%), and thus have been associated with NRAS-driven melanoma progression (122–124). p53 inactivation in melanoma cells can also

be caused by off-target phenomena such as overexpression of p53 regulators MDM2 and/or MDM4, or CDKN2A deletions (50%) (125–127). For this reason, several attempts have been made to reactivate p53, such as through PRIMA-1 (p53 Reactivation of Massive Apoptosis) and its methylated form PRIMA-1Met (APR-246), which have been successfully used, in combination with chemotherapy, in a variety of cancers, showing promising results (128–130). These are only some examples of the many genetic alterations that can lead to constitutive activation of these two very important pathways, which influence cell survival and can lead to drug resistance.

Off-Target Resistance

Off-target resistance mechanisms consist of alterations in the expression or activation of molecules that do not interact directly with cisplatin but ensure cell survival by activating signalling pathways that enable most of the genetic adaptations mentioned in the sections above. Adhesion molecules and membrane receptors play a major role in this by interacting with the extracellular matrix and activating protective signals; this is known as cell adhesion mediated drug resistance (CAM-DR) (77,78,82).

Cancer cells often modify the ECM by overexpressing molecules that can interact with cell receptors and induce survival. This is the case for the matrix proteins, Collagens, which have been observed to be overexpressed and induce CAM-DR in several cancer types (131–136). Cells can also overexpress or upregulate cell receptors that interact with the ECM. Receptors tyrosine kinase (RTK) are most commonly involved in this process. One of the most important genetic alterations in malignant melanoma involves receptor tyrosine kinases and the upregulation of downstream MAPK and PI3K/AKT pathways, both of which play major roles in melanoma progression (4,31). For example, deregulation of the receptor AXL causes MAPK-mediated stabilization of the abovementioned MDMX–MDM2 heterocomplex, and thus p53 inactivation in melanoma cells (137). Another receptor known to be mutated in 20% of melanomas, activating the PI3K/AKT pathway is ERBB4 (31). Moreover, the overexpression of HER-2 of the ERBB growth factor receptor family, has been associated with PI3K/AKT dependent cisplatin resistance through an interesting mechanism that depicts environment-mediated drug resistance perfectly: at first contact with cisplatin, HER-2 activates basal levels of PI3K/AKT pathway, which induce cell-cycle arrest and survival through cyclin-dependent-kinase inhibitor 1A (CDKN1A or p21)(138–140).

This protects the cell from DNA damage and gives the cell time to adapt to treatment stress. As cisplatin stress persists, PI3K/AKT pathway activity increases, not exclusively, as a result of HER-2 overexpression (138). This leads to CDKN1A translocation from the nucleus to the cytoplasm, thereby generating a high proliferative cisplatin resistant phenotype (acquired drug resistance) (138,141).

However, other membrane receptors that do not possess kinase activity, such as integrins and syndecans, can also be activated by components of the ECM, such as fibronectin (FN), laminin (LM) and collagen (Coll), and induce resistance. Integrins, especially the β1 integrin subunit, have been primarily associated with CAM-DR in blood cancers, since this was the first type of cancer in which environment-mediated drug resistance has been studied, as mentioned above (142–146). β1 integrin has later been associated with CAM-DR in several different solid tumours, in which resistance to chemo- and targeted therapy is induced by β1 integrin contact with ECM compounds, such as FN, the main component of bone marrow; and Coll I, the main ligand for β1 integrin and a major matrix protein of tumour microenvironment (147–152).

This binding causes β1 integrin up-regulation, and thus increases activation and expression of important components of the MAPK and PI3K/AKT signalling pathways such as ERK, MEK, ILK, FAK, PI3K, AKT and upregulation of anti-apoptotic proteins such as BCL-2, BCL-X, Bim, MCL-1 and Survivin and downregulation of BAX (147–152). But, so far, there are not many studies connecting β1 to melanoma chemoresistance. Recently, Iyoda et al. were able to demonstrate multiple drug resistance induced by FN in melanoma and breast cancer cells mediated by Bim (153). Moreover, even though the relation between β1 integrin and Coll I in melanoma migration and metastasis has been established since the ‘90s, there is only one report, in uveal melanoma, linking these molecules in the context of chemoresistance, which demonstrates the lack of studies about this interaction (154–158).

In light of these facts, we have concentrated our efforts in investigating the adhesion molecules, integrin, and its co-receptor, syndecan. They interact with the PI3K/AKT pathway and have been associated with tumour malignancy. The importance of these molecules for cancer progression and resistance, as well as their relation to the PI3K/AKT pathway and each other, will be discussed below.

Extracellular matrix

The extracellular matrix (ECM) is a complex non-cellular environment responsible for structural support and stability to cell tissues as well as information exchange between the intra- and extracellular spaces. Cells interact with the ECM through adhesion molecules, mainly integrins and syndecans, which recognise and bind to specific ECM components and carry out these messages. Interestingly, almost all ECM elements present binding sites for these two proteins (159). These bonds affect cell adhesion, polarity, motility, proliferation, differentiation and survival (159–162). For example, although, malignant transformation leads to anchorage-free survival, integrin adhesion to components of the ECM regulates the expression of pro and anti-apoptotic proteins from the BCL-2 family, such as BAX and BCL-2, through FAK/PI3K signalling, promoting cell survival (163,164). As previously mentioned, ECM also offers protective response to cancer cells against cytostatic drugs (147–152). β1 integrin binding to the ECM triggers FAK (focal adhesion kinase) signalling that inhibits p53 through degradation by MDM2 (165,166).

Thus, ECM properties such as composition and physical-chemical properties, namely rigidity, elasticity, topology, and pH, impact cells in different ways (162,167–170). For example, matrix stiffness has often been associated with tumorigenesis and increased cell cycle progression, especially in breast cancer, by adhesion-mediated FAK activation, which initiates proliferation signals through phosphorylation of PI3K and RAS, resulting in ERK activation and nuclear translocation, and cyclin D1 induction (171–175). Mechanotraction also downregulates PTEN expression, thereby upregulating PI3K/AKT signalling, which leads to cell growth and survival (176). The ECM is a versatile and dynamic milieu composed of water; fibrous proteins, such as vitronectin, LM, FN and Coll; glycoproteins; and proteoglycans; soluble factors; polysaccharides and glycosaminoglycans (160).

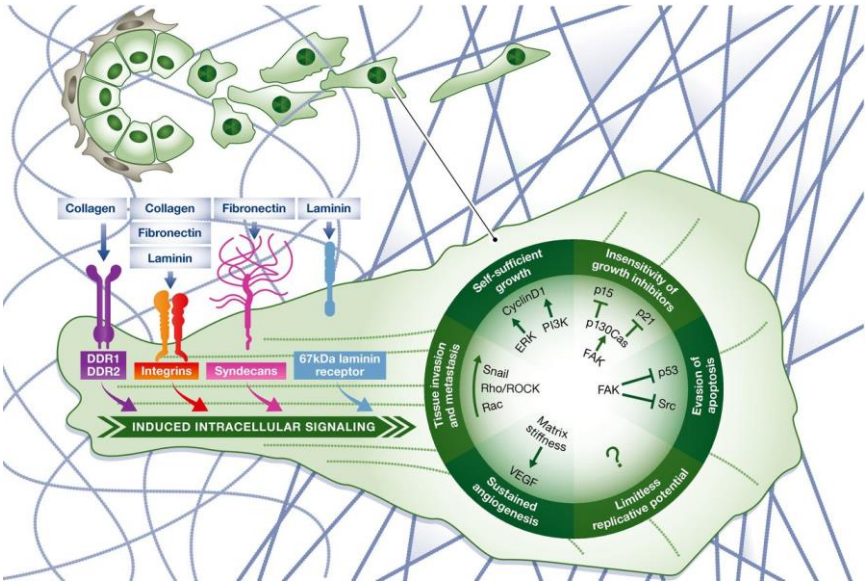

Figure 7. Extracellular matrix influences in cancer progression and maintenance. Cells bind their adhesion molecules, for example discoidin domain receptors (DDR), integrins, syndecans and laminin receptor, to ECM components such as Coll, FN and laminin resulting in a vast array of cell signals that impact cell behaviour, survival and growth (162).

Collagen

Collagens account for 30% of total protein mass in mammals (177). They constitute the largest matrix protein family with at least 28 members and are defined by the presence of triple-helical domains, which can comprise almost all of their structure (96% for Coll I), or very little of it (less than 10% for Coll XII) (177,178). They interact with other collagens and components of the ECM, as well as glycoprotein, proteoglycans, cell surface receptors and adhesion molecules, such as integrins, and contribute to tissue integrity, tensile strength, organization and function (178).

Coll fibrils are a classical example of a quaternary protein structure. The amino acid structure of Coll is translated and folds into α-helices (secondary protein structure) that vary in size from 662 - 3152 amino acids (177). α-helix chains can present several isoforms, which define Coll type, each of these isoforms can suffer alternative splicing or use alternative promoters generating further variability and affect Coll function (177). The triple helices represent the tertiary protein structure and are formed by three left-handed α-helix chains twisted into a right-handed coil (177). The triple-helical general sequence is formed by Gly-Pro-X or Gly-X-Hyp repeats, X representing other amino acids, although 3-hydroxyproline residues have been identified in Coll I, II, III, and V/XI (177,179). This structure is mainly stabilized by glycine, but also inter-chain

hydrogen bonds (25). Fibrillar collagens can associate in various ways to form quaternary structures: Coll fibrils that may contain non-fibrillar counterparts (fibril-associated collagens with interrupted triple-helices - FACIT) (177). For example, cartilage fibrils are made of Coll II, XI and IX (FACIT) or II and III, while skin fibrils are rich in Coll I and III and cornea I and V (177,180,181). Besides FACIT, non-fibrillar Coll includes multiplexins and membrane collagens, and besides the ability to form fibrils, fibrillar collagens present one major triple-helical domain while non-fibrillar bear many (177,178). The most common Coll is type I, it forms hexagonal-like structures by associating groups of five Coll I molecules into supertwisted fibrils, which interdigitate with other fibrils (177,178). Coll assemblies can be observed by electron microscopy as rods of 75 nm – 425 nm of length, as depicted below (177).

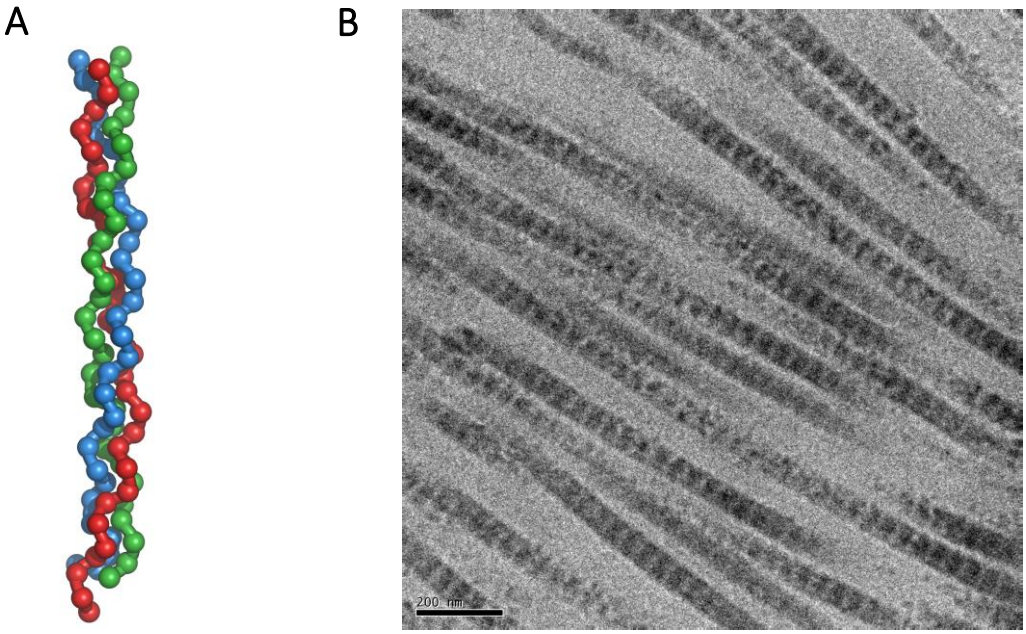

Figure 8. Collagen structure. The amino acid structure of Coll is translated and folds into α-helices (represented in red, green and blue). A. Three α-helix chains twist into a triple helix (182). B. Coll fibrils observed under microscope (183).

The function of Coll in the cell is diverse and dependent on several factors. These factors include, first, the previously mentioned wide Coll family diversity and genetic modifications (177,184). Second, some collagens (IX, XII, XIV, XV, XVIII) function as core proteins for glycosaminoglycans and, therefore, are considered proteoglycans (177,184). They can suffer glyco- or proteolytic cleavage, usually by glycosylases, and matrix metalloproteinases (MMPs) or sheddases, respectively, this leads to the release of bioactive fragments that influence cell behaviour (177,184,185). Third, conformational changes caused by interactions with other collagens or ECM

compounds, denaturation or binding to cell receptors leading to the generation of mechanical forces, as is the case for integrins (177,184). For example, it has been suggested that integrins and FN, together with Coll V and XI, could be involved in fibrillogenesis of Coll I and II (177,186). Coll and FN have been shown to co-localize in the ECM, and there seems to be a mutual cooperation between them (187). FN displays Coll binding (FNI_6 $FNII_{1\text{-}2}FNI_{7\text{-}9}$, see Figure 10.) and is involved in the deposition of Coll, as mentioned above (187,188). Simultaneously, Coll provides structural support that regulates FN stretching (189).

Besides acting as mechanosensors, integrins are involved in several cell functions which are often related to attachment to the ECM. The integrins that show most affinity to Coll are β1 integrins. They are responsible for cell attachment and survival in physiologic conditions, however, in cancer cells other integrin subunits maybe involved. In normal fibroblasts, β1 integrin can lead to apoptosis in response to contraction of Coll I 3D matrices, through the inhibition of the FAK/PI3K/AKT pathway (190). However, the same cells survive following activation of the same integrins and pathway on Coll I coating (no mechanotension) (190). On the other hand, in melanoma cells, Coll I 3D matrices have been shown to lead to cell survival by activating β3 integrin (191). Initial attachment seems to be made by β1 integrins, but extensive incubation in Coll stimulates cells to digest the Coll, exposing its RGD binding site where β3 integrin can attach and lead to cell survival (191). Overexpression of Coll has been associated with CAM-DR in cisplatin-resistant ovarian and lung cancers (131–133,136). Moreover, Bérubé et al. were able to show the presence of the CAM-DR in uveal melanoma cells, where there is a correlation between β1 integrin binding to Coll IV, FN and laminin, and cisplatin resistance (158). β3 integrin also seems to be involved in this process to some extend (158). Additionally, Coll IV has been shown to bind and activate integrin α1 (192). Coll I has been shown to carry different binding sites for heparan sulfate and heparin than for integrins, which means this Coll can bind to integrins and glycosaminoglycan chains of proteoglycans simultaneously, thereby facilitating integrins – syndecans clustering, for example (178).

Fibronectin

Fibronectin (FN) is a very ubiquitous ECM adhesion protein; it is known by its ability to bind simultaneously to a variety of ECM compounds, such as collagens and growth factors, cell surface receptors and adhesion molecules, such as integrins and

proteoglycans (187,188,193). Binding to these molecules and/or mechanotension can lead to conformational alterations in FN, which impact cell behaviour, such as migration and adhesion (187,188,193). FN also presents a quaternary protein fold, it is composed of two approximately 230 – 270 kDa subunits, connected by a pair of disulphide bonds, at their C-termini, forming a dimeric glycoprotein (187,188,193). Each subunit is composed by twelve Type I repeats, two Type II repeats, and 15-17 Type III repeats (187,188,193). These repeats present similar but distinct structures, the main difference being that type I and type II repeats are stabilized by intramodular disulphide bonds, while type III repeat is formed by an antiparallel 7-stranded β-barrel structure that is not stabilized by disulphide bonds, rendering the molecule more flexible and sensitive to chemical or mechanical changes (187,188,193).

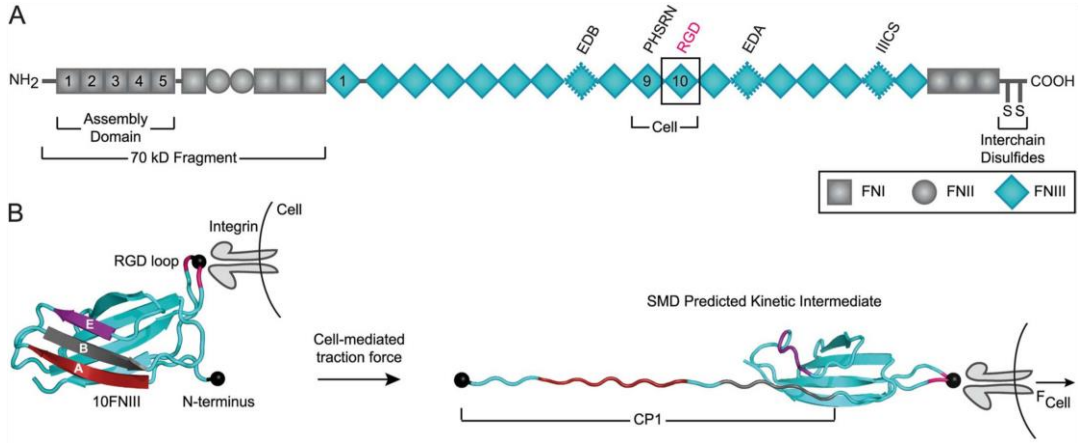

Figure 9. Fibronectin structure and domains. Adapted from Gee et al. (194). **A. Linear depiction of FN**, which is composed of two approximately 230 – 270 kDa subunits, connected by interchain disulphide bonds, at their C-termini, forming a dimeric glycoprotein. Each subunit is composed by twelve Type I repeats (FNI represented by grey squares), two Type II repeats (FNII represented by grey circles), and 15-17 Type III repeats (FNIII represented by blue diamond). The RGD integrin binding site can be identified in pink at the cell binding region of the molecule. Finally, the amino-terminal 70-kDa fragment contains assembly and gelatin-binding domains and is routinely used in FN binding and matrix assembly studies. **B. 3D molecular structure of FN**. FNIII is formed by an antiparallel 7-stranded β-barrel structure, which is not stabilized by disulphide bonds like FNI and FNII, giving the molecule flexibility.

FN is secreted as soluble, covalent dimer (fibres) that associate into supermolecular structures (fibrils) through non-covalent bonds that involve Type I repeat 1-5 and Type III repeat number 1 (187,188,193). Fibril formation is mediated by integrins that enable the cross talk between FN fibres and the actin cytoskeleton, coordinating FN fibril architecture with cell shape and intracellular signalling (188,193,195). Integrins' main binding site is the RGD motif on $FNIII_{9\text{-}10}$, but they can also bind to the CS1 segment of the alternatively spliced V region on FNIII (196–198). The main subunit involved in

FN fibril assembly is integrin α5β1 (188). Its binding to FN RGD motif generates FAK-mediated intracellular signalling, which is essential to FN fibril formation (188,199). This leads integrins to cluster and form adhesion complexes that create contractile forces, exposing FN binding site and allowing fibres approximation and interaction with each other (188). Other cell-adhesion molecules such as α4β1, αvβ1, αvβ3 and αIIbβ3 can also induce fibril formation under specific stimuli, such as activation by Mn^{2+} or specific antibodies (188). Moreover, the proteoglycans syndecan-1 and 2 seem to also be able to contribute to FN association (188).

FN function and affinity to ligands is controlled by several factors, such as structure variability by alternative splicing, which mainly affects subunit size and the presence of specific binding sites; environmental factors, such as contractile forces and pH; and conformational changes in the protein structure (187,188,193). For instance, alternative splicing can alter integrin α4β1 and syndecan ability to bind to FN (197,198,200,201). Moreover, the FN quaternary structure is rendered inactive for transportation in the blood stream (187). Additionally, FN relaxed or stretched state can dictate binding affinity to specific integrin types; for example relaxed FN promotes integrin α5β1 binding, while stretched conformation favours integrin αvβ3 adhesion (187). This integrin subtype switch can have consequences in cell decision-making, such as proliferation in detriment of migration, which will be discussed in the chapter about integrin herein.

This shows that integrins interaction with FN affects several different cell processes besides FN fibril formation. Integrin binding to FN generates survival and proliferation intracellular signalling, which involves FAK, PKC, Src, paxillin, and PI3K/AKT (202). For example, it has been shown that β1 and β3 integrin activation upon FN and vitronectin binding, respectively, leads to FAK phosphorylation and upregulation of BCL-2 pro-survival gene through PI3K-AKT pathway (203). Moreover, blocking of the FN heparin binding site has shown to inhibit αv and α2 melanoma cell adhesion to FN and Coll IV, and reduce cell viability and metastatic potential through downregulation of FAK and ERK 1/2 (204). Finally, FN has been associated with CAM-DR in acute myeloid leukaemia, breast and skin cancers (153,205–208). In addition, blocking of $FNIII_{14}$ has been shown to inactivate β1 integrin and upregulate pro-apoptotic Bim protein (153,205–208).

Another family of cell surface receptors are the proteoglycans syndecans (Syn). They are formed by a central protein core that presents glycosaminoglycans attached to it (178). Even though they will be discussed in depth later, at this point, it is important to point out the relation between syndecans and FN. FN presents three major heparin binding-sites, but the best characterized is Hep II, located in the C-terminal ($FNIII_{12-14}$) (178). Syn can bind to this site through its glycosaminoglycan chains, which enhances integrin-mediated cell spreading and intracellular signalling (159,178). Additionally, Hep II presents a RGD sequence that can bind to integrins, reinforcing the concept of cooperation between Syn and integrins in cell attachment (178,187,202).

Glycosaminoglycans

Glycosaminoglycans are linear polymers of complex sugars, some examples are hyaluronan, heparin (Hep), heparan sulfate, chondroitin sulfate. They are formed by repetitive disaccharide units, constituted by one hexosamine, glucosamine or galactosamine, united by a glycoside bond to a non-nitrogenized sugar residue, uronic acid, β-D-glucuronic acid or α-L-iduronic acid, or even, a neutral sugar such as D-galactose (209). Glycosaminoglycan synthesis is complex and involves a large number of transferases and modifying enzymes, whose role is to regulate their fine structural properties, such as sulfation in specific positions of their molecule (210,211). The reducing portion of the glycosaminoglycan chain, consisting of 50 to 200 repeating disaccharides, is covalently bound to the *core* protein by a link tetrasaccharide, common to all glycosaminoglycans, thereby forming a proteoglycan (209). The only exception is hyaluronan, which is an ECM soluble molecule. Proteoglycans act as adhesion molecules that can bind to other compounds of the ECM, as well as other adhesion molecules, such as integrins (212–215). They present a wide variety of distribution and biological functions such as tissue organization, adhesion, motility and proliferation, which will be discussed below.

The abovementioned heparins are special glycosaminoglycans produced by mast cells with anti-coagulative activity, for this reason they have been widely used as anti-thrombotic agents since 1939 (216). They are similar to heparan sulfate, but generally present a very high amount of iduronic acid, N- and O- sulfation. Hep chain length can vary from 6.000-30.000 Da and researchers have observed that sugar chain length impacts its ability to bind to its ligand thrombin (216,217). This occurs because this glycosaminoglycan facilitates the interaction between anti-thrombin and factor Xa,

firstly by tightly binding to anti thrombin through a specific pentasaccharide; this leads to allosteric changes in the anti-thrombin, which facilitate factor Xa binding; secondly, by loosely connecting to the enzyme and thrombin and allowing anti-thrombin to slide along its sugar chain and approach the complex (32). Thus, there is a minimum length of the Hep chain that allows this interaction, this length is seven sugar units following the pentasaccharide (216,218). This discovery gave rise to two important concepts: unfractionated heparin (UFH), which refers to all Hep molecules isolated from a sample; and low molecular weight heparins (LMWH), which refers to small Hep molecules that still preserve catalytic activity (216,218). Many have been developed through the decades, to improve patient treatment, one example being Tinzaparin, which has molecular weight of 6.500 Da and is one of the biggest LMWH (218). Studies have shown that Tinzaparin has antitumoral properties, such as antimetastatic and impairing neovascularization effects (219–221). LMWH has also been associated with overcoming chemoresistance (222–225). In our group, Schlesinger et al. have shown that heparin can reduce metastatic activity in melanoma, by blocking α4β1 integrin (226,227). In addition, Pfankuchen et al. showed that the heparin tinzaparin can induce resistance against cisplatin treatment in ovarian carcinoma (224,228).

Integrins

Cellular functionality in general is determined by adhesive interactions between cells and their local microenvironment, which allows cells to integrate and detect external changes and influence cell phenotype as well as malignant transformation. Integrins are a key molecule in these exchanges, since they are ubiquitous cell-membrane proteins involved in cell adhesion and signalling. Integrins are heterodimeric transmembrane glycoproteins formed by α and β-subunits, which mediate interactions between cells and their extracellular environments. 18 α- and 8 β-subunits have been mapped on the human genome; composing 24 integrins, they form the biggest family of cell adhesion molecules presenting a large array of ligands and functions (145,229,230). Subunits α and β are each formed by a small cytoplasmic region (40–70 amino acids), which interacts with intercellular messenger proteins; a transmembrane section; and a large extracellular portion, for ligand binding. The transcription of the subunits is performed separately, then they undergo modification with high mannose N-linked oligosaccharides to ensure their correct folding and, finally, are assembled in the endoplasmic reticulum (ER), and transported into the Golgi apparatus (231,232). Integrins are highly glycosylated proteins, and their glycosylation pattern is known to

affect integrin heterodimerization, stabilization, cell membrane placement, function and affinity to ECM compounds and other ligands (217,233–235). Aberrant glycosylation of integrins has been observed in different cancer types, including melanoma (217,236,237). The main alteration is the glycosylation pattern of β1 integrin, which has been shown to be involved in melanoma malignant transformation and to affect integrin affinity to ECM compounds (217,236–239).

The β-subunit is formed by a cysteine-rich membrane proximal-β tail (βTD), followed by four epidermal growth factor (EGF) segments, hybrid and PSI (plexin/semaphorin/integrin) domains and, finally, a βI-like N-terminus, which contains the MIDAS divalent-cation-binding site. The α-subunit is formed by two calf domains, followed by a tight and a folded seven-bladed β-propeller, which harbours four to five divalent-cation-binding sites and can contain an immunoglobulin-like domain. Since the affinity of integrins to their ligands is dependent on the above mentioned divalent-cations (Ca^{2+}, Mg^{2+} and particularly Mn^{2+}) (240), it has been reported that Ca^{2+} binds to the heterodimer to keep it inactive until it has been transported to the plasma membrane (241). Integrin activation is dependent on ligand binding, which changes the conformation of such receptors. Inactive integrins present a folded conformation with the tails of each subunit close together. Upon stimuli, integrins go into an extended conformation, with separated tails, that presents intermediate or high ligand affinity (242).

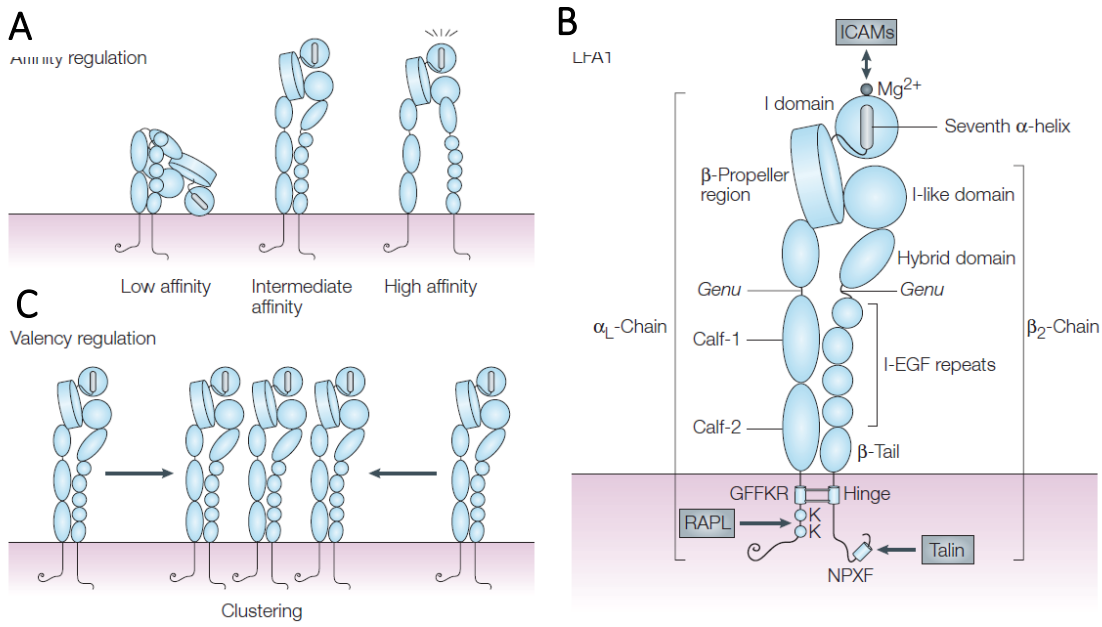

Figure 10. Integrin structure and activation. A. Integrins present one inactive and two active states (intermediate and high affinity). Integrin activation follows ligand binding that induces conformational change. **B. Integrins are transmembrane proteins formed by an α and a β chain.** The β-subunit is formed by a cysteine-rich membrane proximal-β tail (βTD), followed by four epidermal growth factor (EGF) segments, hybrid and PSI (plexin/semaphorin/integrin) domains and, finally, a βI-like N-terminus, which contains one of the metal ion-dependent adhesion sites (MIDAS). The α-subunit is formed by two calf domains, followed by a tight and a folded seven-bladed β-propeller, which harbours four to five divalent-cation-binding sites and can contain an immunoglobulin-like domain. **C.** Upon ligand bidding and conformational change to the high affinity state **integrins can form cooperative clusters** that can mature into focal adhesions (243).

Integrin activation is dependent on the above-mentioned cation, particularly, Mn^{2+}, which can directly affect integrin conformation to the high affinity extended state (242). Once activated, it can bind to components of the ECM (242). Each integrin heterodimer interacts, preferentially, with different ECM molecules such as Coll, FN, and LM among other substances, as depicted bellow (217,242). Integrin binding to ECM is essential to cell survival, since integrin dissociation from the ECM leads to integrin - mediated cell death by anoikis (242).

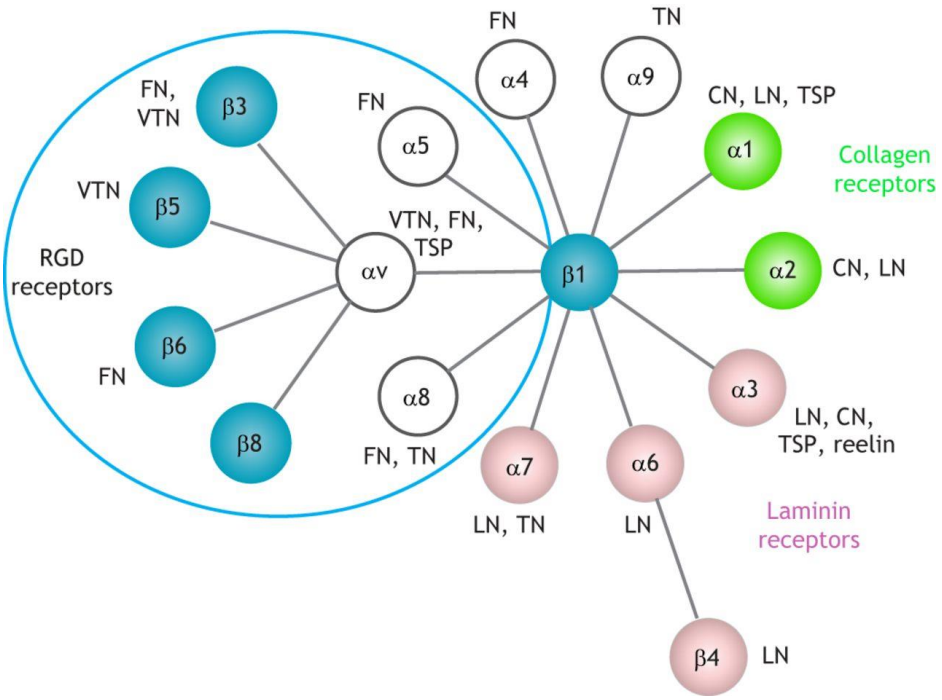

Figure 11. Integrin and their ligands. Integrin heterodimers are formed by α and β-subunits, a variety of 18 α- and 8 β-subunits compose 24 integrins, which mediate interactions between cells and their extracellular environments. Each integrin heterodimer interacts, preferentially, with different extracellular matrix molecules such as Coll (depicted in green as CN), fibronectin (FN, depicted in blue), and laminin (LN, depicted in pink), among other substances such as tenascin (TN), vitronectin (VTN), thrombospondin (TSP) (244).

Integrin binding to the ECM, or to adjacent cell surface receptors has three different functions. First, to regulate the cytoskeleton and ECM fluidity, through physical attachment in association with other proteins, such as talin, forming integrin adhesion complexes, that generate mechanotransduction signals, which influence cell positioning, division and protein expression (245). Second, to form clusters on the cell surface, often in association with syndecans, which affect the expression and concentration of integrin on cell surface, as well as affinity to ligands (246,247). Syndecans have often been described as co-receptors for integrins in the interaction with ECM molecules in physiological and tumoral situations, but the relationship between these two cell adhesion molecules goes far beyond that, this will be discussed in depth in the next section. Third, activate specific signalling pathways by phosphorylating kinases, such as focal-adhesion kinase (FAK), proto-oncogene tyrosine-protein kinase (Src), Rho-family GTPases, integrin-linked kinase (ILK) and lipid kinases, all of which control cell division, migration, differentiation and survival (229,230,248,249); or by acting as cell ligands and interacting with surface receptors, such as growth factor receptors (GFR), or specific immunoglobulins, such as VCAM.

This can affect cell proliferation, survival and angiogenesis through PI3K/AKT pathway, ERK signalling and Rho GTPase – Rac1 cascade (229,230).

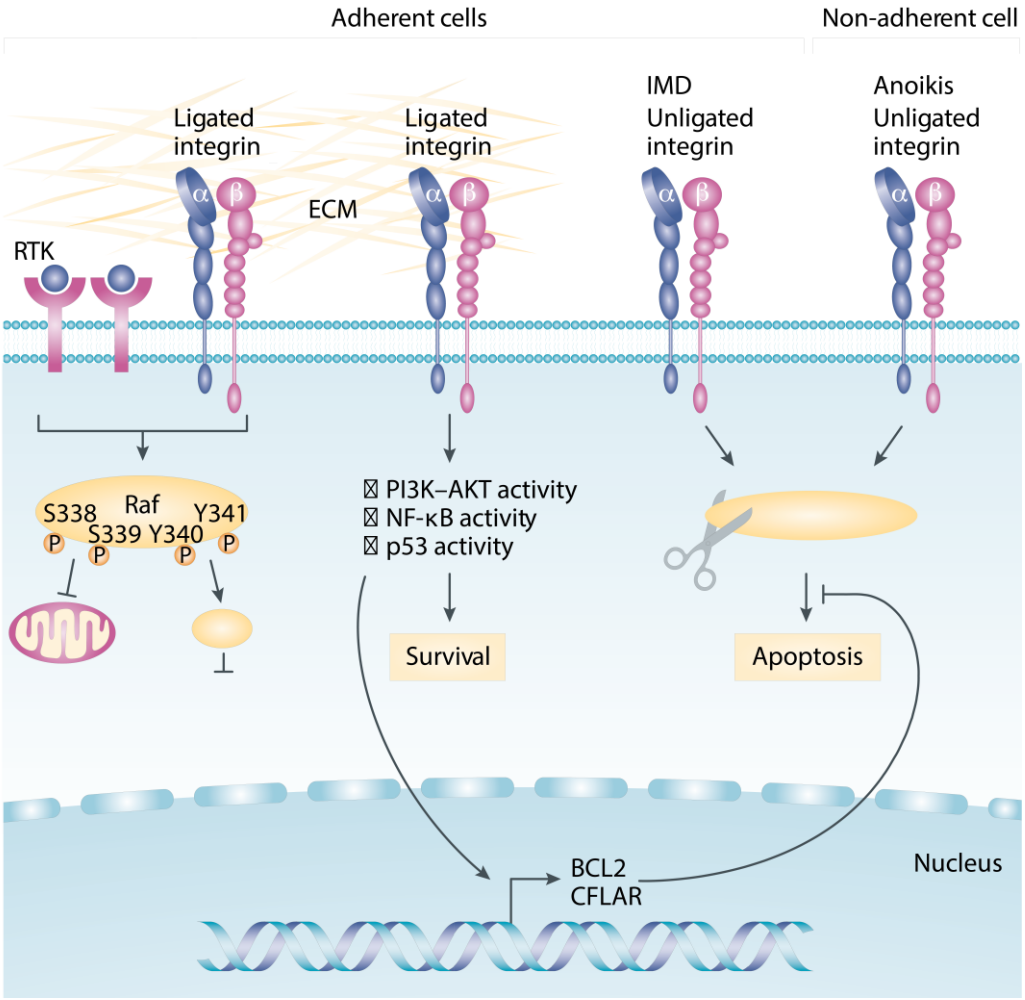

Figure 12. Integrin adhesion regulation of cell survival and apoptosis. Integrins attachment and activation of specific signalling pathways determines cell-fate. Integrin activation and affinity to the ECM can lead to cell survival, while integrin detachment initiates anoikis apoptotic signals. (250).

All these roles of integrins within the cell, associated with the fact that malignant cell transformation often alters the expression of integrins, has led them to be associated with cancer progression, contributing to proliferation, survival, invasion, neoangiogenesis and metastasis (189,195). However, the role of each integrin subunit in different cancer types has been object of controversy. As each integrin subunit has different, specific functions, their association with different heterodimer counterparts influences their specificity to different ECM molecules or receptors and affects function. Moreover, different integrin subunits can cooperate or regulate each other to adapt to modify their microenvironment in a rapid, complex process, not yet fully understood. These changes can be a response to genetic modification, in the case of

malignant transformation, cell density, ECM stiffness, or stress, such as pH variation or the presence of anti-tumour drugs in the tissue. A key integrin subunit in this haemostasis behaviour is β1 integrin. Preferably binding to Coll and FN, β1 integrin can associate with at least 12 α–subunits to ensure cell survival, migration and metastasis, by regulating focal adhesions assembly between the cell and ECM. This integrin subunit has been associated with poor prognosis and metastasis in several cancer types, including melanoma (252–254). Highly metastatic MV3 melanoma cells present increased expression and activation of β1 containing integrins and use them to reorganize Coll matrices and migrate (255–257). Lydolph et al. have shown that β1 integrins can be activated by Mn^{2+} ions, increasing adhesion in a Rho dependent and heparan sulfate independent manner, and that the activating status of β1 integrins controls cell tendency towards migration or proliferative behaviour (focal adhesion formation) (254). Furthermore, as mentioned above, β1 integrin has been linked to drug resistance in hematopoietic and solid tumours (142–144,147–149). But, so far, there are not many studies connecting β1 integrin to melanoma chemoresistance, except for the report from Bérubé et al. about uveal melanoma mentioned above. β1 integrin binding to their ECM ligands leads to integrin-mediated cell survival by activation of several signalling cascades including the FAK/PI3K/AKT pathway (250,252,258). For example, it has been shown that β1 and β3 integrin activation upon FN and vitronectin binding, respectively, leads to FAK phosphorylation and upregulation of the BCL-2 pro-survival gene through the PI3K/AKT pathway (203). For this reason, we thought this would be an interesting target to investigate CAM-DR.

As mentioned above, different integrin subunits can cooperate or regulate each other depending on environmental signals, this is the case for β1 and β3 integrin. There seems to be a very complex regulation between these subtypes. It has been suggested that β1 integrin is involved in strong adhesion and proliferation, while β3 integrin expression favours endothelial to mesenchymal transition and metastasis (259–261). While this is true for β3 integrin, which has been associated with metastasis in many tumour types, including melanoma (191,260–264), β1 integrin has also been shown to drive tumour migration by modifying the ECM, especially Coll and FN fibres, in solid tumours. This can be observed for example in the previously mentioned MV3 melanoma cell lines that show high metastatic potential and increased levels of β1 integrins (255–257). As mentioned before, other melanoma cells have been shown to survive in Coll I 3D matrices by activating β3 integrin (191). Initial attachment seems to be made by β1

integrins, which are able to modify the Coll fibres, exposing its RGD binding site where β3 integrin can attach and lead to cell survival (191). It has also been suggested that the conformation state of FN fibres can favour expression and activation of either integrin subtype, thereby impacting cell behaviour and fate (265–267). Moreover, reports have shown that breast cancer cells, but not normal mammary cells, compensate for β1 integrin downregulation by upregulating β3 integrin expression, which makes sense, if we observe the similarities between these two integrins, especially that both of them are able to bind to ECM components and form focal adhesions, which regulate survival through FAK activation (191,260,262,264). For example, the main ligand for β3 integrin is vitronectin, which can also bind to Coll and induce melanoma cell survival (160,191).

It has been suggested that the switch to β3 integrin makes cells more aggressive and resistant to stress, since this integrin can induce survival upon cell detachment, through non-canonical FAK-independent signalling pathways (260,261). It has also been associated with RTK independency and cancer stem cell phenotype, which is knowingly treatment resistant (261,268,269). Moreover, β3 integrin invasion and metastasis in different cancer types, including melanoma by activating the FAK signalling pathway (191,260–264). Thus, even though the regulating mechanisms that control the balance between β1 and β3 integrin expression are not fully understood, they are certainly accurately regulated by cancer cells and seem to adapt to environmental changes, survive and proliferate.

Syndecans

Syndecans are an important adhesion protein family, often described as co-receptor for integrins and as ubiquitously expressed. The syndecans belong to the so-called heparan sulfate proteoglycans (HSPG), since they constitute a family of type I transmembrane proteins, which present glycosaminoglycans, most commonly heparan sulfate, covalently bound to their ectodomain. Syndecans' *core* proteins range from 20-40 kDa and are divided into three parts: the extracellular domains or ectodomains, which are very sequence-divergent among the four syndecans, apart from the conserved GAG covalent attachment sites, where usually heparan sulfate, but also chondroitin sulfate, can be found; the transmembrane region, which is highly conserved and, finally, the small cytoplasmic domain, which is composed of two highly conserved regions (C1 and C2), and a variable region (V), which is unique to each syndecan (246,247,270).

The V region of syndecan-4 is quite well understood and of great importance, its Tyr180 regulates the effect of proteoglycans on integrin internalization and function. Also the serine residue, adjacent to this tyrosine, harbours the phosphorylation site for PKCδ (270).

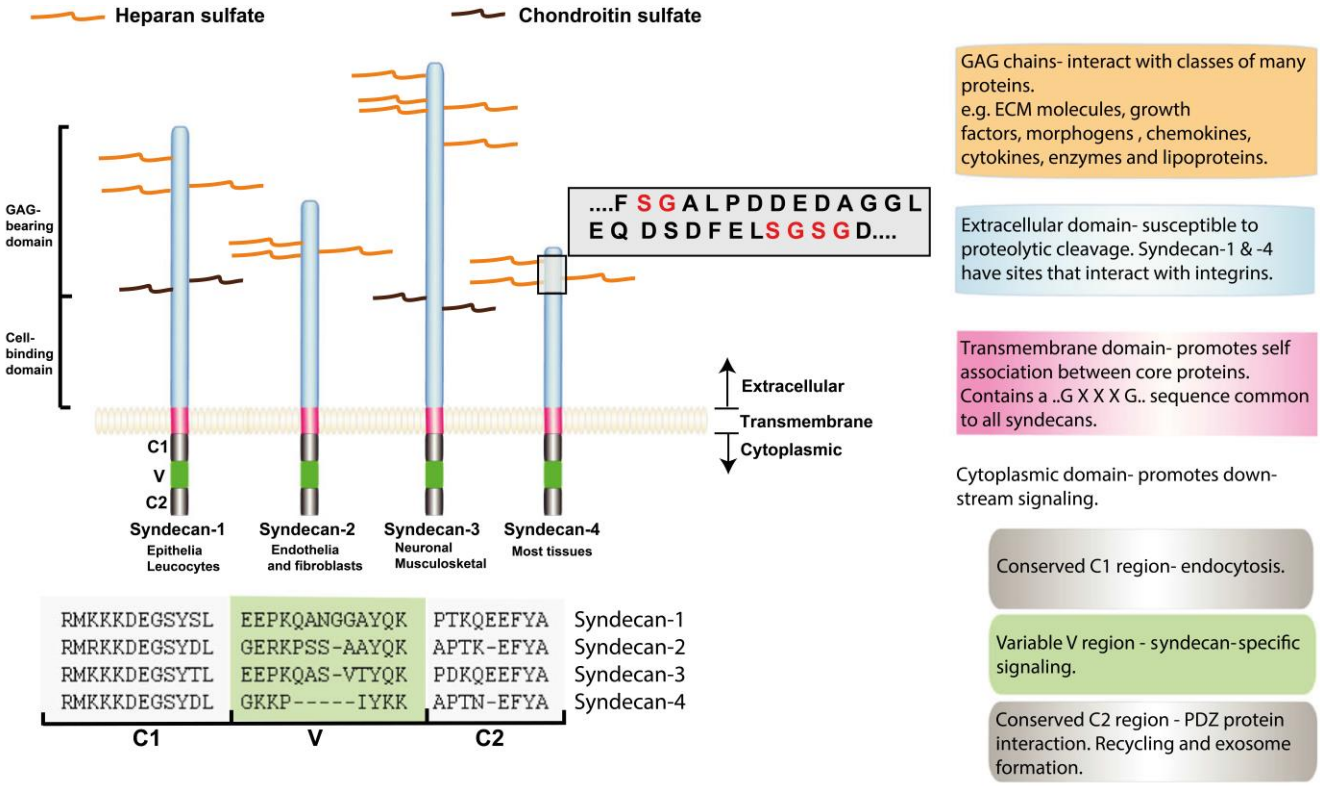

Figure 13. Syndecan subtypes and structure. Syndecans are transmembrane proteins that range from 20-40 kDa and are divided into three parts: ectodomain (blue), where usually heparan sulfate (orange), but also chondroitin sulfate (brown) are bound; the transmembrane region (pink), which is highly conserved; and the cytoplasmic domain, which is composed of two highly conserved regions (C1 and C2 in grey), and a variable region (V in green), which is unique to each syndecan (270).

Syndecans have been known to work as receptors on the cell membrane, in a GAG-dependent manner. The long sugar chains enable these HPSG to concentrate or reach disperse ligands from the ECM. Their importance has been shown in several studies where blocking or digestion of such GAG disrupts syndecan interaction with FN, fibroblast growth factor-2 (FGF2) and vascular endothelial growth factor (VEGF) (271,272). However, there are also reports of direct interactions between syndecan core protein and integrins in a GAG independent manner (273–275). These various interactions with multiple ligands render proteoglycans responsible for a variety of cell processes, such as regulating adhesion, motility and cellular proliferation; activity of cytokines, growth and angiogenic factors and enzymes; and interacting with tyrosine

kinase receptors and integrins (212,246,247,276,277). Thus, they are involved in tissue organization, development and repair, inflammation and tumour progression (276,278).

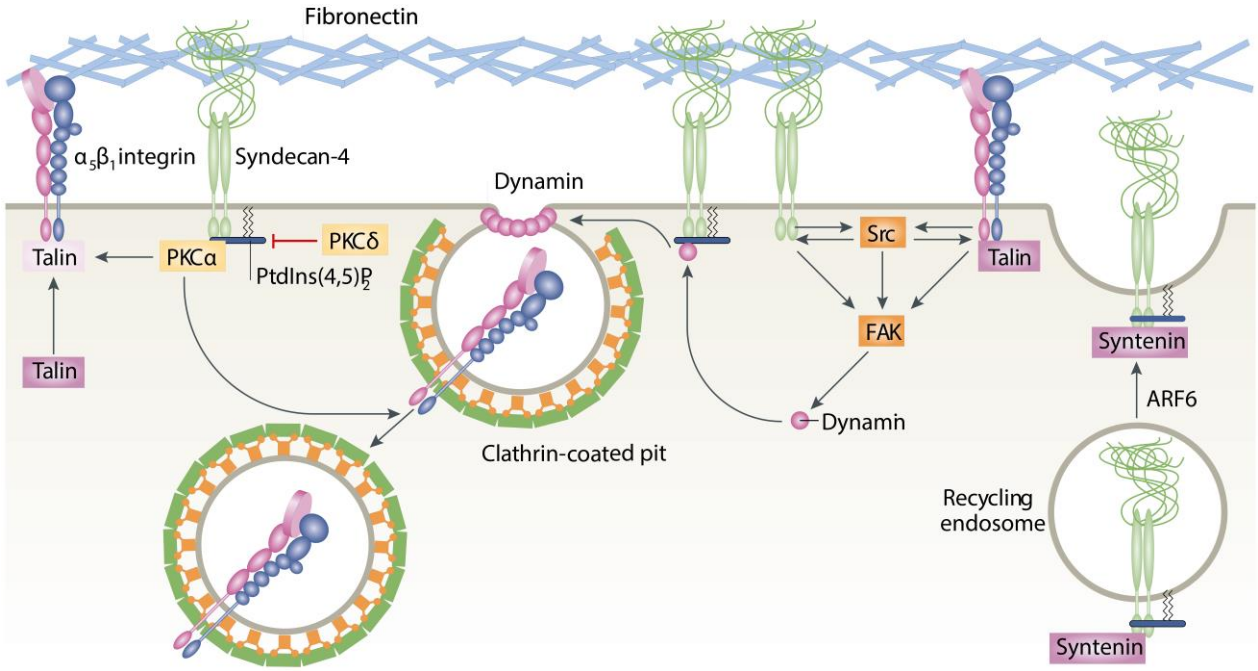

Figure 14. Syndecan – integrin cooperation. Syndecans have been extensively associated with integrins as co-receptors, they can activate or increase integrin bidding affinity interacting with them directly or indirectly through the ECM, leading to outside–in signalling. Syndecans – integrin interaction can also lead to outside-in activation through Src/FAK (246).

Syndecans have been extensively associated with integrins as co-receptors, and therefore inherent in tumour progression through regulation of matrix remodelling, cell adhesion and migration. Syndecan-1 aberrant expression has been associated with poor prognosis in several tumours (270). This proteoglycan has also been demonstrated to co-localize with α2β1 integrin in breast cancer to enhance integrin-mediated adhesion through actin organization on Coll, in a heparan dependent manner (247). Moreover, syndecan-4 altered expression has been shown to enhance cancer progression in breast cancer, melanoma and hepatocarcinoma. In melanoma, for example, downregulation of syndencan-4 blocks FGF2 signalling, increasing cell metastatic potential and decreasing adhesion (270).

Regarding cell adhesion and migration, syndecans have a very specific and important, yet not completely understood, synergic function with integrins; they have a unique role in focal adhesions, which are points of strong attachment formed by membrane receptors that attach to actin filaments (stress fibres), such as integrins and syndecans, interacting with ECM molecules (212,276,279,280). The number of focal adhesions,

their size, and their stability, influences cell anchorage and migration. First, it was believed that only the combinatorial interactions of syndecan-4 and integrin β1 could form focal adhesion. Currently, it is known that integrin αvβ3 and αvβ5, and integrins α2β1 and α6β4 can cooperate with syndecan-1 to adhere to vitronectin and laminin, respectively (273,274,281,282). However, since syndecan-4 is obliquely expressed in all cell tissue, its involvement with integrin β1 in focal adhesion is the most understood, and their interaction has been shown to be the most important combination for ECM-mediated cell survival (283).

The combinatorial interactions of syndecan-4 and β1 integrins involve a series of downstream signalling events, which are also not fully understood. It seems that the syndecan-4 V region recruits phosphatidylinositol 4,5-bisphosphate leading to protein kinase Cα (PKCα) activation and integrin β1 engagement, which promotes phosphorylation of RhoA and Rho kinases, stress fibre recruitment and focal adhesion assembly, enabling migration and adhesion to FN, Coll and laminin (246,284,285).

The synergy between integrin and syndecan-4 and integrin β1 helps such proteins regulate each other, for example syndecan-4 influences β1 integrin endocytosis and recycling, thereby assuring the balance between migration and attachment (246). Integrin and syndecan-4 interaction spans well beyond physical cell attachment since these interactions trigger intracellular survival signals. Since integrins and syndecans lack enzymatic activity, they activate these pathways by recruiting non-receptor kinases, such as PKC, Src, FAK and PI3K/AKT. In fact, syndecan-4 signalling through PKCα has been shown to regulate AKT activation by determining the localization of the mTOR complex 2 (mTORC2), which is responsible for the phosphorylation of AKT at S473 residue, and PDK1 (3 – phosphoinositide-dependent protein kinase 1), the kinase responsible for the T308 phosphorylation of this protein (286–288).

FAK / PI 3-Kinase / AKT Signalling Pathway

As previously mentioned, integrins can activate several different signalling pathways, which control cell survival, growth, migration and differentiation, such as the PI3K/AKT cascade, which can be activated as a result of integrin clustering via phosphorylation of focal adhesion kinase (FAK).

FAK is a cytoplasmic tyrosine kinase formed by an amino-terminal FERM domain, a central kinase region, proline-rich domains and a C-terminal focal adhesion-targeting

(FAT) domain (289). FAK expression is associated with p53 and NF-κB (290,291). FAK overexpression or upregulation is often linked to tumour progression and survival, since this kinase can be activated by integrins upon extracellular stimuli, and trigger survival signals through PI3K/AKT cascade, for example (292).

Although FAK can be activated by different stimuli, the best characterized involves integrin clustering upon binding to the ECM. This causes FAK dimerization and FAK auto-phosphorylation at Y397, which leads to Src protein kinases recruitment, binding and phosphorylation of FAK at Y576 and Y577, generating an active FAK–Src complex. The FAK-Src complex activates PI3K/AKT signalling through phosphatidylinositol-3,4,5-diphosphate [PtdIns(3,4,5)P2] (PIP2) (289,292–294). In head and neck cancer, the blockade of integrin-FAK signalling by integrin β1 antibodies sensitized cells to radiotherapy and delayed tumour growth *in vivo* (295). Moreover, it has been described that integrin activation in ovarian cancer induces resistance to paclitaxel and prevents cell-death in an integrin – FAK – AKT-dependent manner (296,297). Furthermore, FAK inhibitors have been shown to enhance cancer cell sensitivity to cytotoxic drugs (297,298).

FAK activation can be regulated by an intramolecular occlusion, by which the FAK FERM domain binds to the kinase domain, blocking accessibility to Y397 and auto-phosphorylation. FAK FERM conformational changes can be triggered by interactions with phosphoinositide lipids (PIPs), cell binding to ECM (integrins, syndecans), FERM binding to receptor tyrosine kinases (RTK), pH alterations and increased cell-ECM tension (289,299–302). The latter has been observed in breast cancer mouse models in which FAK Y397 phosphorylation and tumour progression increased upon Coll fibre crosslinking (301,302).

As mentioned above, phosphatidylinositol 3-kinase (PI3K) and its downstream effector AKT are frequently inappropriately activated and associated with malignancy in several different tumours, including melanoma (303–306). PI3K are heterodimers formed by a p85 regulatory subunit, which inhibits the p110 catalytic subunit. PI3K activation occurs when this inhibition is relieved by a conformational change, induced by the engagement of phosphotyrosines on p85 Src-homology 2 (SH2) domain (158,158,304,305). This also translocates PI3K to the plasma membrane, where its substrate PIP2 resides.

FAK phosphorylation creates a motif at the FAT domain, which allows interaction with the SH2 domain of PI3K. This can be triggered by cell membrane receptors such as integrins and receptor tyrosine kinases (RTK), whose modulation is also dependent on integrins (31,158). Thus, integrins play a crucial role in the incorrect activation of PI3K. As mentioned above, another PI3K over-activation mechanism is the loss of the PTEN tumour suppressor gene, which is considered to be part of the malignant transformation of melanoma cells, reported in up to 30% of cases (16,31,33–35,304). PTEN is responsible for dephosphorylating PIP3, consequently terminating PI3K signalling. (304).

Accumulation of PIP3 generated by PI3K recruits AKT to the cell membrane and allows its phosphorylation by PDK1 (3 – phosphoinositide-dependent protein kinase 1) on T308 phosphorylation site, which results in partial activation of AKT (30,307). However, to be fully active, AKT must be phosphorylated into two critical residues: T308 and S473, since phosphorylation of S473 stabilizes T308 phosphorylation. The kinase responsible for S473 phosphorylation is, in most cases, the mTOR complex 2 (mTORC2) (289,304,308,309). Once activated, AKT phosphorylates several substrates, such as FOXO, mTORC1 and GSK3, which are involved in various cellular processes, including cell growth, proliferation, survival, and metabolism, all of which are crucial for the establishment and maintenance of the tumorigenic phenotype (30).

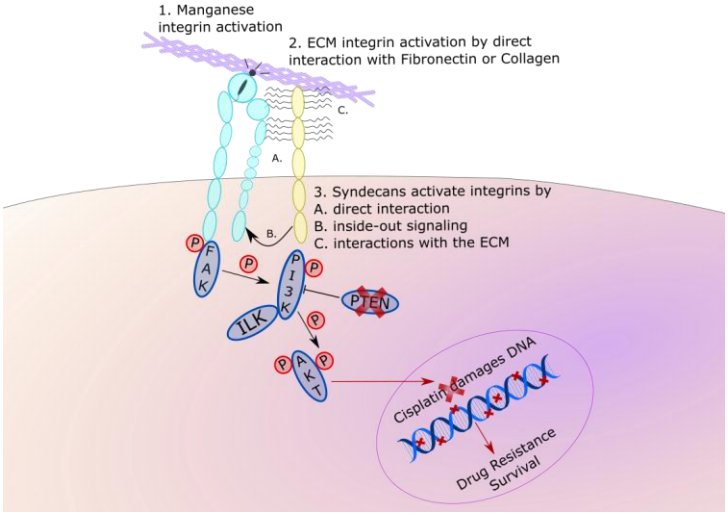

Figure 15. Integrin FAK/PI3K/AKT signalling pathway. FAK auto-phosphorylation upon integrin activation creates a motif at the focal adhesion-targeting domain of FAK, which allows interaction with the SH2 domain of PI3K. Accumulation of PIP3 generated by PI3K recruits AKT to the cell membrane and allows its phosphorylation by PDK1 (3 – phosphoinositide-dependent protein kinase 1) on T308 phosphorylation site, and phosphorylation of S473, in most cases, by the mTOR complex 2 (mTORC2). The integrin-linked kinase (ILK) acts as a co-activator of AKT, together with PI3K, upon integrin activation. FAK - PI3K – AKT signalling leads to cell survival and drug resistance.

2. Aim

Minimal residual disease (MRD) has first been identified in hematopoietic cancers. This phenomenon consists of a three-step process, of which environment-mediated drug resistance (EM-DR) is the most essential. Extracellular matrix components shelter cells from chemotherapeutic stress through a vast array of mechanisms that ensure cell survival and enable cells to go to the next step, acquired drug resistance. Drug-resistance development of melanocytes is a complex process, which involves interactions of environmental and genetic factors leading to loss of regulation of cell proliferation, apoptosis and cell-cell interactions.

Cell membrane proteins that adhere to the extracellular matrix and to other cells, and lead to survival in face of chemotherapeutic stress are pivotal in this assemblage. The most important of these proteins are integrins. Their importance in cell-cell and cell-matrix vital interactions is recognized and well understood. Furthermore, their impact on cell malignant transformation is established, although the mechanisms of such process are still under investigation. Moreover, integrins can directly activate focal adhesion kinase (FAK) that can phosphorylate PI3K and activate PI3K-AKT signalling.

However, a potential role of integrins to chemoresistance of highly metastatic malignant melanoma has not yet been elucidated. Therefore, this project aims to provide an insight into the resistance phenomena of melanoma cells; investigate a potential link between beta-1 integrin and melanoma anti-apoptotic PI3K-AKT pathway, in response to cisplatin treatment; as well as elucidate the potential synergistic role of syndecans and integrins in underlying mechanisms of chemoresistance.

Materials

Chemicals and primary compounds

Chemical substances

Denomination	Manufacturer
(3-(4,5-dimetiytiazol-2-yl)-2,5-diphenyltetrazoliumbromate), MTT	AppliChem GmbH, Darmstadt, Germany
4′,6-diamidino-2-phenylindole, DAPI	Sigma-Aldrich Chemie GmbH, Steinheim, Germany
Acetone	Merck Chemicals GmbH, Schwalbach, Germany
AlamarBlue™	Sigma-Aldrich Chemie GmbH, Steinheim, Germany
Annexin V-FITC Apoptosis Detection Kit	Bender MedSystems GmbH, Vienna, Fromtria
Bacillol® AF	Paul Hartmann AG, Heidenheim, Germany
BEZ235 (Dactolisib)	Selleck Chemicals, Munich, Germany
Bovine Serum Albumin, BSA	Sigma-Aldrich Chemie GmbH, Steinheim, Germany
Carbon dioxide, CO_2	AIR LIQUIDE Deutschland GmbH, Düsseldorf, Germany
CASY®ton	Schärfe Systems GmbH, Reutlingen, Germany
Cell Extraction Buffer	Thermo Fisher Scientific Inc., Waltham, USA
CellTiter-Fluor™	Promega GmbH, Mannheim, Germany
cis- diamminedichloridoplatinum(II), cisplatin	Sigma-Aldrich Chemie GmbH, Steinheim, Germany

Clarity™ ECL Western Blotting Substrate	Bio-Rad Laboratories GmbH, Munich, Germany
Collagen I (rat tail)	Roche Diagnostics GmbH, Mannheim, Germany
Dimethyl sulfoxide, DMSO	Sigma-Aldrich Chemie GmbH, Steinheim, Germany
Dulbecco's Modified Eagle Medium, DMEM	PAN Biotech GmbH, Aidenbach, Germany
Dulbecco's Phosphate-Buffered Saline, DPBS, without calcium, without magnesium, sterile	PAN Biotech GmbH, Aidenbach, Germany
Ethanol 96% (v/v)	Merck Chemicals GmbH, Schwalbach, Germany
Foetal bovine serum, FBS, F7524	Sigma-Aldrich Chemie GmbH, Steinheim, Germany
FuGENE® HD transfection reagent	Promega GmbH, Mannheim, Germany
Gigasept® Instru AF	Schülke & Mayr GmbH, Norderstedt, Germany
Glycine	AppliChem GmbH, Darmstadt, Germany
Halt™ Protease Inhibitor Cocktail (100X)	Thermo Fisher Scientific, Waltham, USA
Hydrochloric acid 1M	Sigma-Aldrich Chemie GmbH, Steinheim, Germany
Isopropanol 100%	Merck Chemicals GmbH, Schwalbach, Germany
L-Glutamine Solution (200mM)	PAN Biotech GmbH, Aidenbach, Germany
Liquid nitrogen, LN_2	Linde AG, Düsseldorf, Germany
Manganese(II) chloride, $MnCl_2$	Merck Chemicals GmbH, Schwalbach, Germany
Melsept® SF	B. Braun AG, Melsungen, Germany
Methanol 99,9%	Merck Chemicals GmbH, Schwalbach, Germany

Milk powder	Carl Roth GmbH, Karlsruhe, Germany
Paraformaldehyde	Carl Roth GmbH, Karlsruhe, Germany
Penicillin / Streptomycin Solution (10.000 I.E./mL / 10 mg/mL)	PAN Biotech GmbH, Aidenbach, Germany
Phenylmethylsulfonyl fluoride, PMSF	Sigma-Aldrich Chemie GmbH, Steinheim, Germany
Pierce™ BCA Protein Assay Kit	Thermo Fisher Scientific Inc., Darmstadt, Germany
Polybrene® (hexadimethrine bromide)	Santa Cruz Biotechnology Inc., Heidelberg
Precision Plus Protein™ Unstained Standards	Bio-Rad Laboratories GmbH, Munich, Germany
Precision Protein™ StrepTactin-HRP Conjugate	Bio-Rad Laboratories GmbH, Munich, Germany
Proteome Profiler™ Human Soluble Receptor Array	R&D Systems Europe Ltd., Abingdon, UK
Puromycin	Carl Roth GmbH, Karlsruhe, Germany
Roti®-CELL PBS/EDTA Solution	Carl Roth GmbH, Karlsruhe, Germany
RPMI-1640® medium	PAN Biotech GmbH, Aidenbach, Germany
Sample Laemmli buffer, 2× concentrate	Sigma-Aldrich Chemie GmbH, Steinheim, Germany
Sodium azide, NaN_3	Carl Roth GmbH, Karlsruhe, Germany
Sodium carbonate, Na_2CO_3	AppliChem GmbH, Darmstadt, Germany
Sodium chloride, NaCl	Grüssing GmbH, Filsum, Germany
Sodium hydroxide Solution 1M, NaOH	Sigma-Aldrich Chemie GmbH, Steinheim, Germany
Sodium hydroxide, NaOH	Grüssing GmbH, Filsum, Germany
TRIS-Base	AppliChem GmbH, Darmstadt, Germany
Tri-sodium citrate dehydrate, $C_6H_5Na_3O_7 * 2 H_2O$	Merck KGaA, Darmstadt, Germany

Triton X-100	Carl Roth GmbH, Karlsruhe, Germany
Trypsin/EDTA 0.25% Solution	PAN Biotech GmbH, Aidenbach, Germany
Tween™ 20	AppliChem GmbH, Darmstadt, Germany
VitroGel 3D-RGD	The Well Bioscience, Newark, USA

Transfection plasmids

Transfection system	**Manufacturer**
Control shRNA Lentiviral Particles-A	Santa Cruz Biotechnology Inc., Heidelberg, Germany
Integrin β1 shRNA (h) Lentiviral Particle: sc - 35674 - V	Santa Cruz Biotechnology Inc., Heidelberg, Germany

Primary Antibodies

Antibody	**Epitope**	**Host and Isotype**	**Manufacturer**
β1 Integrin (P5D2)	human β1 Integrin from epidermal keratinocytes	Mouse, monoclonal, IgG_1	Santa Cruz Biotechnology Inc., Heidelberg, Germany
β3 Integrin (B-7)	Against amino acids 635-730 of the C-terminus of human β3 - Integrin	Mouse, monoclonal, IgG_1	Santa Cruz Biotechnology Inc., Heidelberg, Germany
β-actin (C4)	whole length of β-actin from avian gizzard actin	Mouse, monoclonal, IgG_1	Santa Cruz Biotechnology Inc., Heidelberg, Germany
AKT1 (C – 20)	Against the C-terminus of human AKT1	Goat, polyclonal, IgG	Santa Cruz Biotechnology Inc., Heidelberg, Germany
p-AKT1 (Thr 308)	Against amino acid sequence containing	Rabbit, polyclonal, IgG	Santa Cruz Biotechnology

	Thr 308 phosphorylated human Akt1		Inc., Heidelberg, Germany
ERK-1/2	ERK1 and ERK2	Rabbit, polyclonal, IgG	Cell Signalling Technology, Frankfurt am Main, Germany
p-ERK-1/2 (Thr202/Tyr204)	Double-phosphorylated Thr202 and Tyr204 or simple-phosphorylated Thr202 of ERK1 and ERK2	Rabbit, monoclonal IgG_1	Cell Signalling Technology, Frankfurt am Main, Germany
FAK (C – 20)	Against the C-terminus of human FAK	Rabbit, polyclonal, IgG	Santa Cruz Biotechnology Inc., Heidelberg, Germany
p-FAK (2D11)	Against the amino acid residues surrounding Tyr397 of human FAK	Mouse, monoclonal, IgG_1	Santa Cruz Biotechnology Inc., Heidelberg, Germany
GAPDH (GT239)	Against the central region of human GAPDH	Mouse, monoclonal, IgG_{2b}	Gene Tex Inc, Irvine, USA
p-MEK-1/2 (7E10)	Amino acids of the T-E-Y Sequence	Mouse, monoclonal, IgG_1	Santa Cruz Biotechnology Inc., Heidelberg, Germany
PI3K p85α (Z – 8)	Against amino acids 333-430 of human PI 3-kinase p85α	Rabbit, polyclonal, IgG	Santa Cruz Biotechnology Inc., Heidelberg, Germany
p-PI3K p85α (Tyr 508)	Against a short amino acid sequence containing Tyr-508 phosphorylated PI3-kinase p85α of human origin.	Goat, polyclonal, IgG	Santa Cruz Biotechnology Inc., Heidelberg, Germany

Secondary Antibodies

Antibody	**Epitope**	**Host and Isotype**	**Manufacturer**
Donkey F(ab´)2 Anti Goat IgG	Goat-IgG light chain	Donkey, polyclonal, F(ab´)2 fragment, Alexa Fluor488	Abcam plc, Cambridge, UK
Donkey Anti-Mouse IgG	Mouse-IgG	Donkey, polyclonal, Alexa Fluor488	Abcam plc, Cambridge, UK
Donkey Anti-Rabbit IgG	Rabbit-IgG	Donkey, polyclonal, Alexa Fluor405	Abcam plc, Cambridge, UK
Donkey Anti-Goat IgG	Goat-IgG	Donkey, polyclonal, FITC	Santa Cruz Biotechnology Inc., Heidelberg, Germany
Donkey Anti-Goat IgG	Goat-IgG	Donkey, polyclonal, HRP conjugated	Santa Cruz Biotechnology Inc., Heidelberg, Germany
Goat Anti-Rabbit IgG	Rabbit-IgG	Goat, polyclonal, HRP conjugated	Santa Cruz Biotechnology Inc., Heidelberg, Germany
mIgGκ BP	Mouse-IgGκ light chain	Binding protein, HRP conjugated	Santa Cruz Biotechnology Inc., Heidelberg, Germany

Reagents solutions

Antibody solutions

Antibody (dilution)	**Composition**	**Amount**
β1 Integrin (1:200)	sodium azide	10 mg
	BSA	500 mg
	β1 Integrin (P5D2)	50 µL
	TBS-T	10 mL

β3 Integrin (1:200)	sodium azide	10 mg
	BSA	500 mg
	β3 Integrin	50 µL
	TBS-T	10 mL
β-actin (C4) (1:200-1000)	sodium azide	10 mg
	BSA	500 mg
	β-actin (C4)	10-50 µL
	TBS-T	10 mL
AKT1 (C – 20) (1:100)	1% BSA solution	100 µL
	AKT1 (C – 20)	1 µL
p-AKT1 (Thr 308) (1:100)	1% BSA solution	100 µL
	p-AKT1 (Thr 308)	1 µL
ERK-1/2 (1:200)	sodium azide	10 mg
	BSA	500 mg
	ERK-1/2	50 µL
	TBS-T	10 mL
p-ERK-1/2 (Thr202/Tyr204) (1:200)	sodium azide	10 mg
	BSA	500 mg
	p-ERK-1/2 (Thr202/Tyr204)	50 µL
	TBS-T	10 mL
FAK (C – 20) (1:100)	1% BSA solution	100 µL
	FAK (C – 20)	1 µL
p-FAK (2D11) (1:100)	1% BSA solution	100 µL
	p-FAK (2D11)	1 µL
GAPDH (1:20000)	sodium azide	10 mg
	BSA	500 mg
	GAPDH (GT239)	0.5 µL
	TBS-T	10 mL

p-MEK-1/2 (1:200)	sodium azide	10 mg
	BSA	500 mg
	p-MEK-1/2 (7E10)	50 µL
	TBS-T	10 mL
PI3K p85α (Z – 8) (1:100)	1% BSA solution	100 µL
	PI3K p85α (Z – 8)	1 µL
p-PI3K p85α (Tyr 508) (1:100)	1% BSA solution	100 µL
	p-PI3K p85α (Tyr 508)	1 µL
TCF4 (1:200)	sodium azide	10 mg
	BSA	500 mg
	TCF4	50 µL
	TBS-T	10 mL
Donkey Anti Goat IgG Alexa Fluor488 (1:200)	1% BSA solution	200 µL
	Donkey F(ab´)2 Anti Goat IgG Alexa Fluor488	1 µL
Donkey Anti-Mouse IgG Alexa Fluor 488 (1:200)	1% BSA solution	200 µL
	Donkey Anti-Mouse IgG Alexa Fluor488	1 µL
Donkey Anti-Rabbit IgG Alexa Fluor 405 (1:200)	1% BSA solution	200 µL
	Donkey Anti-Rabbit IgG Alexa Fluor 405	1 µL
Donkey Anti-Goat IgG FITC (1:200)	1% BSA solution	200 µL
	Donkey Anti-Goat IgG FITC	1 µL
Donkey Anti-Goat IgG HRP conjugated (1:1000)	Milk powder	1 g
	Donkey Anti-Goat IgG	1 µL
	Streptactin from Precision Plus Protein™ WesternC™ Pack	0.5 µL
	TBS-T	20 mL

Goat Anti-Rabbit IgG HRP conjugated (1:1000)	Milk powder	1 g
	Goat Anti-Rabbit IgG	1 µL
	Streptactin from Precision Plus Protein™ WesternC™ Pack	0.5 µL
	TBS-T	20 mL
mIgGκ BP (1:1000)	Milk powder	1 g
	Anti-Mouse binding protein	1 µL
	Streptactin from Precision Plus Protein™ WesternC™ Pack	0.5 µL
	TBS-T	20 mL

Buffers and solutions

Denomination	**Composition**	**Amount**
Blocking –solution	Milk powder	5 g
	TBS - T	to final Vol. 100 mL
BSA – Solution 0.5%	BSA	250 mg
	Sodium azide	50 mg
	DPBS	50 mL
BSA – Solution 1%	BSA	500 mg
	Sodium azide	50 mg
	DPBS	50 mL
BSA – Solution 3%	BSA	1.5 g
	Sodium azide	50 mg
	DPBS	50 mL
Cisplatin stock solution (5 mM)	Cisplatin	15 mg
	DPBS	to final Vol. 10 mL
Cisplatin work solution (1 mM)	Cisplatin stock solution (5 mM)	0.200 mL
	DPBS	0.800 mL

Cisplatin work solution (3,1mM)	Cisplatin stock solution (5 mM)	0.600 mL
	DPBS	0.400 mL
Cryopreservation medium	DMSO	5 mL
	FBS	45 mL
Electrode buffer 10X	Glycine	72 g
	TRIS-Base	15 g
	SDS	5 g
	Purelab® water	to final Vol. 500 mL
Electrode buffer 1X	Electrode buffer 10X	100 mL
	Purelab® water	900 mL
Ethanol 10%	Ethanol 96%	10.4 mL
	DPBS	to final Vol. 100mL
Glycine solution (0,1 M)	Glycine	375 mg
	DPBS	to final Vol. 50 mL
Luminol - peroxide solution	Clarity Western peroxide reagent	4 mL
	Clarity Western luminol reagent	4 mL
Lysis buffer	PMSF stock solution (0.3 mol/L)	34 µL
	Halt™ Protease Inhibitor Cocktail (100X)	500 µL
	Cell Extraction Buffer	10 mL
Manganese(II) chloride stock solution (100 mM)	Manganese(II) chloride	0.629 mg
	Purelab® water	to final Vol. 50 mL
Manganese(II) chloride work solution (10 mM)	Manganese(II) chloride S. Sol	5.0 mL
	Purelab® water	to final Vol. 50 mL
MTT solution (5 mg/mL)	MTT salt	50 mg
	DPBS	to final Vol. 10 mL
NVP-BEZ235, Dactolisib stock solution (1 mM)	NVP-BEZ235	1 mg
	DMF	to final Vol. 2.13mL

NVP-BEZ235, Dactolisib work solution (5 µM)	NVP-BEZ235 stock solution (1 mM)	50 µL
	DPBS	9.950 mL
NVP-BEZ235, Dactolisib work solution (1 µM)	NVP-BEZ235 stock solution (1 mM)	10 µL
	DPBS	9.990 mL
Paraformaldehyde solution 2 %	Paraformaldehyde	1 g
	DPBS	to final Vol. 50 mL
PMSF stock solution (0.3 mol/L)	PMSF	250 mg
	DMSO	4.783 mL
Protein standard solution (0,2 mg/mL)	BSA	2 mg
	Purelab® water	to final Vol. 10 mL
Puromycin 5 mg/mL	Puromycin	50 mg
	DPBS	10 ml
Selection medium	RPMI 1640	500 mL
	FBS	50 mL
	Penicillin / Streptomycin Solution	10 mL
	Puromycin (2.75 µg/mL)	152.6 µL
RPMI complete medium	RPMI 1640	100 mL
	FBS	50 mL
	Penicillin / Streptomycin Solution	10 mL
TBS 10x	Sodium chloride	40 g
	TRIS-Base	60.06
	Purelab® water	to final Vol. 500 mL
	Adjust pH to 7.3 with 1 M Hydrochloric acid	
TBS 1X	TBS 10X	100 mL
	Purelab® water	900 mL
TBS - T	TBS 10X	100 mL
	Tween™ 20	2 mL
	Purelab® water	to final Vol. 1 L

Transduction medium	RPMI complete medium	2.5 ml
	Polybrene® (10mg / ml)	1 ul
Transfer buffer 10X	Glycine	72 g
	TRIS-Base	15 g
	Purelab® water	final Vol. 0.500 mL
Transfer buffer 1X	Transfer buffer 10X	100 mL
	Purelab® water	900 mL
Triton stock solution 0.1 %	Triton X-100	50 µL
	DPBS	50 mL
Triton work solution 0.001 %	Triton stock solution 0.1 %	500 µL
	DPBS	50 mL

Disposable materials

Denomination	**Manufacturer**
CASY®cups	Schärfe System GmbH, Reutlingen, Germany
Cell culture bottles, 250 mL, 75 cm², PS	Greiner Bio-One GmbH, Frickenhausen, Germany
Cell culture bottles, 50 mL, 25 cm², PS	Greiner Bio-One GmbH, Frickenhausen, Germany
Cell culture bottles, 550 mL, 175 cm², PS	Greiner Bio-One GmbH, Frickenhausen, Germany
Cell culture bottles, 650 mL, 175 cm², CELLCOAT Collagen Type I	Greiner Bio-One GmbH, Frickenhausen, Germany
Centrifuge tube, 15 mL, PP, sterile	Greiner Bio-One GmbH, Frickenhausen, Germany
Centrifuge tube, 50 mL, PP, sterile	Greiner Bio-One GmbH, Frickenhausen, Germany
Combitips advanced® 1.0 mL; 0.5 mL; 0.1 mL	Eppendorf AG, Hamburg, Germany

Cryovial tube PP, with screw cap, sterile	Greiner Bio-One GmbH, Frickenhausen, Germany
CytoOne® 24-Well-Platte, TC-treated	Starlab GmbH, Ahrensburg, Germany
CytoOne® 96-Well-Platte, TC-treated	Starlab GmbH, Ahrensburg, Germany
Disposable pipetting reservoirs	Argos Technologies, Inc., Illinois, USA
Disposable syringes Injekt® Solo (10 mL)	B. Braun Melsungen AG, Melsungen, Germany
Disposable syringes Injekt® Solo (20 mL)	B. Braun Melsungen AG, Melsungen, Germany
Filter paper 50/PKG, Mini T/B	Bio-Rad Laboratories GmbH, Munich, Germany
Gel- Pipette tips MµltiFlex Round	Sorenson BioScience Inc., Salt Lake City, UT, USA
Micro plate, 96-Well, PS, V-bottom, transparent	Greiner Bio-One GmbH, Frickenhausen, Germany
Micro tube (0.6 mL)	Corning B. V. Life Sciences, Amsterdam, Holland
Micro tube (1.5 mL)	Sarstedt AG & Co., Nümbrecht, Germany
Micro tube (2.0 mL)	Sarstedt AG & Co., Nümbrecht, Germany
Mini-PROTEAN® TGX™ stainfree	Bio-Rad Laboratories GmbH, Munich
Nunc™ F96 MicroWell™ Polystyrolplate, black	Thermo Fisher Scientific GmbH, Langenselbold, Germany
Nunc™ F96 MicroWell™ Polystyrolplate, white	Thermo Fisher Scientific GmbH, Langenselbold, Germany
Pasteur pipette, Glass	Brand GmbH & Co. KG, Wertheim, Germany
Pipette tips (101-1000 µL), blue	Starlab GmbH, Ahrensburg, Germany
Pipette tips (1-10 µL), transparent	Starlab GmbH, Ahrensburg, Germany
Pipette tips (1-200 µL), yellow	Starlab GmbH, Ahrensburg, Germany
Pipette tips (5 mL) Plastibrand®, transparent	Brand GmbH & Co. KG, Wertheim, Germany

Roti®-PVD, 0.45 µm	Carl Roth GmbH & Co. KG, Karlsruhe, Germany
Serological pipette (10 mL)	Sarstedt AG & Co., Nümbrecht, Germany
Serological pipette (25 mL)	Sarstedt AG & Co., Nümbrecht, Germany
TC-Platte 6 Well, Standard, F	Sarstedt AG & Co., Nümbrecht, Germany

Equipment

Equipment	**Manufacturer**
Accu-Jet®	BRAND GmbH & Co. KG, Wertheim, Germany
Accu-Jet® pro	BRAND GmbH & Co. KG, Wertheim, Germany
Analytical balance Kern 770	Kern & Sohn GmbH, Balingen-Frommern, Germany
Analytical balance Mettler Toledo Classic Plus AB135-S	Mettler-Toledo GmbH, Giessen, Germany
Analytical balance Sartorius basic BA210S	Sartorius AG, Göttingen, Germany
Analytical balance Sartorius R160P	Sartorius AG, Göttingen, Germany
Aspiration system BVC 21 NT	Vacuubrand GmbH & Co. KG, Wertheim, Germany
Cell counter CASY® 1 Model TT	Schärfe System GmbH, Reutlingen, Germany
Centrifuge Allegra™ 25R	Beckmann-Coulter GmbH, Krefeld, Germany
Centrifuge Avanti J-25	Beckmann-Coulter GmbH, Krefeld, Germany
Centrifuge Micro 200 R	Andreas Hettich GmbH & Co. KG, Tuttlingen, Germany
Centrifuge Mini Spin	Eppendorf AG, Hamburg, Germany
Centrifuge Universal 32 R	Andreas Hettich GmbH & Co. KG, Tuttlingen, Germany

Centrifuge Universal 320 R	Andreas Hettich GmbH & Co. KG, Tuttlingen, Germany
ChemiDoc™ XRS+ System	Bio-Rad Laboratories GmbH, Munich, Germany
CO_2-incubator ICO105med	Memmert GmbH + Co. KG, Schwabach, Germany
CO_2-Incubator MCO-170 AIC (UV)	Panasonic Healthcare Co., Kadoma, Japan
CO_2-Incubator NuAire™ DH AutoFlow	NuAire Inc., Plymouth, MN, USA
Drying cabinet 60°C	Heraeus Holding GmbH, Hanau, Germany
Freezing container, Nalgene® Mr. Frosty	Sigma-Aldrich Chemie GmbH, Steinheim, Germany
FLUOstar OPTIMA fluorescence scanner	BMG Labtech, Offenburg, Germany
sigmaGuava® easyCyte HT	Merck KGaA, Darmstadt, Germany
Laboratory shaker KS-15	Edmund Bühler GmbH, Hechingen, Germany
Laminar-Air-Flow - Heraeus HeRASafe HSP 12	Heraeus Holding GmbH, Hanau, Germany
Laminar-Air-Flow - Holten safe 2010	Heto-Holton A/S, Allerød, Denmark
Light microscope Axiovert 200	Carl Zeiss Microscopy GmbH, Jena, Germany
Light microscope Wilovert 30	Helmut Hund GmbH, Wetzlar, Germany
Light microscope Wilovert Standard HF/K	Helmut Hund GmbH, Wetzlar, Germany
Magnetic stirrer MR 3001	Heidolph Elektro GmbH & Co. KG, Kelheim, Germany
Magnetic stirrer RCT basics	IKA®-Werke GmbH & CO. KG, Staufen, Germany
Mini-PROTEAN® Tetra Cell and Blotting Module with PowerPac 300	Bio-Rad Laboratories GmbH, Munich, Germany
Multipette® M4	Eppendorf AG, Hamburg, Germany

Multiscan® EX	Thermo Scientific GmbH, Langenselbold, Germany
Multiwellreader FLUOstar™ OPTIMA	BMG Labtech GmbH, Offenburg, Germany
Multiwellreader POLARstar™ OPTIMA	BMG Labtech GmbH, Offenburg, Germany
PARAFILM® M	BRAND GmbH & Co. KG, Wertheim, Germany
pH-Meter S20 SevenEasy™ pH	Mettler-Toledo GmbH, Giessen, Germany
Pipette (10 µL) Ranin	BRAND GmbH & Co. KG, Wertheim, Germany
Pipette (10 µL) Research®	Eppendorf AG, Hamburg, Germany
Pipette (100 µL) Research®	Eppendorf AG, Hamburg, Germany
Pipette (100 µL) Transferpette® S	BRAND GmbH & Co. KG, Wertheim, Germany
Pipette (1000 µL) Research®	Eppendorf AG, Hamburg, Germany
Pipette (1-5 mL) Finnpipette®	Thermo Fisher Scientific GmbH, Langenselbold, Germany
Pipette (200 µL) Transferpette® S-12	BRAND GmbH & Co. KG, Wertheim, Germany
Pipette (200 µL) Transferpette®-12 electronic	BRAND GmbH & Co. KG, Wertheim, Germany
Purelab® Flex water treatment filter	ELGA LabWater, Celle, Germany
Purelab® Plus water treatment filter	ELGA LabWater, Celle, Germany
Repeating pipette HandyStep® electronic	BRAND GmbH & Co. KG, Wertheim, Germany
Repeating pipette HandyStep® S	BRAND GmbH & Co. KG, Wertheim, Germany
Shaking incubator Unimax® 1010	Heidolph Instruments GmbH, Schwabach, Germany

Spatula, various	Carl Roth GmbH, Karlsruhe, Germany
Steri-Cycle® CO_2 cell incubator	Thermo Electron GmbH, Dreieich, Germany
Thermomixer comfort (IsoTherm 1.5 mL)	Eppendorf AG, Hamburg, Germany
Tweezers, diverse	Carl Roth GmbH, Karlsruhe, Germany
Ultrasonic bath Sonorex® Super RK 103 H	BANDELIN electronic GmbH & Co. KG, Berlin, Germany
Vacuum- Chemistry pumping unit PC5	Vacuubrand GmbH & Co. KG, Germany
Volumetric flask BLAUBRAND®, Klasse A (10 mL, 50 mL, 100 mL, 250mL, 500mL)	Carl Roth GmbH, Karlsruhe, Germany
Vortex-Genie 2	Scientific industries, New York, USA

Software

Denomination/Version	**Developer**
Ascent Software™ v2.6	© Thermo Labsystems Oy 1996-2002
ChemSketch Ultra v14.01	© ACD/Labs 2012
Image Lab v6.0	© Bio-Rad Laboratories 2010
InCyte™	© Merck KGaA
Microsoft Office v14.0.7190.5000	© Microsoft Corporation 2010
Microsoft Visio v14.0.7188.5002	© Microsoft Corporation 2010
Optima v.2.20R2	© BMG Laptech
Prism 5 for Windows v5.00	© GraphPad Software Inc. 1992-2007
ZEN 2012 v.1.1.2.0	© Carl Zeiss
Zotero 5.0.44	© Roy Rosenzweig Center for History and New Media

Cell Culture

The MV3 cell line (kindly donated by Dr. Reiner Zeisig, EPO Berlin) was established from a xenotransplantation in nude mice of lymph-node metastases from a 76-year-old male patient that suffered from a primary cutaneous amelanotic malignant melanoma (310). These undifferentiated cells present aneuploid karyotype, cell polymorphism, large abnormal nucleoli and multinucleated cells (310,311). They are also known to display high affinity to Coll type I and IV and increased expression of integrin β1 and CD44, which have been linked to various steps of the metastatic cascades and tumour malignancy (257,312,313).

MV3 Syn-4 knockdown (MV3 Syn-4 kd) was established by Dr. Patrick Schmitz from Dr. Bendas' group using lipid-based shRNA-plasmid (Mission®*sh*RNA, Sigma-Aldrich) transfection (314). Cells stably expressing anti Syn-4 shRNA were selected under permanent puromycin treatment (314). Syn-4 expression was measured via western blot (315).

MV3 cell lines were kept in RPMI 1640 medium supplemented with penicillin (10 IU/mL), streptomycin (100 µg/mL) and 10% FBS. The cell medium of transfected cells was also supplemented with puromycin (2.75 µg/mL).

NW1539 and Mel_1956 cells are novel and recently established melanoma cell lines, which are currently under further characterization. They were kept in DMEM medium containing 10 mM HEPES buffer, L-arginine (84 mg/L), L-glutamine (584 mg/L), penicillin (10 IU/mL), streptomycin (100 µg/mL), and 10% FBS.

All cells were kept at humidified atmosphere, at 37°C, containing 5% CO_2. All media was stored at 2°C - 8°C and used at room temperature, media supplements (antibiotics, FBS, L-glutamine and HEPES buffer) were stored at -20°C until use.

Cells were grown to 80 – 90% confluence before sub-cultivation and media was changed every 2-3 days depending on consumption, which was evaluated by the colour of the pH marker. For sub-cultivation, old media was aspirated, and cells were washed once with DPBS at room temperature. Then cells were detached, using a commercial solution of 0,025 % EDTA, for 3-5 min, at 37 °C. Detached cells were collected with the appropriate full media into centrifugation tubes and centrifuged at 4°C, 310 g for 5 min, after which supernatant was aspirated and cell pellet suspended in 5mL fresh full

media. Cell suspension was then counted (see below) and seeded into the new desired cell culture container. Since cell culture is inherently subject to fluctuations and excessive cultivation and detachment results in the genetic diversification of the cell line, every sub-cultivation was counted as one passage, to create a record of the age of the cells used. When cells were deemed too old (over 20 – 25 passages) or presented abnormal growth or morphology, they were discarded, and a new cell vial was thawed (see below).

CASY® cell counter was used to determine cell concentration in our suspension. The equipment isolates cells by aspirating them through a capillary, which generates an electric field that can measure cell resistance and thus, cell concentration. 20 µL of cell suspension obtained after centrifugation was transferred to a CASY® cup containing 10 mL of CASY® ton (dilution 1: 500). Cell concentration in this new suspension was measured using the CASY® cell counter. Since each cell, depending on its size, specifically modifies the resistance, in addition to the absolute cell count, the device also presents a cell population size distribution. Particularly small particles represent cell metabolites, contaminants or dead cells, which are automatically removed from the cell count by the device. Based on the number of viable cells measured, it is possible to deduce cell concentration in cell suspensions and seed cells in the desired density.

Cell lines can be maintained for many years in liquid nitrogen through cryopreservation. This assures scientists fresh supplies of the studied cell lines to replace cells that have been in culture for too long and present numerous passages or abnormal growth or morphology. For this purpose, once detached, cells were resuspended in media and counted. As described above, they were centrifuged again, and cell pellet collected in cryopreservation medium for a final concentration of 1 million cells per mL. This solution was distributed into previously identified cryovials and stored overnight in a freezing container filled with 96% ethanol at 80ºC. In the following morning, the cell vials were transferred to liquid nitrogen for long term storage. The ethanol in the freezing container and dimethyl sulfoxide (DMSO) present in the freezing medium cause cells to freeze slowly and prevent the formation of water crystals that could rupture cell membranes and lead to cell death. When necessary, cryopreservation vials were thawed by taking cells from the nitrogen tank and quickly resuspending them in warm, full medium. Subsequently, cells were centrifuged to remove toxic DMSO and cell debris and seeded into the desired cell-culture containers.

Transduction

Transduction is the specific name given to viral transfections, in other words, the introduction of foreign DNA by means of viral particles into a host cell (316). The underlying principle is based on the ability of viruses to introduce and integrate their genetic material into the genome of target cells. This allows scientists to take advantage of the natural mechanism of survival of viruses to introduce genetic modifications in culture cell lines (316). These modifications can induce gene silencing as well as overexpression (316). In the present case, we aimed to silence the β1 integrin gene and thus protein expression.

For this purpose, modified lentiviruses were used. These viral particles have had the desired DNA sequence integrated into their genome, creating a viral vector (316). Since the viruses are no longer capable of replication, it is necessary to incubate the cells with enough virus particles to ensure that the desired gene sequence is effectively integrated into the host genome (316). Typically, the integrated gene sequence will contain multiple copies of the desired DNA segments, to allow a proportionally high level of target RNA; in our case a small hairpin RNA (shRNA) directed against the β1 integrin gene sequence to inhibit protein translation (316,317).

Small or short hairpin RNAs, known as shRNAs, are artificial constructs used for molecular biology because of their double strand stable structure (316,317). In the nucleus, the sequence introduced by the virus into the cell genome is transcribed by RNA polymerase III or II, depending on the promoter used in the vector, generating a double strand RNA molecule bound by a loop (hairpin) (see Figure 16) (316,317). This RNA molecule is processed by Drosha and results in a pre-shRNA, which is exported into the cytoplasm where it can be cleaved by Dicer into a double-stranded siRNA (316,317). An enzyme complex of argonaut proteins and the RNA-induced silencing complex (RISC) bind to the double-stranded siRNA and convert it into two single-stranded RNAs (316,317). The sense strand (passenger) is degraded, while the antisense strand (guide) recognizes the complementary target messenger RNA (mRNA) and can direct RISC to bind to the target (316,317). Depending on complementarity, RISC cleaves the mRNA through argonaut proteins with endonuclease activity, or represses mRNA translation into protein (316,317). In both these cases, this leads to reduced target protein expression. In our case, the produced guide siRNA is complementary to the mRNA that encodes β1 integrin protein, thus blocking β1 integrin translation. This

process is referred to as knock-down, as it results in greatly reduced production of functioning β1 integrins.

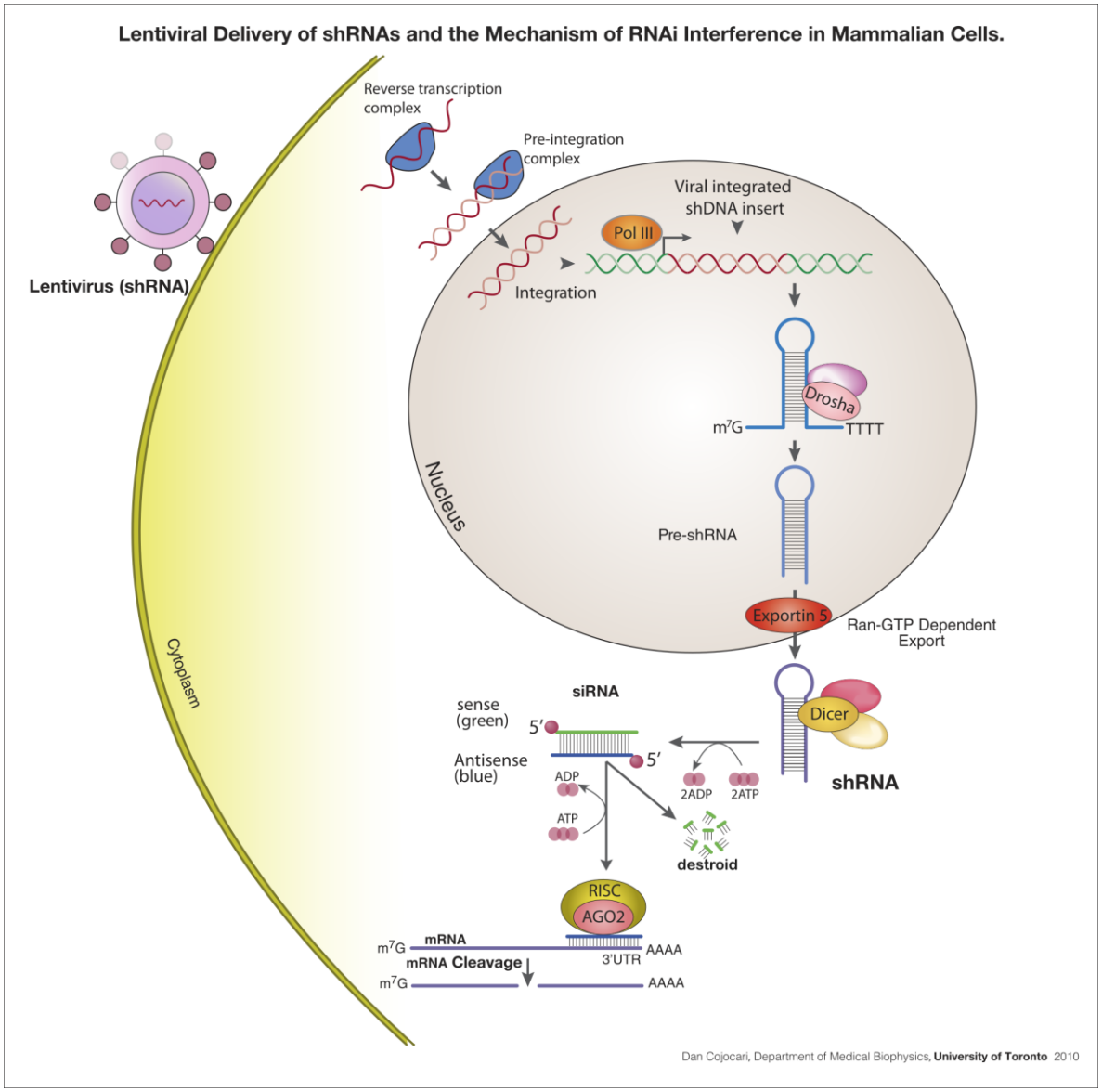

Figure 16. Cell transduction with lentivirus and shRNA processing. DNA sequence for shRNA is introduced into the cell by lentivirus particles. After inserted into cell DNA, the sequence is transcribed into a hairpin shRNA, which is processed by Drosha, exported to the cytoplasm and cleaved by Dicer into a siRNA. The siRNA binds to the RISC – argonaut complex and sense strand (green) is degraded, while the antisense strand (blue) recognizes, binds to and cleaves the complementary target mRNA. Modified from Cojocari (318).

Typically, most viral vectors also contain a sequence that allows the detection and/or selection of successfully transduced cells. The most common are the so-called reporter genes that code for the synthesis of a fluorescent protein, which can be visualized under a fluorescence microscope or selected through fluorescence cell sorting; or an enzyme that can modify the media (ex. *lac*-Z) (316). Antibiotics resistance genes can be

considered as a type of reporter gene, since they enable cells to produce enzymes that can deactivate toxic substances (antibiotics) present in cell media. This confers transduced cells resistance to a specific antibiotic and allows selection of transduced in detriment of non–transduced cells (316). Moreover, continuous treatment with the antibiotic creates selective pressure because it pressures cells to keep the foreign, introduced DNA and not lose their transduced properties, even if the transcription of the DNA introduced is uncomfortable to the cell (toxic, lacks important protein, high energy costs) (316). It is crucial that the toxicity of the antibiotics in a specific cell line to be determined prior to transduction, this can be done by using a kill curve method (see below) (316).

Besides the shRNA sequence, the viral vector used contains a sequence for puromycin resistance. Puromycin is a nucleoside antibiotic that inhibits protein biosynthesis in eukaryotic cells. The successfully transduced cells are capable of producing puromycin N-acetyltransferase (PAC), which deactivates the puromycin added to the cell medium (319). The cells can be selected accordingly in puromycin-containing medium. Thus, puromycin-added medium is referred to as the selection medium.

In order to exclude possible misleading effects generated by the cell transduction process and not by protein downregulation, wild type MV3 cells were also transduced with viral particles that are identical to the knockdown vectors, except that they encode a scramble sequence that results in a siRNA with no function (Control shRNA Lentiviral Particles A) (316). This is particularly important in lentiviral transfections because these viruses have the ability to integrate into sections of transcriptionally active chromatin. On the one hand, this is an advantage because it allows the genetic modification to be passed on to progeny cells, but, on the other hand, increases the risk of insertional mutagenesis, which can be reduced by using an integrase-deficient lentivirus (316).

Even though, my colleagues that performed the syn-4 knockdown had already tested the best concentration of puromycin for the MV3 cells, I decided to repeat this step and make a puromycin kill curve for these cells to ensure that the concentration used was still suitable. For this purpose, the cells were seeded at 60% confluence, in 24-well plates, and let adhere overnight. On the following day, a curve with increasing concentration of puromycin, including the concentration previously used, was added to cell medium. Cells were monitored for one week, in the end of which, we could confirm

that optimal dose (lowest dose of puromycin that killed all cells) was the previously established one: 2.75 µg/mL. We could also observe a minimum dose, in the presence of which none or a few cells were affected after one week, and a maximum puromycin dose, in the presence of which all cells died within three days. Thus, the selection medium for all transfected cells (MV3 Syn-4 kd, MV3 β1 kd and MV3 scramble) is the same (complete RPMI 1640 plus puromycin 2.75 µg/mL).

For transduction, a fresh cell vial of MV3 cells was thawed and cells were kept in normal cell culture conditions for one week. On the first transduction day, cells were seeded in a 96-well plate at a density of 1000 cells / well and let adhere overnight. On the second day, complete cell medium was substituted by 100 µL / well of transduction medium (Polybrene® 4µg / mL in complete cell medium). Polybrene serves as a polycationic reagent that saturates negative charges between the cell surface and the viral capsid. In the next step, the viral particles were thawed and carefully resuspended. In one well, 4 µL of integrin β1 shRNA (h) lentiviral particles were added to the medium, the same procedure was carried out for the control shRNA lentiviral particles in another well. In addition to these two wells, two additional wells were used as controls. In order to exclude a harmful influence of the polybrene on the cells, the first well of the controls was mixed only with polybrene-containing medium. The second well was incubated with cell medium, without supplements and switched together with the other samples 24 hours after the transduction to complete medium. The addition of puromycin on the fourth day enabled stable clones to be selected.

The medium with the infectious viruses of this approach was used again to transduce another approach in the same way (referred to as clone 2 in the following statements).

Over a period of four weeks, the cells were further cultured and repeatedly transferred to larger growth plates and cell culture bottles until a cell count of approximately 10^6 was reached and cryovials could be made. The polybrene control grew in full medium analogously to normal cells. As expected, the puromycin control died after a one-week incubation period. After transduction, MV3 β1 kd and MV3 scramble were submitted to the kill curve assay again and optimal and maximum doses were confirmed.

Plate Coating

As described, the extracellular matrix plays an essential role in the activation of integrins and the interaction between this protein and syndecans. To observe the influence of ECM components on CAM-DR, cells were grown in commercially pre-coated Coll I bottles, as well as plates manually coated with FN or Coll I, in our laboratory, using commercial stock solutions.

Coll and FN at a 10 µg / cm^2 density were used for all experiments. Based on the density, coating area (cm^2) and volume (µL), the concentration of work solution (µg / mL) required was calculated using equation 1:

$$\frac{well\ area\ (cm^2)\ x\ coating\ density\ (\mu g/cm^2)}{vol\ per\ well\ (\mu L)} = work\ solution\ concentration\ (\mu g/\mu L)$$

Equation 1. Calculation of the concentration of Coll or FN based on desired density.

Based on the number of wells to be coated and the volume required per well, the total volume of work solution can be calculated, in this step an excess amount of 10% was added to make up for pipetting mistakes.

$$number\ of\ wells\ x\ vol\ per\ well\ (mL) = total\ work\ solution\ vol\ (mL)$$

Equation 2. Calculation of total volume of work solution based on the number of wells to be coated.

Taking this into account, we can calculate the amount of Coll or FN (mg) to form the work solution:

$$work\ solution\ concentration\ (mg/mL)\ x\ total\ work\ solution\ vol\ (mL) = work\ solution\ coll/FN\ amount\ (mg)$$

Equation 3. Calculation of the mass of Coll or FN required for the work solution, based work solution total volume.

Finally, the volume of stock solution needed to be diluted with PBS to form the work solution can be calculated:

$$\frac{work\ solution\ coll/FN\ amount\ (mg)}{stock\ solution\ concentration\ (mg/mL)} = stock\ solution\ vol\ (mL)$$

Equation 4. Calculation of stock solution volume based on amount of coating protein required.

The amount of PBS is then calculated by subtracting the volume of stock solution from the total volume of work solution. Then, the specific volume was pipetted into each well and plates were incubated, for at least 1 hour for Coll, and 4 hours for FN, at 37ºC; wells were briefly rinsed once with DPBS before cell seeding. Coll plates can be dried under the laminar air flow after washed with DPBS and kept sterile at 4ºC for up to a month.

Establishment of 3D cell culture model

Throughout the years, mainly due to ethical problems, there has been a constant search for science models that accurately mimic the *in vivo* environment, but do not necessarily demand animal research (320,321). Solid tumours grow three-dimensionally *in vivo* and it has been known that cells behave and express different proteins in 3D models, which suggests this model mimics the *in vivo* environment more accurately if compared to 2D cultures (320,322). In line with this, 3D cell culture models were developed. There are two types of 3D models: spheroids and embedding. The spheroid technique is based on cell aggregation properties; when cells are cultured in suspension or in a non-adhesive environment. Cells are forced to form a 3D structure by adhering amongst themselves due to environmental conditions, such as agitation, hanging drop system or non-adherent bottom conditions, such as agarose or non-adherent U-bottom plates (320,321). These models present the advantage of enabling the observation of the cells and their capability to adhere to themselves and produce ECM, without the interference of artificial ECM added by the researcher (320,321). However, there are a couple of disadvantages, for example, the cells in the bottom of the sphere are still in contact with plastic or agarose and might grow two-dimensionally, also it is hard to control sphere size and stability, lose spheres might disaggregate in time (320,321). The embedding model consists of resuspending the cells in an extracellular protein (Coll) or ECM proteins mixture (Matrigel®, VitroGel™ 3D) before it can polymerize into a gel. However, it is important to ensure that the gel is not dense to the point that the cells are petrified into it and cannot receive nutrients. The advantage of this system is that the cells are round, completely in contact with ECM and still present cell-cell contact, exchanges and interactions (320,321).

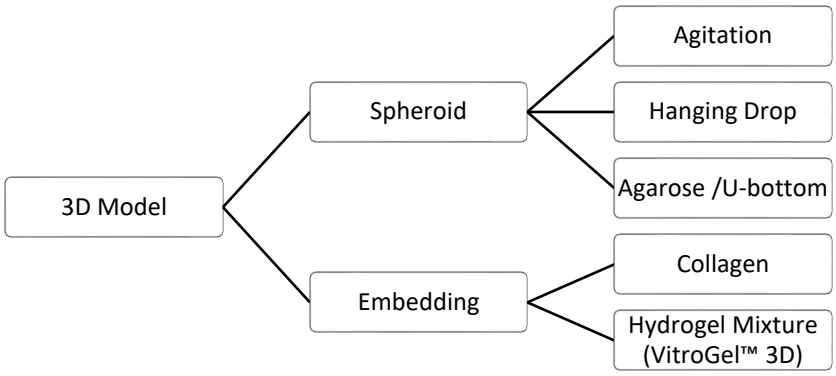

Figure 17. 3D Model techniques schema

After testing many different 3D cell culture model approaches, we opted for the embedding of the cells in a commercial hydrogel mixture called VitroGel™ 3D - RGD, since this technique showed the most success and least variability. Cells were detached from cell bottles and counted as described above, then cell pellet was resuspended in complete cell medium and mixed 1:1 with VitroGel™ 3D – RGD, diluted in DPBS (1:3), for a final concentration of 10^2 cells/µL or 2×10^2 cells/µL, according to instructions of the manufacturer for melanoma cells. VitroGel-cell solutions were distributed 50µL/well in black clear flat bottom 96-well plates in accordance to our established resazurin cytotoxicity assay protocol (see below). Plates were incubated for 15 min, at 37ºC, before addition of 40µL/well of complete cell medium. On the following day, a 10µL/well of cisplatin logarithmic concentration curve was applied to the cells and resazurin cytotoxicity assays were performed as described below.

Cytotoxicity assays

Cell cytotoxicity assays are based on the ability of mitochondria to metabolize substances upon ATP spending, usually generating a coloured or fluorescent product. There are many different assays based on this concept. One of which is the thiazolyl blue tetrazolium bromide (MTT), which measures the cytotoxic effect of cisplatin. This assay is based on the capacity of the mitochondria to convert tetrazolium salt (3-(4,5-dimetyltiazol-2-yl)-2,5-diphenyltetrazoliumbromate) into formazan crystals (316,323). This process is carried out by the succinate dehydrogenase enzyme and requires ATP; therefore, it can only be performed by viable cells. The resulting formazan crystals can be solubilized in dimetylsulfoxide (DMSO) creating a purple solution whose colour intensity can be measured by spectrophotometry and is proportional to the amount of living cells (316,323).

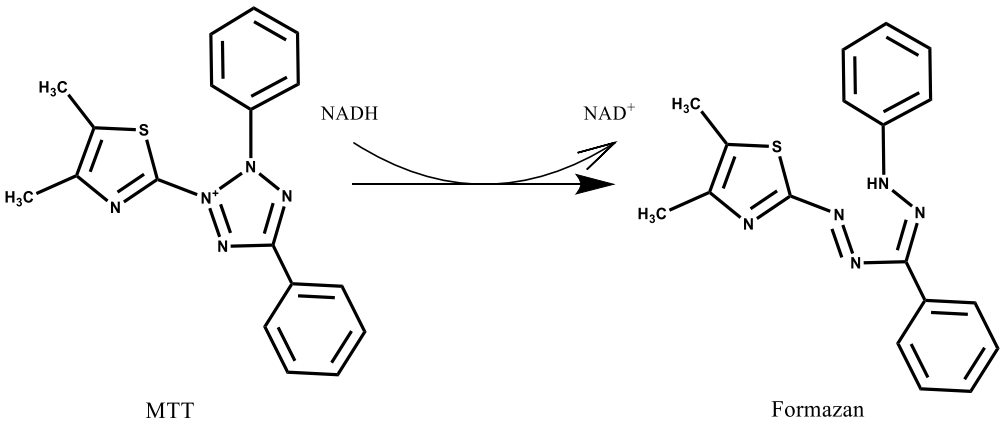

Figure 18. Conversion of MTT salt to formazan

Another example is the alamarBlue™ assay, which was performed using a commercial resazurin solution to measure the 3D cell culture assays. Resazurin is a blue, non-toxic, cell-permeable, non-fluorescent reagent, which can passively enter cells (316,323). In viable cells, it is then converted to resorufin, a highly fluorescent compound that can be detected by fluorescence plate reader (316,323).

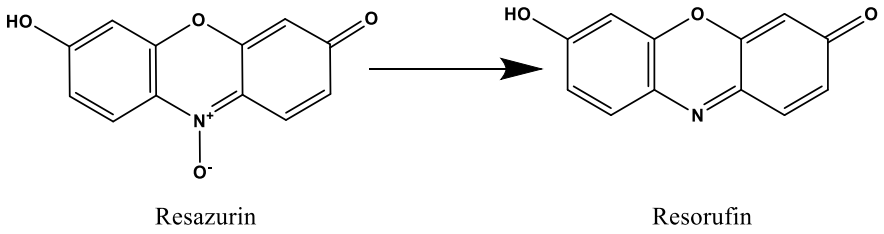

Figure 19. Conversion of resazurin to resorufin

For the cell cytotoxicity assays, cells were first seeded at two different cell densities in triplicates (B, C, D 5000 cells / well and E, F, G 10000 cells / well) onto the 60 inner wells of black clear bottom (resazurin) or transparent (MTT) flat bottom 96-well plates, with or without coating, as described above, and let to adhere overnight. The outer wells (A and H) were filled with 90µL DPBS per well, to avoid medium evaporation (see plate scheme). Cells were usually let to adhere overnight, and appropriate treatment was given on the following day.

For treatment with manganese (Mn^{2+}), cells were incubated for 5 minutes with 1 mM solution of manganese chloride ($MnCl_2$), for final concentration of 100µM Mn^{2+} per well. After incubation, cell medium was discarded, and new cell medium added to all cell plates, before cisplatin addition.

BEZ235 (NVP-BEZ235, Dactolisib) is an imidazole[4,5-c]quinolone derivative dual pan-PI3K/mTOR inhibitor developed by Novartis, which is currently in phase I/II clinical trials for use as co-adjuvant anti-tumour therapy (308,324,325). It binds, reversibly and competitively, to the ATP-binding cleft of PI3K and mTOR, working as potent and selective inhibitor of PI3K pathway. BEZ235 presents very low affinity to other down or upstream effectors, such as FAK, AKT and PDK1, but has been shown to interfere in 50% of AKT phosphorylation in a reversible manner (308). It interferes in cell proliferation, and it has been shown to lead to apoptosis, when associated to platinum derivatives and taxanes (326,327).

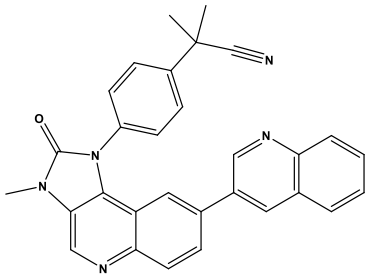

Figure 20. Structure of dual pan-PI3K/mTOR inhibitor BEZ235 (NVP-BEZ235, Dactolisib)

For this reason, cells were treated with 500 nM and 100 nM of BEZ235, for 30 minutes, before different concentrations of cisplatin were added.

Administration of 10 μg tinzaparin (500 μg/mL) was performed at two different time points, 0 h, which means tinzaparin was administered to cells immediately after cell seeding; and 6 h, which means cells were let to adhere for 6 hours prior to tinzaparin treatment. On the following day, cisplatin was added.

Heparan sulfate digestion with heparitinase I was performed 6 hours after cell seeding, using 10 μL of heparitinase I (0.1 U/mL). On the following day, cisplatin was added.

Treatment was followed by a logarithmic concentration curve of cisplatin for a final volume of 100ul per well. The cisplatin logarithmic concentration curve was obtained by diluting 5 mM cisplatin stock solution with PBS into a concentration of 1μmol (10^{3}) and 3.162μmol ($10^{-2.5}$) and making sequential 1:10 dilutions from these solutions.

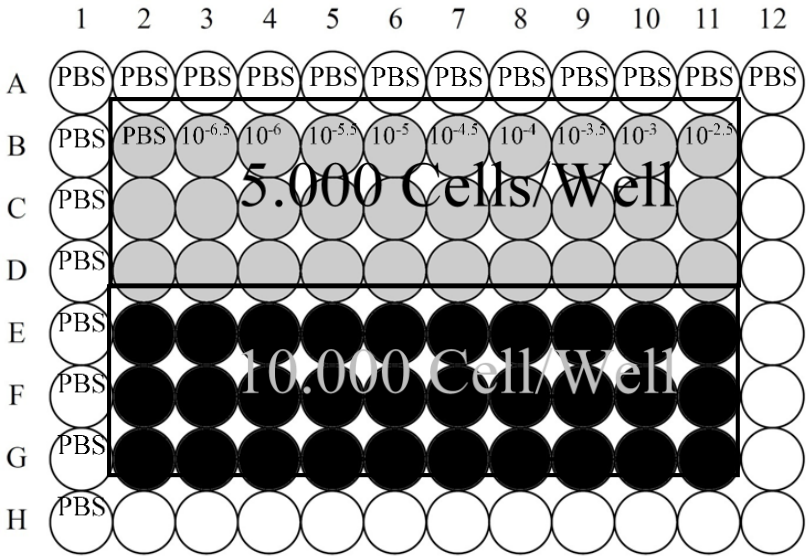

Figure 21. Exemplary distribution of a cell cytotoxicity assay. Cisplatin logarithmic dilution series starting with DPBS as 0 value and ending with 3.162µmol cisplatin (10-2.5). The outermost row of panels contains the DPBS evaporation protection.

Cells were then incubated, for 72 h, at 37ºC, with 5% CO_2. Subsequently, the assays were developed according to the cytotoxicity assay protocol. In the case of MTT, 20 µL of MTT reagent solution (5 mg/mL in PBS) was added to each well and incubated for 1 h, at 37ºC, until formazan crystals were formed. The supernatant was removed, and the formazan crystals were solubilized with 100 µL of dimetylsulfoxide. Plates were analysed under spectrophotometer at 570 nm, with background subtraction at 690 nm, using Thermomultiscan EX plate reader. For the alamarBlue™ assay, resazurin stock solution (10 mg/mL in DPBS) was diluted to a work solution of 0.15 mg/mL in DPBS. After that, 20 µL of this solution was added to each well and incubated for 2 hours., at 37ºC. After that, plates were analysed using FLUOstar OPTIMA fluorescence scanner, with a 560 nm excitation / 590 nm emission filter.

In order to determine cisplatin IC_{50} and the pIC_{50} values on the different cell lines, under different conditions, results were analysed by generating sigmoidal concentration-response curves using the software Prism™ GraphPad. IC_{50} is defined as molar concentration of drug, which produces 50% of the maximum possible response, while pIC_{50} is its negative logarithm ($pIC_{50} = -\log IC_{50}$). pIC_{50} values were later used for statistical analyses using Student's t-test or ANOVA, since the logarithm of IC_{50} values can be regarded as normally distributed (328).

The difference between cell lines or treatments can also be evaluated using the resistance factor (RF), which is the quotient between the IC_{50} of treated cells and the IC_{50} of untreated (only cisplatin) as depicted in formula 5:

$$RF = \frac{IC_{50}\ (treated\ cells)}{IC_{50}\ (untreated\ cells)}$$

Equation 5. Calculation of the resistance factor

RF values greater than one indicate resistance, whereas values lower than one show sensitization of cells. The statistical evaluation of RF mean and SD was carried out through one-way ANOVA and Dunnett's test. The significance level is represented by asterisks as follows: * $p < 0.05$; ** $p < 0.01$; *** $p < 0.001$.

Flow cytometry

Fluorescence flow cytometry was used to measure changes in the mount and activation of surface and internal cell proteins, thus evaluated the cell signalling events, which take place in the cell. Proteins can be labelled with specific antibodies that are subsequently marked with secondary fluorescence labelled antibodies (329). Since the methodology also permits the observation of single cell size and surface condition, it enables the examination of, for example, the vitality of the cell population, or if the treatment used gives rise to two separate cell populations (329).

First, cells are separated by a capillary that allows single cell measurements (329). As the laser focus passes through, the apparatus detects both the forward scattered light (FSC) and the side scattered light (SSC), which is deflected at an angle of 90° to the sample (329). The FSC correlates with the size of the cell, while the SSC describes granularity (329). Both parameters are usually displayed against each other in a dot-plot diagram (Figure 23).

The fluorescence generated by the previously labelled cell structures is also measured at an angle of 90°, but separately (329). The emitted light is first deflected using dichroic mirrors, then, it goes through a specific filter, corresponding to the different wavelengths, to adjust the detection of the emission spectrum of the fluorophore used (329). Finally, the signals are amplified by means of a photomultiplier and converted into electrical signals that can be measured (329).

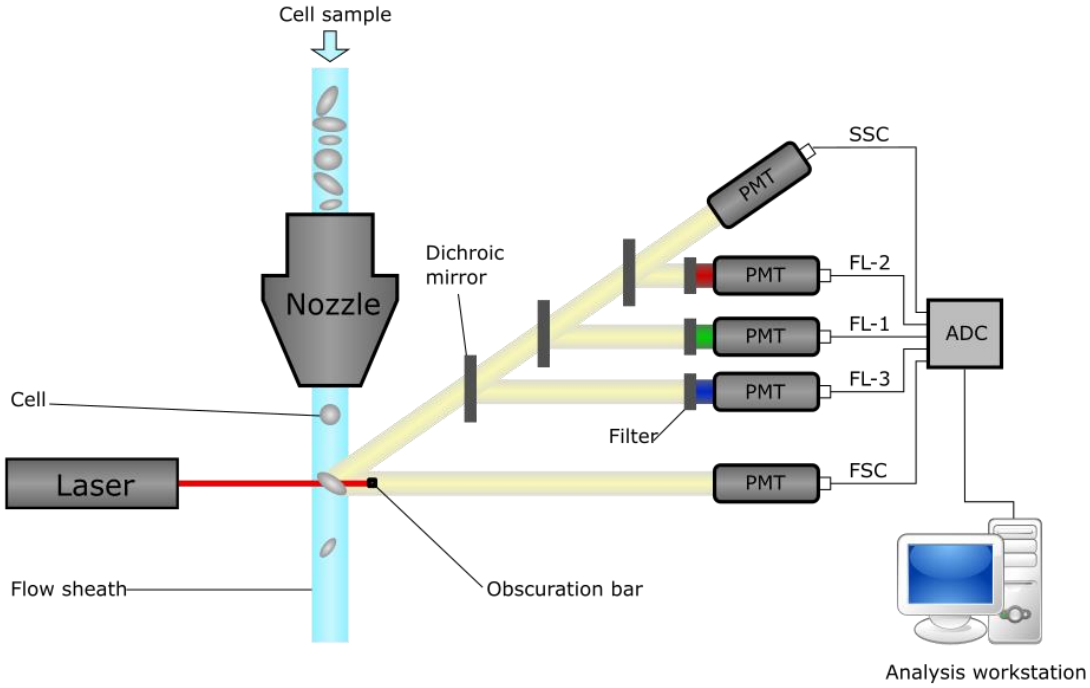

Figure 22. Fluorescence flow cytometer (330). Cells enter the equipment and are separated by a capillary which allows single cell measurements. As the laser focus passes through, the apparatus detects forward scattered light (FSC) and side scattered light (SSC). The fluorescence generated by the previously labelled cell structures is first deflected using dichroic mirrors, then, goes through a specific filter, corresponding to the different wavelengths; to adjust the detection of the emission spectrum of the fluorophore used. Finally, the signals are amplified by means of a photomultiplier and converted into electrical signals that can be measured.

The fluorescence detected is displayed in a histogram where the shift between the maximum fluorescence of the sample can be compared to the corresponding control (Figure 23B).

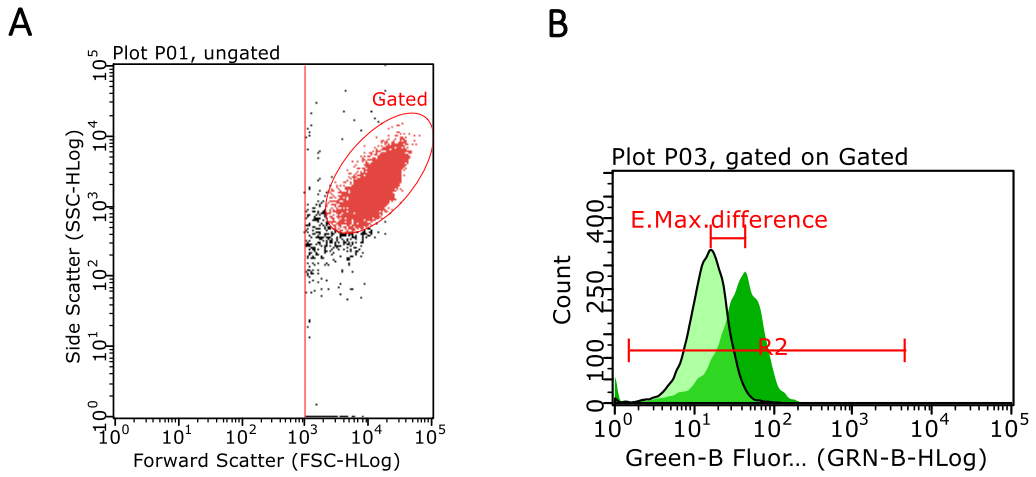

Figure 23. A. FSC x SSC dot-plot diagram. The forward scattered light (FSC), that correlates with the size of the cell, is displayed against the side scattered light (SSC), which describes cell granularity. **B. Fluorescence maxima comparison histogram.** Cell structures are labelled with fluorophores, which can then be excited by specific wave lengths. The emission maxima or fluorescence maxima are displayed as a histogram showing the cell count against log fluorescence intensity. The measured value consists of the difference between the emission maxima of cells only labelled with secondary antibody (light green) and cells labelled with primary and secondary antibodies (dark green).

To ensure a trustworthy measurement, it is important to set adequate experimental parameters, such as threshold value, measuring time, laser intensity and the number of cells per measurement (329). The threshold value is of great importance because it determines from which size in the FSC a cell is included in the measurement, it is appropriate to choose a value that excludes background noise, as effectively as possible, without interfering with the readout, which means without excluding cells that might be significant (329).

One advantage of this technique is that it allows the labelling of multiple cell structures within the same well. This reduces the number of samples needed to perform the assay, but also permits almost direct comparison of a protein and its phosphorylated form within the exact same well, at the same time, which is not possible with the western blot technique, for example. However, when multiple fluorophores are used within the same well, as is in our case, it is essential to ensure that their emission spectra are far enough from each other in the light spectrum. A fluorophore overlap would lead to one fluorophore influencing the measurement results of other fluorophores, thus making it impossible to evaluate the data (329). In such cases, compensation may be beneficial.

When using two or more fluorophores, in some cases, the emitted light of one fluorophore radiates into the channel (filter) of another, and creates an overlap (see below) (329). Compensating means identifying the overlap region and excluding its influence from the measurement (329). The closer the emission spectra of the fluorophores used to each other, the more likely is an overlap to occur. Most modern equipment have built-in software that can calculate, define and apply the compensation required for each fluorophore, however, it is most important to choose fluorophore that can be well paired together to minimize the compensating effect.

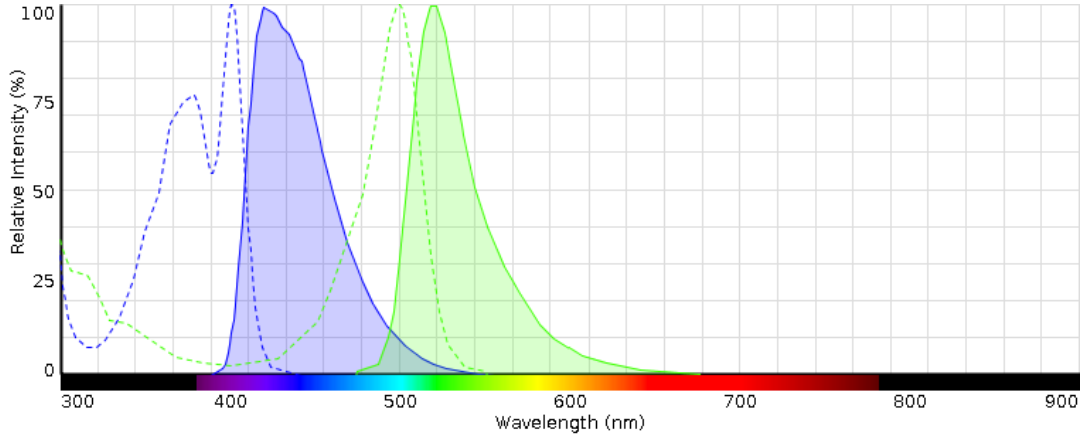

Figure 24. Fluorescence histogram with compensating area. The absorption spectrum (dotted line), as well as the emission spectrum (coloured curve with continuous line) for two fluorophores can be observed here, AlexaFluor 405 (blue) and AlexaFluor 488 (green). The overlap of the emission spectra can be observed between 473 and 540nm. Image generated using Fluorescence SpectraViewer from ThermoFisher (331).

Finally, the measurements obtained can be further broken down, after the completion of the measurements, using regions and gates (329). By means of a gate, a cell population can be limited to a specific area on the dot-blot. Subsequently, it is possible to consider parameters, such as fluorescence, only for this range (329). Regions, on the other hand, can be used to isolate and assess certain areas of the fluorescence histogram. So, it is possible to define a respective region for the two emission maxima for a fluorophore and thus to display the number of cells in this region.

Two different protocols were used to prepare cells for the fluorescence flow cytometry, depending on the location of the target structure in the cell. In both cases, cells were washed with PBS and then detached from cell culture bottles, counted and centrifuged as described above. For cell membrane proteins, cell pellets were then resuspended, in 2 mL wash buffer (BSA solution 0.5%), and centrifuged at 310 g, for 5 min, at 4°C.

After the first washing step, cells were resuspended in 3% BSA blocking solution for a final concentration of 5×10^5 cells per 90 µL, distributed in a 96-well V bottom plate (90 µL per well), and incubated for 15 minutes to block unspecific antibody binding. Subsequently, cells were centrifuged at 1370g, for 5 minutes, at 4 °C, and supernatant aspirated. Then, 25 µL of specific primary antibody solution (1:100 in 1% BSA) was added to each well. Cells were resuspended and incubated with the primary antibody for 45 minutes, at room temperature, protected from light. This was followed by a wash and centrifugation step, and resuspension in 10 µL / well of secondary antibodies solution (1:200 in 1% BSA). Cells were incubated for 35 minutes, at room temperature, protected from light. This was followed by centrifugation, two washes and cells uptake in 100 µL / well wash buffer, for assessment on the Guava® easyCyte Flow Cytometer.

The protocol used for labelling intracellular structures was modified from Barbosa et al. (332). After detachment, counting and centrifugation, the supernatant was aspirated, and pellet resuspended in 5 mL 2% PFA-solution in PBS and fixated for 30 min., at room temperature (RT). After fixation, samples were centrifuged, the supernatant aspirated, and pellet was washed with 5 mL 0.1 M glycine solution in PBS. Remaining pellet was then resuspended and permeabilized with 5 mL 0.001% Triton solution in PBS, for 30 minutes, at RT. After permeabilization, cells were centrifuged, the supernatant aspirated, and pellet was resuspended with 5 mL 0.1 M glycine solution for a final concentration of 5×10^5 cells per 90 µL, distributed in a 96-well V bottom plate (90µL / well). Plate was centrifuged at 1370 g, for 5 minutes, at 4° C, glycine was aspirated and 25 µL of specific primary antibodies solution (1:100 in 1% BSA) was added to each well and incubated for 2 hours, at RT, protected from light. After that, the cells were washed once with 1% BSA solution, and incubated for 2 hours, at RT, protected from light, with 10 µL / well of the appropriate secondary antibody solution (1:200 in 1% BSA). This was followed by a wash and centrifugation step, and cells uptake in 100 µL / well wash buffer, before assessment on the Guava® easyCyte Flow Cytometer.

Results were plotted into a graph, where standard deviation (SD) from at least 3 measurements is given. Statistical analysis was performed using one-way ANOVA and Dunnett's test (* $p < 0.05$; ** $p < 0.01$; *** $p < 0.001$)

Western Blot

To validate the effectiveness of the β1 integrin knock-down, the transduced cells were evaluated via western blot. For this purpose, cell protein lysate was obtained using the following protocol. First, cells were detached from cell culture bottles with EDTA and counted, as described above. After centrifugation, cell pellet was washed once in cold DPBS and resuspended in cell lysis buffer, freshly prepared as described in buffers and solutions. The volume of cell lysis buffer used varied between 100-1000 µL and was determined based on the number of cells in the sample, in order to ensure maximal cell-lysis and high final protein concentration lysates. Cell lysates were then incubated for 30 minutes, at 0° C, on a shaker. After incubation, tubes were centrifuged for 10 minutes, at 20,635 g, 4° C, in order to exclude non-solvated cell constituents, which accumulate as pellets. Supernatant was aliquoted in reaction tubes 100 µL / tube and stored at -80° C for up to six months.

The total protein amount of the lysates obtained was determined using Pierce™ BCA Protein Assay Kit. This assay is based on a biuret reaction in which molecules with two peptide bonds to complex divalent copper ions in alkaline solution. Following this principle, the copper (II) ions, contained in a copper sulfate solution, during the BCA assay, are reduced to copper (I) ions by the reductive groups of the amino acids of the total protein. It could be shown that cysteine, cystine, tryptophan, tyrosine and the peptide bond itself act as reducing agents. Bicinchoninic acid (BCA) then complexes the copper (I) ions formed into a violet-blue colour (Figure 25), which remains stable in an alkaline environment, thus enabling the assessment of protein amounts through spectrophotometry.

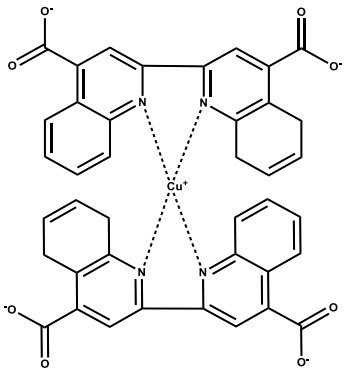

Figure 25. BCA complex with copper (I) ions

To work within the limits of Lambert-Beer's law (< 10 mM), dilutions of 1:20, 1:50 and 1:100, from the lysate in Purelab® water, were prepared from a 1:10 starting dilution. These three dilutions were distributed, in duplicates 20 µL / well, onto a transparent 96-well flat–bottom plate. In addition, a series of previously prepared references that are used to generate a calibration curve of 0 - 400 µg BSA / mL of Purelab® water; and three quality controls (QC) (150 µg / mL, 250 µg / mL and 350 µg / mL) were also added in duplicates onto the plate. The correlation coefficient of the calibration line should be 0.99 and the QCs should not deviate more than ± 5%.

The copper sulfate solution and the BCA reagent were mixed 1:50, and 200 µL / well of this mixture was added to the samples. The incubation was carried out at 60° C, for one hour. The plates were then cooled to RT and measured at 570 nm.

After the protein quantification of the lysates, samples were submitted to protein gel electrophoresis, in order to separate proteins according to their sizes, in a polymerized SDS gel, using electric current. SDS polyacrylamide gel electrophoresis is based on the principle of disk electrophoresis. Disk is the short form for discontinuous and refers to the separation of the gel in a wide-pore stacking gel before entering the narrow-pore running gel, and to the fact that the buffer in the gel and the electrophoresis chamber are different. This allows samples to be collected and concentrated in the stacking gel so they can be specifically separated in the narrow-pore gel. The stacking gel has a lower concentration of acrylamide, lower pH, and a different ionic content than the running gel. This allows the proteins in a loaded sample to be concentrated into one tight band during the first few minutes of electrophoresis, before entering the resolving portion of a gel. Important for this is the use of a Tris-HCl / Tris - glycine system. Typically, the system is set up with a stacking gel of pH 6.8 (Tris-HCl), a running gel of pH 8.8 (Tris-HCl) and an electrophoresis buffer at pH 8.3 (Tris - glycine). The glycine present in the buffer is negatively-charged at pH 8.3, but upon application of an electrical voltage, it is forced to enter the stacking gel, where the pH is 6.8, close to the isoelectric point of glycine. So, glycine switches predominantly to its zwitterionic state. This loss of charge causes them to move very slowly in the electric field. In contrast, the chloride ions contained in the buffer have high electrophoretic mobility and create an ion-migrating front ahead of the glycine. This creates the highly mobile Cl^- front, followed by the slower, mostly neutral glycine front. Since the proteins present an intermediate electrophoretic mobility, they form a stack between the two

mobility zones. At the transition between collecting gel and separating gel, the difference in density leads proteins to concentrate, since the gelatinous nature of the gel counteracts the increased resistance of the sample.

Once in the separating gel, the mobility of the proteins is strongly dependent on their molecular size, since the sodium dodecyl sulfate (SDS) denatures and binds to proteins to make them uniformly negatively charged. The intrinsic charge of the proteins thereby no longer plays a role in the separation. Depending on the size of the targeted protein, it is additionally possible to make the pore size of the separating gel variable by changing gel density during the polymerization of the acrylamide (usually 7.5 - 12%).

In order to properly separate the proteins of the sample, it is common to use a Laemmli buffer, which reduces the proteins of the sample. This contains β-mercaptoethanol, which reductively cleaves the sulphur bridges between the cysteines. In some cases, such as ours, it may be necessary to dispense with these reducing properties in order to preserve the quaternary structure of the protein and thereby the antibody binding site intact. The anti-integrin β1 antibody also acts as an inhibitor of protein activation, for this reason, according to the instruction of the antibody manufacturer, non-reducing Laemmli buffer was used.

Non-reducing Laemmli buffer was added to the sample in accordance with protein concentration in each sample, samples were diluted 1:1 in Laemmli buffer, and total volume was pipetted in each gel pocket, as well as 5 µl of Precision Plus Protein™ Unstained Standards. Proteins were then separated via electrophorese at 200 V for 40 - 60 minutes, depending on gel density. The commercial precast gels were cracked open so that western blot could be performed.

First, proteins were transferred from the SDS acrylamide gel to a polyvinylidene fluoride (PVDF) membrane using an electric current. For this purpose, PVDF membranes were activated with methanol for 20 seconds, to reduce their hydrophobia, then blot sandwiches were assembled, from outside to inside, consisting of two sponges, two filter papers, the membrane and the gel. In the presence of the electric current, the negatively charged proteins from the gel are pulled to the positively charged anode site, where the membrane has been placed. Blot was performed at 100 V for 1 hour, after that, membranes were blocked, with 50 ml of BSA blocking solution for 1 hour, to avoid antibody unspecific binding. Subsequently, membranes were washed three times

with 20 ml TBS-T for 10 minutes, before addition of 10 mL of primary antibody solution. After incubation for 1 hour, membranes were washed three times with 20 ml TBS-T for 10 minutes, and 10 mL of secondary antibody solution was added for 1 hour. The secondary antibody binds to the primary antibody and allows sample detection by chemiluminescence since it is coupled to horseradish peroxidase (HRP) that can catalyse the chemiluminescence reaction between luminol and peroxide, generating a luminescence signal that can be quantified. Cells were washed again, before the 5-minute incubation with luminol-peroxide reagent. Immediately after incubation, membranes were analysed on the ChemiDoc ™ XRS + system.

Proteome Profiler™ Human Soluble Receptor Array

The Proteome Profiler™ Human Soluble Receptor Array was used to screen for the membrane proteins of the cell lines and analyse the impact of cisplatin treatment on the expression of such proteins. It can identify 119 soluble receptors, to which respective antibodies are fixated in duplicates on the nitrocellulose membranes present in the kit. It essentially works as a dot blot. The preparation and storage of the lysates used for the implementation of Proteome Profiler™ Human Soluble Receptor Array was carried out as per manufacturer's instructions, and protein concentration was determined using BCA protein assay, as described above. Membranes were incubated with cell lysates, then washed and incubated with a cocktail of biotinylated detection antibodies and detected with streptavidin-HRP and a chemiluminescent reagent, similar to the western blot technique. Membranes were analysed on the ChemiDoc ™ XRS + system.

As a result, a dot blot was obtained, which was evaluated by pixel analysis, as advised by the manufacturer. In order to ensure comparability between the membranes, all membranes were evaluated after the same development time. First, all relevant dots were marked as a 2.0 mm^2 circumference. Then, background noise, based on the mean value of the PBS dots on the membrane, was subtracted from each marked dot. Membranes also present reference dots, which serve as landmarks, and positive control dots, which were used for the normalization value. Mean and standard deviation were calculated from each samples' duplicates, after subtraction of the background noise (PBS dot). Results were plotted into a graph, where the SD is represented. Statistical analysis was performed using one-way ANOVA and Dunnett's test and the significance level is represented by asterisks as follows: * $p < 0.05$; ** $p < 0.01$; *** $p < 0.001$.

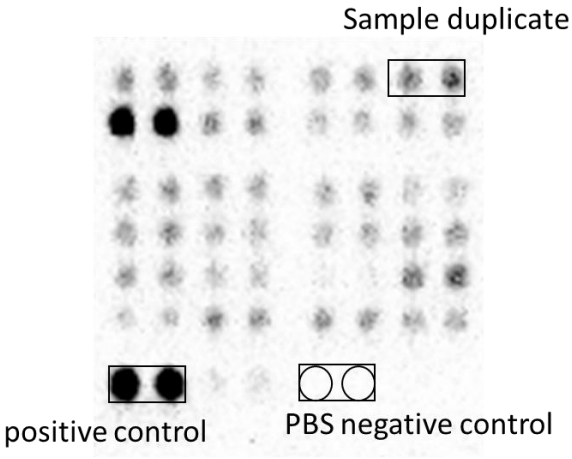

Figure 26. Pixel analysis of Proteome Profiler™ Human Soluble Receptor Array membrane. All relevant dots are marked as a 2.0 mm^2 blue circumference. PBS negative control corresponds to background noise, and were subtracted from each sample dot. Reference spots, serve as landmarks, and the positive control were used for sample normalization.

Evaluation of different melanoma cell lines in our experimental model

Characterization of NW1539 and Mel_1956 cell lines with Proteome Profiler™ Human Soluble Receptor Array

First, three different melanoma cell lines (MV3, NW1539 and Mel_1956) were assessed under experimental conditions with the purpose of determining which was the most appropriate cell line with which to continue our studies. Since literature regarding the NW1539 and Mel_1956 cell lines was sparse, we submitted these cell lines to Proteome Profiler™ Human Soluble Receptor Array, in order to better understand and characterize the cells.

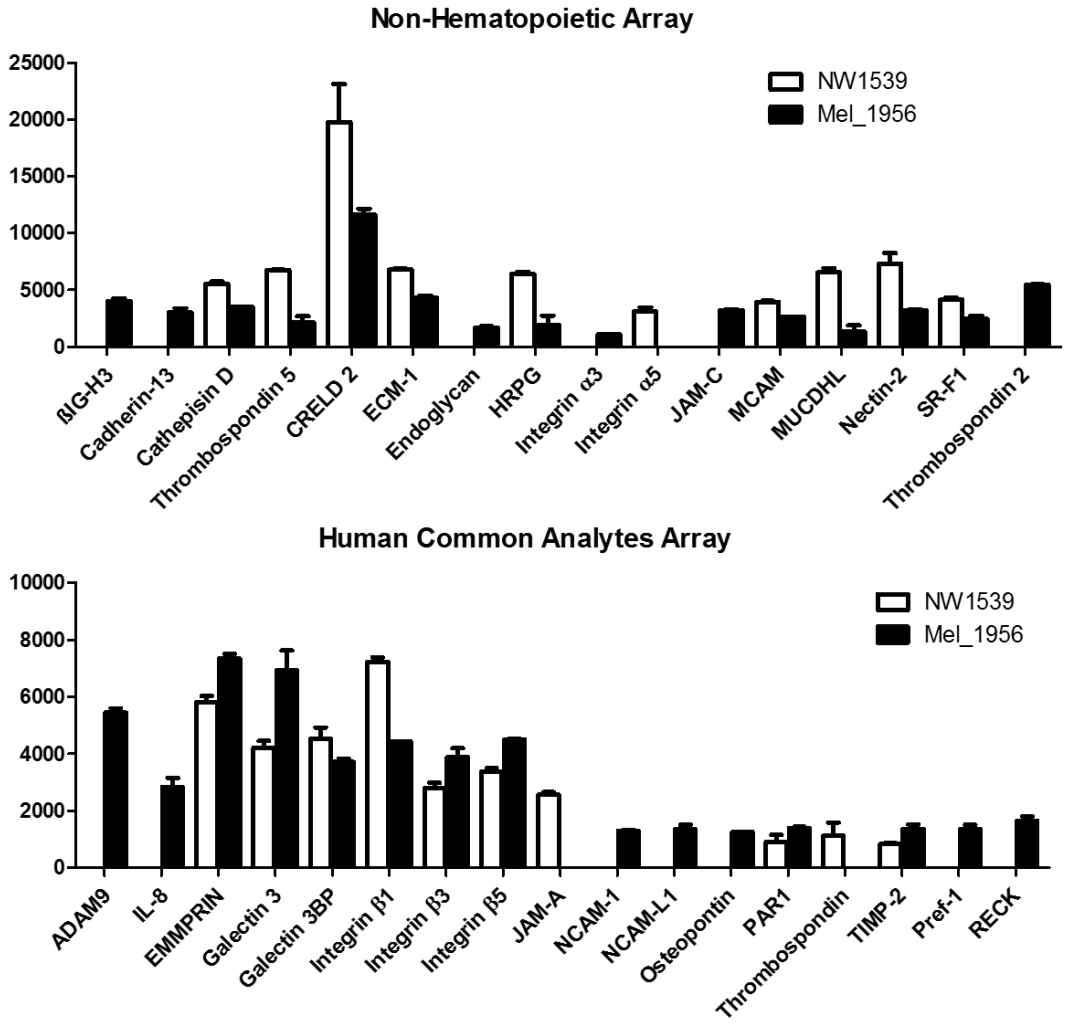

Figure 27. Proteome Profiler ™ Human Soluble Receptor Array of Mel_1956 and NW1539 melanoma cell lines. Cell lysate of Mel_1956 and NW1539 cell lines were incubated overnight with the Proteome Profiler ™ Human Soluble Receptor Array, as described above, to quantify the expression of specific cell membrane proteins.

It was observed that NW1539 cells express more β1 integrin then Mel_1956 cell line, whereas Mel_1956 cells were shown to express higher levels of β3 and β5 integrins than NW1539. This is in line with reports, discussed in the introduction, that suggest a complex regulation and cooperation system between β1 and β3 integrins. Generally, these integrins are associated to opposing function in the cell, β1 integrin has been more associated with strong adhesion and proliferation, while β3 integrin has been thought to lead to metastatic and EMT phenotypes (259–261). However, it has also been shown that they can cooperate, normally β3 integrin is not capable to attach to Coll. But the interaction between β1 integrin and Coll leads to modifications that expose the RGD binding site of this ECM component enabling β3 integrin to attach (191). Additionally, downregulation of β1 integrin has been shown to provoke β3 integrin upregulation in breast cancer cells, with the purpose of maintaining the malignant phenotype (260), however, not in normal mammary cells. This also impressively demonstrates cancer cells plasticity and ability to adapt in relation to normal tissue. To sum up, the results observed in the array suggest a more metastatic phenotype for the Mel_1956 cell line and a more proliferative and, possibly, CAM-DR associated profile for NW1539.

Regarding the α subunits, Mel_1956 cells are the only ones to produce α3 integrin, while α5 integrin is only produced by NW1539 cells, according to data from the Proteome Profiler™ Antibody Array. In this assay, we could also observe the expression of several proteins that interact with integrins, thus enhancing tumorigenesis, some of which had already been identified as overexpressed in metastatic melanoma compared to primary melanomas, such as thrombospondin, osteopontin, and NCAM1 (333).

The results show that thrombospondin 5 is expressed in both cell lines evaluated, although with a higher expression in NW1539. Moreover, thrombospondin 1 was only expressed in NW1539 cells, while thrombospondin 2 was only expressed in Mel_1956, which could indicate a regulation system between subunits similar to the one observed for β integrins, which has not yet been investigated. Thrombospondins are extracellular matrix molecules formed by glycoprotein subunits, with EGF-like and calcium-binding domains. They can bind to other ECM molecules or cell membrane proteins, such as chemokines, integrins and growth factors, and thus interfere in cell attachment, proliferation and differentiation (334–337). For example, all three thrombospondins expressed by the cells studied are involved in enhancing adhesion in an integrin-dependent way and have been associated with cancer malignancy (337–342).

Furthermore, thrombospondin 5, which is known to interact with several ECM proteins, such as FN, Coll and proteoglycans, has been shown to co-localize with FN and integrins on chondrocytes (343,344). Accordingly, thrombospondin 5 binding to FN is significantly enhanced by Mn^{2+}, demonstrating an integrin involvement (343,344).

Thrombospondin 1 is not expressed in normal melanocytes; however, it has been largely studied in melanoma. Its expression is acquired with the malignant progression of this type of cancer and acts in an autocrine manner, correlating with invasiveness, drug resistance, higher cell proliferation and tumour thickness, as well as reduced expression of genes involved in pigmentation (334,335). Thrombospondin 1 binding to integrins is mediated by CD47 and shows different cell effects depending on the integrin subunit. Interaction with β3 integrin stimulates invasion and metastasis, while α4β1 integrin-binding increases cell adhesion and spreading (334,338), which is consistent with the reports about cooperation and regulation between these two integrin subtypes discussed above and show that the integrins dictate cell fate upon ligation (259–261). The combination of thrombospondin 1 and β1 integrin in the NW1539 cell line reinforces the proliferative and adhesive profile expected from these cells. In contrast, thrombospondin 2 expression on Mel_1956 reinforces the metastatic profile suggested by β3 integrin expression, since thrombospondin 2 is usually strongly expressed in metastatic melanoma, but not on primary tumours (336).

Another ECM protein present in our assay, which interacts with integrins leading to a poor outcome in tumorigenesis, is osteopontin (OPN), a chemokine-like protein secreted by many cells as part of the ECM. OPN has been shown to bind to cells in an integrin-dependent manner stimulating adhesion (345–347). Elevated levels of OPN expression and secretion have been associated with enhanced malignancy in several cancers, including melanoma, and is used as a prognostic marker (333,348,349). This is due to the fact that OPN secreted by tumour stroma, or tumour cells themselves, promotes tumour progression by interacting with ECM factors and cell membrane receptors, such as integrins, activating multiple signalling cascades, which regulate cell proliferation, survival, angiogenesis and metastasis (345–349). In this assay, Mel_1956 cells have been shown to express this protein, which is in accordance with other reports that analysed different stages of melanoma, and revealed that enhanced OPN expression correlates with metastatic melanoma phenotype (333,348). This has been associated to OPN-integrin binding (345–347,350).

Mel_1956 also displayed a high and exclusive expression of ADAM9, which is a membrane-anchored protein with catalytic activity, such as FN and gelatin hydrolyzation, and ectodomain shedding, which helps regulate and remodel the ECM. Besides metalloprotease activity, ADAM9 also interacts with different integrins and has been implicated in cancer progression (351–354). ADAM9 expression positively correlates with tumour progression in several cancers including melanoma (354–357), and the inhibition of its expression has been shown to sensitize chemotherapy resistant prostate cancer and melanoma (353,357). It is know that ADAM9 can bind to α6β1 and αvβ5 integrins, in a Mn^{2+} and Ca^{2+} dependent and RGD-independent manner, in fibroblast and myeloma cell lines, respectively (353,358), demonstrating that different cell types may use different integrins to mediate binding to ADAM9. More specifically, Zigrino et al. showed that ADAM9, produced by melanoma cells, mediates interactions between these cells and fibroblasts by binding to β1 integrins on fibroblast surface in a Mn^{2+} dependent manner, enhancing metastasis (354). In the case of the Mel_1956 cell line it is possible that ADAM9 expression indicates ECM remodelling and an invasive phenotype.

Interleukin-8 (IL-8) was also only expressed by Mel_1956, which also indicates a more aggressive behaviour of this cell line, as IL-8 is a chemokine, which is not normally produced by melanocytes. However, it is overexpressed by melanoma cells, accompanied by the expression of its receptors, CXCR1 and CXCR2 (359,360), thus demonstrating not only a paracrine, but also an autocrine effect (359). IL-8 and its receptors interact with integrins and correlate with melanoma malignancy and metastatic potential through the activation of multiple cell signalling pathways and by affecting proliferation, apoptosis resistance and cytoskeletal dynamics (359–361).

Finally, both cell lines express high levels of galectin 3, an ECM protein, which has been associated with several biological processes and pathologies, including cancer (362–366). Its overexpression and/or changes in location are indicators of poor prognosis, since they affect cell growth and differentiation, chemoattraction, apoptosis, immunosuppression, angiogenesis, adhesion, invasion and metastasis. For example, galectin-3 binding to integrin αvβ3 can induce angiogenesis (364,365). Moreover, galectin-3 has been associated with metastatic behaviour of melanoma, through association with FN mediated by α3β1 integrin (362,363,365). According to the data, integrins β1 and β3, as well as galectin-3 are expressed by both cell lines tested, which shows their malignant potential.

Taken together these results show that, even though NW1539 and Mel_1956 cell lines are both malignant metastatic melanoma cell lines, they display different profiles; Mel_1956 presents a more metastatic phenotype, while NW1539 could be described as more adherent and proliferative. These differences are strongly connected to the integrin pattern of these cells, as we were able to demonstrate. This shows the importance of targeting such integrins and integrin related adhesion events for the improvement of anticancer therapy.

Sensitivity of melanoma cell lines to cisplatin

Cisplatin was selected as the cytostatic agent for this project in order to investigate a potential relation between integrin activity and loss of apoptotic response, in all three cell lines. Cisplatin is usually used a second line treatment in extreme cases of aggressive tumours, including melanoma, which means that it is implemented when other treatments have failed (52). For this reason, this cytostatic drug seamed like a suitable system to simulate therapy resistance. Two parameters were taken into consideration to select the optimal seeding density of each cell line: first, cisplatin impact on cell proliferation, and second the proliferation rate observed for each cell line. Thus, the cytotoxicity assays were performed using 5000 cells/well and 10000 cells/well for the Mel_1956 and MV3 cell lines; and 2500 cells/well and 5000 cells/well for the NW1539 cell lines. As mentioned, the MV3 cells are known to display high affinity to Coll type I and IV and have high expression of integrin β1 and CD44 (257,312,313). Furthermore, Maaser et al. were able to demonstrate a hierarchal interaction between these two adhesion molecules. They have shown that α2β1, but not CD44, is necessary for the interaction of MV3 cells with Coll matrix containing hyaluronan (256). The MV3 cell line has also been shown to stimulate pro-coagulatory factors, as well as, glycosaminoglycan synthesis by other cell on their surroundings , which demonstrates the ability of these cells to manipulate and adapt to their environment (367,368). The data from the Proteome Profiler™ Antibody Array (Figure 27) together with literature about the MV3 cells show that although all three cell lines are derived from highly metastatic human melanomas, they differ in various characteristics, such as, expression pattern of integrins and other proteins, and proliferative or invasive profile. Accordingly, the cell lines display a slightly different, but not statically significant, sensitivity to cisplatin.

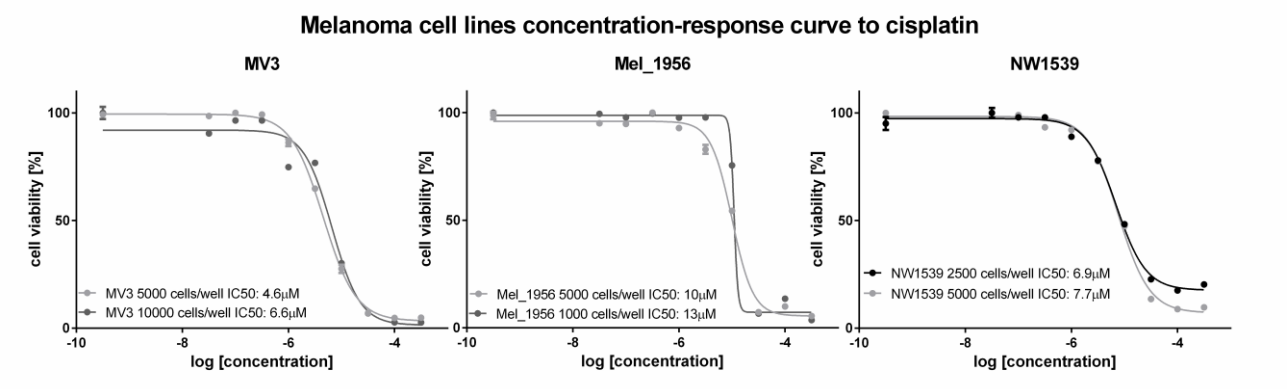

Figure 28. Melanoma cell lines sigmoidal concentration-response curves. Exemplary curves that represent one of at least three measurements. The sensitivity of all three cell lines to cisplatin was assessed by quantifying the number of living cells after a 72-hour incubation period with drug logarithmic concentration curve, using MTT assay. The data obtained were plotted into sigmoidal concentration-response curves and used to determine the IC_{50} values.

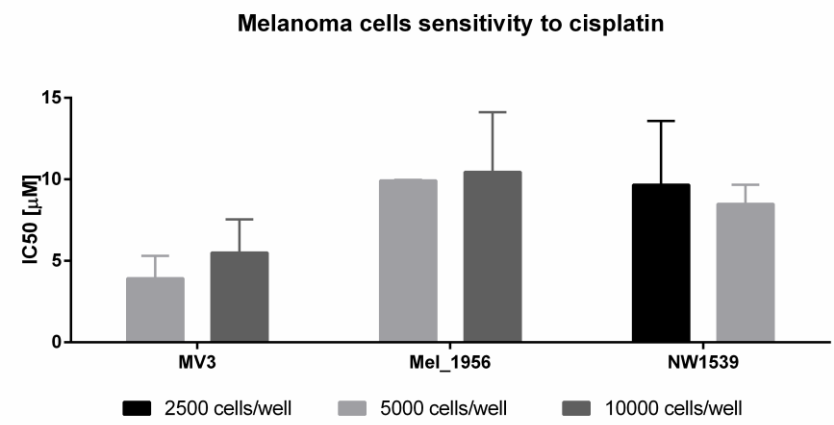

Figure 29. Melanoma cell lines sensitivity to cisplatin. Sensitivity of all three cell lines to cisplatin represented using the mean value and SEM of IC_{50} values from at least three MTT concentration-response curves. ANOVA statistical analysis, asterisks indicate statistical significance in comparison to cells treated solely with cisplatin: * P<0.05; ** P<0.01; *** P<0.001.

Interestingly, even though the cell lines present different protein expression profiles and, based on that, diverse phenotypes, only a slight difference between their sensitivity to cisplatin was found. The MV3 cells displayed the highest sensitivity, while the other two cell lines exhibited similar IC_{50} concentrations; as expected from their aggressive metastatic protein expression Mel_1956 cells were the most resistant.

Impact of integrin activation by FN and Mn^{2+} on cisplatin resistance

Based on these findings, the melanoma cells were investigated with respect to their sensitivity to cisplatin in relation to integrin activation. Since our expression data confirmed that multiple integrins were expressed by the cells, fibronectin (FN) was used as a universal integrin binding substrate. Thus, cells were either treated with 1 mM solution of Mn^{2+} for a final concentration of 100 µM in each well, which induces integrin clustering and a high affinity binding state; or grown on FN coated surfaces. Alternatively, a combination of both treatments was used. Cell sensitivity to cisplatin was measured using MTT cytotoxicity assay. The Mel_1956 cell line was evaluated first.

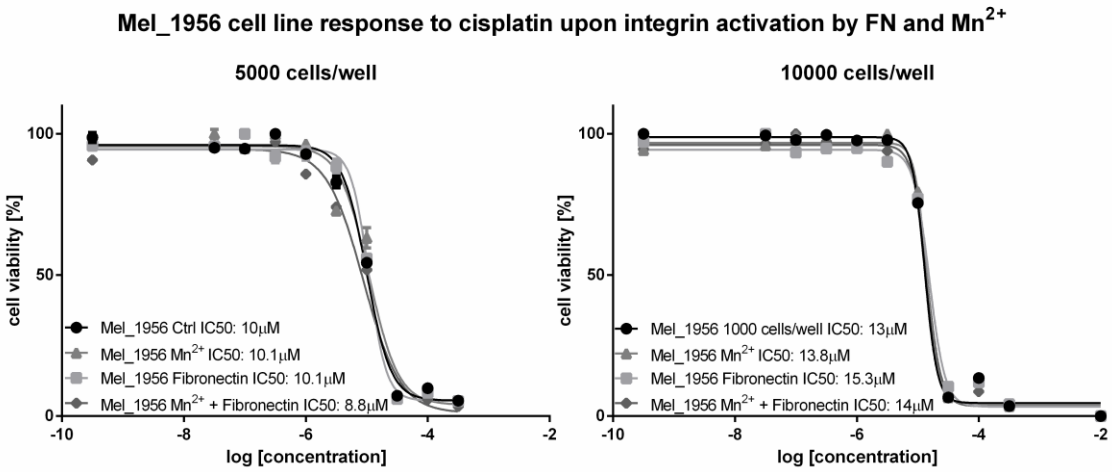

Figure 30. Mel_1956 sigmoidal concentration-response curves upon integrin activation. Curves exemplify results from one of at least three MTT assays. Cells were platted on FN coated plates and/or incubated with final concentration in well of 100 µM Mn^{2+}, before a 72-hour incubation with cisplatin logarithmic concentration curve. Sigmoidal concentration-response curves were used to calculate the IC_{50} values of each treatment.

Table 1. Cisplatin IC_{50} on Mel_1956 cell line upon Mn^{2+} and FN treatment

Cell Density	Treatment	pIC_{50} ± SEM	IC_{50} (µM)
5000 cells / well	Cisplatin	5.00 ± 0.05	9.9
	Mn^{2+}	5.04 ± 0.11	9.1
	Fibronectin	5.05 ± 0.13	8.8
	Mn^{2+} + FN	5.09 ± 0.05	8.1
10000 cells / well	Cisplatin	5.00 ± 0.18	9.9
	Mn^{2+}	4.97 ± 0.13	10.8
	Fibronectin	5.13 ± 0.32	7.4
	Mn^{2+} + FN	5.00 ± 0.13	10.0

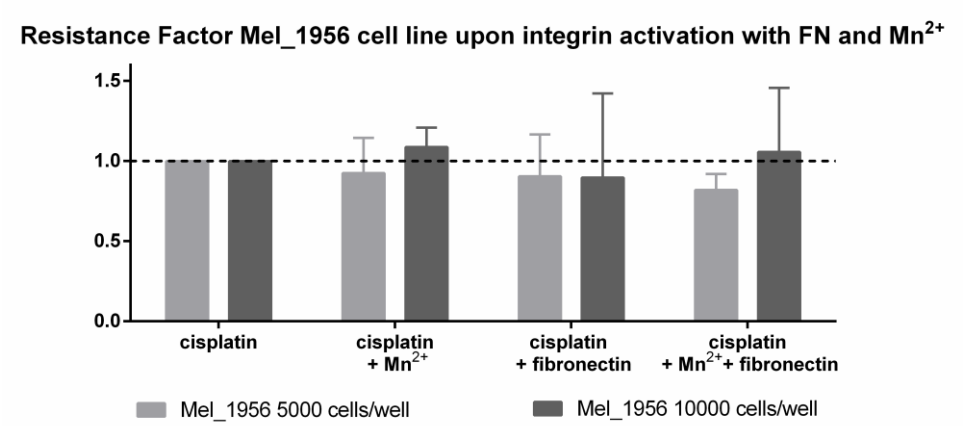

Figure 31. Integrin activation in Mel_1956 cells. IC_{50} values of each MTT were used to estimate the resistance factor (RF), which consists of the quotient between the IC_{50} of cisplatin-treated cells and the IC_{50} of cells that received other treatment in addition to cisplatin, in this case FN and/or Mn^{2+}. The data displayed here correspond to the mean value and SD of the RF of at least 3 assays. Statistical analysis was performed by one-way ANOVA; asterisks indicate statistical significance in relation to cisplatin-treated cells only: * P<0.05; ** P<0.01; *** P<0.001.

Contrary to expectations, treatments for triggering integrins barely increased Mel_1956 sensitivity to cisplatin. Only Mn^{2+} was able to slightly increase cell resistance factor (RF: ratio of IC_{50} of cisplatin *vs.* treated cells) in the high cell-density sample. Regrettably, however, most treatments decreased cell sensitivity to cisplatin, which can be observed by RF lower than 1. Although unfortunate, these results confirm the hypothesis that the Mel_1956 cell line is a highly metastatic melanoma cell, which concentrates cell effort, most likely on migration, rather than adhesion and CAM-DR formation. NW1539 cells were evaluated next.

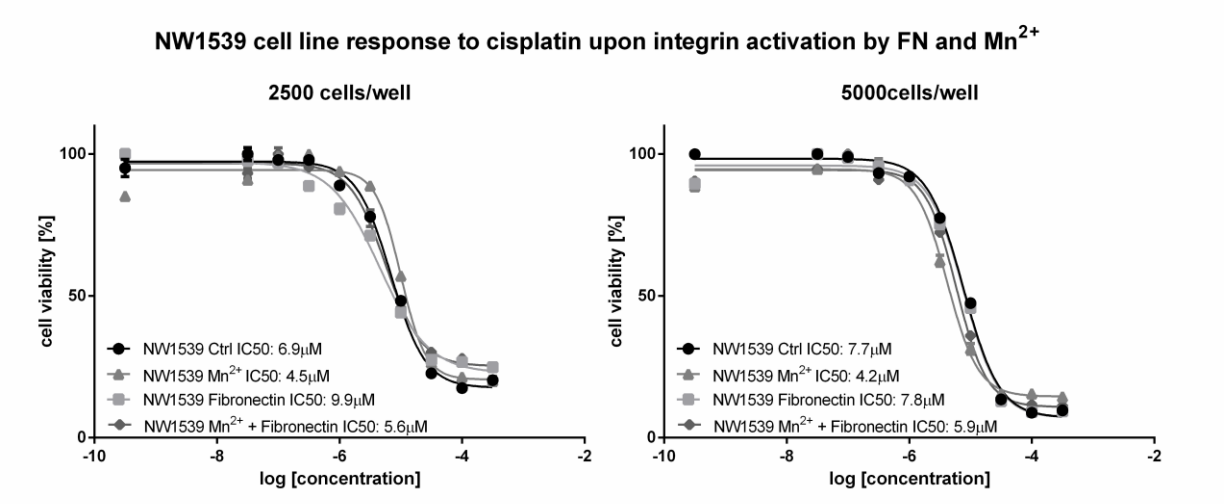

Figure 32. Sigmoidal concentration-response curves of NW1539 upon integrin activation. The curves shown here represent one of at least three MTT experiments. Cells were seeded on FN coated plates and/or incubated with 1 mM solution of Mn^{2+}, before incubation with drug logarithmic concentration curve for 72 hours. Sigmoidal concentration-response curves were used to determine the impact of each treatment on cisplatin IC_{50} values.

Table 2. Cisplatin IC_{50} on NW1539 cell line upon Mn^{2+} and FN treatment

Cell Density	Treatment	pIC_{50} ± SEM	IC_{50} (µM)
2500 cells / well	Cisplatin	5.03 ± 0.18	9.3
	Mn^{2+}	5.19 ± 0.22	6.5
	Fibronectin	4.97 ± 0.04	10.6
	Mn^{2+} + FN	5.12 ± 0.19	7.7
5000 cells / well	Cisplatin	5.07 ± 0.06	8.5
	Mn^{2+}	5.31 ± 0.09	4.9
	Fibronectin	5.12 ± 0.02	7.5
	Mn^{2+} + FN	5.18 ± 0.08	6.7

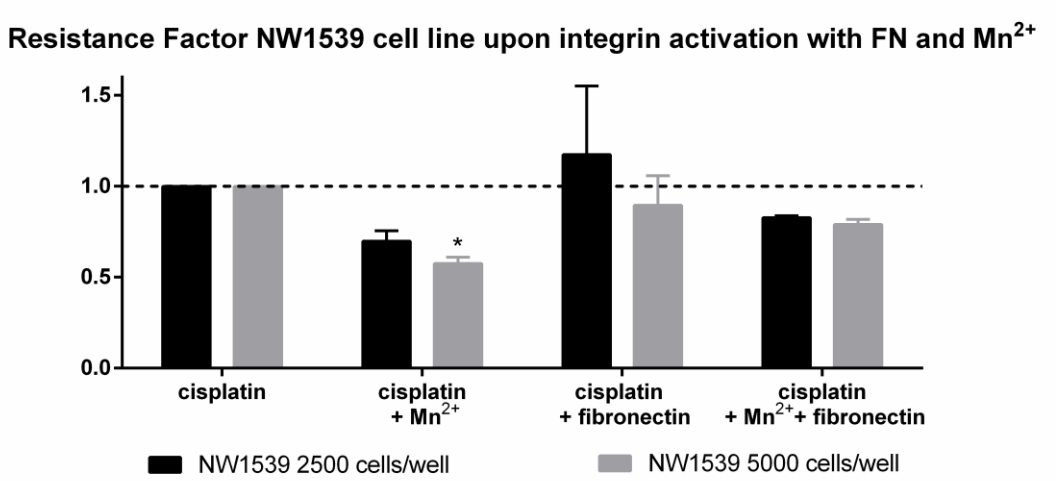

Figure 33. Effect of integrin activation on NW1539 cells. Resistance factors (RF) were estimated using the IC_{50} values obtained from MTT sigmoidal concentration-response curves. Mean value and SD of the RF of at least 3 measurements can be observed. Data were submitted to one-way ANOVA statistical analysis; asterisks indicate statistical significance in relation to cisplatin-treated cells only: * P<0.05; ** P<0.01; *** P<0.001.

Unexpectedly, sensitivity of NW1539 cells to cisplatin increased with almost all integrin-activating stimuli. In the case of Mn^{2+}, even showing a statistically significant sensitization of cells to cisplatin. This was very surprising, as the Proteome Profiler™ Antibody Array (Figure 27) had indicated that these were high proliferative and adhesive cells that overexpress several integrin-binding proteins. The difficulty in detecting an increase in cell sensitivity to cisplatin in the abovementioned melanoma cell line may be a result of the fact that these cells already have highly activated integrins and, therefore, cannot be overactivated by the treatments used.

Unfortunately, the treatments used to increase integrin-binding, and thus induce chemoresistance in Mel_1956 and NW1539, were not able to generate a resistance factor greater than 1. For this reason, we carried out our work only with the MV3 cell line, which had shown more promising results.

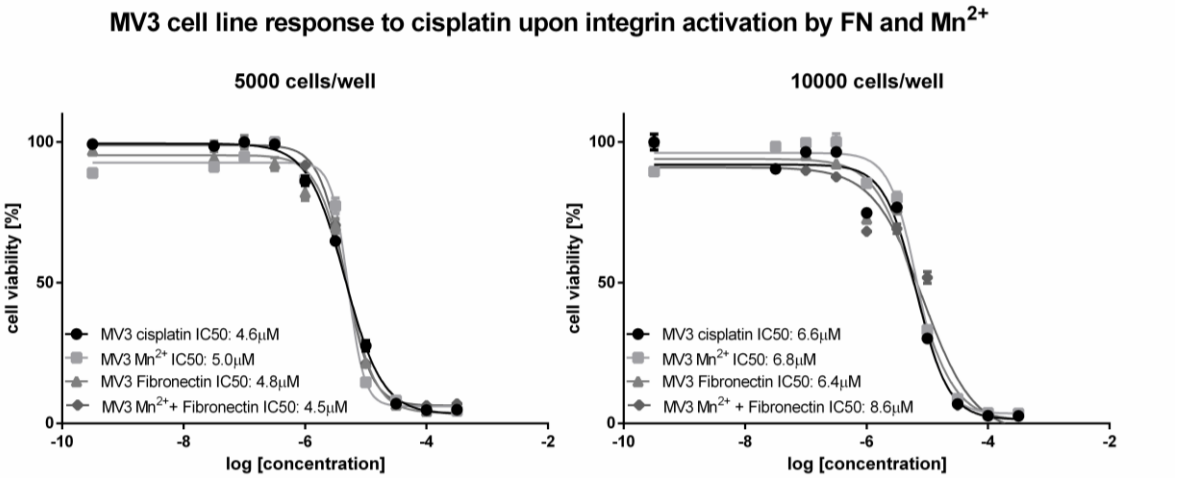

Figure 34. Sigmoidal concentration-response curves of MV3 cells treated with integrin activating stimuli, FN and Mn^{2+}. The exemplary curves illustrate one of at least three MTT experiments. Cells were seeded on FN coated plates and/or incubated with a final concentration of 100 µM Mn^{2+} in well, then incubated for 72 hours with cisplatin logarithmic concentration curve. Sigmoidal concentration-response curves were used to calculate IC_{50} values.

Table 3. Cisplatin IC_{50} on MV3 cell line upon Mn^{2+} and FN treatment

Cell Density	Treatment	pIC_{50} ± SEM	IC_{50} (µM)
5000 cells / well	Cisplatin	5.42 ± 0.15	3.8
	Mn^{2+}	5.04 ± 0.25	4.0
	Fibronectin	5.37 ± 0.17	4.2
	Mn^{2+} + FN	5.35 ± 0.24	4.5
10000 cells / well	Cisplatin	5.22 ± 0.19	5.9
	Mn^{2+}	5.14 ± 0.26	6.6
	Fibronectin	5.16 ± 0.06	7.0
	Mn^{2+} + FN	5.07 ± 0.18	8.6

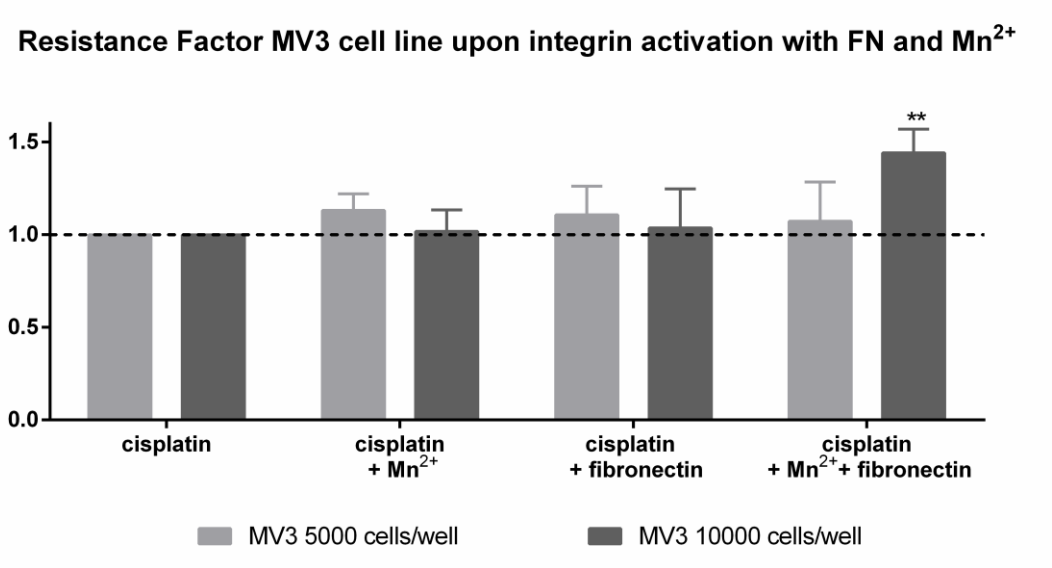

Figure 35. Impact of integrin activation by FN and Mn^{2+} on the resistance factor of MV3 cell line. IC_{50} values obtained from at least three MTT experiments were used to estimate the resistance factor (RF) by dividing the IC_{50} of cells that received other treatment in addition to cisplatin, in this case FN and/or Mn^{2+} by the IC_{50} of cisplatin treated cells. RD mean value and SD was analysed by one-way ANOVA; asterisks indicate statistical significance compared to cisplatin-treated cells only: * $P<0.05$; ** $P<0.01$; *** $P<0.001$.

It can be observed that the MV3 cells showed an interesting response. All integrin-activating treatments were able to increase RF above 1, in different intensities, depending on the number of cells per well. Sensitivity of MV3 cells to CDDP was affected by cultivation in contact with FN, a known integrin activator. Additionally, integrin activation by Mn^{2+} also shifted the sensitivity of MV3 cells to higher IC_{50} values, indicating an impact of integrin activity on resistance phenomena. Furthermore, the combination of FN coating and Mn^{2+} resulted in higher resistance, especially in the 10000 cells per well density, thus showing a strong statistic correlation. This is a promising set of data that shows a clear dependency of cellular sensitivity towards cisplatin and integrin stimulation. This is in obvious accordance with our hypothesis that the other melanoma cell lines tested already had highly activated integrins, which could not be overactivated by the treatments, the cell line with the intrinsically highest cisplatin sensitivity, MV3, showed the most promising results.

MV3 melanoma cell line

Integrin activation in MV3 melanoma leads to decreased sensitivity against cisplatin cytotoxicity.

As discussed in the introduction, another important component of the ECM are collagens. Coll type I, specifically, is a known binding partner of the β1 integrin subunit, which is abundantly expressed in most cell types, including the MV3 cells, and has been often associated with cancer malignancy and chemoresistance (255–257). Thus, cells were grown on Coll I-coated surfaces, and, in some cases, treated with Mn^{2+}, for a combination of both treatments, before being submitted to the MTT cytotoxicity assay.

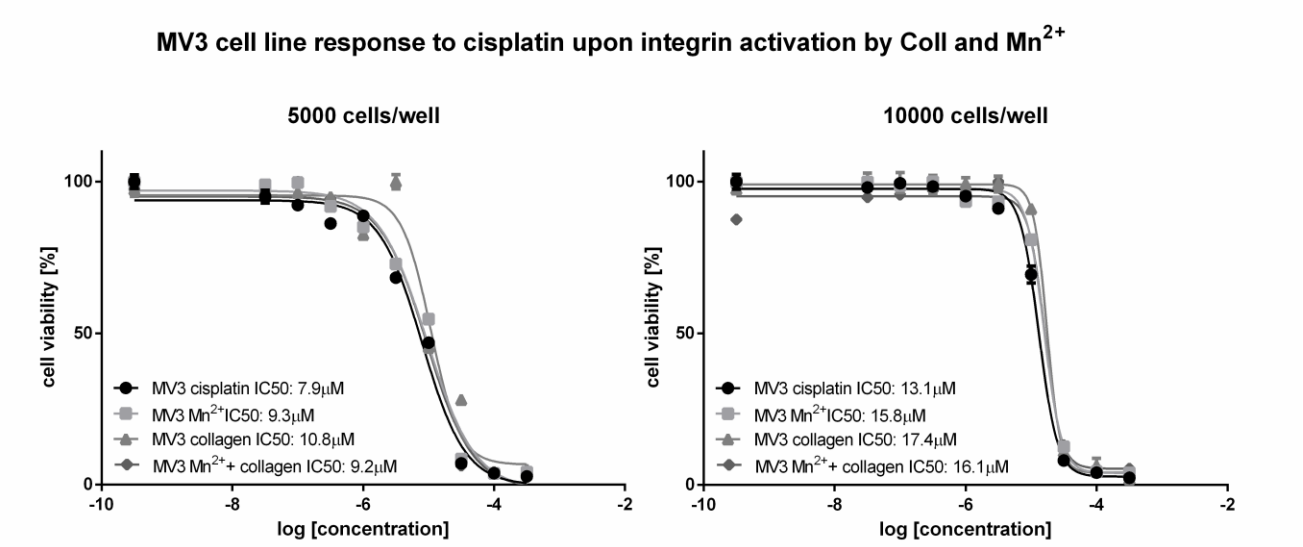

Figure 36. MV3 cell line sigmoidal concentration-response curves upon integrin activation by Coll. One of at least three curves obtained by MTT assay is represented here. Cells were platted on Coll-coated plates and, in some cases, incubated with a final concentration in well of 100 μM Mn^{2+}, previously to incubation with cisplatin logarithmic concentration curves for 72 hours. Sigmoidal concentration-response curves were used to determine the IC_{50} values of each treatment.

Table 4. Cisplatin IC_{50} on MV3 cell line upon Mn^{2+} and Coll treatment

Cell Density	Treatment	pIC_{50} ± SEM	IC_{50} (μM)
5000 cells / well	Cisplatin	5.13 ± 0.33	7.4
	Mn^{2+}	5.11 ± 0.39	7.8
	Collagen	5.02 ± 0.33	9.7
	Mn^{2+} + Coll	5.04 ± 0.05	9.1
10000 cells / well	Cisplatin	4.93 ± 0.39	11.7
	Mn^{2+}	4.92 ± 0.45	12.1
	Collagen	4.78 ± 0.12	16.6
	Mn^{2+} + Coll	4.84 ± 0.12	14.5

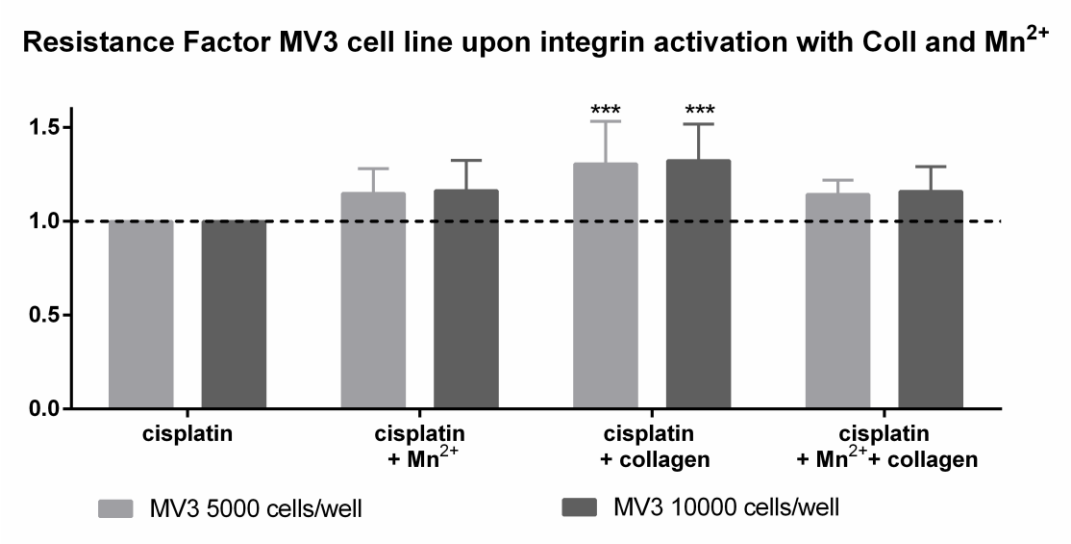

Figure 37. Resistance factors of MV3 cells as indicators for attenuated cisplatin cytotoxicity upon integrin activation by Coll and Mn^{2+}. Cells were submitted to MTT assay, after 72 hours of incubation with cisplatin, under integrin activating stimuli 1 mM Mn^{2+} solution and/or Coll coating. The data displayed here corresponds to the mean value and SD of RF (ratio between IC_{50} of treated vs. untreated) of at least three measurements. One-way ANOVA statistical analysis was used; asterisks indicate statistical significance compared to cells treated solely with cisplatin: * P<0.05; ** P<0.01; *** P<0.001.

MTT assay results revealed a consistent decrease in sensitivity of MV3 melanoma cells, when subjected to all integrin-activating stimuli. Mn^{2+} and Coll increased cell resistance to cisplatin in both cell densities. The effect of Coll seems to be more robust, showing strong statistical significance. Despite the fact that these findings suggest a functional axis of β1 integrin activity and loss in chemosensitivity, a synergistic effect between the two integrin-activators could not be observed, as it was the case for FN and Mn^{2+}. Nevertheless, this clearly indicates that the functional consequences of the different integrin activations, integrin clustering and conformational changes by Mn^{2+} *vs*. ligand-triggered activation, affect the loss in sensitivity differently and deserve closer examination. Integrins are known to control cell proliferation through activation of different signalling pathways (36,37,38). In order to test the possibility that the lack of synergy between the integrin activating stimuli or the resistance effects observed were associated with integrins interfering in the cell proliferation rate, cell counts were observed microscopically, after 72 hours, in the presence or absence of 7.5 µM cisplatin.

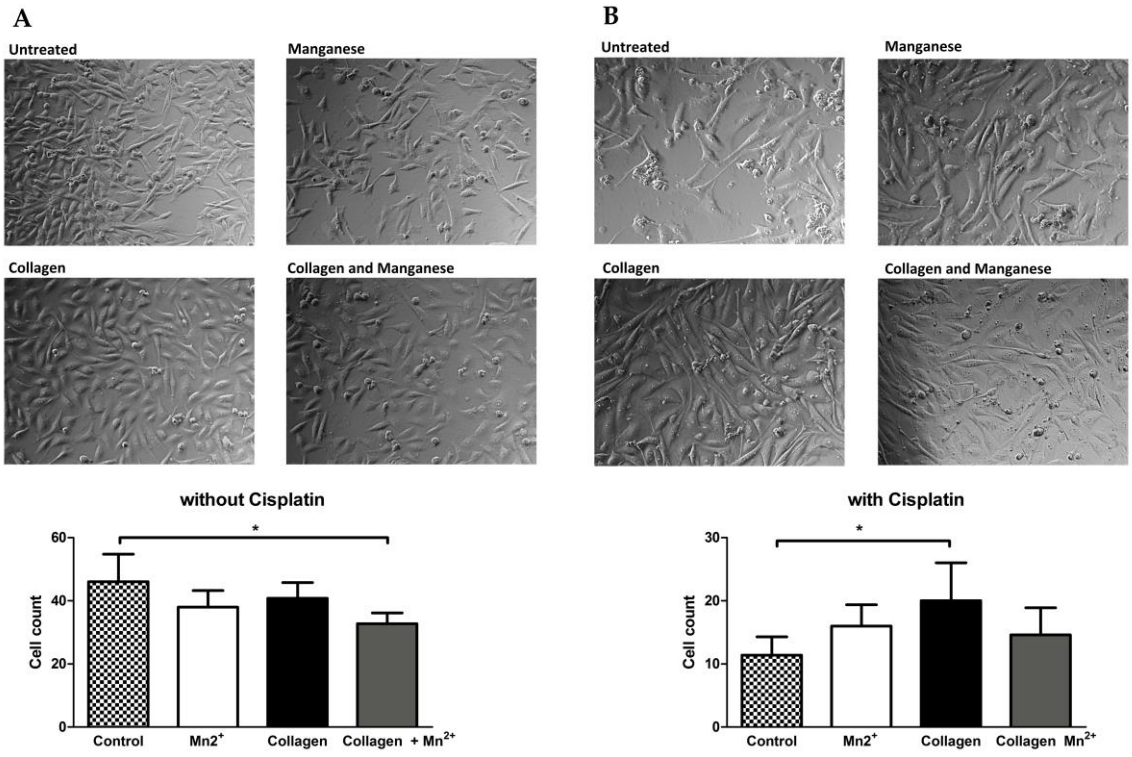

Figure 38. Evaluation of integrin activators impact on MV3 cell proliferation rate observed by microscopy. A. Exemplary microscopy images of MV3 cells cultured for 72 hours without cisplatin, under the indicated conditions (control, Coll or/and Mn^{2+}). **B.** Exemplary microscopic pictures of MV3 cells, cultured for 72 hours, under the same indicated conditions in the presence of 7.5 μM of cisplatin. Pictures were taken at five different growth spots and counted. The graph displays the mean value and SD of the cell-count for the different spots. Results were analysed by one-way ANOVA. Statistical significance: * P<0.05; ** P<0.01; *** P<0.001. From Piva et al. (369).

Neither the Mn^{2+} nor Coll, or the combined treatment increased cell proliferation rate. On the contrary, cell growth and density seemed to be slightly reduced, in relation to the control cells. In strict contrast, when cells were exposed to a cisplatin for 72 hours, the integrin-activated cells displayed a clearly higher proliferation capacity than the untreated control cells (Figure 38B). Consequently, the changes in IC_{50} values presented in Figure 37 do not originate from an integrin-activated accelerated cell proliferation rate, but it appears to be the first indication of a lower sensitivity to cisplatin cytotoxicity in the integrin-activated cells compared to the respective controls. These findings show a role for integrins in cisplatin chemoresistance of the MV3 cell line. Additionally, as mentioned, β1 integrins are the main ligands for Coll I, and have been often associated with cancer malignancy and chemoresistance, which suggests they could be the integrin subunit responsible for this process in the MV3 cells as well (255–257).

Resistance of MV3 cells is mediated by the FAK/PI3K/AKT pathway

To further elucidate the path of integrin activation, we investigated the downstream key effectors of integrin signalling FAK, PI3K, and its direct target of phosphorylation, AKT, by flow cytometry adopting the same treatment regimens as used for the MTT assays, but without cisplatin, for 72 hours.

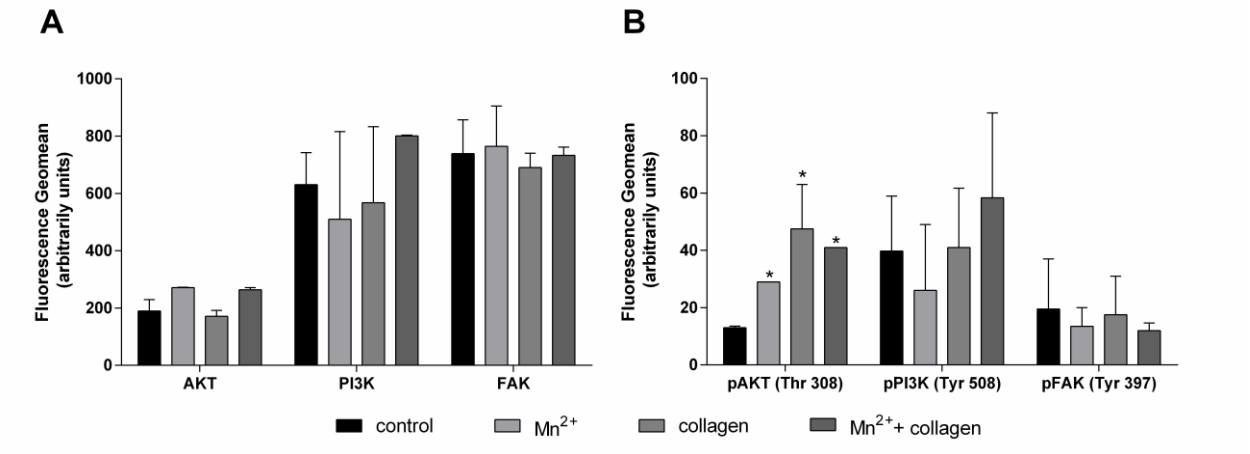

Figure 39. Integrin-signalling effector proteins quantified by flow cytometry. A. Total protein levels of integrin effectors AKT, PI3K and FAK. **B.** Levels of phosphorylated (active) AKT, PI3K and FAK signalling proteins. MV3 cells were cultivated for 72 hours in uncoated or Coll-coated cell culture flasks, and, depending on the treatment, incubated with 2 ml of 1 mM Mn^{2+} solution for 5 minutes. Presenting geomean and SEM of at least three measurements. One-way ANOVA statistical analysis was used to calculate statistical significance in relation to control (uncoated), which is indicated by asterisks: * $P<0.05$; ** $P<0.01$; *** $P<0.001$.

It could be observed that the integrin activating treatments induced a statistically significant increase only in AKT phosphorylation. Since AKT is the last effector in this signalling pathway, this might be a consequence of the time point observed and does not exclude the hypothesis of integrin involvement. Moreover, these results show the behaviour of untreated MV3 cells and, as discussed above, cisplatin treatment by itself can alter expression and activation state of cell proteins (73). In order to investigate if this was the case of our experimental model, we would have to analyse the cell in an environment that really simulated the MTT assays. For this purpose, cells were submitted to the same treatment regimens plus a cisplatin concentration of 7.5 µM, for 72 hours, before integrin signalling effectors were analysed and this data was compared to the expression and activation rates of the untreated cells.

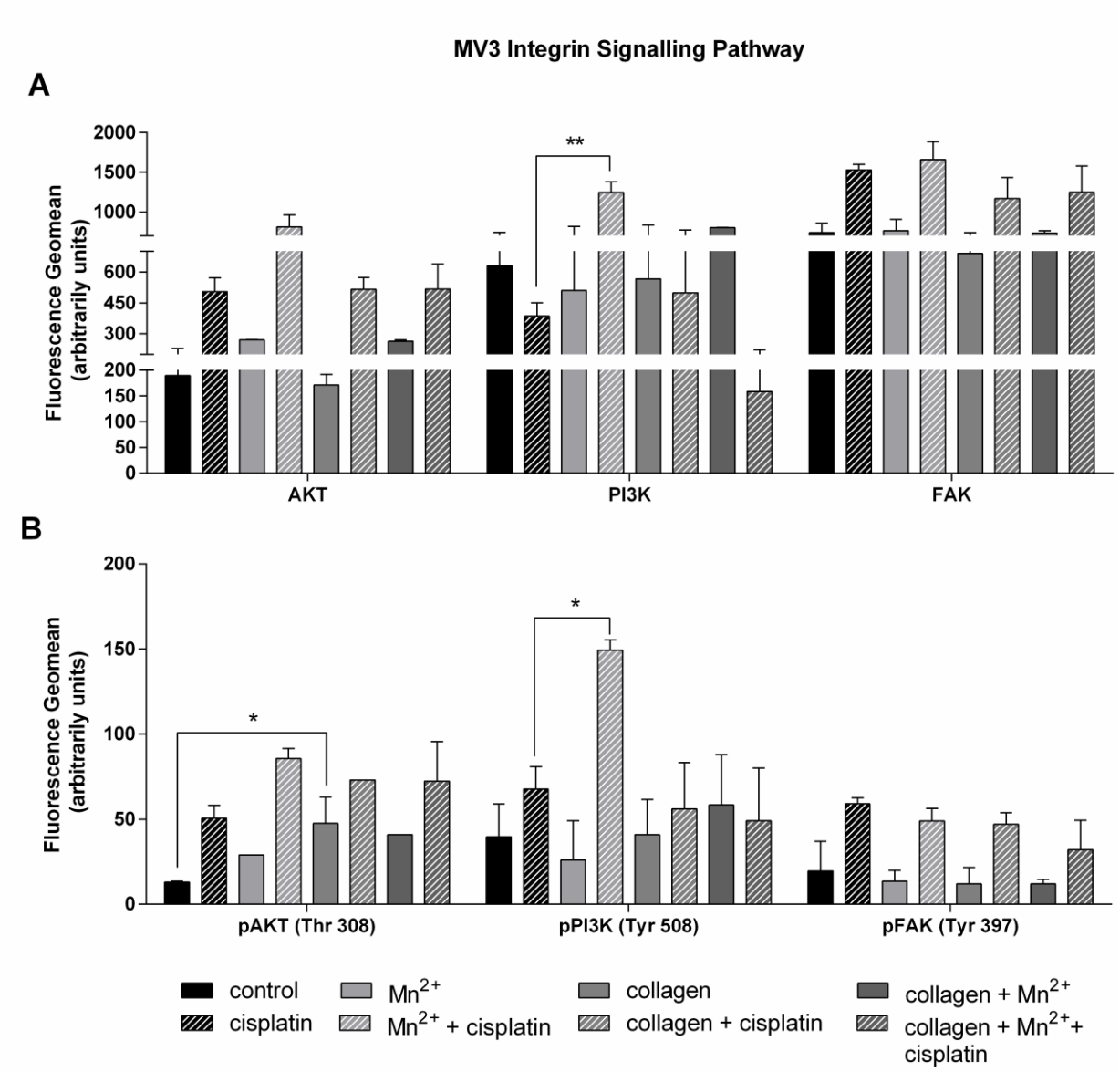

Figure 40. Effect of cisplatin on integrin cell signalling assed via flow cytometry. A. Total protein levels of AKT, PI3K and FAK. **B.** Levels of phosphorylated AKT, PI3K and FAK, which indicate activation. The MV3 cell line was grown in cell-culture flasks, either coated with Coll type I, or uncoated and, depending on the treatment, incubated with 100 µM final concentration of Mn^{2+}, for 5 minutes, prior to the addition of 7.5 µM cisplatin. Cells were Collected after 72 hours and submitted to FACS. Graphs display geomean and SEM of at least 3 assessments. ANOVA statistical analysis, statistical significance in relation to control or only cisplatin: * P<0.05; ** P<0.01; *** P<0.001

As expected, the incubation with cisplatin triggered an intracellular survival response. It induced a general increase in the expression and activation of FAK, PI3K and AKT, which shows the importance of this pathway for the cells. This survival pathway was obviously activated in response to cisplatin stress. Interestingly, in the cisplatin treated cells, an integrin activation through downstream signalling molecules could only be observed under Mn^{2+} stimulation, but not under Coll treatment, or both treatments combined. A significant upregulation of PI3K and phosphorylated PI3K is evident, indicating an activation most likely through FAK. Furthermore, PI3K activity was confirmed by an upregulation of AKT and an increase in AKT phosphorylation.

The activation of the PI3K/AKT axis in the presence of cisplatin only under Mn^{2+} treatment is another indicator of the complexity of integrin regulation and activation. It shows, once again, that each integrin-activating stimulus provokes a different integrin-functional consequence, thus triggering distinct mechanisms. This is confirmed by the lack of synergistic effect between these two integrin-activators shown in the combined treatments.

Sensitization of MV3 cells to cisplatin by inhibition of FAK/PI3K/AKT pathway

Considering the strong upregulation of the FAK/PI3K/AKT signalling pathway in cisplatin treated cells, associated with increased expression of PI3K and phosphorylated PI3K in the Mn^{2+} treated cells, we aimed to associate these findings with cisplatin sensitivity. Thus, PI3K was blocked, with the PI3K inhibitor BEZ235, in order to investigate its impact on sensitivity. BEZ235 binds reversibly and competitively to the ATP-binding cleft of PI3K and mTOR, working as potent and selective inhibitor of PI3K pathway. BEZ235 presents very low affinity to other down- or upstream effectors, such as FAK, and PDK1, but has been shown to interfere in 50% of AKT phosphorylation in a reversible manner (308). BEZ235 has been shown to decrease cell proliferation and migration, and display synergistic effects to platinum drugs and taxanes (325–327).

First, a MTT cytotoxicity assay with different concentrations of the inhibitor was performed to establish the optimal concentration for our cisplatin assays.

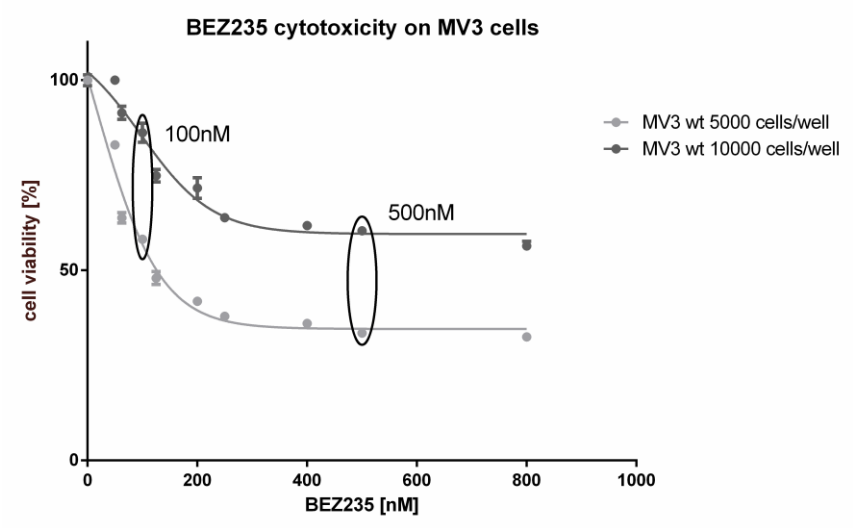

Figure 41. BEZ235 cytotoxicity curves on MV3 cells. Exemplary curves that represent one of at least three measurements obtained by MTT assay. Cells were incubated with a series of concentrations of the PI3K inhibitor BEZ235 for 72 hours, to simulate cisplatin assay conditions, before cytotoxicity assessment by MTT assay.

PI3K inhibitor BEZ235 showed an IC_{50} of approximately 200 nM for the lower cell density of the MV3 cell line. Unfortunately, we were not able to observe an IC_{50} for the higher cell count. This is a consequence of the well-established ability of BEZ235 to induce a cell cycle arrest with no apoptosis induction, which can be observed by the concentration plateau reached in our assay (308,324,370). Based on these results, cells were submitted to MTT assay under integrin activating stimuli (Coll and Mn^{2+}) in the presence of two concentrations of BEZ235, a non-cytotoxic final concentration in the well of 100 nM and a higher final concentration of 500 nM in the well, which induces cell cycle arrest, both of which have been shown to inhibit mainly PI3K (308). Cells were treated with BEZ235 for a period of 6 hours, before cisplatin was added; subsequently, cells were incubated with both compounds simultaneously, for 72 hours.

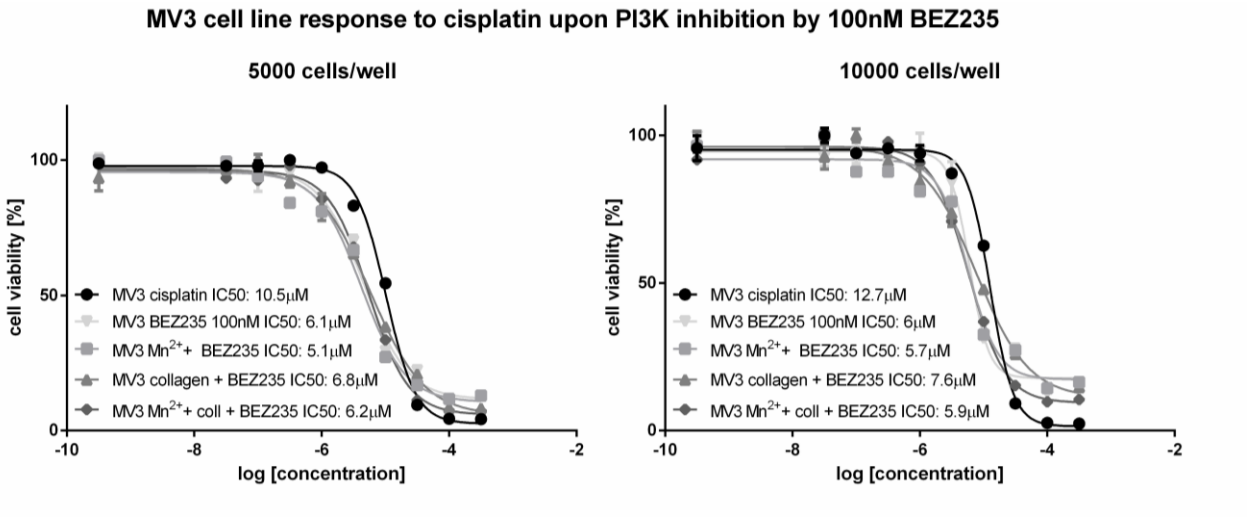

Figure 42. MV3 cell line sigmoidal concentration-response curves. Exemplary curves that represent one of at least three experiments. Cells were incubated with integrin activators (1 mM Mn^{2+} or Coll coating) concomitantly with 100 nM of BEZ235, for 6 hours, before the addition of cisplatin. After 6 hours, cisplatin logarithmic concentration curve was added and cells grown for 72 hours prior to MTT assay. Sigmoidal concentration-response curves were used to determine IC_{50} values.

Table 5. Cisplatin IC_{50} on MV3 cell line upon treatment with 100 nM BEZ235

Cell Density	Treatment	pIC_{50} ± SEM	IC_{50} (μM)
5000 cells / well	Cisplatin	4.98 ± 0.11	10.4
	100 nM BEZ235	5.27 ± 0.08	5.4
	BEZ235 + Mn^{2+}	5.40 ± 0.15	4.0
	BEZ235 + Coll	5.12 ± 0.06	7.6
	BEZ235 + Mn^{2+} + Coll	5.18 ± 0.04	6.6
10000 cells / well	Cisplatin	4.88 ± 0.32	13.2
	100 nM BEZ235	5.22 ± 0.31	6.0
	BEZ235 + Mn^{2+}	5.25 ± 0.28	5.7
	BEZ235 + Coll	5.12 ± 0.27	7.6
	BEZ235 + Mn^{2+} + Coll	5.23 ± 0.31	5.9

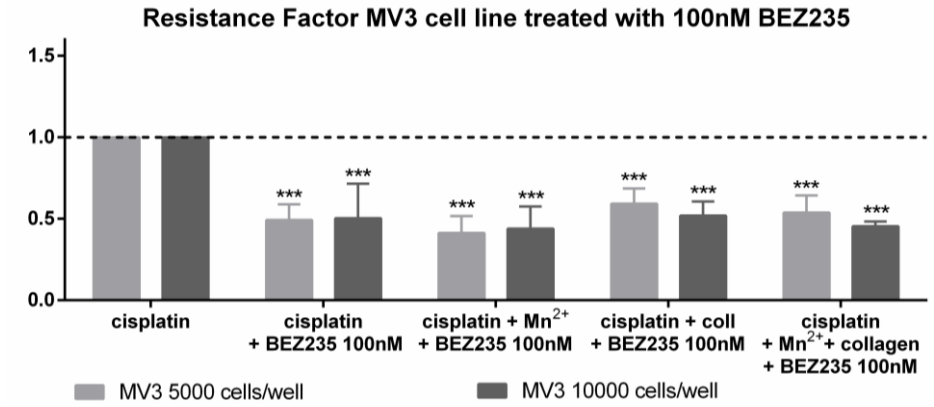

Figure 43. Change in resistance factors under PI3K inhibition with 100 nM BEZ235. Cells were seeded on Coll and/or 1 mM Mn^{2+}, then incubated for 6 hours with 100 nM BEZ235. After that, cisplatin logarithmic concentration curve was added and incubated for 72 hours, prior to MTT assay. Data was analysed by ANOVA; statistical significance in relation to control: * P<0.05; ** P<0.01; *** P<0.001. Extracted from Piva et al. (369).

The non-cytotoxic concentration of 100 nM of BEZ235 greatly increased cell sensitivity to cisplatin and reduced MV3 resistance factor to about 50%, which results from a synergy with cisplatin and not from the cytotoxic effect of BEZ235 alone. As mentioned above, the ability of other drugs to increase BEZ235 cytotoxicity, and even overcome the cell cycle arrest provoked by this inhibitor, has been show in previous reports (325–327). As observed above, BEZ235 was not only able to increase sensitivity to cisplatin, but also circumvent integrin-activating stimuli. On one hand, Mn^{2+} treated cells were slightly more affected, which is in line with their PI3K activation status shown by flow cytometry (Figure 40 and Figure 39). On the other hand, Coll showed a slightly protective effect against BEZ235, which is in accordance with the increase in the RFs observed in Figure 37. This also indicates that other signalling pathways, in addition to the PI3K pathway, might be involved in integrin-signal transduction upon activation by Coll, which has been seen in the flow cytometry data (Figure 40). This, associated with the fact that Mn^{2+} – Coll combination treatment, once again, demonstrated an intermediate response, reinforces the theory that these two integrin-activating stimuli have different mechanisms of action. In contrast, the concentration 500 nM of BEZ showed a high and unspecific cell cytotoxicity when combined with cisplatin.

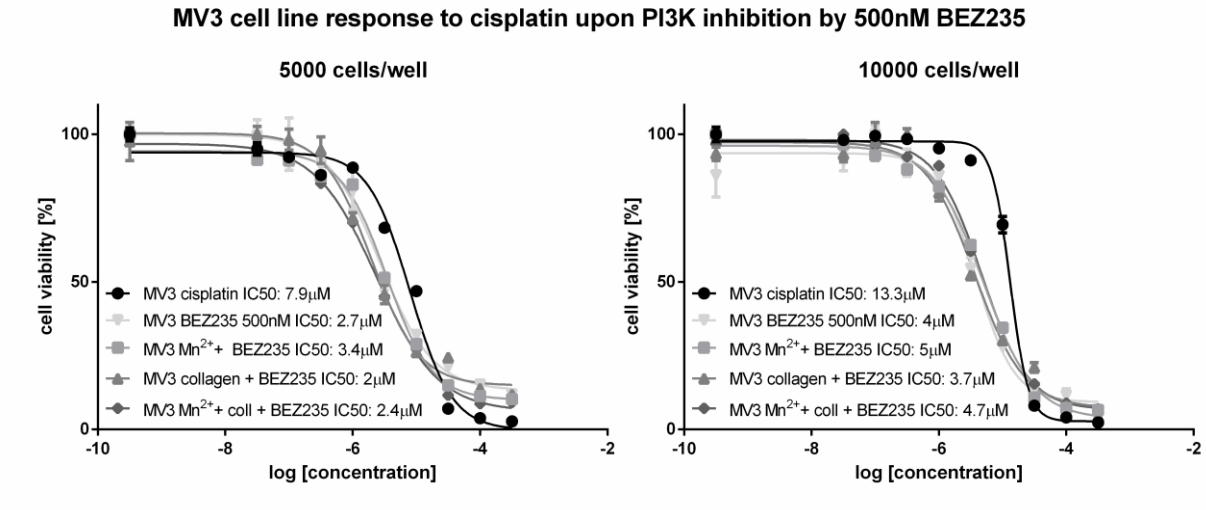

Figure 44. Sigmoidal concentration-response curves of MV3 cells treated 500 nM BEZ235. One of at least three measurements obtained by MTT assay is represented here. Cells were platted on Coll and/or incubated with a final concentration of 100 µM Mn^{2+} in well, before addition of 500 nM of PI3K inhibitor BEZ235 for 6 hours. Subsequently, cells were incubated for 72 hours with cisplatin logarithmic concentration curve. IC_{50} values were determined using the sigmoidal concentration-response curves.

Table 6. Cisplatin IC_{50} on MV3 cell line upon treatment with 500nM BEZ235			
Cell Density	**Treatment**	**pIC_{50} ± SEM**	**IC_{50} (µM)**
5000 cells / well	Cisplatin	5.13 ± 0.33	7.4
	500 nM BEZ235	5.52 ± 0.14	3.0
	BEZ235 + Mn^{2+}	5.44 ± 0.07	3.6
	BEZ235 + Coll	5.70 ± 0.07	2.0
	BEZ235 + Mn^{2+} + Coll	5.58 ± 0.12	2.6
10000 cells / well	Cisplatin	4.88 ± 0.32	13.2
	500 nM BEZ235	5.29 ± 0.10	5.1
	BEZ235 + Mn^{2+}	5.30 ± 0.04	5.0
	BEZ235 + Coll	5.36 ± 0.23	4.4
	BEZ235 + Mn^{2+} + Coll	5.29 ± 0.05	5.2

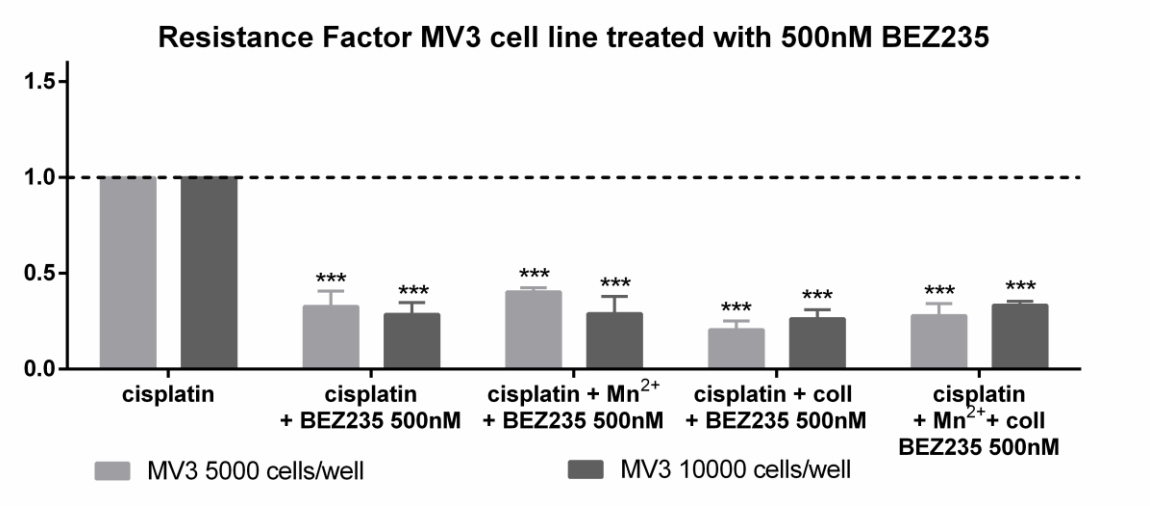

Figure 45. Effect of 500 nM of PI3K inhibitor BEZ235 on the resistance factor of MV3 cells. Cells were submitted to integrin activation by Coll or Mn^{2+} solution (1mM), prior to a 6-hour incubation period with 500 nM PI3K inhibitor BEZ235. Afterwards, plates were given a cisplatin logarithmic concentration curve, which was incubated with cells for 72 hours, before MTT quantification. ANOVA statistical test was performed; asterisks indicate statistical significance in relation to control: * P<0.05; ** P<0.01; *** P<0.001.

Interestingly, even though both cell densities were differently affected by BEZ235 alone, when associated with cisplatin, cells demonstrated equally high cytotoxicity, which demonstrates the advantage of a combination treatment, compared to the inhibitor alone. As it has been suggested by many reports, the biggest advantage of combinatory therapy is the ability to reduce drug concentration to achieve the same effect with lower side effects for the patient. More specifically, the 500 nM concentration of the PI3K inhibitor lead to high unspecific cytotoxicity and a massive gain in sensitivity in all treatment groups, reducing the RF of MV3 cells by 50-60%, independently of cell density. Despite the slight differences between the integrin

activation stimuli, the combination of cisplatin and inhibitor clearly overcomes cell cycle arrest and prevents the formation of the plateau observed for this concentration of inhibitor alone. This is in accordance with several previous reports that establish the synergy between BEZ235 and other platinum drugs and taxanes (325–327).

In summary, this highlights the relevance of PI3K signalling for cells to survive cisplatin treatment and suggests the blockade of PI3K to be a highly promising target to affect chemosensitivity of melanoma cells. This also impressively confirms the role of integrins in steering the cells into a chemoresistant state, the massive sensitization showed by the RFs 50% smaller than 1 supports our hypothesis.

Microscopy of β1 integrin-blocking antibody on MV3 cell line

The protective effect showed by Coll against BEZ235 associated with the fact that treatment with Coll was the most effective in increasing the RF, points to the involvement of the β1 integrin subunit, which is the main ligand to Coll, in the cisplatin chemoresistance phenomena of MV3 melanoma cells. Aiming to test this hypothesis, MV3 cells were grown on Coll-coated 24-well plates for 48 hours and then treated with 1.75µg/ml P5D2 β1 integrin-blocking antibody for 24 hours. Subsequently, cells were analysed by microscopy.

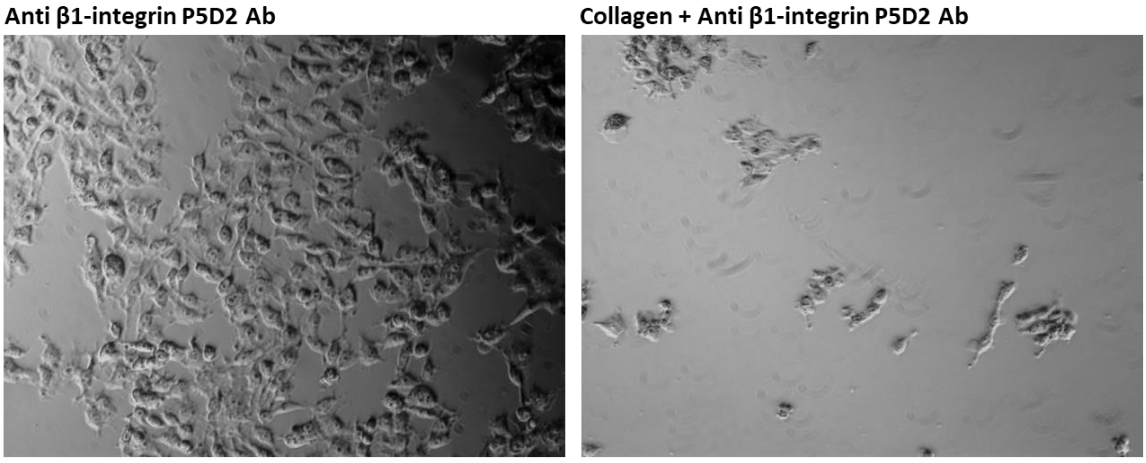

Figure 46. Microscopic images of MV3 wt treated with β1 integrin-blocking antibody. Exemplary pictures of one of at least three experiments. Cells were cultured for 48 hours, on 24-well plates, in the presence or absence of Coll coating. Then, cells were treated with 1.75µg/ml P5D2 β1 integrin-blocking anti-body for 24 hours, prior to microscopy analysis.

Data clearly shows that the antibody had a massive effect on cells platted on the Coll-coated surface, which corroborates the hypothesis that CAM-DR formation in MV3 is

mediated by β1 integrin through activation by Coll binding. This, taken together with our previous data which shows that Coll increases cells RF (Figure 37) by impacting cell signalling (Figure 39), led us to the conclusion that β1 integrin is one of the main factors responsible for cell adhesion-mediated cisplatin resistance in MV3 melanoma cell line.

MV3 β1 integrin kd cell line

β1 integrin knockdown on MV3 wt cells

After the promising results shown by the inhibition of β1 integrin by the P5D2 blocking antibody, the next logical step was to establish an MV3 mutant cell line with reduced expression of this integrin subunit. This was performed as described in the materials and methods section by a lentiviral approach and the resulting knockdown (kd) cells were called MV3 β1 integrin kd cell line. With the purpose of confirming the efficiency of the knockdown cells, they were submitted to western blot, as advised by the plasmid manufacturer, to measure the amount of β1 integrin in the kd cells in relation to the wild type (wt) MV3 cells.

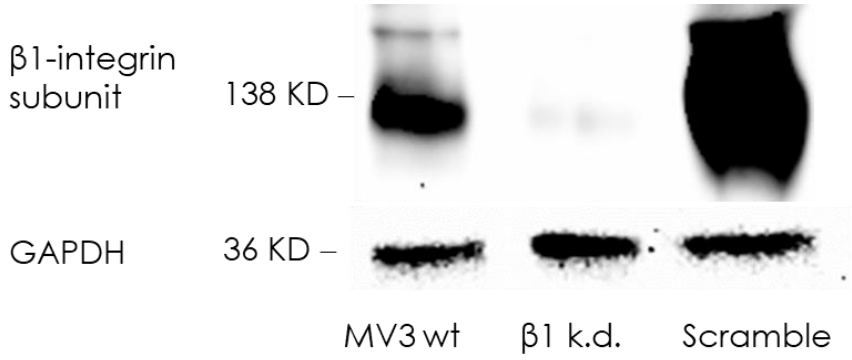

Figure 47. Western blot of MV3 β1-integrin kd to confirm downregulation. Exemplary picture represents one of at least three assessments. MV3 wt, MV3 β1-integrin kd and MV3 scramble cell lines were grown to 80% confluence, in uncoated cell flasks, before cell lysates were harvested and prepared for SDS page followed by western blot. Membranes were developed by chemiluminescence and analysed using ChemiDoc ™ XRS + system.

Wild type MV3 cells showed high levels of β1 integrin expression, while the protein could barely be detected in the knockdown cells. This confirmed that the cell transduction had massively reduced β1 integrin levels in the MV3 β1 integrin kd cells without any apparent changes in cell morphology or viability. However, MV3 scramble cells showed an unexpected increase in β1 integrin expression when compared to the wild type. We believe this to be the result of a random point integration.

A major disadvantage of delivery systems for stable transfections is that, even though constructs are engineered to avoid random integration in the genome of the cell, it can still occur and lead to undesirable effects, such as insertional mutagenesis or different levels of expression of shRNA, depending on the area of integration (316,371). As stated in the materials and methods chapter, the lentiviral particles were commercially acquired, thus the construct sequence is protected by intellectual property. The scramble lentivirus particles encode a non-targeted sequence, which works as negative control for targeted shRNA lentiviral particles, which possess the same construct, but several different knockdown targets. For this reason, it is possible that the scramble sequence has inserted itself in a different location in the cell genome other than the targeted knockdown.

Other experiments showed that the MV3 scramble cell line presents a completely different behaviour and protein expression than the wild type cells (data not shown). This associated with the western blot data, that clearly shows that the scramble sequence interferes with the expression of our target protein, β1 integrin; led us to the conclusion that a comparison between MV3 β1 integrin kd and MV3 scramble would not represent an accurate picture of cell behaviour and knockdown effect. For this reason, the effect of β1 integrin knockdown will be evaluated considering the wild type and not the scramble cells.

MV3 β1 integrin kd cell line sensitivity to cisplatin and integrin activating stimuli

To test the new cell line sensitivity to cisplatin, wild type MV3 and MV3 β1 integrin kd cells were submitted to MTT cell cytotoxicity assay.

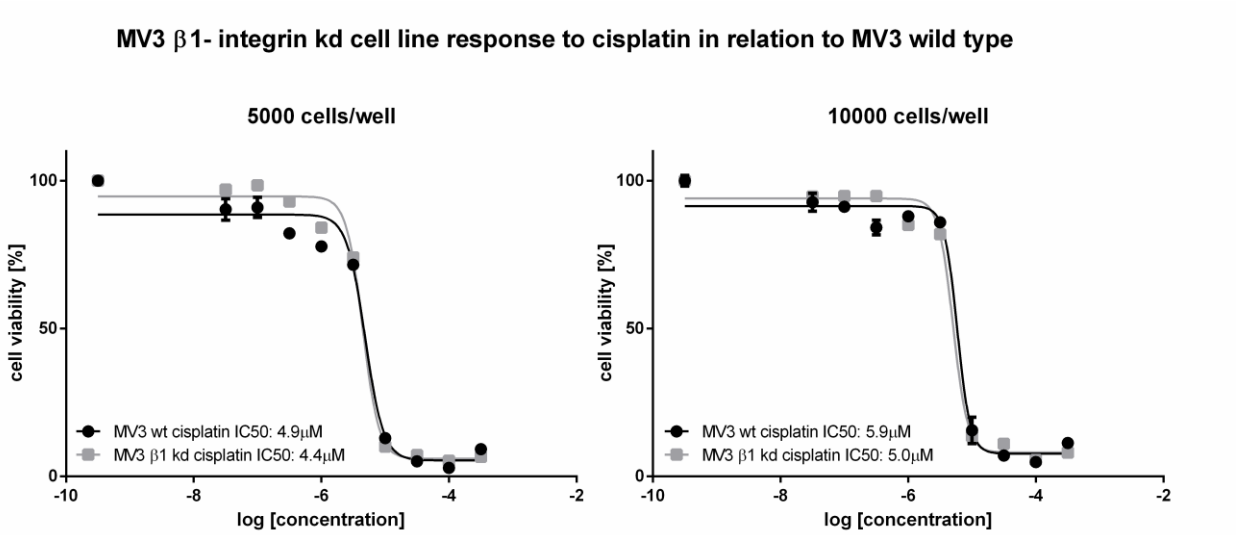

Figure 48. Impact of β1-integrin knockdown on sigmoidal concentration-response curves. Curves represent one of at least three MTT assays. The sensitivity of MV3 β1-integrin kd cell line to cisplatin was compared to the wild type after a 72-hour incubation period with drug logarithmic concentration curve. The sigmoidal concentration-response curves were used to determine IC_{50} values.

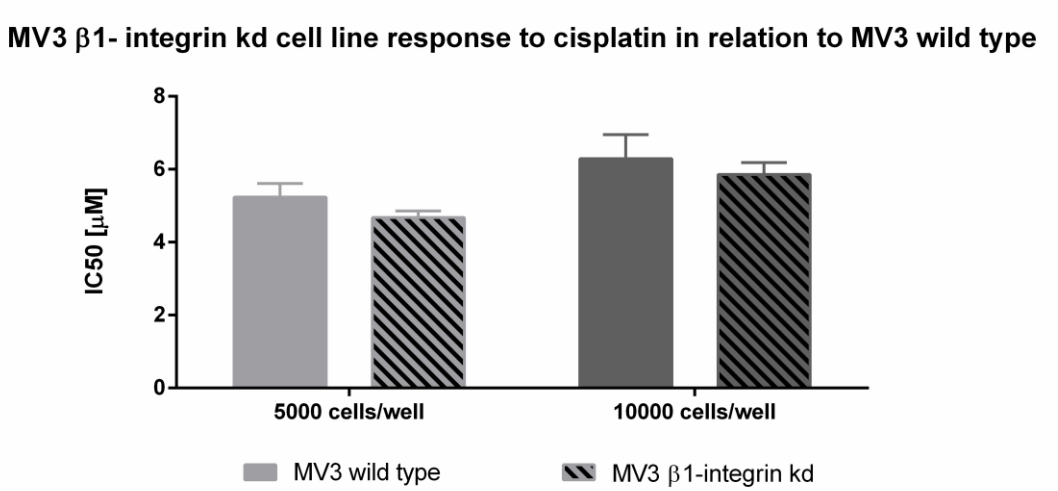

Figure 49. Evaluation of the cisplatin resistance factor of MV3 β1-integrin kd cells. Here represented mean value and SEM of IC_{50} values from each cell line obtained from at least three MTT experiments. One-way ANOVA statistical analysis was used; asterisks indicate statistical significance * P<0.05; ** P<0.01; *** P<0.001.

The knockdown of β1 integrin only led to a slight sensitization to cisplatin, compared to wild type cells. Since the β1 integrin by the P5D2 blocking antibody only showed an

effect when associated to Coll, this could also be the case for the MV3 β1 integrin kd cells. With the aim of testing if integrin activating stimuli would have an effect on such cells, they were grown on Coll-coated plates or treated with 1μM Mn^{2+} solution. Since, from the beginning, the combination of these treatments had constantly shown an intermediated response instead of a synergistic one, combinatory treatments were not performed in the knockdown cells.

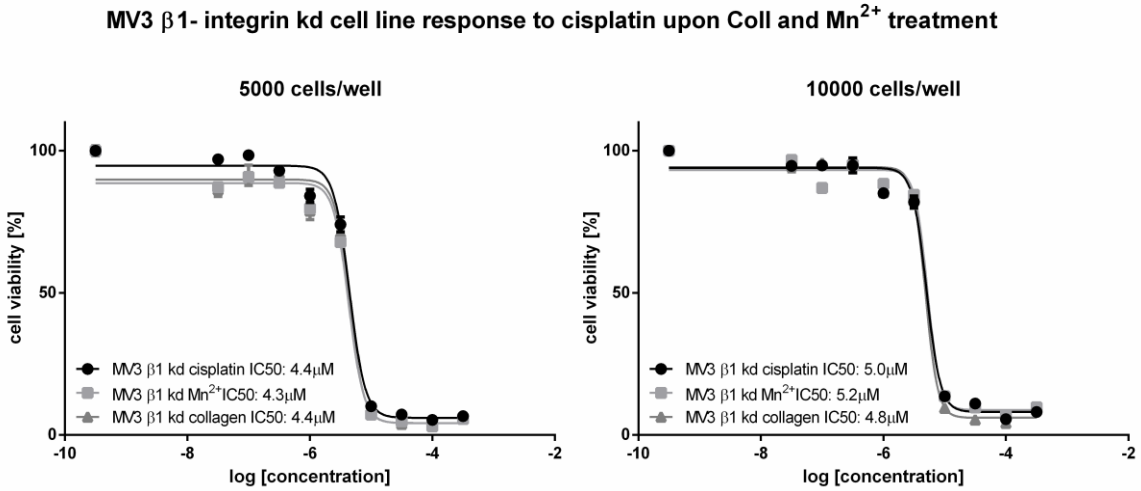

Figure 50. MV3 β1-integrin kd cell line sigmoidal concentration-response curves upon integrin activation by Coll and Mn^{2+}. Curves shown represent one of at least three assays. Cells were platted on Coll or incubated with a final concentration in well of 100 μM Mn^{2+}, then incubated for 72 hours with cisplatin logarithmic concentration curve. Cell sensitivity to the drug was assessed by quantifying the number of living cells using MTT assay. The data obtained was plotted into sigmoidal concentration-response curves and used to determine the IC_{50} values.

Table 7. Cisplatin IC_{50} on MV3 β1-integrin kd cell line upon Mn^{2+} and Coll treatment

Cell Density	Treatment	pIC_{50} ± SEM	IC_{50} (μM)
5000 cells / well	Cisplatin	5.38 ± 0.08	4.2
	Mn^{2+}	5.42 ± 0.07	3.8
	Collagen	5.42 ± 0.09	3.8
10000 cells / well	Cisplatin	5.24 ± 0.05	5.7
	Mn^{2+}	5.30 ± 0.02	5.0
	Collagen	5.29 ± 0.16	5.1

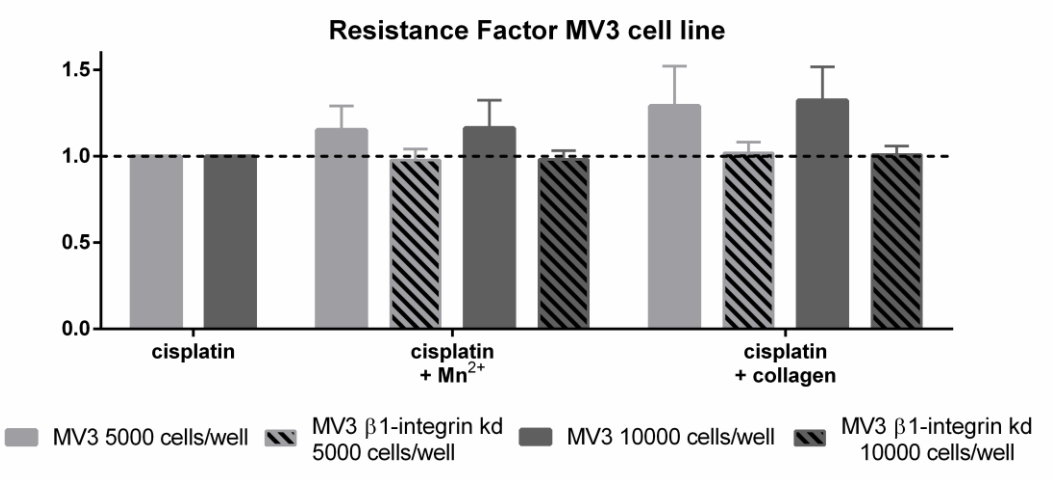

Figure 51. Resistance factors of MV3 β1-integrin kd after treatment with cisplatin concomitant to Coll or Mn^{2+}. Cells were submitted to MTT assay, after 72 hours of incubation with cisplatin under integrin activating stimuli 1 mM Mn^{2+} solution or Coll coating. The data displayed here correspond to the mean value and SD of the RF (ratio between IC_{50} of treated vs. untreated) of at least three measurements. One-way ANOVA statistical analysis was used; asterisks indicate statistical significance only in relation to cisplatin treated cells: * P<0.05; ** P<0.01; *** P<0.001.

While wild type cells presented statistically significant increase in the resistance factor on Coll-coated surfaces and slight increase upon Mn^{2+} treatment (Figure 37), MV3 β1 integrin kd cells were irresponsive to integrin activating stimuli. Even thought, the treatment with cisplatin alone had not been able to display a significant difference between wild type and β1 integrin knockdown cells, there was a possibility that this would change once integrins were activated through Coll coating or Mn^{2+} treatment. Unfortunately, this was not the case, while MV3 wt consistently exhibited an augmented cisplatin resistance when treated with integrin activators (Figure 37), we were neither able to replicate this in the MV3 β1 integrin kd cells, nor show an increase in cell sensitivity to cisplatin. These observations were difficult to accept considering that all the experimental evidence from the wild type cells points to a strong β1 integrin–Coll axis and the involvement of the two proteins in the resistance formation of these cells. For this reason, it became clear that further investigation was required, so, first we decided to compare the wild type cells and MV3 β1 integrin kd cells under the microscope on Coll-coated surfaces to the effects observed in the P5D2 β1 integrin-blocking antibody by microscopy.

β1 integrin kd affects cells differently than β1 integrin-blocking antibody

Although the previous data obtained with the wild type cells were quite promising and strongly indicated that β1 integrin was a key molecule in the chemoresistance of the cells upon Coll activation, the reduction in the resistance factor of MV3 β1 integrin kd cells was only slightly lower than the wild type MV3, and no response could be observed from the integrin activators. In order to gain a better understanding of the reasons for these somewhat disappointing data, MV3 β1 integrin kd and wild type cell lines were observed via microscopy. Cells were seeded on 24-well plates, with or without Coll coating, and grown for 72 hours and analysed via microscopy. Results were compared to the effect of the P5D2 β1 integrin-blocking antibody on MV3 wild type cells.

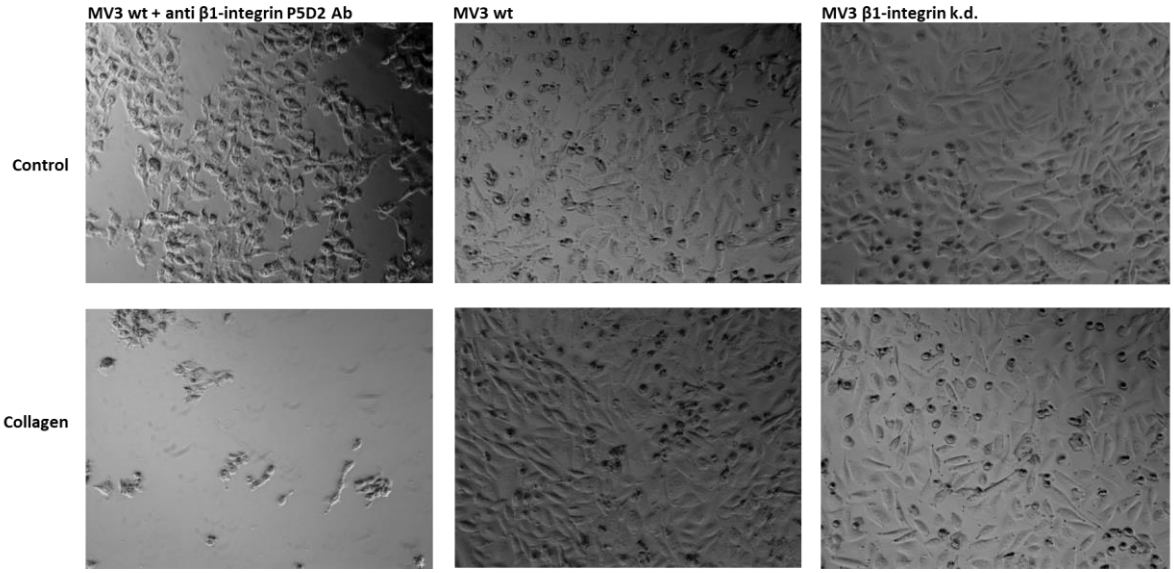

Figure 52. Microscopy images of MV3 β1 integrin kd. Knockdown and wild type MV3 cells were cultured on 24-well plates in the presence or absence of Coll coating and photographed after 72 hours. Pictures represent results observed in of one of at least three experiments.

It can be observed in the pictures that the considerable reduction of the β1 integrin did not provoke any apparent change in cell morphology or viability. Besides, β1 integrin kd cells seem to be slightly less confluent on the Coll surface, which could indicate that, similarly to the P5D2 β1 integrin-blocking antibody, integrin activation by Coll triggers cell signalling pathways that would usually be reinforced or carried forward by β1 integrin. Since this integrin is not present, the signal cannot be transmitted and it is difficult for cells to adhere, thus they proliferate less or die.

This is in accordance with above-mentioned literature that has linked β1 integrin to a more adhesive and proliferative cell-profile in normal and cancer cells (259–261).

Nevertheless, the phenotype provoked by P5D2 β1 integrin-blocking antibody definitely could not be observed, which is, unfortunately, in accordance with the only slight reduction on the RF value of the knockdown cells under cisplatin (Figure 49) and irresponsive to integrin activating stimuli observed in the MTT assay (Figure 50). A reason for the difference between β1 integrin knockdown and inhibition by antibody could be that, on one hand, knockdown cells suffer a genetic change that provokes cell-signal rewiring, which ensures cell survival. Moreover, these adaptive changes have taken place before cells come into contact with Coll. On the other hand, inhibition by antibodies is a quick environmental change that demands a rapid adaptive response from the cells. More importantly, cells were put into contact with Coll first and β1 integrin was blocked after a 24-hour adhesion period. This means that cells had been activated and were strongly relying on the Coll induced β1 integrin signalling, when it was suddenly interrupted, causing cell death. In order to investigate if the abovementioned integrin signalling rewiring did occur in the β1 integrin knockdown, cells were submitted to flow cytometry assay.

Evaluation of β1 integrin kd on the FAK/PI3K/AKT signalling pathway of MV3 cell line by flow cytometry

The unexpected data obtained from the MV3 β1 integrin kd cell line, more precisely, the inability of β1 integrin downregulation to sensitize cells to cisplatin, led us to investigate how integrin signalling had been affected by the knockdown. Moreover, up to this point, the evidence gathered pointed to the involvement of the FAK/PI3K/AKT cell-signalling pathway in the resistance formation of the wild type cells, so this pathway was investigated on MV3 β1 integrin kd cells as well, in the presence of cisplatin.

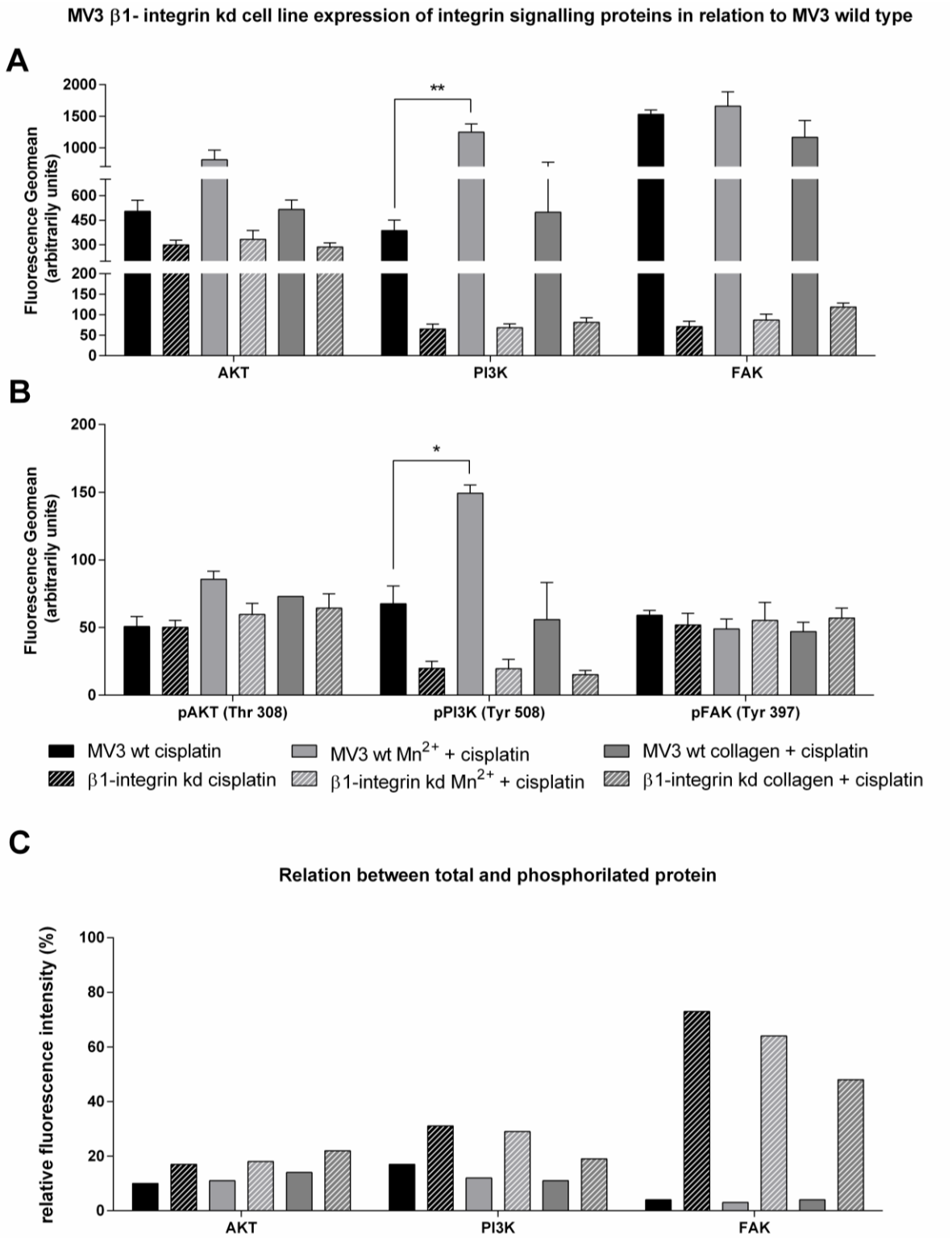

Figure 53. Changes on integrins signalling triggered by β1 integrin knockdown observed by flow cytometry. A. Total protein levels of AKT, PI3K and FAK. **B.** Levels of active AKT, PI3K and FAK. MV3 β1 integrin kd cells were either incubated with final concentration of 100 µM Mn^{2+} for 5 minutes or cultivated in Coll-coated or uncoated cell flasks before treatment with 7.5 µM cisplatin for 72 hours. Depicted, geomean and SEM obtained from at least three flow cytometry experiments. Asterisks indicate statistical significance calculated by ANOVA: * P<0.05; ** P<0.01; *** P<0.001. **C.** Representation of signalling pathway activation as relative comparison between the total and phosphorylated protein amounts in percentage.

Interestingly, we could observe a general reduction of total protein expression in the MV3 β1 integrin kd, while the phosphorylated forms of AKT and FAK remained the same as in the wild type cells. Moreover, the amount of active PI3K, which had been significantly increased in MV3 wt, was massively reduced in the absence of β1 integrin.

This indicates, first that β1 integrin downregulation puts cells under stress, which they try to compensate by increasing protein activation, as we can observe in Figure 53C, which shows the difference in the activation levels of cell signalling proteins between the two cell lines. In the wild type cell only approximately 4% of total FAK, 13% of total PI3K, and 12% of total AKT is activated, while in the knockdown cells, a much higher activation percentage can be observed: 60% for FAK, 26% for PI3K, 20% for AKT. Second, while in the wild cell the signalling is amplified from one effector to the other, in the β1 integrin deficient counterpart, the signalling fades, since activation decreases according to how downstream the effector is. These results indicate that there could be a compensation mechanism involved and that the activation seen could be initiated by other integrin subtypes that are unable to efficiently carry the message all the way to the nucleus. It has been discussed in the introduction of this work that the expression and cooperation between β1 and β3 integrins is a very complex and not completely understood cell mechanism; and that breast cancer cells have been shown to compensate for the downregulation β1 integrin with increased expression of β3 integrins (260). Thus, it is possible that this integrin subtype could be responsible for this compensation mechanism in MV3 β1 integrin kd cells as well, which was tested by submitting cell lysates to western blot.

β3 integrin expression on MV3 β1 integrin kd cell line

As discussed above, literature reports of cooperation and regulation between β1 and β3 integrins, led us to suspect the involvement of the later integrin subtype in a possible compensation mechanism. For this reason, we evaluated the wild type and β1 integrin kd MV3 cell lysates via western blot to assess the amount of β3 integrin present in these cells.

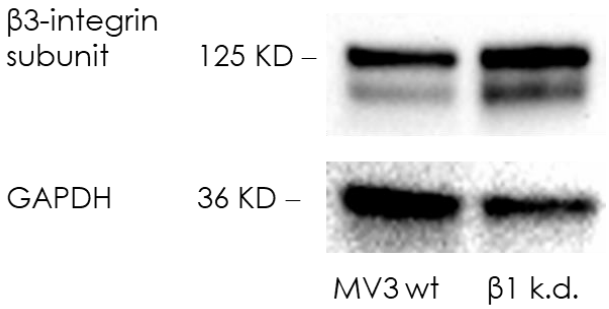

Figure 54. Expression level of β3-integrin subunit on MV3 β1-integrin kd cells obtained by western blot. The image shown represents one of at least three experiments. Cell lysates were obtained from 80% confluent cells, cultivated in uncoated cell flasks. SDS page followed by western blot, membranes analysis was performed as previously described.

The western blot data confirmed the increase of β3 integrin in the β1 integrin kd cell line, in relation to the wild type MV3. This compensation mechanism has been reported in breast cancer cells (260), it is an adaptive survival response that leads to the upregulation of a different integrin subunit to compensate for the integrin deficit. This explains the only slight reduction in the resistance factor in the knockdown cells and demonstrates the importance of β1 integrins for cells. Moreover, even though β3 integrin displays some protective effect against cisplatin, it does not achieve exact the same effect as β1 integrin, since cells were irresponsive to Mn^{2+} and Coll stimuli and PI3K signalling was reduced. This might result from the fact that β3 integrin preferable binding partner is vitronectin and not Coll (160). Besides, in order for β3 integrins to be able to attach to Coll, there must be an initial attachment made by β1 integrins that exposes the RGD binding site of Coll (191).

Cisplatin treatment changes protein profile of MV3 cell line

Alterations in integrin expression pattern of wild type MV3 cells caused by cisplatin

With the intention of looking for other interesting targets that could be involved in association with β1 integrin in resistance formation, cells were submitted to the Proteome Profiler ™ Human Soluble Receptor Array, which provides a broad view of cell membrane proteins expressed. Since cisplatin has been known to alter cell expression pattern (51,73,109), we looked into how cisplatin influences the integrin status in terms of general toxicity to the cells. Therefore, the assay was performed under the influence of cisplatin at a concentration of 7.5 µM.

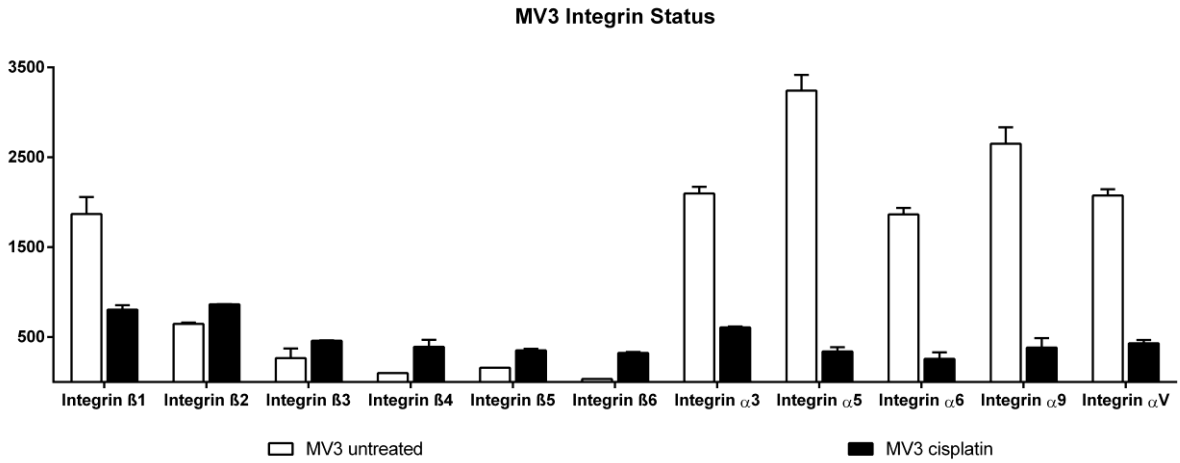

Figure 55. Impact of cisplatin treatment on the integrin status of MV3 melanoma cell line. Cells were incubated for 72 hours in the presence (white) or absence (black) of 7.5 µM cisplatin. Cell lysates were then submitted to Proteome Profiler ™ Human Soluble Receptor Array. Results of cisplatin-treated cells (white) were compared to untreated cells (black). Measurements were conducted in duplicates. Adapted from Piva et al. (369).

The array revealed a strong decrease in a great variety of proteins (data not shown) and a shift in integrin distribution among its subunits representing one of only a few up-regulations in proteins, under cisplatin treatment. Interestingly, the overall integrin expression pattern undergoes a shift in the sub-type expressions, during which there is a down-regulation of several of those integrin subunits, which are important for Coll binding, such as β1 and α3. All α-chains of integrins investigated were strongly down-regulated, while the ratio of β-chain containing integrins was, with exception of β1, upregulated. Integrin subunits β2, β3, β4, β5 and β6, which are barely detectable in untreated cells, were more strongly expressed under cisplatin stress. Cisplatin clearly alters the integrin expression pattern of MV3 cells, possibly indicating a direct link to

the different responses in cell sensitivity to cisplatin. For example, the decrease of Coll binding integrins β1 and α3 and shift to other integrin subtypes serves as first hallmark for the differences in integrin activation observed above (Figure 40).

Transformation of the syndecan profile of MV3 wt cells

Other proteins present in the Proteome Profiler ™ Human Soluble Receptor Array are syndecans-1 and 4. As explained above, cisplatin treatment led to a general downregulation of cell membrane proteins, which is an interesting contrast to flow cytometry results, presented in Figure 40, that show intracellular proteins upregulation and increased activation upon cisplatin treatment, as a survival adaptive response. This indicates that, under stress, cell machinery concentrates protein transcription efforts to express proteins that are essential to cell survival, mostly intracellular signalling molecules, but also a few crucial cell membrane proteins. As it was the case of syndecan-1, which was the only protein from the array that exhibited a statistically significant increase in expression upon cisplatin treatment.

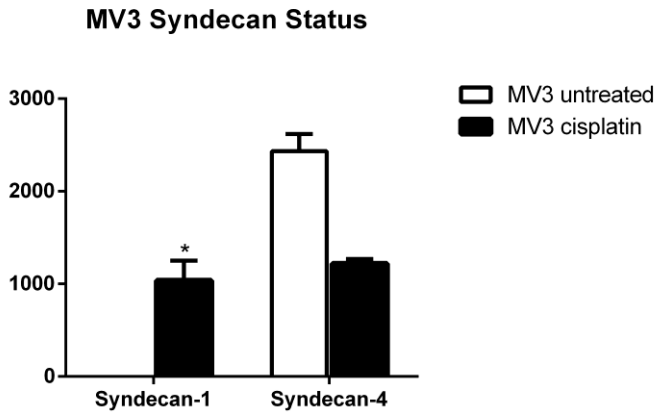

Figure 56. Cisplatin treatment alters syndecan profile of MV3 melanoma cell line. Cell lysates were harvested from untreated cells (white) or cells kept in the presence of 7.5μM cisplatin (black) for 72 hours. Results obtained with Proteome Profiler™ Human Soluble Receptor Array were analysed by comparing cisplatin-treated (black) to untreated (white) cells. Measurements were conducted in duplicates.

Interestingly, similar to integrin, the syndecan status showed a shift from the expression of exclusively syndecan-4, to the expression of about 50% syndecan-1, which demonstrates the importance of this proteoglycan for cell survival. As discussed in the introduction, both syndecan-1 and 4 have been shown to cooperate with β1 integrin in focal adhesions, and their aberrant expression has been associated with tumour malignancy respectively (270,273,274,281,282). Specifically, in breast cancer, syndecan-1 co-localization with α2β1 integrin enhances integrin-mediated adhesion through actin organization on Coll, in a heparan sulfate-dependent manner (247). However, syndecan-4 cooperation with β1 integrin in focal adhesion is the most understood and has been shown to be the most important combination for ECM-mediated cell survival (283). Actually, it was not until recently that it could be shown that syndecan-1 can also cooperate with several integrins (αvβ3, αvβ5, α2β1 α6β4) to form focal adhesions on vitronectin and laminin (273,274,281,282). In comparison with the results of the Proteome Profiler ™ Human Soluble Receptor Array, it is evident that the shift in syndecan expression pattern is intimately connected with the change in the integrin profile, since upregulation of syndecan-1 was followed by upregulation of its binding partners β3, β5 and β4 (Figure 55). The contrary being true for syndecan-4 and β1 integrin, as well. Thus, these two syndecans would definitely be involved in the CAM-DR phenomena triggered by integrins.

MV3 Syn-4 kd cell line

Syndecan-4 knockdown on MV3 wt cells

As observed above, upon cisplatin treatment MV3 cells showed a diversification in their syndecan profile (Figure 56). There was a reduction in syndecan-4 expression of about 50%, with a simultaneous increase of approximately 50% in syndecan-1 expression. With the purpose of evaluating if syndecan-1 alone could still trigger cell resistance to cisplatin, we used the MV3 syndecan-4 knockdown (MV3 Syn-4 kd) cell line, stablished in our group as described in methods.

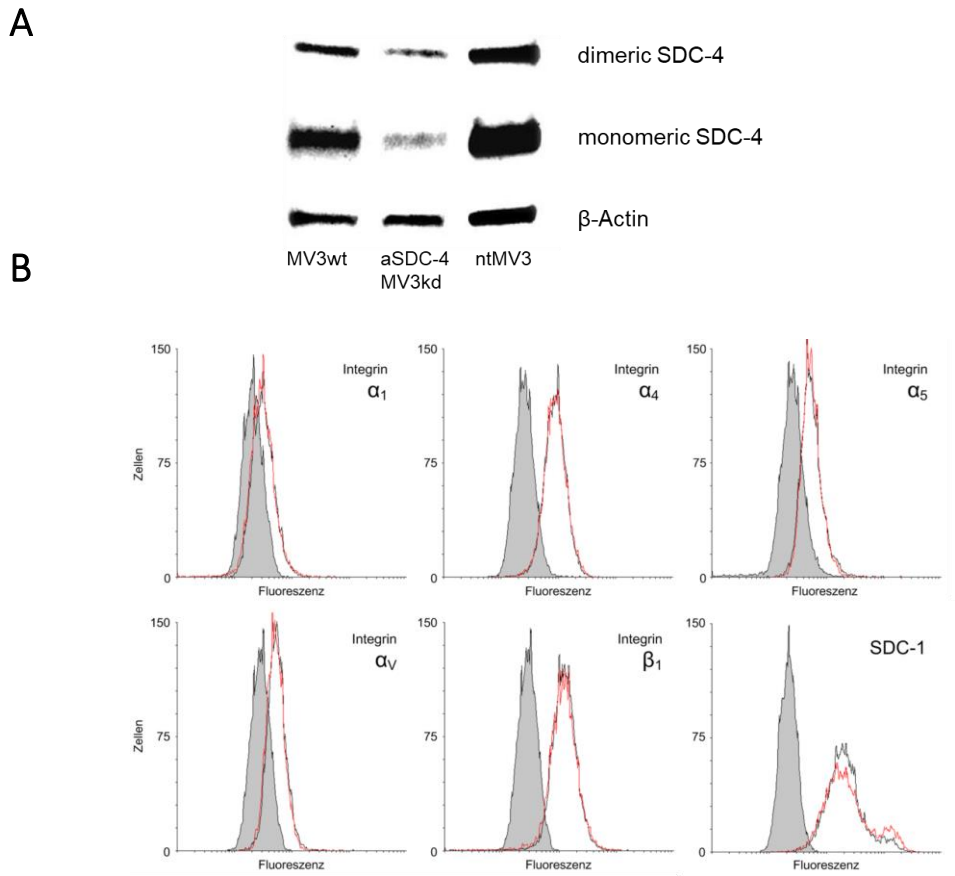

Figure 57. Establishment of MV3 syndecan-4 knockdown cell line and cell functional consequences. **A.** Knockdown confirmation by western blot. MV3 Syn-4 kd cells (aSDC-4 MV3kd) were compared to MV3 wt and MV3 negative control (ntMV3) with respect to syndecan-4 expression. SDC-4 monomer 32 kDa, SDC-4 dimer 68.2 kDa, β-actin 42k Da. **B.** Flow cytometry data to determine the impact of syndecan-4 knockdown on the expression pattern of different integrin subunits and syndecan-1. The grey peak represents the secondary antibody control, MV3 wt is represented in black and MV3 Syn-4 kd cells in red. Adapted from Gerber et al. (315).

As demonstrated by our group, syndecan-4 knockdown reduced target protein expression without interfering in the syndecan-1 or integrin profile of the cells (315,372). As discussed above, syndecans are a known co-receptor for numerous integrins, syndecan-4, particularly, has been associated with focal adhesion complexes formation and mediating adhesive and migratory capacities (270). For this reason, the syndecan profile shift caused by cisplatin seemed strange, but gave us the opportunity to investigate if syndecan-1 alone is capable of maintaining the resistant phenotype.

Syndecan-4 kd increases cell sensitivity to cisplatin

First, MV3 Syn-4 kd cells were submitted to MTT assay aiming to demonstrate their response to cisplatin in relation to the wild type cell line and a negative control. MV3 NT represents the negative control for the MV3 Syn-4 kd cells similar to the MV3 scramble cell line. NT stands for non-transfecting plasmid.

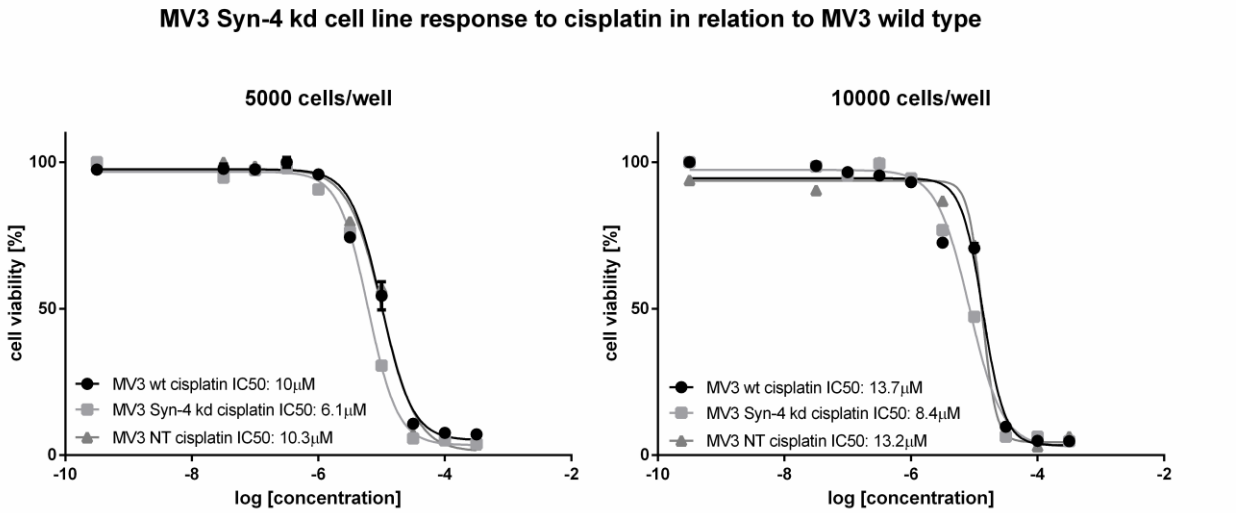

Figure 58. MV3 Syn-4 kd cell line sigmoidal concentration-response curve in response to cisplatin cytotoxicity. MV3 Syn-4 kd cell line sensitivity to cisplatin was assessed in relation to MV3 wt and negative control MV3 NT. Exemplary curves that represent one of at least three measurements obtained by MTT assay. Cells were left to adhere over night after seeding. In the following day, cisplatin logarithmic concentration curve was added and incubated for 72 hours. Sigmoidal concentration-response curves were used to estimate IC_{50} values.

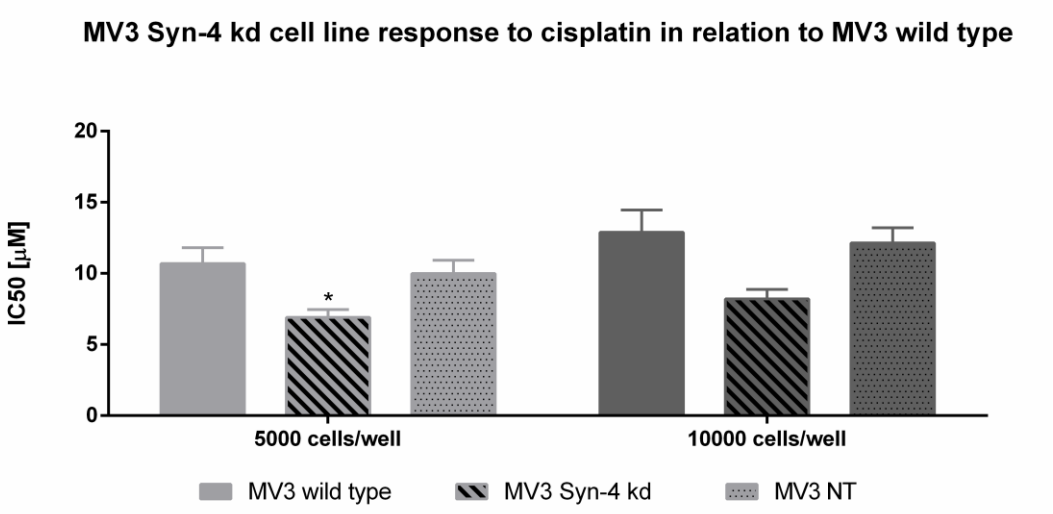

Figure 59. MV3 Syn-4 kd cell line sensitivity to cisplatin. Sensitivity of all three cell lines to cisplatin is represented using the mean value and SEM of IC_{50} values from at least three MTT concentration-response curves. ANOVA statistical analysis was used to calculate statistical significance, which is indicated by asterisks: * P<0.05; ** P<0.01; *** P<0.001.

The data clearly indicated that the knockdown of syndecan-4 increased cell sensitivity to cisplatin treatment. This impressively illustrated, on the one hand, that syndecan-1 alone cannot maintain the resistant phenotype, and on the other hand, the importance of syndecan-4 itself, possibly in triggering integrin activity and the role of integrins in the resistance phenomena in MV3. Since the MV3 NT positive control cell line consistently presented the same behaviour as the wild type cells in this and other works (315,372), we decided it was safe to carry out the integrin activating experiments only with MV3 wt and Syn-4 kd cell lines.

MV3 Syn-4 kd cell line sensitivity to cisplatin upon integrin activating stimuli

The results presented above show that cisplatin treatment induced a change in the pattern of syndecan expression in the wild type MV3 cells (Figure 56). Under cisplatin stress, cells reduced their expression of syndecan-4 and upregulated the expression of syndecan-1, which indicated that this specific proteoglycan sub-type is important for cell survival under these conditions. However, we could also show that syndecan-4 also plays a role in this phenomenon, since cells deficient in this proteoglycan sub-type were more sensitive to cisplatin. Integrin – syndecan cooperation and synergy has been discussed throughout this work and is well stablished in literature, the best understood example being the cooperation of β1 integrins and syndecan-4 in focal adhesions (283). Since our main goal was to investigate the mechanisms of CAM-DR and the role of integrins in this process, the next step was to determine the impact of syndecan-4 loss in the activation of integrins in cells treated with cisplatin.

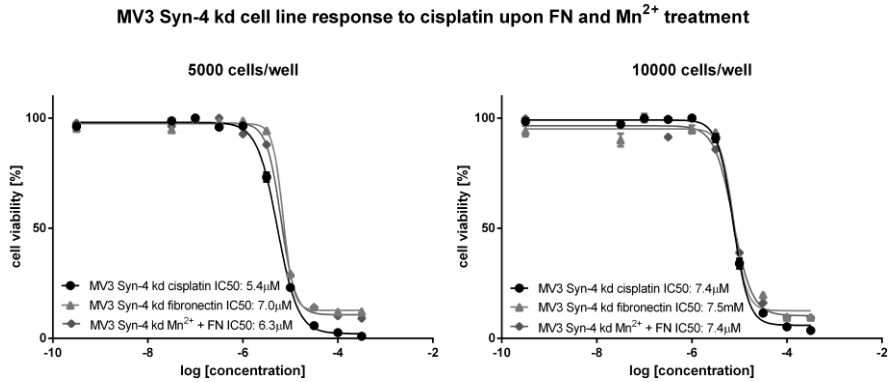

Figure 60. MV3 Syn-4 kd cell line response to integrin activation by FN and Mn^{2+}. Sigmoidal concentration-response curves are representative of one of at least three MTT experiments. Cells were platted on FN and, sometimes, incubated with a final concentration in well of 100 μM Mn^{2+} previous to a 72-hour incubation period with cisplatin logarithmic concentration curve. Sigmoidal concentration-response curves were used to estimate IC_{50} values.

Table 8. Cisplatin IC_{50} on MV3 Syn-4 kd cell line upon Mn^{2+} and FN treatment			
Cell Density	**Treatment**	**pIC_{50} ± SEM**	**IC_{50} (µM)**
5000 cells / well	Cisplatin	5.24 ± 0.05	5.8
	Fibronectin	5.19 ± 0.05	6.4
	Mn^{2+} + FN	5.17 ± 0.03	6.7
10000 cells / well	Cisplatin	5.13 ± 0.14	7.5
	Fibronectin	5.10 ± 0.05	7.9
	Mn^{2+} + FN	5.13 ± 0.16	7.4

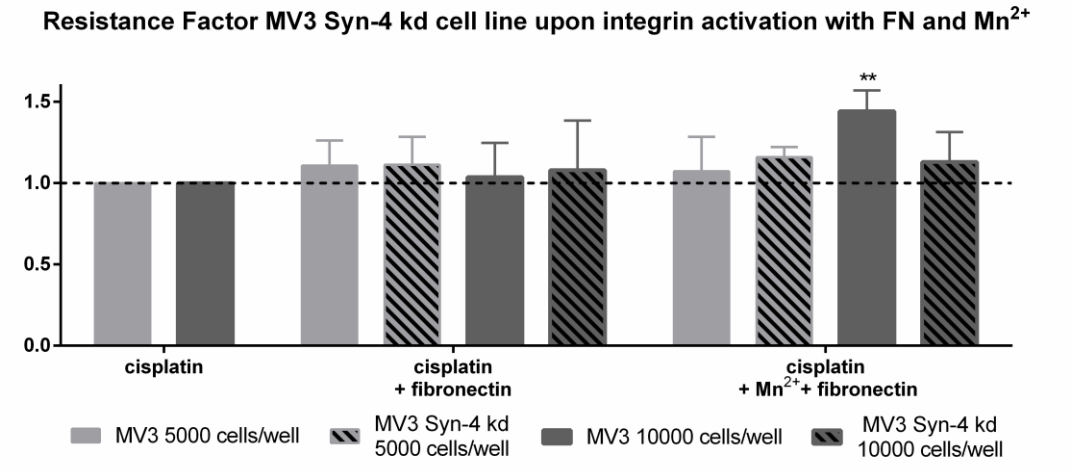

Figure 61. Integrin activation by FN and Mn^{2+} in MV3 Syn-4 kd cells. IC_{50} values of each measurement were used to estimate the resistance factor (ratio between IC_{50} of treated *vs*. untreated cells). The results shown here correspond to the mean value and SD of the RF of at least 3 assessments. ANOVA statistical analysis was used; asterisks indicate statistical significance in relation to cells treated solely with cisplatin: * P<0.05; ** P<0.01; *** P<0.001.

MV3 Syn-4 cells were able to increase their resistance factor to the same levels as the wild type cells in almost all cases. The data clearly indicates that the sensitization induced by knockdown of syndecan-4 could be reverted, in most cases almost completely, by external integrin activating stimuli. This suggests that syndecan-4 is not required for integrin interaction, activation and resistance formation in the presence of FN, possibly because several different integrin subtypes can bind to FN, and syndecan-1 has shown to have a more diverse integrin biding profile, than syndecan-4. As previously mentioned, syndecan-4 has been shown to cooperate with β1 integrins in focal adhesions, including to Coll, which is the main binding partner for these integrin subtypes (283,373). In order to investigate the effect of this ligand, the MTT assay was performed with Coll-coated plates.

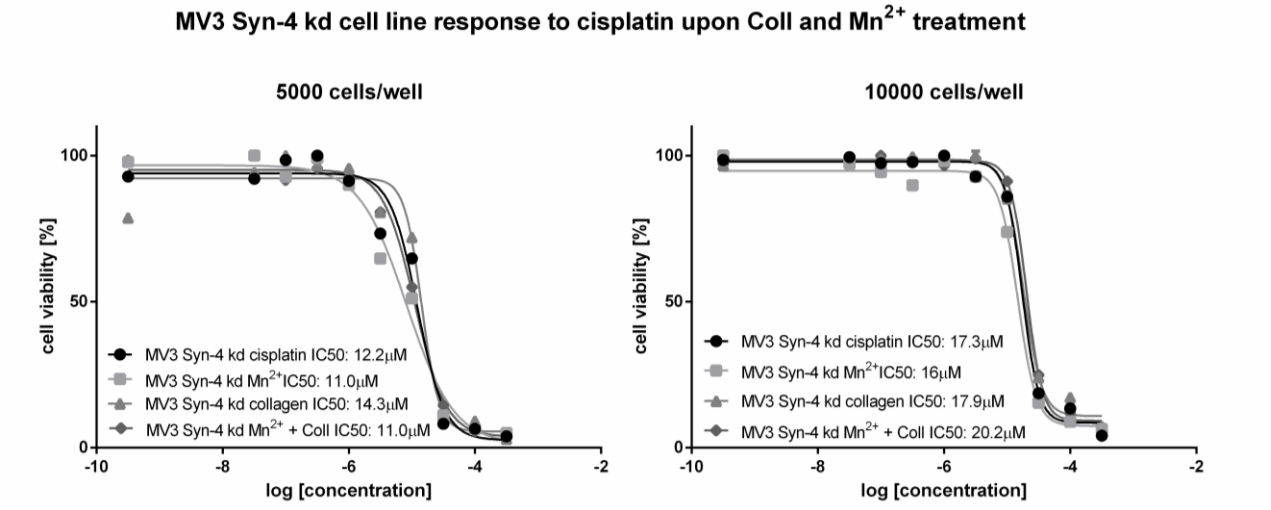

Figure 62. Sigmoidal concentration-response curves of MV3 Syn-4 kd cell line in response to cisplatin in the presence of Coll and Mn^{2+}. Exemplary curves that represent one of at least three MTT assays. Cells were submitted to cisplatin activating stimuli Coll coating and/or incubation with Mn^{2+}, before a 72-hour incubation with cisplatin logarithmic concentration curve. The IC_{50} values were calculated from the sigmoidal concentration-response curves obtained.

Table 9. Cisplatin IC_{50} on MV3 Syn-4 kd cell line upon Mn^{2+} and Coll treatment

Cell Density	Treatment	pIC_{50} ± SEM	IC_{50} (µM)
5000 cells / well	Cisplatin	4.87 ± 0.08	13.5
	Mn^{2+}	4.94 ± 0.16	11.5
	Collagen	4.85 ± 0.11	14.2
	Mn^{2+} + Coll	4.89 ± 0.10	12.8
10000 cells / well	Cisplatin	4.70 ± 0.28	20.1
	Mn^{2+}	4.61 ± 0.29	24.61
	Collagen	4.66 ± 0.27	22.0
	Mn^{2+} + Coll	4.68 ± 0.11	21.0

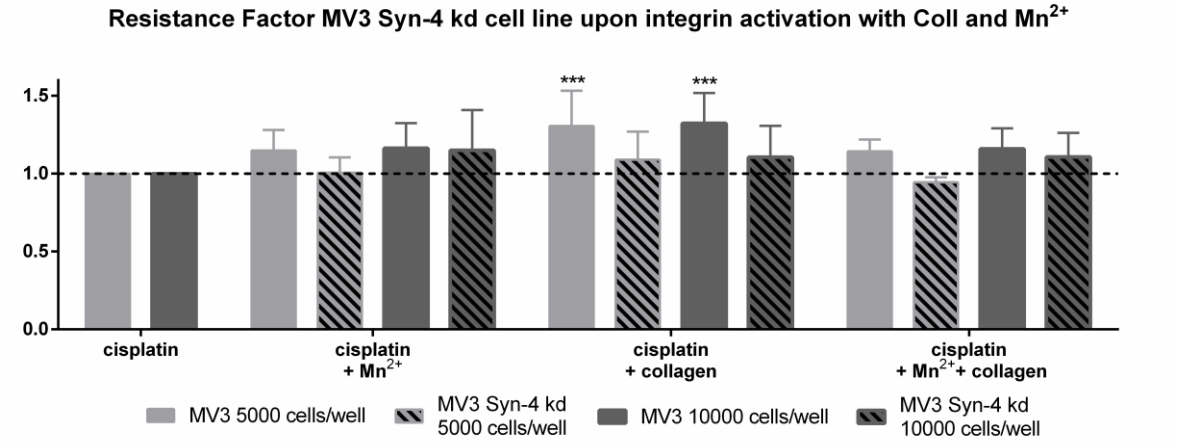

Figure 63. Impact of integrin activation by Coll and Mn^{2+} on the resistance factors of MV3 Syn-4 kd cells. IC_{50} values of each measurement were used to calculate the resistance factor (RF) as indicator of sensitivity to cisplatin cytotoxicity. Graph represents mean value and SD of the RF of at least three measurements, analysed using ANOVA statistical test in relation only to cisplatin-treated cells; asterisks indicate statistical significance: * P<0.05; ** P<0.01; *** P<0.001.

Indeed, it can be observed that Coll treatment had an inferior impact on increasing the resistance factor of MV3 Syn-4 kd cell. Even though Coll increased knockdown cell resistance factors, RFs on Coll were lower than on FN and did not reach the same activation levels as MV3 wt. Coll was not able to cause on MV3 Syn-4 kd the same effect it has on wild type cells. This might be a result of the integrin pattern shift we also observed in the array (Figure 55). It showed that although MV3 cells have a high β1 integrin expression, this specific subunit is downregulated upon cisplatin stress. Since β1 integrin is the main cell ligand to Coll, its reduction, combined with syndecan-4 deficiency, makes it harder for this ECM protein to induce resistance.

Curiously, Mn^{2+} treatment was only able to compensate for the lack of syndecan-4 on the higher cell count, even in the presence of Coll, which is unsurprising, considering the results of Mn^{2+}-Coll combinatory treatment observed so far. Most likely, the outcome of the higher cell density is not a reflex of Mn^{2+} itself, but rather of the cell-cell contacts facilitated by the physical proximity among the cells. As explained before, the Proteome Profiler ™ Human Soluble Receptor Array allows for the evaluation of many different cell membrane proteins, some of which could be involved in the result observed in the higher cell count.

Evaluation of FAK/PI3K/AKT signalling pathway on MV3 Syn-4 kd cell line by flow cytometry

The intriguing data presented above led us to investigate the underlying cell-signalling pathways. Flow cytometry experiments were performed aiming to evaluate the cell integrin-signalling behaviour of MV3 Syn-4 kd cells under cisplatin stress.

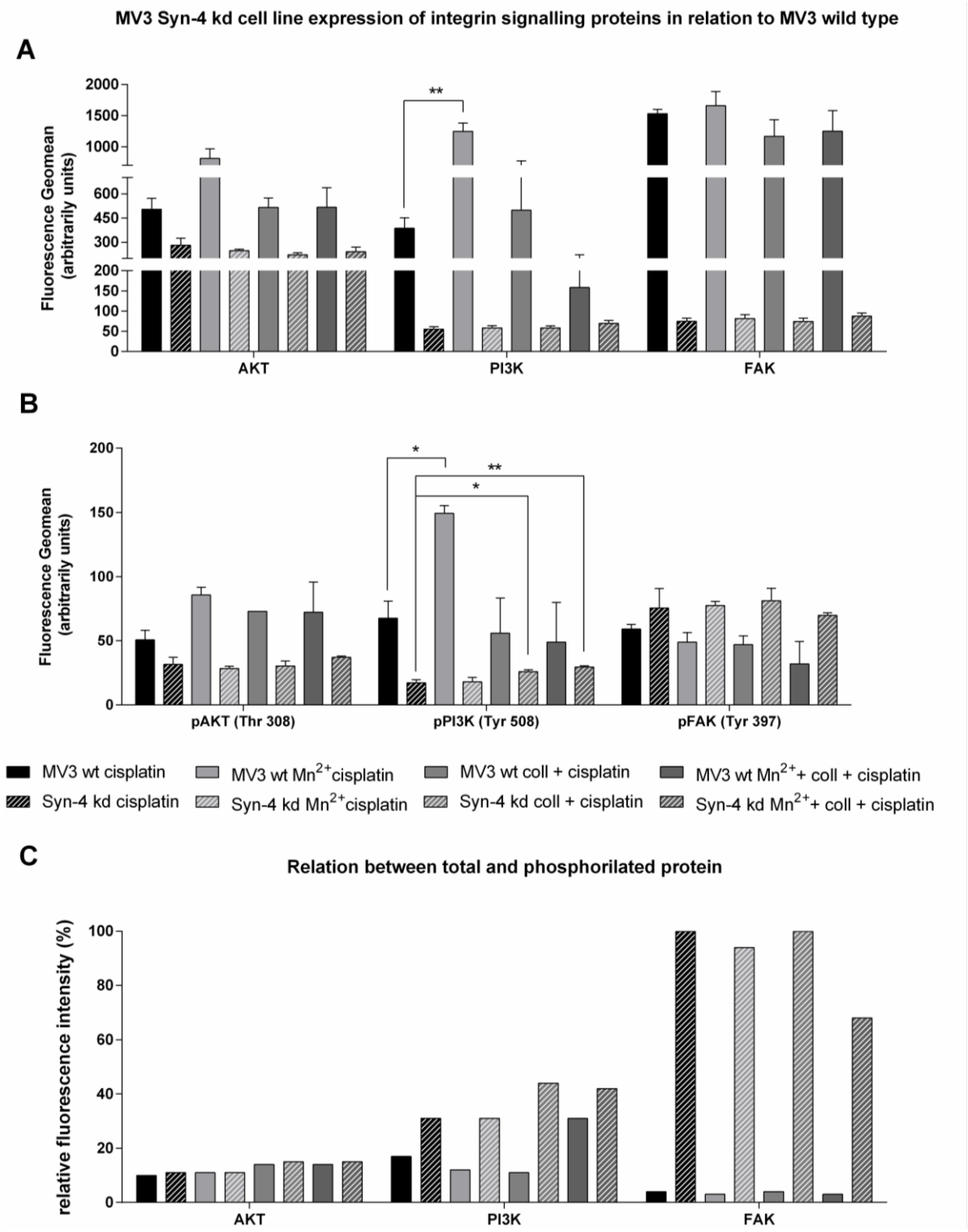

Figure 64 Flow cytometry data corresponding to integrin signalling proteins on MV3 Syn-4 kd cell line. A. Total protein levels of AKT, PI3K and FAK. **B.** Levels of phosphorylated AKT, PI3K and FAK, active form of the effectors. MV3 Syn-4 kd cells were grown on culture flasks, either coated with Coll or uncoated. After that, depending on treatment, incubated with 1 mM Mn^{2+} solution for 5 minutes, prior to addition of 7.5µM of cisplatin and incubation for 72 hours. Flow cytometry results are represented as geomean and SEM of at least 3 assays. Statistical significance between treatments was calculated using ANOVA and symbolized by asterisks: * P<0.05; ** P<0.01; *** P<0.001. **C.** Depicts the quotient of the total and phosphorylated protein amounts of integrin signalling effectors, which corresponds to perceptual activation of each molecule.

As expected MV3 Syn-4 kd cells show a lower expression and activation of the PI3K/AKT signalling pathway compared to wild type cells. As previously discussed, this results from the deficiency of an important integrin-binding partner, syndecan-4, that contributes to integrin activation in an outside-in, e.g. integrin clustering, as well as, an inside-out manner. From the data gathered so far, we can conclusively state that syndecan-4 is an important integrin partner, whose absence impacts the formation of cell resistance against cisplatin. The lack of this proteoglycan leads to decreased integrin activation and signalling, and consequently, a cisplatin-sensitive phenotype.

Similar to the β1 integrin knockdown, the amount of phosphorylated FAK is higher in Syn-4 kd cells than in their wild type counterpart. This could be observed independently of integrin-activating treatment, which indicates that this is a specific adaptive response to the Syn-4 deficiency. Moreover, in the wild type cells only a small percentage of the expressed FAK is activated, while in the knockdown cells, 100% of the expressed FAK is activated into phosphorylated form. This shows that the cells are desperately trying, without success, to initiate the FAK/PI3K/AKT survival signalling pathway, through integrin activation, with the purpose of enduring cisplatin stress. However, this signal cannot be transmitted to the downstream effectors PI3K and AKT, and to the nucleus, due to the absence of specific activating kinases such as PDK1 and mTORC2. This is because syndecan-4 is responsible for recruiting these kinases to the cell membrane where they can interact with AKT and the phosphate donor PIP3, formed by PI3K (304,309). As explained in the introduction, for AKT full activation this protein must be phosphorylated in two critical residues, namely T308 and S473, by PDK1 and mTORC2, respectively. Syndecan-4 mediates the recruitment of these kinases to the cell membrane, thus indirectly regulating AKT phosphorylation (286–288). Accordingly, when we compare the relative activation of FAK, PI3K and AKT in the Syn-4 kd cells, it becomes evident that the integrin survival signal gradually fades away at every step of the pathway due to lack of signalling supporting molecules such as the above-mentioned kinases. These results are not only in accordance with previous reports, but also corroborate what was observed in the previous MTT assay (Figure 63), where Coll was not able to re-establish knockdown cell resistance.

Impact of PI3K/AKT pathway inhibition by BEZ235

In face of this data, further investigation into the role of PI3K/AKT signalling pathway in these cells was needed. The PI3K inhibitor BEZ235 was used for this purpose. First, a cytotoxicity assay was performed to ensure the cells would be treated with the right dose of inhibitor.

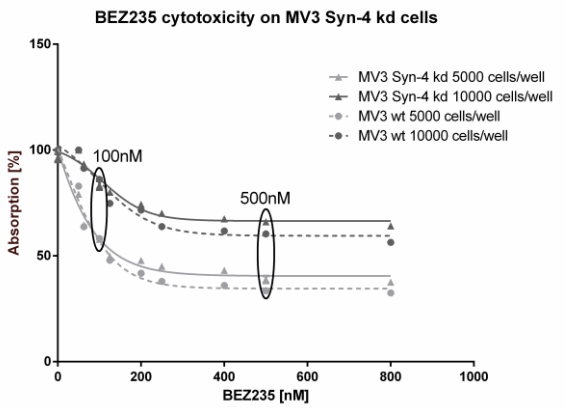

Figure 65. BEZ235 cytotoxicity on MV3 Syn-4 kd cell line. Representation of one of at least three measurements. Cell sensitivity to PI3K inhibitor BEZ235 was obtained by incubating cells for 72 hours with a series of concentrations of the inhibitor before MTT cytotoxicity assay.

Fortunately, MV3 Syn-4 kd cells had a similar response as the wild cells to the PI3K inhibitor BEZ235. They showed an IC_{50} of approximately 200 nM for the lower cell count and a plateau at the higher cell count, possibly as a consequence of the ability of BEZ235 to induce a cell cycle arrest (308). Therefore, the dose previously used for the MV3 wild type cells could be used to treat the knockdown cells. Thus, cells were submitted to MTT assay with two different concentrations of BEZ235 (500 nM and 100 nM) under the same conditions as wild type cells, with Coll and Mn^{2+} used as integrin activating stimuli. Unfortunately, the higher concentration of 500 nM BEZ235 showed a high unspecific cytotoxicity when combined with cisplatin, which did not allow experiments to be conducted with this dosage of inhibitor. The non-cytotoxic concentration of BEZ235, however, showed interesting results.

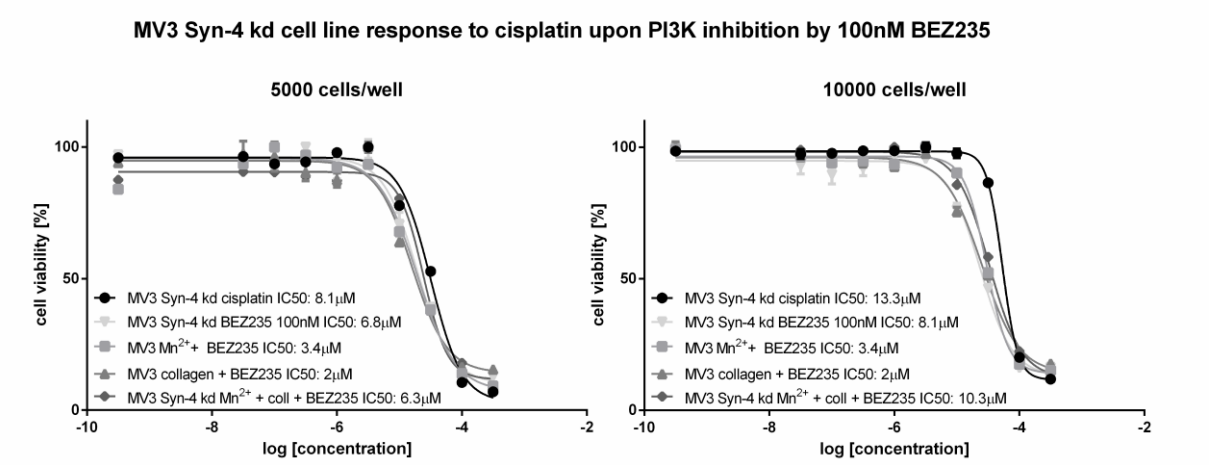

Figure 66. MV3 Syn-4 kd cell line sigmoidal concentration-response curves upon PI3K inhibition. One of at least three MTT curves obtained is represented here. Cells were incubated with integrin activators (Mn^{2+} or Coll) concomitantly with 100 nM of PI3K inhibitor BEZ235 for 6 hours, before the addition of cisplatin logarithmic concentration curve. MTT assay was performed after 72 hours and results used to draw the sigmoidal concentration-response curves used to determine IC_{50}.

Table 10. Cisplatin IC_{50} on MV3 Syn-4 cell line upon treatment with 100nM BEZ235

Cell Density	Treatment	pIC_{50} ± SEM	IC_{50} (μM)
5000 cells / well	Cisplatin	4.87 ± 0.08	13.5
	100nM BEZ235	4.96 ± 0.14	11.0
	BEZ235 + Mn^{2+}	4.97 ± 0.16	10.7
	BEZ235 + Coll	5.01 ± 0.17	9.7
	BEZ235 + Mn^{2+} + Coll	4.97 ± 0.20	10.8
10000 cells / well	Cisplatin	4.70 ± 0.28	20.1
	100nM BEZ235	4.90 ± 0.27	12.6
	BEZ235 + Mn^{2+}	4.95 ± 0.34	11.3
	BEZ235 + Coll	4.91 ± 0.36	12.2
	BEZ235 + Mn^{2+} + Coll	4.84 ± 0.24	14.5

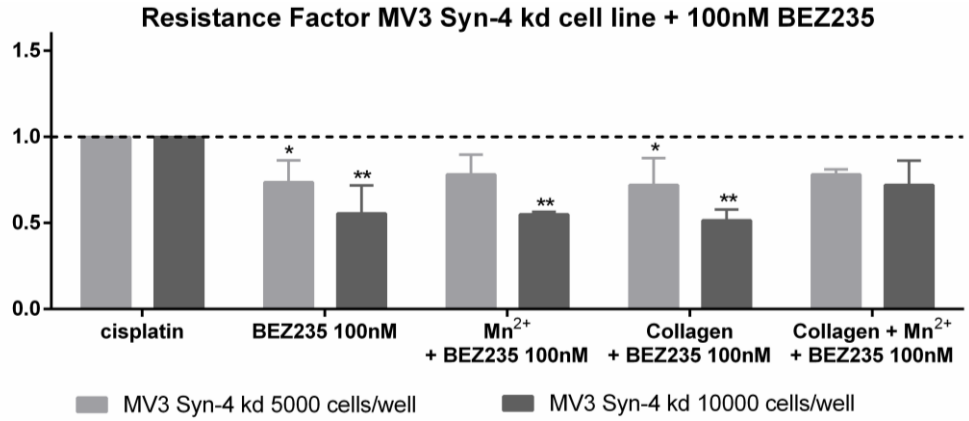

Figure 67. Impact of PI3K inhibition on the resistance factors of MV3 Syn-4 kd cell line. Integrin activating stimuli was given to the cells prior to a 6-hour incubation period with 100 nM BEZ235. Subsequently, cells were kept on cisplatin logarithmic concentration curve for 72 hours until MTT assay. Represented mean value and SD of the RF of at least three experiments. Asterisks indicate statistical significance calculated by ANOVA: * P<0.05; ** P<0.01; *** P<0.001.

As expected, in spite of the non-cytotoxic concentration of 100 nM of BEZ235 still being able to sensitize MV3 Syn-4 kd cells, the reduction of the resistance factors was smaller than that of the wild type cells, and greatly dependent on cell density. In the previous MTT (Figure 63), the high cell count facilitated the increase of the resistance factor in the absence of syndecan-4, due to physical proximity and cell–cell contact. This shows that the low cell density was more affected by the reduction of Syn-4. Thus, cell seeding at 5000 cells per well showed a lower sensitivity to BEZ235, with a reduction of 20-25% in the resistance factors, as a consequence of cell adaptation to syndecan-4 deficiency through rewiring of signalling pathways to decrease dependency on PI3K/AKT signalling. Conversely, the higher cell count, which was able to partially compensate for the low Syn-4 levels due to greater cell-cell contact (Figure 63), still depended greatly on PI3K/AKT signalling, thus was more affected by BEZ245 and showed a reduction of about 50% in the resistance factor.

This variation in effect is unsurprising, if we consider that the function of CAM-DR is to quickly protect cells from unexpected stress. It is expected that the adaptive changes provoked by this phenomenon would be rapid and influenced by many environmental factors, including cell count. Furthermore, MV3 cell dependency on syndecan for integrin resistance formation; cell-signalling adaptive rewiring to reduced level of syndecan-4; and the effect of cell density in this process, could also be observed in the following experiment, in which cell surface heparan sulfate (HS) and heparin (Hep) were digested with heparitinase.

Impact of glycosaminoglycans on sensitivity against cisplatin cytotoxicity

In summary, the results presented above highlight the importance of syndecans on cell signalling and survival by interacting with integrins and regulating their function. Additionally, the glycosaminoglycans present in these proteins play an essential role in these interactions, as it can be observed in the experiments bellow where wild type MV3 and MV3 Syn-4 kd cell lines were submitted to heparan sulfate and heparin digestion by heparitinase for 6 hours before cisplatin was added.

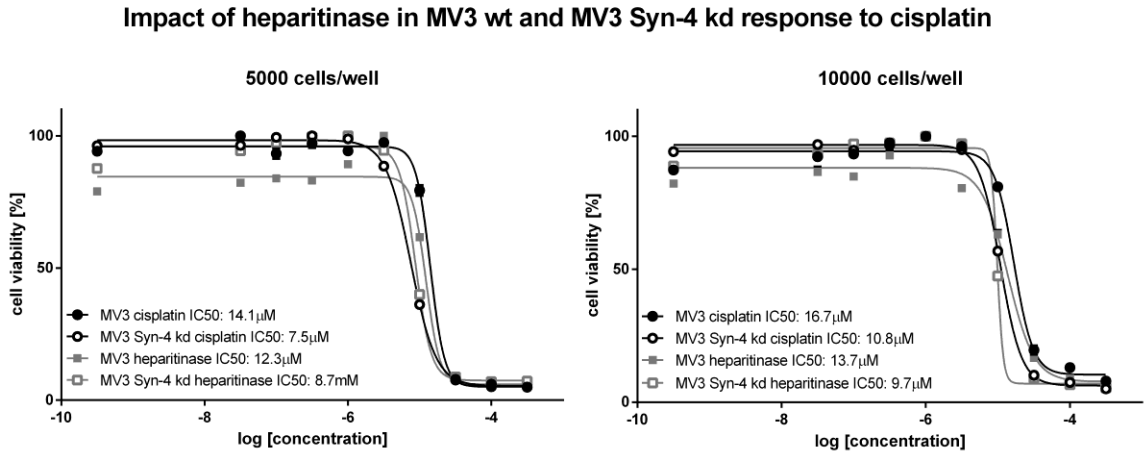

Figure 68. Sigmoidal concentration-response curves of MV3 wt and MV3 Syn-4 kd cell lines in response to HS and Hep digestion by heparitinase. Exemplary curves that represent one of at least three measurements obtained via MTT assay. Cells were incubated with 10 μL of heparitinase I (0.1 U/mL), 6 hours after cell seeding. On the following day, cisplatin logarithmic concentration curve was added to all plates and incubated for 72 hours. Sigmoidal concentration-response curves were used to estimate IC_{50} values.

Table 11. Cisplatin IC_{50} on MV3 and MV3 Syn-4 kd cell line upon heparitinase I treatment

Cell Density	Cell Line	Treatment	pIC_{50} ± SEM	IC_{50} (μM)
5000 cells / well	MV3	Cisplatin	4.95 ± 0.42	11.2
		Heparitinase	5.26 ± 0.48	5.5
	MV3 Syn-4 kd	Cisplatin	5.06 ± 0.08	8.6
		Heparitinase	5.07 ± 0.02	8.5
10000 cells / well	MV3	Cisplatin	4.80 ± 0.09	15.9
		Heparitinase	5.00 ± 0.12	9.9
	MV3 Syn-4 kd	Cisplatin	4.92 ± 0.06	11.9
		Heparitinase	4.96 ± 0.05	11.1

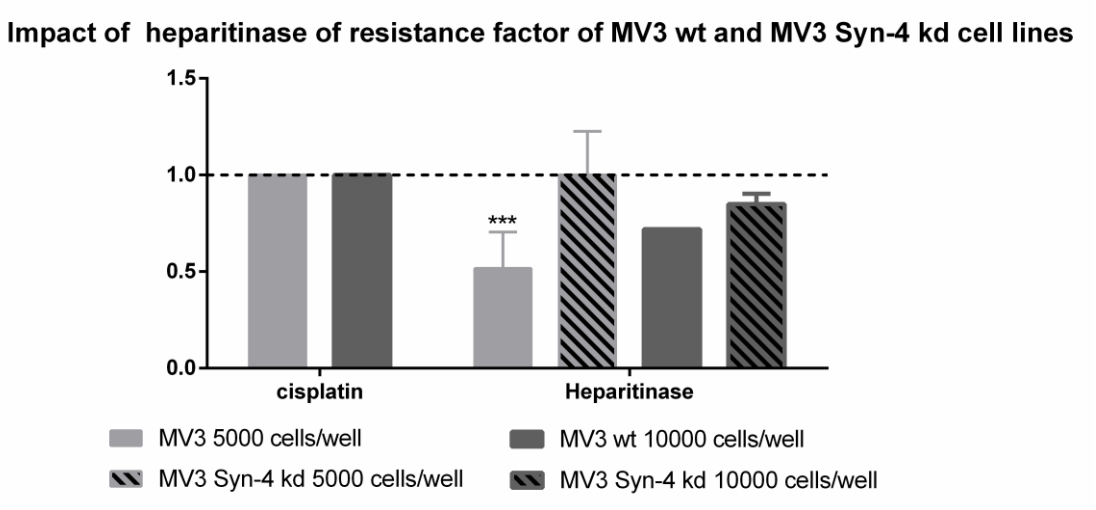

Figure 69. Resistance factors of MV3 wt and MV3 Syn-4 kd cell lines in the presence of heparitinase. IC_{50} values of each experiment were used to calculate the resistance factors as indicators of sensitivity to cisplatin. Results correspond to the mean value and SD of the RF of at least three assays. ANOVA statistical analysis was used; asterisks indicate statistical significance compared to cells treated solely with cisplatin: * P<0.05; ** P<0.01; *** P<0.001.

It can be observed that digestion of HS and Hep glycosaminoglycan chains by heparitinase affects the wild type cells, more than the knockdown cell line. Moreover, in MV3 Syn-4 kd the higher cell density was slightly more affected than the lower cell count. Taken together these results confirm the findings that cells undergo cell-signalling rewiring in order to minimize the effects of syndecan-4 downregulation, and that this is dependent on cell density. Besides, this illustrates the importance of HS and Hep in the interactions between syndecan and integrin.

The data obtained so far clearly show the influence of proteoglycans and their GAG chains on integrin resistance formation. It has been suggested that LMWH (low molecular weight heparins) could sensitize cells to cisplatin by interfering with integrin-mediated resistance formation by directly binding to specific integrins or inhibiting the anti-apoptotic Wnt pathway (374–376). Aiming to investigate if this was the case for the MV3 cell line, cells were submitted to MTT in the presence of Tinzaparin, a LMWH.

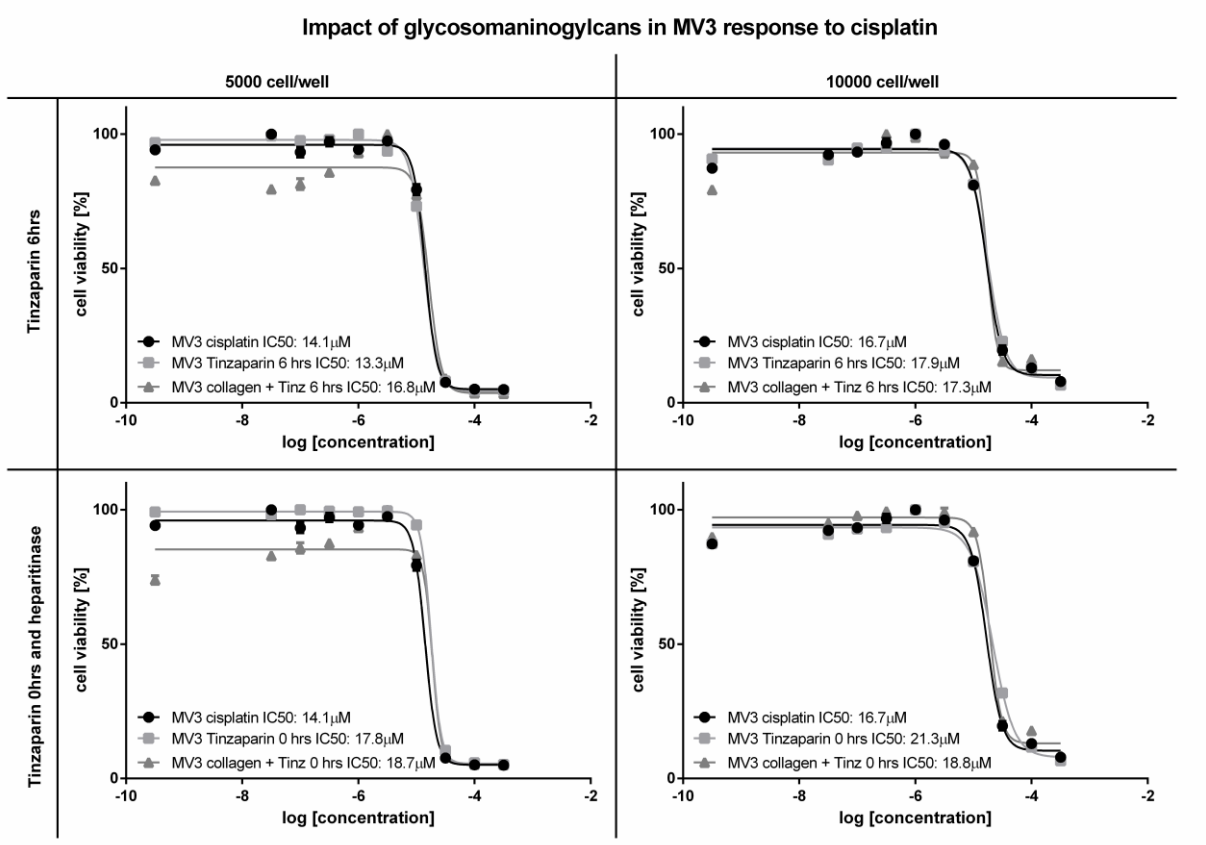

Figure 70. The impact of LMWH Tinzaparin on cisplatin cytotoxicity towards MV3 wt cell line grown on Coll. Sigmoidal concentration-response curves shown represent one of at least three MTT assays. Depending on treatment, cells were platted on Coll-coated plates and/or incubated with 10 μg tinzaparin (500 μg/mL), 6 hours after cell seeding, or immediately after (0 hrs). Subsequently, cells were incubated with cisplatin logarithmic concentration curve for 72 hours. IC_{50} values were obtained from sigmoidal concentration-response curves.

Table 12. Cisplatin IC_{50} on MV3 cell line upon treatment with LMWH Tinzaparin

Cell Density	Treatment	pIC_{50} ± SEM	IC_{50} (μM)
5000 cells / well	Cisplatin	4.95 ± 0.42	11.2
	Tinzaparin 6 h	4.92 ± 0.14	12.1
	Tinzaparin 6 h + Coll	4.86 ± 0.24	13.7
	Tinzaparin 0 h	4.86 ± 0.16	13.7
	Tinzaparin 0 h + Coll	4.85 ± 0.18	14.0
10000 cells / well	Cisplatin	4.80 ± 0.09	15.9
	Tinzaparin 6 h	4.76 ± 0.06	17.5
	Tinzaparin 6 h + Coll	4.75 ± 0.02	17.6
	Tinzaparin 0 h	4.74 ± 0.09	18.4
	Tinzaparin 0 h + Coll	4.72 ± 0.05	18.9

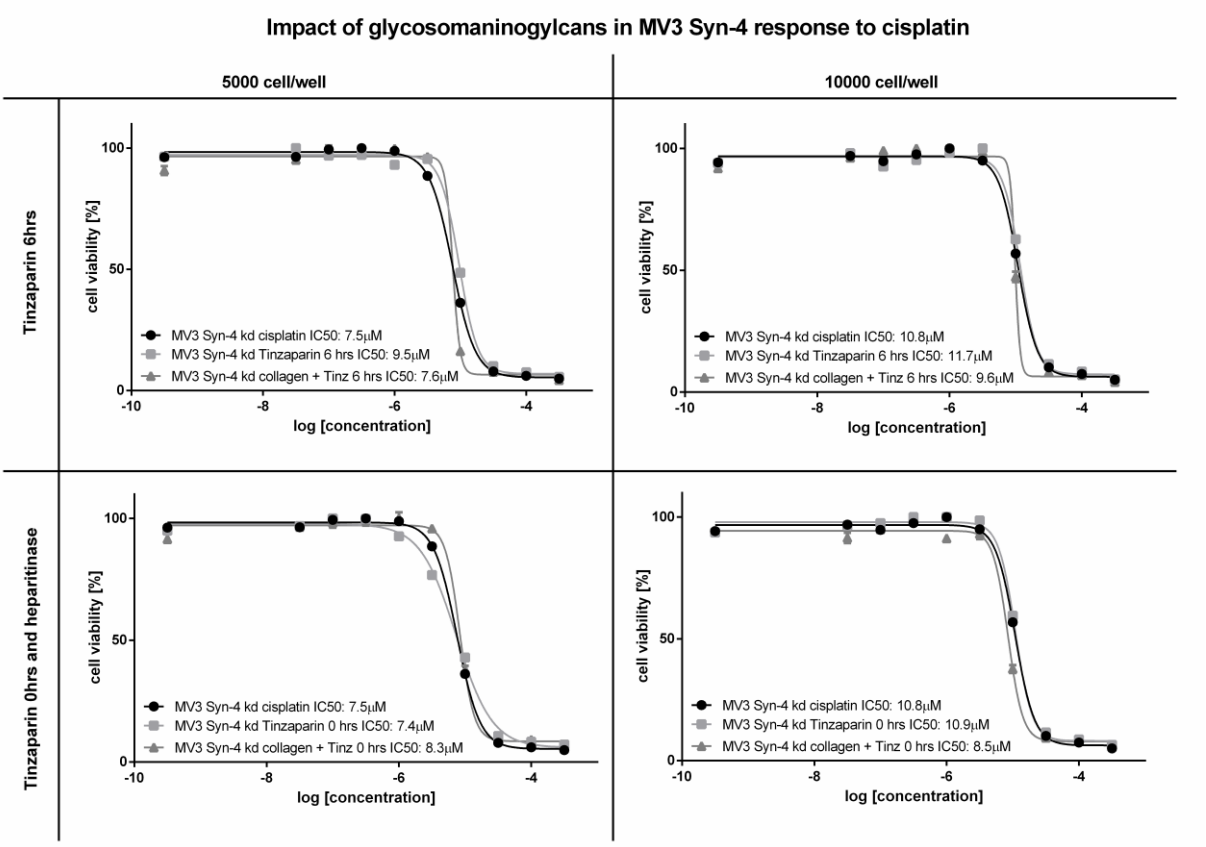

Figure 71. LMWH Tinzaparin affects cisplatin cytotoxicity towards MV3 Syn-4 kd cell line grown on Coll. Sigmoidal concentration-response curves shown represent one of at least three MTT assays. Depending on treatment, cells were platted on Coll-coated plates and/or incubated with 10 μg tinzaparin (500 μg/mL), 6 hours after cell seeding, or immediately after (0 hrs). Subsequently, cells were incubated with cisplatin logarithmic concentration curve for 72 hours. IC_{50} values were obtained from sigmoidal concentration-response curves.

Table 13. Cisplatin IC_{50} on MV3 Syn-4 cell line upon treatment with LMWH Tinzaparin

Cell Density	Treatment	pIC_{50} ± SEM	IC_{50} (μM)
5000 cells / well	Cisplatin	5.06 ± 0.08	8.6
	Tinzaparin 6 h	4.97 ± 0.21	10.8
	Tinzaparin 6 h + Coll	5.08 ± 0.29	8.3
	Tinzaparin 0 h	5.10 ± 0.25	8.0
	Tinzaparin 0 h + Coll	4.97 ± 0.15	10.7
10000 cells / well	Cisplatin	4.92 ± 0.06	11.9
	Tinzaparin 6 h	4.85 ± 0.09	14.1
	Tinzaparin 6 h + Coll	4.94 ± 0.10	11.4
	Tinzaparin 0 h	4.92 ± 0.06	12.0
	Tinzaparin 0 h + Coll	4.96 ± 0.16	11.0

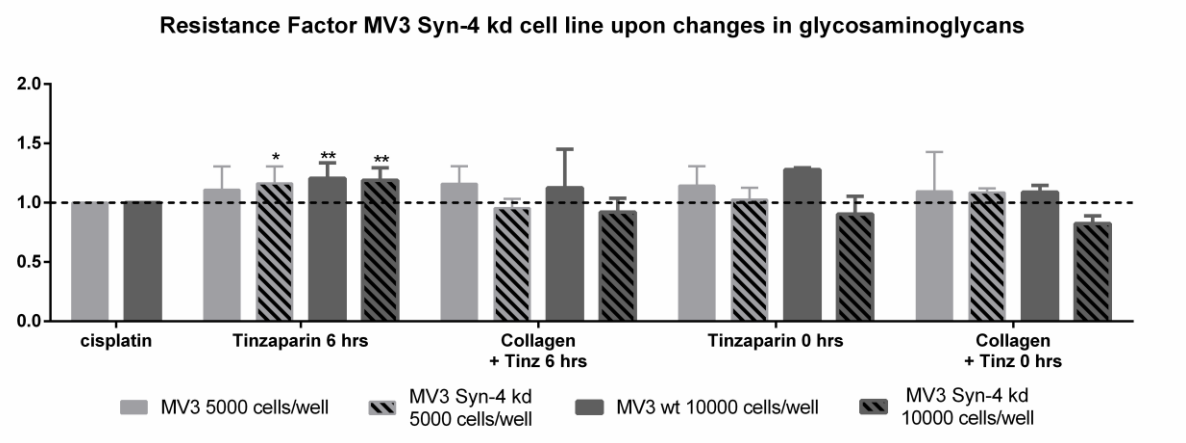

Figure 72. Effect of Tinzaparin on the response of MV3 wt and MV3 Syn-4 kd cell lines to cisplatin in the presence of Coll. RFs were calculated based on the IC_{50} values of each measurement and correspond to the mean value and SD of the RF of at least 3 assays. Statistical analysis was performed using ANOVA; asterisks indicate statistical significance in relation to cisplatin treated cells: * P<0.05; ** P<0.01; *** P<0.001.

Although it has been shown by our group that Tinzaparin is able to sensitize ovarian cancer cisplatin-resistant cells (375,376), this could not be shown for the MV3 wt or MV3 Syn-4 kd cells. In fact, wild type cells show lower sensitivity to cisplatin when treated with this heparin analogue, while the MV3 Syn-4 kd cells display a decrease in RF in almost all treatments. The mechanism of Tinzaparin is not fully understood and currently under investigation in our laboratory. So far, Schlesinger et al. have shown that Tinzaparin binds to α4β1 integrins with lower affinity than the physiological ligand VCAM-1, but with a similar dissociation ratio, which causes a weak inhibition of cell binding (374). Furthermore, Pfankuchen et al. were able to show that Tinzaparin can overcome cisplatin-resistance in ovarian cancer cells by antagonizing the Wnt pathway (375,376).

Taken together, these results confirm our hypothesis of MV3 Syn-4 kd rewiring to decrease syndecan dependency. This can be corroborated by the fact that MV3 wt, which relies on syndecan for cell survival, show an increase in its resistance factor, most likely because Tinzaparin acts as shed syndecan in the ECM. In comparison, MV3 Syn-4 kd, which underwent signalling rewiring due to syndecan-4 deficiency, are not responsive to syndecan shedding, thus showed reduced RFs.

The only exception was when cells were treated with Tinzaparin alone, 6 hours after cell seeding. In this case, resistance factor increased substantially in both cell lines. In the case of MV3 Syn-4 kd, this is most likely a syndecan–integrin unrelated effect. Shed syndecan can also bind to heparin-binding growth factors, such as fibroblast growth

factor (FGF), vascular endothelial growth factor (VEGF) and platelet-derived growth factor (PDGF) (377). Once cells have adhered, Tinzaparin can no longer bind to integrin and remains free in the ECM and can influence growth factor receptors, which are probably responsible for the effect observed. In contrast, Coll prompts signalling syndecan-4 - β1 integrin axis, which cannot be supported because of syndecan-4 deficiency, independent of when Tinzaparin is added. In Conclusion, this shows, first the importance of GAG for the interaction between syndecan and integrins. Second, how the delicate balance between these cell components can alter cell fate.

3D Model

After many attempts to generate a 3D Model in our laboratory we opted for embedding all three MV3 cell line variants in VitroGel™ 3D - RGD, which is a mixture of many different ECM compounds. The results obtained were a bit disappointing, but nevertheless interesting.

Table 14. Cisplatin IC_{50} on MV3 wt, MV3 β1 integrin kd and MV3 Syn-4 kd cell lines on 3D Model

Cell Density	Cell Line	Treatment	pIC_{50} ± SEM	IC_{50} (µM)
5000 cells / well	MV3	2D Cisplatin	4.89 ± 0.33	12.8
		3D Cisplatin	4.98 ± 0.31	10.5
	MV3 β1 integrin kd	2D Cisplatin	5.01 ± 0.23	9.7
		3D Cisplatin	4.98 ± 0.05	**10.5**
	MV3 Syn-4 kd	2D Cisplatin	4.98 ± 0.29	10.4
		3D Cisplatin	5.04 ± 0.08	9.2
10000 cells / well	MV3	2D Cisplatin	4.57 ± 0.37	27.0
		3D Cisplatin	4.64 ± 0.42	22.8
	MV3 β1 integrin kd	2D Cisplatin	4.71 ± 0.02	19.5
		3D Cisplatin	4.69 ± 0.15	**20.5**
	MV3 Syn-4 kd	2D Cisplatin	4.61 ± 0.40	24.8
		3D Cisplatin	4.76 ± 0.24	17.45

We can observe that, the cells that responded well to integrin activating stimuli in 2D, MV3 wt and MV3 Syn-4 kd, were sensitized to cisplatin by the matrix embedding in comparison with their counterparts, which were grown on 2D surfaces. This is probably a consequence of cell adaptation to being grown in layers, the time window for the assay (96 hours) is not enough for cells to re-acquire their 3D capacities.

Curiously, in the case of the MV3 β1 integrin kd cell line, which were unresponsive to the Mn^{2+} and Coll treatments, the 3D matrix demonstrated to be a protective environment against cisplatin. As discussed above, the absence of β1 integrin was not able to reduce the RF of MV3 cells because of a compensation mechanism that triggered the increase in β3 integrin expression (Figure 54). As previously explained, β3 integrin is not able to connect to Coll alone. The interaction of β1 integrin with this matrix protein is necessary to expose the RGD binding site, where β3 integrin can bind (191). However, in a mixed matrix as VitroGel™ 3D - RGD there are many other binding partners for the β3 integrins which possess RGD binding sites available, such as its preferable binding partner vitronectin (160). For this reason, this more varied matrix was able to trigger a protective effect on these cells.

5. Conclusion

In the present work we were able to provide evidence that, first, different cell lines from the same cancer type (melanoma) can present completely different protein expression profiles, proliferation and response to therapy. Second, we were able to demonstrate the importance of the ECM in resistance formation of the MV3 melanoma cell line, specifically the effect of Coll I on integrin activation. We showed that the interaction between Coll and integrins triggers cell signalling pathways that increase cell resistance to cisplatin treatment. This activation can be blocked by using β1 integrin-blocking antibody P5D2, which leads to cell death, establishing not only the involvement, but also the importance of this integrin subtype, as main Coll ligand in resistance development. Moreover, we were able to observe that Mn^{2+} activation of integrins also induces cisplatin resistance, but at a lower level and non-synergistic manner to Coll, indicating that more than one signalling pathway might be involved.

Nevertheless, it could be observed by flow cytometry that both treatments promoted activation of the FAK/PI3K/AKT signalling pathway, at different levels. Additionally, the inhibition of this pathway by BEZ235, a PI3K blocking molecule, induced massive sensitization of cells to cisplatin; and this effect could not be reverted by treatments with Coll or Mn^{2+}. This corroborates the involvement of this pathway in the transmission of the survival-signal initiated by the contact between β1 integrin and Coll, or integrin activation through Mn^{2+} binding, from the cell membrane, through the cytoplasm, into the nucleus, where it will affect protein transcription and lead to cell survival.

MV3 β1 integrin knockdown was also performed and, unfortunately, did not produce the expected results. Even though, the knockdown greatly reduced the levels of β1 integrin in MV3 cells, the new cell line displayed only a slight reduction in the resistance factor, when compared to the wild type. Although it might seem that our attempt to demonstrate the importance of β1 integrin on MV3 cisplatin resistance failed, this is not true. It allowed us to observe the effect of a genetic change, such as a knockdown, as a powerful selective tool that leaves only the cells that were able to somehow adapt to the genetic modification to be evaluated. In contrast, the antibody treatment to block β1 integrin is a rapid environmental change that forces cells to adapt quickly. Therefore, knockdown is more similar to the acquired drug resistance, which leads to permanent genetic changes, such as the upregulation of β3 integrin observed; while the antibody treatment can be compared to environmentally-mediated drug

resistance, and, for this reason, is more appropriate to demonstrate our hypothesis. This being said, we can at this point state with confidence that the data reported in this work illustrates the importance and involvement of β1 integrin in the resistance mechanism of MV3 melanoma cells treated with cisplatin. Moreover, this mechanism is mediated by integrin activation through Coll Type I.

Next, the effect of cisplatin on the MV3 cell line was evaluated and a shift in the integrin and syndecan profiles could be observed. All integrins α-chains were strongly down-regulated while the ratio of β-chain containing integrins was, with exception of β1, up-regulated. In the syndecan profile, we could observe a switch from the expression of only syndecan-4, to a 50 – 50 distribution between syndecans 1 and 4. Another knockdown was performed to reduce the expression of syndecan-4. The lack of this important integrin partner led to increased cisplatin sensitivity; FN was able to restore resistant factors even in the absence of Syndecan-4. This was not the case for Coll, which demonstrated the importance of this proteoglycan for β1 integrin activation, specifically.

Similarly, in the β1 integrin knockdown, we could observe a massive increase in FAK activation in the knockdown cells, as a desperate attempt to initiate survival signalling. However, since Syndecan-4 is responsible for the recruitment of kinases that phosphorylate AKT to the cell membrane, the signal cannot be transmitted to the downstream effectors PI3K and AKT, which was observed by a decreased expression and activation of the PI3K/AKT signalling pathway, in comparison to wild type cells. Thus, the genetic modification induced by us forced cells to adapt by rewiring and becoming less dependent on this pathway and syndecan-4 to survive. Accordingly, syndecan-4-deficient cells were less affected by the BEZ235 PI3K inhibitor and HS and Hep ablation with heparitinase, than the wild type cells. This confirms that the knockdown leads cells to adapt by becoming less dependent on the signalling pathways activated by the missing protein, in this case syndecan-4.

Finally, due to several reports about the benefit of LMWH in sensitizing cells to cisplatin, cells were treated with Tinzaparin (374–376). This was the case for syndecan-4 knockdown cells, but not the for MV3 cell line, which became slightly resistant. This is probably also a reflex of the independency of syndecan-4-deficient cells from this proteoglycan, which the MV3 cells do not present. However, the Tinzaparin mechanism of action is still not completely understood and more investigation is necessary.

Taken together, these results demonstrate the importance and complexity of the interaction of integrins and syndecans with the ECM in supporting cell adaptation and survival. Moreover, they show the plasticity of cancer cells and give some insight into the challenges of cancer biology and therapy development. Certainly, extensive research is still needed in this field, but hopefully this work will have made a small, yet, significant contribution.

6. References

1. Haridy Y, Witzmann F, Asbach P, Schoch RR, Fröbisch N, Rothschild BM. Triassic Cancer-Osteosarcoma in a 240-Million-Year-Old Stem-Turtle. JAMA Oncol. 2019 Feb 7;

2. Barbosa FH de S, Pereira PVLG da C, Bergqvist LP, Rothschild BM. Multiple neoplasms in a single sauropod dinosaur from the Upper Cretaceous of Brazil. Cretaceous Research. 2016 Jul 1;62:13–7.

3. Jiménez-Serrano A, Martínez de Dios JL, de la Torre Robles Y, Barba Colmenero V, Bardonova M, Moya E, et al. Proyecto Qubbet el-Hawa: Las Tumbas nº 31, 33, 34aa, 34bb, 35n, 35p y 122. Vol. 25. 2016. 11 p.

4. Bandarchi B, Jabbari CA, Vedadi A, Navab R. Molecular biology of normal melanocytes and melanoma cells. J Clin Pathol. 2013 Aug;66:644–8.

5. International Agency for Research on Cancer. Global Cancer Observatory (GCO). GLOBOCAN 2018: cancer incidence, mortality and prevalence worldwide. [Internet]. 2018. Available from: http://gco.iarc.fr/

6. Sullivan RJ, Fisher DE. Understanding the Biology of Melanoma and Therapeutic Implications. Hematology/Oncology Clinics of North America. 2014 Jun;28(3):437–53.

7. Kanzler B, Foreman RK, Labosky PA, Mallo M. BMP signaling is essential for development of skeletogenic and neurogenic cranial neural crest. Development. 2000 Mar 1;127(5):1095–104.

8. Sharma SV, Lee DY, Li B, Quinlan MP, Takahashi F, Maheswaran S, et al. A Chromatin-Mediated Reversible Drug-Tolerant State in Cancer Cell Subpopulations. Cell. 2010 Apr;141(1):69–80.

9. Ravindran Menon D, Das S, Krepler C, Vultur A, Rinner B, Schauer S, et al. A stress-induced early innate response causes multidrug tolerance in melanoma. Oncogene. 2015 Aug;34(34):4448–59.

10. Luskin MR, Murakami MA, Manalis SR, Weinstock DM. Targeting minimal residual disease: a path to cure? Nature Reviews Cancer. 2018 Jan 29;18(4):255–63.

11. Amaral T, Sinnberg T, Meier F, Krepler C, Levesque M, Niessner H, et al. The mitogen-activated protein kinase pathway in melanoma part I - Activation and primary resistance mechanisms to BRAF inhibition. Eur J Cancer. 2017;73:85–92.

12. Amaral T, Sinnberg T, Meier F, Krepler C, Levesque M, Niessner H, et al. MAPK pathway in melanoma part II-secondary and adaptive resistance mechanisms to BRAF inhibition. Eur J Cancer. 2017;73:93–101.

13. Mitra D, Luo X, Morgan A, Wang J, Hoang MP, Lo J, et al. An ultraviolet-radiation-independent pathway to melanoma carcinogenesis in the red hair/fair skin background. Nature. 2012 Nov;491(7424):449–53.

14. Cui R, Widlund HR, Feige E, Lin JY, Wilensky DL, Igras VE, et al. Central role of p53 in the suntan response and pathologic hyperpigmentation. Cell. 2007 Mar 9;128(5):853–64.

15. Akbani R, Akdemir KC, Aksoy BA, Albert M, Ally A, Amin SB, et al. Genomic Classification of Cutaneous Melanoma. Cell. 2015 Jun;161(7):1681–96.

16. Sullivan RJ, LoRusso PM, Flaherty KT. The Intersection of Immune-Directed and Molecularly Targeted Therapy in Advanced Melanoma: Where We Have Been, Are, and Will Be. Clinical Cancer Research. 2014 Oct 1;19(19):5283–91.

17. Eggermont AM, Spatz A, Robert C. Cutaneous melanoma. Lancet. 2014 Mar;383:816–27.

18. Hartman ML, Czyz M. MITF in melanoma: mechanisms behind its expression and activity. Cellular and Molecular Life Sciences. 2015 Apr;72(7):1249–60.

19. Sturm RA, Fox C, McClenahan P, Jagirdar K, Ibarrola-Villava M, Banan P, et al. Phenotypic Characterization of Nevus and Tumor Patterns in MITF E318K Mutation Carrier Melanoma Patients. Journal of Investigative Dermatology. 2014 Jan;134(1):141–9.

20. Garraway LA, Widlund HR, Rubin MA, Getz G, Berger AJ, Ramaswamy S, et al. Integrative genomic analyses identify MITF as a lineage survival oncogene amplified in malignant melanoma. Nature. 2005 Jul;436(7047):117–22.

21. Kumar SM, Dai J, Li S, Yang R, Yu H, Nathanson KL, et al. Human skin neural crest progenitor cells are susceptible to BRAF V600E -induced transformation. Oncogene. 2014 Feb;33(7):832–41.

22. Lister JA, Capper A, Zeng Z, Mathers ME, Richardson J, Paranthaman K, et al. A Conditional Zebrafish MITF Mutation Reveals MITF Levels Are Critical for Melanoma Promotion vs. Regression In Vivo. Journal of Investigative Dermatology. 2014 Jan;134(1):133–40.

23. Yokoyama S, Woods SL, Boyle GM, Aoude LG, MacGregor S, Zismann V, et al. A novel recurrent mutation in MITF predisposes to familial and sporadic melanoma. Nature. 2011 Nov 13;480(7375):99–103.

24. Cancer Genome Atlas Network. Genomic Classification of Cutaneous Melanoma. Cell. 2015 Jun;161(7):1681–96.

25. Davies H, Bignell GR, Cox C, Stephens P, Edkins S, Clegg S, et al. Mutations of the BRAF gene in human cancer. Nature. 2002 Jun;417(6892):949–54.

26. Sosman JA, Kim KB, Schuchter L, Gonzalez R, Pavlick AC, Weber JS, et al. Survival in BRAF V600–Mutant Advanced Melanoma Treated with Vemurafenib. New England Journal of Medicine. 2012 Feb 23;366(8):707–14.

27. Omholt K, Platz A, Kanter L, Ringborg U, Hansson J. NRAS and BRAF mutations arise early during melanoma pathogenesis and are preserved throughout tumor progression. Clin Cancer Res. 2003 Dec 15;9(17):6483–8.

28. Najem A, Krayem M, Salès F, Hussein N, Badran B, Robert C, et al. P53 and MITF/Bcl-2 identified as key pathways in the acquired resistance of NRAS-mutant melanoma to MEK inhibition. European Journal of Cancer. 2017 Sep;83:154–65.

29. Houben R, Becker JC, Kappel A, Terheyden P, Bröcker E-B, Goetz R, et al. Constitutive activation of the Ras-Raf signaling pathway in metastatic melanoma is associated with poor prognosis. J Carcinog. 2004 Mar 26;3:6.

30. Manning BD, Toker A. AKT/PKB Signaling: Navigating the Network. Cell. 2017 Apr;169(3):381–405.

31. Kwong LN, Davies MA. Navigating the therapeutic complexity of PI3K pathway inhibition in melanoma. Clin Cancer Res. 2013 Oct 1;19(19):5310–9.

32. Hocker T, Tsao H. Ultraviolet radiation and melanoma: a systematic review and analysis of reported sequence variants. Hum Mutat. 2007 Jun;28(6):578–88.

33. Teng DH, Hu R, Lin H, Davis T, Iliev D, Frye C, et al. MMAC1/PTEN mutations in primary tumor specimens and tumor cell lines. Cancer Res. 1997 Dec 1;57(23):5221–5.

34. Tsao H, Zhang X, Benoit E, Haluska FG. Identification of PTEN/MMAC1 alterations in uncultured melanomas and melanoma cell lines. Oncogene. 1998 Jul 2;16(26):3397–402.

35. Tsao H, Zhang X, Fowlkes K, Haluska FG. Relative reciprocity of NRAS and PTEN/MMAC1 alterations in cutaneous melanoma cell lines. Cancer Res. 2000 Apr 1;60(7):1800–4.

36. Goel VK, Lazar AJF, Warneke CL, Redston MS, Haluska FG. Examination of mutations in BRAF, NRAS, and PTEN in primary cutaneous melanoma. J Invest Dermatol. 2006 Jan;126(1):154–60.

37. Davies MA, Stemke-Hale K, Tellez C, Calderone TL, Deng W, Prieto VG, et al. A novel AKT3 mutation in melanoma tumours and cell lines. Br J Cancer. 2008 Oct 21;99(8):1265–8.

38. Davies MA, Stemke-Hale K, Lin E, Tellez C, Deng W, Gopal YN, et al. Integrated Molecular and Clinical Analysis of AKT Activation in Metastatic Melanoma. Clin Cancer Res. 2009 Dec 15;15(24):7538–46.

39. Stahl JM, Sharma A, Cheung M, Zimmerman M, Cheng JQ, Bosenberg MW, et al. Deregulated Akt3 activity promotes development of malignant melanoma. Cancer Res. 2004 Oct 1;64(19):7002–10.

40. Carpten JD, Faber AL, Horn C, Donoho GP, Briggs SL, Robbins CM, et al. A transforming mutation in the pleckstrin homology domain of AKT1 in cancer. Nature. 2007 Jul 26;448(7152):439–44.

41. Cheung M, Sharma A, Madhunapantula SV, Robertson GP. Akt3 and mutant V600E B-Raf cooperate to promote early melanoma development. Cancer Res. 2008 May 1;68(9):3429–39.

42. Hodis E, Watson IR, Kryukov GV, Arold ST, Imielinski M, Theurillat J-P, et al. A landscape of driver mutations in melanoma. Cell. 2012 Jul 20;150(2):251–63.

43. Omholt K, Kröckel D, Ringborg U, Hansson J. Mutations of *pik3ca* are rare in cutaneous melanoma. Melanoma Research. 2006 Apr 1;16(2):197–200.

44. Yang AS, Chapman PB. The History and Future of Chemotherapy for Melanoma. Hematol Oncol Clin North Am. 2009 Jun;23(3):583–x.

45. Megahed AI, Koon HB. What Is the Role of Chemotherapy in the Treatment of Melanoma? Curr Treat Options in Oncol. 2014 Jun 1;15(2):321–35.

46. Bhatia S, Tykodi SS, Thompson JA. Treatment of Metastatic Melanoma: An Overview. Oncology (Williston Park). 2009 May;23(6):488–96.

47. Bollag G, Tsai J, Zhang J, Zhang C, Ibrahim P, Nolop K, et al. Vemurafenib: the first drug approved for BRAF-mutant cancer. Nature Reviews Drug Discovery. 2012 Oct 12;11(11):873–86.

48. Williams TE, Subramanian S, Verhagen J, McBride CM, Costales A, Sung L, et al. Discovery of RAF265: A Potent mut-B-RAF Inhibitor for the Treatment of Metastatic Melanoma. ACS Med Chem Lett. 2015 Aug 3;6(9):961–5.

49. Delord J, Houede N, Awada A, Taamma A, Faivre SJ, Besse-Hammer T, et al. First-in-human phase I safety, pharmacokinetic (PK), and pharmacodynamic (PD) analysis of the oral MEK-inhibitor AS703026 (two regimens [R]) in patients (pts) with advanced solid tumors. Journal of Clinical Oncology. 2010 May 20;28(15_suppl):2504–2504.

50. Houede N, Faivre SJ, Awada A, Raymond E, Italiano A, Besse-Hammer T, et al. Safety and evidence of activity of MSC1936369, an oral MEK1/2 inhibitor, in patients with advanced malignancies. Journal of Clinical Oncology. 2011 May 20;29(15_suppl):3019–3019.

51. Mirmohammadsadegh A, Mota R, Gustrau A, Hassan M, Nambiar S, Marini A, et al. ERK1/2 Is Highly Phosphorylated in Melanoma Metastases and Protects Melanoma Cells from Cisplatin-Mediated Apoptosis. Journal of Investigative Dermatology. 2007 Sep;127(9):2207–15.

52. Chemotherapy for Melanoma Skin Cancer [Internet]. [cited 2018 Dec 26]. Available from: https://www.cancer.org/cancer/melanoma-skin-cancer/treating/chemotherapy.html

53. Probst U, Fuhrmann I, Beyer L, Wiggermann P. Electrochemotherapy as a New Modality in Interventional Oncology: A Review. Technol Cancer Res Treat [Internet]. 2018 Jul 9 [cited 2019 Feb 19];17. Available from: https://www.ncbi.nlm.nih.gov/pmc/articles/PMC6048674/

54. Testori A, Tosti G, Martinoli C, Spadola G, Cataldo F, Verrecchia F, et al. Electrochemotherapy for cutaneous and subcutaneous tumor lesions: a novel therapeutic approach. Dermatol Ther. 2010 Dec;23(6):651–61.

55. Wichtowski M, Murawa D. Electrochemotherapy in the treatment of melanoma. Contemp Oncol (Pozn). 2018;22(1):8–13.

56. Siegel R, Naishadham D, Jemal A. Cancer statistics, 2013. CA Cancer J Clin. 2013 Jan;63(1):11–30.

57. Zahnreich S, Mayer A, Loquai C, Grabbe S, Schmidberger H. Radiotherapy with BRAF inhibitor therapy for melanoma: progress and possibilities. Future Oncol. 2016 Jan;12(1):95–106.

58. Cruz Zambrano C, Schuler MH, Machiels J-PH, Hess D, Paz-Ares L, Awada A, et al. Phase lb study of buparlisib (BKM120) plus either paclitaxel (PTX) in advanced solid tumors (aST) or PTX plus trastuzumab (TZ) in HER2+ breast cancer (BC). JCO. 2014 May 20;32(15_suppl):627–627.

59. Menzies AM, Long GV. Dabrafenib and trametinib, alone and in combination for BRAF-mutant metastatic melanoma. Clin Cancer Res. 2014 Apr 15;20(8):2035–43.

60. Kauffman GB, Pentimalli R, Doldi S, Hall MD. Michele Peyrone (1813-1883), Discoverer of Cisplatin. Platinum Metals Review. 2010 Oct 1;54(4):250–6.

61. Rosenberg B, Van Camp L, Krigas T. Inhibition of Cell Division in Escherichia coli by Electrolysis Products from a Platinum Electrode. Nature. 1965 Feb 13;205(4972):698–9.

62. Rosenberg B, Vancamp L, Trosko JE, Mansour VH. Platinum Compounds: a New Class of Potent Antitumour Agents. Nature. 1969 Apr 26;222(5191):385–6.

63. Kelland LR. Preclinical perspectives on platinum resistance. Drugs. 2000;59 Suppl 4:1–8; discussion 37-38.

64. Dasari S, Tchounwou PB. Cisplatin in cancer therapy: molecular mechanisms of action. Eur J Pharmacol. 2014 Oct 5;740:364–78.

65. Lazarević T, Rilak A, Bugarčić ŽD. Platinum, palladium, gold and ruthenium complexes as anticancer agents: Current clinical uses, cytotoxicity studies and future perspectives. Eur J Med Chem. 2017 Apr 18;

66. Waissbluth S, Daniel SJ. Cisplatin-induced ototoxicity: transporters playing a role in cisplatin toxicity. Hear Res. 2013 May;299:37–45.

67. Zhu S, Pabla N, Tang C, He L, Dong Z. DNA damage response in cisplatin-induced nephrotoxicity. Arch Toxicol. 2015 Dec;89(12):2197–205.

68. Yotsuyanagi T, Usami M, Noda Y, Nagata M. Computational consideration of cisplatin hydrolysis and acid dissociation in aqueous media: effect of total drug concentrations. Int J Pharm. 2002 Oct 10;246(1–2):95–104.

69. Eastman A. The formation, isolation and characterization of DNA adducts produced by anticancer platinum complexes. Pharmacol Ther. 1987;34(2):155–66.

70. el-Khateeb M, Appleton TG, Gahan LR, Charles BG, Berners-Price SJ, Bolton AM. Reactions of cisplatin hydrolytes with methionine, cysteine, and plasma ultrafiltrate studied by a combination of HPLC and NMR techniques. J Inorg Biochem. 1999 Oct;77(1–2):13–21.

71. Gale GR, Morris CR, Atkins LM, Smith AB. Binding of an antitumor platinum compound to cells as influenced by physical factors and pharmacologically active agents. Cancer Res. 1973 Apr;33(4):813–8.

72. Gately DP, Howell SB. Cellular accumulation of the anticancer agent cisplatin: a review. Br J Cancer. 1993 Jun;67(6):1171–6.

73. Galluzzi L, Senovilla L, Vitale I, Michels J, Martins I, Kepp O, et al. Molecular mechanisms of cisplatin resistance. Oncogene. 2012 Apr 12;31(15):1869–83.

74. Bellon SF, Coleman JH, Lippard SJ. DNA unwinding produced by site-specific intrastrand cross-links of the antitumor drug cis-diamminedichloroplatinum(II). Biochemistry. 1991 Aug 13;30(32):8026–35.

75. Esteban-Fernández D, Moreno-Gordaliza E, Cañas B, Palacios MA, Gómez-Gómez MM. Analytical methodologies for metallomics studies of antitumor Pt-containing drugs. Metallomics. 2010 Jan 1;2(1):19–38.

76. Rapanotti MC, Campione E, Spallone G, Orlandi A, Bernardini S, Bianchi L. Minimal residual disease in melanoma: circulating melanoma cells and predictive role of MCAM/MUC18/MelCAM/CD146. Cell Death Discov. 2017 Mar 6;3:17005.

77. Meads MB, Hazlehurst LA, Dalton WS. The bone marrow microenvironment as a tumor sanctuary and contributor to drug resistance. Clin Cancer Res. 2008 May 1;14(9):2519–26.

78. Meads MB, Gatenby RA, Dalton WS. Environment-mediated drug resistance: a major contributor to minimal residual disease. Nat Rev Cancer. 2009 Sep;9(9):665–74.

79. Rambow F, Rogiers A, Marin-Bejar O, Aibar S, Femel J, Dewaele M, et al. Toward Minimal Residual Disease-Directed Therapy in Melanoma. Cell. 2018 Aug 9;174(4):843-855.e19.

80. Curti BD, Urba WJ. Clinical deployment of antibodies for treatment of melanoma. Molecular Immunology. 2015 Oct 1;67(2, Part A):18–27.

81. Fedorenko IV, Gibney GT, Sondak VK, Smalley KSM. Beyond BRAF: where next for melanoma therapy? Br J Cancer. 2015 Jan 20;112(2):217–26.

82. Sebens S, Schafer H. The tumor stroma as mediator of drug resistance--a potential target to improve cancer therapy? Curr Pharm Biotechnol. 2012 Sep;13:2259–72.

83. Nezos A, Msaouel P, Pissimissis N, Lembessis P, Sourla A, Armakolas A, et al. Methods of detection of circulating melanoma cells: a comparative overview. Cancer Treat Rev. 2011 Jun;37(4):284–90.

84. Schatton T, Frank MH. Cancer stem cells and human malignant melanoma. Pigment Cell Melanoma Res. 2008 Feb;21(1):39–55.

85. Wantoch von Rekowski AK. Untersuchungen der molekularen Mechanismen für Cisplatinresistenzen der Ovarialkarzinomzelllinie W1 und W1CR. Bonn: Universitäts- und Landesbibliothek Bonn; 2017.

86. Galluzzi L, Vitale I, Michels J, Brenner C, Szabadkai G, Harel-Bellan A, et al. Systems biology of cisplatin resistance: past, present and future. Cell Death Dis. 2014;5:e1257.

87. Lambert IH, Sørensen BH. Facilitating the Cellular Accumulation of Pt-Based Chemotherapeutic Drugs. Int J Mol Sci [Internet]. 2018 Aug 1 [cited 2018 Nov 22];19(8). Available from: https://www.ncbi.nlm.nih.gov/pmc/articles/PMC6121265/

88. Schober AL, Wilson CS, Mongin AA. Molecular composition and heterogeneity of the LRRC8-containing swelling-activated osmolyte channels in primary rat astrocytes. J Physiol (Lond). 2017 Nov 15;595(22):6939–51.

89. Shen M-R, Droogmans G, Eggermont J, Voets T, Ellory JC, Nilius B. Differential expression of volume-regulated anion channels during cell cycle progression of human cervical cancer cells. J Physiol. 2000 Dec 1;529(Pt 2):385–94.

90. Lewis AD, Hayes JD, Wolf CR. Glutathione and glutathione-dependent enzymes in ovarian adenocarcinoma cell lines derived from a patient before and after the onset of drug resistance: intrinsic differences and cell cycle effects. Carcinogenesis. 1988 Jul;9(7):1283–7.

91. Hertzman Johansson C, Azimi A, Frostvik Stolt M, Shojaee S, Wiberg H, Grafström E, et al. Association of MITF and other melanosome-related proteins with chemoresistance in melanoma tumors and cell lines: Melanoma Research. 2013 Oct;23(5):360–5.

92. Xie T, Nguyen T, Hupe M, Wei ML. Multidrug Resistance Decreases with Mutations of Melanosomal Regulatory Genes. Cancer Research. 2009 Jan 20;69(3):992–9.

93. Kalayda GV, Wagner CH, Buss I, Reedijk J, Jaehde U. Altered localisation of the copper efflux transporters ATP7A and ATP7B associated with cisplatin resistance in human ovarian carcinoma cells. BMC Cancer. 2008;8:175.

94. Liedert B, Materna V, Schadendorf D, Thomale J, Lage H. Overexpression of cMOAT (MRP2/ABCC2) is associated with decreased formation of platinum-DNA adducts and decreased G2-arrest in melanoma cells resistant to cisplatin. J Invest Dermatol. 2003 Jul;121(1):172–6.

95. Morales JC, Li L, Fattah FJ, Dong Y, Bey EA, Patel M, et al. Review of Poly (ADP-ribose) Polymerase (PARP) Mechanisms of Action and Rationale for Targeting in Cancer and Other Diseases. Crit Rev Eukaryot Gene Expr. 2014;24(1):15–28.

96. Ossovskaya V, Koo IC, Kaldjian EP, Alvares C, Sherman BM. Upregulation of Poly (ADP-Ribose) Polymerase-1 (PARP1) in Triple-Negative Breast Cancer and Other Primary Human Tumor Types. Genes Cancer. 2010 Aug;1(8):812–21.

97. Ge R, Liu L, Dai W, Zhang W, Yang Y, Wang H, et al. Xeroderma Pigmentosum Group A Promotes Autophagy to Facilitate Cisplatin Resistance in Melanoma Cells through the Activation of PARP1. Journal of Investigative Dermatology. 2016 Jun;136(6):1219–28.

98. Song L, McNeil EM, Ritchie A-M, Astell KR, Gourley C, Melton DW. Melanoma cells replicate through chemotherapy by reducing levels of key homologous recombination protein RAD51 and increasing expression of translesion synthesis DNA polymerase ζ. BMC Cancer. 2017 Dec 18;17(1):864.

99. McNeil EM, Melton DW. DNA repair endonuclease ERCC1–XPF as a novel therapeutic target to overcome chemoresistance in cancer therapy. Nucleic Acids Res. 2012 Nov 1;40(20):9990–10004.

100. Li W, Melton DW. Cisplatin regulates the MAPK kinase pathway to induce increased expression of DNA repair gene *ERCC1* and increase melanoma chemoresistance. Oncogene. 2012 May;31(19):2412–22.

101. Song L, Ritchie A-M, McNeil EM, Li W, Melton DW. Identification of DNA repair gene Ercc1 as a novel target in melanoma. Pigment Cell & Melanoma Research. 2011 Oct 1;24(5):966–71.

102. McNeil EM, Astell KR, Ritchie A-M, Shave S, Houston DR, Bakrania P, et al. Inhibition of the ERCC1–XPF structure-specific endonuclease to overcome cancer chemoresistance. DNA Repair. 2015 Jul 1;31:19–28.

103. Helleday T. The underlying mechanism for the PARP and BRCA synthetic lethality: clearing up the misunderstandings. Mol Oncol. 2011 Aug;5(4):387–93.

104. Bradbury PA, Middleton MR. DNA repair pathways in drug resistance in melanoma: Anti-Cancer Drugs. 2004 Jun;15(5):421–6.

105. Lage H, Christmann M, Kern MA, Dietel M, Pick M, Kaina B, et al. Expression of DNA repair proteins hMSH2, hMSH6, hMLH1, O6-methylguanine-DNA methyltransferase and N-methylpurine-DNA glycosylase in melanoma cells with acquired drug resistance. Int J Cancer. 1999 Mar 1;80(5):744–50.

106. Korabiowska M, Brinck U, Dengler H, Stachura J, Schauer A, Droese M. Analysis of the DNA mismatch repair proteins expression in malignant melanomas. Anticancer Res. 2000 Dec;20(6B):4499–505.

107. Bassett E, Vaisman A, Tropea KA, McCall CM, Masutani C, Hanaoka F, et al. Frameshifts and deletions during in vitro translesion synthesis past Pt-DNA adducts by DNA polymerases beta and eta. DNA Repair (Amst). 2002 Dec 5;1(12):1003–16.

108. McCubrey JA, Steelman LS, Abrams SL, Lee JT, Chang F, Bertrand FE, et al. Roles of the RAF/MEK/ERK and PI3K/PTEN/AKT pathways in malignant

transformation and drug resistance. Advances in Enzyme Regulation. 2006;46(1):249–79.

109. Ikeguchi M, Kaibara N. Changes in survivin messenger RNA level during cisplatin treatment in gastric cancer. Int J Mol Med. 2001 Dec;8(6):661–6.

110. Tsao H, Atkins MB, Sober AJ. Management of Cutaneous Melanoma. New England Journal of Medicine. 2004 Sep 2;351(10):998–1012.

111. Jakob JA, Bassett RL, Ng CS, Curry JL, Joseph RW, Alvarado GC, et al. NRAS mutation status is an independent prognostic factor in metastatic melanoma. Cancer. 2012 Aug 15;118(16):4014–23.

112. Serrone L, Hersey P. The chemoresistance of human malignant melanoma: an update. Melanoma Research. 1999 Feb;9(1):51–8.

113. Yajima I, Kumasaka MY, Thang ND, Goto Y, Takeda K, Iida M, et al. Molecular Network Associated with MITF in Skin Melanoma Development and Progression. Journal of Skin Cancer. 2011;2011:1–7.

114. Hsiao JJ, Fisher DE. The roles of microphthalmia-associated transcription factor and pigmentation in melanoma. Archives of Biochemistry and Biophysics. 2014 Dec;563:28–34.

115. Hartman ML, Czyz M. Pro-Survival Role of MITF in Melanoma. Journal of Investigative Dermatology. 2015 Feb;135(2):352–8.

116. Haq R, Shoag J, Andreu-Perez P, Yokoyama S, Edelman H, Rowe GC, et al. Oncogenic BRAF Regulates Oxidative Metabolism via PGC1α and MITF. Cancer Cell. 2013 Mar;23(3):302–15.

117. Goding CR. A picture of Mitf in melanoma immortality. Oncogene. 2011 May;30(20):2304–6.

118. Hientz K, Mohr A, Bhakta-Guha D, Efferth T, Hientz K, Mohr A, et al. The role of p53 in cancer drug resistance and targeted chemotherapy. Oncotarget. 2016 Nov 19;8(5):8921–46.

119. Xie X, He G, Siddik ZH. Functional activation of mutant p53V172F by platinum analogs in cisplatin-resistant human tumor cells is dependent on serine-20 phosphorylation. Mol Cancer Res. 2017 Mar;15(3):328–39.

120. Yu J, Li L, Huang C. Downregulation of Inhibition of Apoptosis-Stimulating Protein of p53 (iASPP) Suppresses Cisplatin-Resistant Gastric Carcinoma In Vitro. Med Sci Monit. 2017 Nov 21;23:5542–9.

121. Feng X, Liu H, Zhang Z, Gu Y, Qiu H, He Z. Annexin A2 contributes to cisplatin resistance by activation of JNK-p53 pathway in non-small cell lung cancer cells. J Exp Clin Cancer Res [Internet]. 2017 Sep 8 [cited 2018 Dec 4];36. Available from: https://www.ncbi.nlm.nih.gov/pmc/articles/PMC5591524/

122. Siroy AE, Boland GM, Milton DR, Roszik J, Frankian S, Malke J, et al. Beyond BRAF V600 : Clinical Mutation Panel Testing by Next-Generation Sequencing

in Advanced Melanoma. Journal of Investigative Dermatology. 2015 Feb;135(2):508–15.

123. Dovey M, White RM, Zon LI. Oncogenic NRAS Cooperates with *p53* Loss to Generate Melanoma in Zebrafish. Zebrafish. 2009 Dec;6(4):397–404.

124. Bardeesy N, Bastian BC, Hezel A, Pinkel D, DePinho RA, Chin L. Dual Inactivation of RB and p53 Pathways in RAS-Induced Melanomas. Molecular and Cellular Biology. 2001 Mar 15;21(6):2144–53.

125. Marine J-CW, Dyer MA, Jochemsen AG. MDMX: from bench to bedside. Journal of Cell Science. 2007 Feb 1;120(3):371–8.

126. Curtin JA, Fridlyand J, Kageshita T, Patel HN, Busam KJ, Kutzner H, et al. Distinct Sets of Genetic Alterations in Melanoma. New England Journal of Medicine. 2005 Nov 17;353(20):2135–47.

127. Momand J, Zambetti GP, Olson DC, George D, Levine AJ. The mdm-2 oncogene product forms a complex with the p53 protein and inhibits p53-mediated transactivation. Cell. 1992 Jun;69(7):1237–45.

128. Deben C, Lardon F, Wouters A, Op de Beeck K, Van den Bossche J, Jacobs J, et al. APR-246 (PRIMA-1 MET) strongly synergizes with AZD2281 (olaparib) induced PARP inhibition to induce apoptosis in non-small cell lung cancer cell lines. Cancer Letters. 2016 Jun;375(2):313–22.

129. Mohell N, Alfredsson J, Fransson Å, Uustalu M, Byström S, Gullbo J, et al. APR-246 overcomes resistance to cisplatin and doxorubicin in ovarian cancer cells. Cell Death & Disease. 2015 Jun;6(6):e1794–e1794.

130. Synnott NC, Murray A, McGowan PM, Kiely M, Kiely PA, O'Donovan N, et al. Mutant p53: a novel target for the treatment of patients with triple-negative breast cancer?: Mutant p53. International Journal of Cancer. 2017 Jan 1;140(1):234–46.

131. Sherman-Baust CA, Weeraratna AT, Rangel LBA, Pizer ES, Cho KR, Schwartz DR, et al. Remodeling of the extracellular matrix through overexpression of collagen VI contributes to cisplatin resistance in ovarian cancer cells. Cancer Cell. 2003 Apr;3(4):377–86.

132. Ismail RS, Baldwin RL, Fang J, Browning D, Karlan BY, Gasson JC, et al. Differential gene expression between normal and tumor-derived ovarian epithelial cells. Cancer Res. 2000 Dec 1;60(23):6744–9.

133. Januchowski R, Wojtowicz K, Sujka-Kordowska P, Andrzejewska M, Zabel M. MDR Gene Expression Analysis of Six Drug-Resistant Ovarian Cancer Cell Lines. Biomed Res Int [Internet]. 2013 [cited 2015 Sep 30];2013. Available from: http://www.ncbi.nlm.nih.gov/pmc/articles/PMC3591129/

134. Sethi T, Rintoul RC, Moore SM, MacKinnon AC, Salter D, Choo C, et al. Extracellular matrix proteins protect small cell lung cancer cells against apoptosis: a mechanism for small cell lung cancer growth and drug resistance in vivo. Nat Med. 1999 Jun;5(6):662–8.

135. Rintoul RC, Sethi T. The role of extracellular matrix in small-cell lung cancer. Lancet Oncol. 2001 Jul;2(7):437–42.

136. Su C, Su B, Tang L, Zhao Y, Zhou C. Effects of Collagen IV on Cisplatin-Induced Apoptosis of Non-Small Cell Lung Cancer Cells. Cancer investigation. 2007 Nov 1;25:542–9.

137. de Polo A, Luo Z, Gerarduzzi C, Chen X, Little JB, Yuan Z-M. AXL receptor signalling suppresses p53 in melanoma through stabilization of the MDMX–MDM2 complex. Journal of Molecular Cell Biology [Internet]. 2016 Nov 9 [cited 2018 Dec 11]; Available from: https://academic.oup.com/jmcb/article-lookup/doi/10.1093/jmcb/mjw045

138. Zhou BP, Liao Y, Xia W, Spohn B, Lee MH, Hung MC. Cytoplasmic localization of p21Cip1/WAF1 by Akt-induced phosphorylation in HER-2/neu-overexpressing cells. Nat Cell Biol. 2001 Mar;3(3):245–52.

139. Menendez JA, Mehmi I, Lupu R. Heregulin-triggered Her-2/neu signaling enhances nuclear accumulation of p21WAF1/CIP1 and protects breast cancer cells from cisplatin-induced genotoxic damage. Int J Oncol. 2005 Mar;26(3):649–59.

140. Sigurðsson HH, Olesen CW, Dybboe R, Lauritzen G, Pedersen SF. Constitutively active ErbB2 regulates cisplatin-induced cell death in breast cancer cells via pro- and antiapoptotic mechanisms. Mol Cancer Res. 2015 Jan;13(1):63–77.

141. Xia X, Ma Q, Li X, Ji T, Chen P, Xu H, et al. Cytoplasmic p21 is a potential predictor for cisplatin sensitivity in ovarian cancer. BMC Cancer. 2011 Sep 21;11:399.

142. Damiano JS. Integrins as novel drug targets for overcoming innate drug resistance. Curr Cancer Drug Targets. 2002 Mar;2(1):37–43.

143. Damiano JS, Cress AE, Hazlehurst LA, Shtil AA, Dalton WS. Cell adhesion mediated drug resistance (CAM-DR): role of integrins and resistance to apoptosis in human myeloma cell lines. Blood. 1999 Mar 1;93(5):1658–67.

144. Hazlehurst LA, Damiano JS, Buyuksal I, Pledger WJ, Dalton WS. Adhesion to fibronectin via beta1 integrins regulates p27kip1 levels and contributes to cell adhesion mediated drug resistance (CAM-DR). Oncogene. 2000 Sep 7;19:4319–27.

145. Hazlehurst LA, Argilagos RF, Emmons M, Boulware D, Beam CA, Sullivan DM, et al. Cell adhesion to fibronectin (CAM-DR) influences acquired mitoxantrone resistance in U937 cells. Cancer Res. 2006 Feb 15;66:2338–45.

146. Damiano JS, Hazlehurst LA, Dalton WS. Cell adhesion-mediated drug resistance (CAM-DR) protects the K562 chronic myelogenous leukemia cell line from apoptosis induced by BCR/ABL inhibition, cytotoxic drugs, and gamma-irradiation. Leukemia. 2001 Aug;15:1232–9.

147. Zhu B, Zhao L, Zhu L, Wang H, Sha Y, Yao J, et al. Oroxylin A reverses CAM-DR of HepG2 cells by suppressing Integrinβ1 and its related pathway. Toxicology and Applied Pharmacology. 2012 Mar;259(3):387–94.

148. Nakagawa Y, Nakayama H, Nagata M, Yoshida R, Kawahara K, Hirosue A, et al. Overexpression of fibronectin confers cell adhesion-mediated drug resistance (CAM-DR) against 5-FU in oral squamous cell carcinoma cells. Int J Oncol. 2014 Apr;44(4):1376–84.

149. Yan L, Wang C, Lin B, Liu J, Liu D, Hou R, et al. Lewis y enhances CAM-DR in ovarian cancer cells by activating the FAK signaling pathway and upregulating Bcl-2/Bcl-XL expression. Biochimie. 2015 Jun;113:17–25.

150. El Azreq M-A, Naci D, Aoudjit F. Collagen/β1 integrin signaling up-regulates the ABCC1/MRP-1 transporter in an ERK/MAPK-dependent manner. Chernoff J, editor. Molecular Biology of the Cell. 2012 Sep;23(17):3473–84.

151. Hanker AB, Estrada MV, Bianchini G, Moore PD, Zhao J, Cheng F, et al. Extracellular Matrix/Integrin Signaling Promotes Resistance to Combined Inhibition of HER2 and PI3K in HER2+ Breast Cancer. Cancer Res. 2017 15;77(12):3280–92.

152. Naci D, Vuori K, Aoudjit F. Alpha2beta1 integrin in cancer development and chemoresistance. Seminars in Cancer Biology. 2015 Dec;35:145–53.

153. Iyoda T, Nagamine Y, Nakane Y, Tokita Y, Akari S, Otsuka K, et al. Coadministration of the FNIII14 Peptide Synergistically Augments the Anti-Cancer Activity of Chemotherapeutic Drugs by Activating Pro-Apoptotic Bim. PLoS One [Internet]. 2016 Sep 13 [cited 2018 Dec 13];11(9). Available from: https://www.ncbi.nlm.nih.gov/pmc/articles/PMC5021278/

154. Eriksson J, Le Joncour V, Nummela P, Jahkola T, Virolainen S, Laakkonen P, et al. Gene expression analyses of primary melanomas reveal CTHRC1 as an important player in melanoma progression. Oncotarget [Internet]. 2016 Mar 22 [cited 2018 Dec 14];7(12). Available from: http://www.oncotarget.com/fulltext/7604

155. Foy M, Anézo O, Saule S, Planque N. PRL-3/PTP4A3 phosphatase regulates integrin β1 in adhesion structures during migration of human ocular melanoma cells. Experimental Cell Research. 2017 Apr;353(2):88–99.

156. Melchiori A, Mortarini R, Carlone S, Marchisio PC, Anichini A, Noonan DM, et al. The α3β1 Integrin Is Involved in Melanoma Cell Migration and Invasion. Experimental Cell Research. 1995 Jul;219(1):233–42.

157. Schön M, Schön MP, Kuhröber A, Schirmbeck R, Kaufmannn R, Klein CE. Expression of the human alpha2 integrin subunit in mouse melanoma cells confers the ability to undergo collagen-directed adhesion, migration and matrix reorganization. J Invest Dermatol. 1996 Jun;106(6):1175–81.

158. Bérubé M, Talbot M, Collin C, Paquet-Bouchard C, Germain L, Guérin SL, et al. Role of the extracellular matrix proteins in the resistance of SP6.5 uveal melanoma cells toward cisplatin. Int J Oncol. 2005 Feb;26(2):405–13.

159. Morgan MR, Humphries MJ, Bass MD. Synergistic control of cell adhesion by integrins and syndecans. Nat Rev Mol Cell Biol. 2007;8(12):957–69.

160. Seetharaman S, Etienne-Manneville S. Integrin diversity brings specificity in mechanotransduction. Biology of the Cell. 2018;110(3):49–64.

161. Geiger B, Spatz JP, Bershadsky AD. Environmental sensing through focal adhesions. Nature Reviews Molecular Cell Biology. 2009 Jan;10(1):21–33.

162. Pickup MW, Mouw JK, Weaver VM. The extracellular matrix modulates the hallmarks of cancer. EMBO reports. 2014 Dec 1;15(12):1243–53.

163. Gilmore AP, Metcalfe AD, Romer LH, Streuli CH. Integrin-mediated survival signals regulate the apoptotic function of Bax through its conformation and subcellular localization. J Cell Biol. 2000 Apr 17;149(2):431–46.

164. Frisch SM, Vuori K, Ruoslahti E, Chan-Hui PY. Control of adhesion-dependent cell survival by focal adhesion kinase. J Cell Biol. 1996 Aug;134(3):793–9.

165. Lewis JM, Truong TN, Schwartz MA. Integrins regulate the apoptotic response to DNA damage through modulation of p53. Proc Natl Acad Sci U S A. 2002 Mar 19;99(6):3627–32.

166. Golubovskaya VM, Cance WG. FAK and p53 Protein Interactions. Anticancer Agents Med Chem. 2011 Sep 1;11(7):617–9.

167. Frantz C, Stewart KM, Weaver VM. The extracellular matrix at a glance. J Cell Sci. 2010;123:4195–200.

168. Hynes RO. Extracellular matrix: not just pretty fibrils. Science. 2009 Nov 27;326(5957):1216–9.

169. Gattazzo F, Urciuolo A, Bonaldo P. Extracellular matrix: a dynamic microenvironment for stem cell niche. Biochim Biophys Acta. 2014 Aug;1840(8):2506–19.

170. Lu P, Takai K, Weaver VM, Werb Z. Extracellular Matrix Degradation and Remodeling in Development and Disease. Cold Spring Harb Perspect Biol [Internet]. 2011 Dec [cited 2019 Jan 9];3(12). Available from: https://www.ncbi.nlm.nih.gov/pmc/articles/PMC3225943/

171. Pylayeva Y. Ras- and PI3K dependent breast tumorigenesis in mice and humans requires focal adhesion kinase signaling. J Clin Invest. 2009;119:252–66.

172. Provenzano PP, Inman DR, Eliceiri KW, Knittel JG, Yan L, Rueden CT, et al. Collagen density promotes mammary tumor initiation and progression. BMC Med. 2008 Apr 28;6:11.

173. Bae YH. A FAK-Cas-Rac-Lamellipodin Signaling Module Transduces Extracellular Matrix Stiffness into Mechanosensitive Cell Cycling. Sci Signal. 2014;7:ra57.

174. Chambard J-C, Lefloch R, Pouysségur J, Lenormand P. ERK implication in cell cycle regulation. Biochim Biophys Acta. 2007 Aug;1773(8):1299–310.

175. Provenzano PP, Keely PJ. Mechanical signaling through the cytoskeleton regulates cell proliferation by coordinated focal adhesion and Rho GTPase signaling. J Cell Sci. 2011 Apr 15;124(Pt 8):1195–205.

176. Mouw JK, Ou G, Weaver VM. Extracellular matrix assembly: a multiscale deconstruction. Nat Rev Mol Cell Biol. 2014 Dec;15(12):771–85.

177. Ricard-Blum S. The collagen family. Cold Spring Harb Perspect Biol. 2011;3(1):a004978.

178. Xian X, Gopal S, Couchman JR. Syndecans as receptors and organizers of the extracellular matrix. Cell and Tissue Research. 2010;339(1):31–46.

179. Weiss L. Metastatic inefficiency. Adv Cancer Res. 1990;54:159–211.

180. Wu J-J, Weis MA, Kim LS, Eyre DR. Type III collagen, a fibril network modifier in articular cartilage. J Biol Chem. 2010 Jun 11;285(24):18537–44.

181. Bruckner P. Suprastructures of extracellular matrices: paradigms of functions controlled by aggregates rather than molecules. Cell Tissue Res. 2010 Jan;339(1):7–18.

182. Fancy cartoon model of the collagen triple helix [Internet]. Wikimedia Commons. [cited 2019 Jan 25]. Available from: https://commons.wikimedia.org/wiki/File:Collagentriplehelix.png

183. Sherman VR, Lopez MI. Transmission electron micrograph of the collagen fibrils in rabbit skin. [Internet]. 2014 [cited 2019 Jan 25]. Available from: https://commons.wikimedia.org/wiki/File:Collagen_fibrils_in_rabbit_skin.jpg

184. Ricard-Blum S, Ballut L. Matricryptins derived from collagens and proteoglycans. Front Biosci (Landmark Ed). 2011 Jan 1;16:674–97.

185. Franzke C-W, Bruckner P, Bruckner-Tuderman L. Collagenous Transmembrane Proteins: Recent Insights into Biology and Pathology. J Biol Chem. 2005 Nov 2;280(6):4005–8.

186. Kadler KE, Hill A, Canty-Laird EG. Collagen fibrillogenesis: fibronectin, integrins, and minor collagens as organizers and nucleators. Curr Opin Cell Biol. 2008 Oct;20(5):495–501.

187. Zollinger AJ, Smith ML. Fibronectin, the extracellular glue. Matrix Biol. 2017;60–61:27–37.

188. Schwarzbauer JE, DeSimone DW. Fibronectins, their fibrillogenesis, and in vivo functions. Cold Spring Harb Perspect Biol. 2011 Jul 1;3(7).

189. Sottile J, Hocking DC. Fibronectin Polymerization Regulates the Composition and Stability of Extracellular Matrix Fibrils and Cell-Matrix Adhesions. Mol Biol Cell. 2002 Oct;13(10):3546–59.

190. Xia H, Nho RS, Kahm J, Kleidon J, Henke CA. Focal adhesion kinase is upstream of phosphatidylinositol 3-kinase/Akt in regulating fibroblast survival

in response to contraction of type I collagen matrices via a beta 1 integrin viability signaling pathway. J Biol Chem. 2004 Jul 30;279(31):33024–34.

191. Montgomery AM, Reisfeld RA, Cheresh DA. Integrin alpha v beta 3 rescues melanoma cells from apoptosis in three-dimensional dermal collagen. Proc Natl Acad Sci U S A. 1994 Sep 13;91(19):8856–60.

192. Weinreb PH, Li S, Gao SX, Liu T, Pepinsky RB, Caravella JA, et al. Dynamic structural changes are observed upon collagen and metal ion binding to the integrin α1 I domain. J Biol Chem. 2012 Sep 21;287(39):32897–912.

193. Singh P, Carraher C, Schwarzbauer JE. Assembly of fibronectin extracellular matrix. Annu Rev Cell Dev Biol. 2010;26:397–419.

194. Gee EPS, Yüksel D, Stultz CM, Ingber DE. SLLISWD Sequence in the 10FNIII Domain Initiates Fibronectin Fibrillogenesis. Journal of Biological Chemistry. 2013 Jul 19;288(29):21329–40.

195. Wierzbicka-Patynowski I, Schwarzbauer JE. The ins and outs of fibronectin matrix assembly. J Cell Sci. 2003 Aug 15;116(Pt 16):3269–76.

196. Pierschbacher MD, Ruoslahti E. Cell attachment activity of fibronectin can be duplicated by small synthetic fragments of the molecule. Nature. 1984 May 3;309(5963):30–3.

197. Wayner EA, Garcia-Pardo A, Humphries MJ, McDonald JA, Carter WG. Identification and characterization of the T lymphocyte adhesion receptor for an alternative cell attachment domain (CS-1) in plasma fibronectin. The Journal of Cell Biology. 1989 Sep 1;109(3):1321–30.

198. Guan JL, Hynes RO. Lymphoid cells recognize an alternatively spliced segment of fibronectin via the integrin receptor alpha 4 beta 1. Cell. 1990 Jan 12;60(1):53–61.

199. Ilić D, Kovačič B, Johkura K, Schlaepfer DD, Tomašević N, Han Q, et al. FAK promotes organization of fibronectin matrix and fibrillar adhesions. Journal of Cell Science. 2004 Jan 15;117(2):177–87.

200. Nojima Y, Humphries MJ, Mould AP, Komoriya A, Yamada KM, Schlossman SF, et al. VLA-4 mediates CD3-dependent CD4+ T cell activation via the CS1 alternatively spliced domain of fibronectin. Journal of Experimental Medicine. 1990 Oct 1;172(4):1185–92.

201. Mostafavi-Pour Z, Askari JA, Parkinson SJ, Parker PJ, Ng TTC, Humphries MJ. Integrin-specific signaling pathways controlling focal adhesion formation and cell migration. J Cell Biol. 2003 Apr 14;161(1):155–67.

202. Ruoslahti E. Fibronectin and its integrin receptors in cancer. Adv Cancer Res. 1999;76:1–20.

203. Matter ML, Ruoslahti E. A signaling pathway from the alpha5beta1 and alpha(v)beta3 integrins that elevates bcl-2 transcription. J Biol Chem. 2001 Jul 27;276(30):27757–63.

204. Tang N, Wang X, Huang T, Wu Y, Chen Y. Role of Ets-1 in fibronectin-derived heparin-binding domain polypeptides alleviating melanoma cell invasiveness and chemoresistance. Exp Dermatol. 2014 Jul;23(7):512–3.

205. Fukai F, Mashimo M, Akiyama K, Goto T, Tanuma S, Katayama T. Modulation of apoptotic cell death by extracellular matrix proteins and a fibronectin-derived antiadhesive peptide. Exp Cell Res. 1998 Jul 10;242(1):92–9.

206. Fukai F, Kamiya S, Ohwaki T, Goto S, Akiyama K, Goto T, et al. The fibronectin-derived anti-adhesive peptide III14-2 suppresses adhesion and apoptosis of leukemic cell lines through down-regulation of protein-tyrosine phosphorylation. Cell Mol Biol (Noisy-le-grand). 2000 Feb;46(1):145–52.

207. Kato R, Ishikawa T, Kamiya S, Oguma F, Ueki M, Goto S, et al. A new type of antimetastatic peptide derived from fibronectin. Clin Cancer Res. 2002 Jul;8(7):2455–62.

208. Kamiya S, Kato R, Wakabayashi M, Tohyama T, Enami I, Ueki M, et al. Fibronectin peptides derived from two distinct regions stimulate adipocyte differentiation by preventing fibronectin matrix assembly. Biochemistry. 2002 Mar 5;41(9):3270–7.

209. Esko JD, Zhang L. Influence of core protein sequence on glycosaminoglycan assembly. Curr Opin Struct Biol. 1996 Oct;6(5):663–70.

210. Bishop JR, Schuksz M, Esko JD. Heparan sulphate proteoglycans fine-tune mammalian physiology. Nature. 2007;446:1030–7.

211. Nadanaka S, Kitagawa H. Heparan sulphate biosynthesis and disease. J Biochem. 2008 Jul;144(1):7–14.

212. Couchman JR, Pataki CA. An introduction to proteoglycans and their localization. J Histochem Cytochem. 2012 Dec;60:885–97.

213. Couchman JR. Transmembrane signaling proteoglycans. Annu Rev Cell Dev Biol. 2010;26:89–114.

214. Sarrazin S, Lamanna WC, Esko JD. Heparan sulfate proteoglycans. Cold Spring Harb Perspect Biol. 2011 Jul;3(7).

215. Häcker U, Nybakken K, Perrimon N. Heparan sulphate proteoglycans: the sweet side of development. Nat Rev Mol Cell Biol. 2005;6:530–41.

216. Hemker HC. A century of heparin: past, present and future. J Thromb Haemost. 2016;14(12):2329–38.

217. Marsico G, Russo L, Quondamatteo F, Pandit A. Glycosylation and Integrin Regulation in Cancer. Trends in Cancer. 2018 Aug;4(8):537–52.

218. Messmore HL, Wehrmacher WH, Coyne E, Fareed J. Heparin to pentasaccharide and beyond: the end is not in sight. Semin Thromb Hemost. 2004 Feb;30 Suppl 1:81–8.

219. Auer R, Scheer A, Wells PS, Boushey R, Asmis T, Jonker D, et al. The use of extended perioperative low molecular weight heparin (tinzaparin) to improve disease-free survival following surgical resection of colon cancer: a pilot randomized controlled trial. Blood Coagulation & Fibrinolysis. 2011 Dec;22(8):760–2.

220. Amirkhosravi A, Mousa SA, Amaya M, Francis JL. Antimetastatic effect of tinzaparin, a low-molecular-weight heparin. J Thromb Haemost. 2003 Sep;1(9):1972–6.

221. Mousa SA, Mohamed S. Anti-angiogenic mechanisms and efficacy of the low molecular weight heparin, tinzaparin: anti-cancer efficacy. Oncol Rep. 2004 Oct;12(4):683–8.

222. Mousa SA, Petersen LJ. Anti-cancer properties of low-molecular-weight heparin: Preclinical evidence. Thrombosis and Haemostasis [Internet]. 2009 Jul 6 [cited 2016 Apr 21]; Available from: http://www.schattauer.de/index.php?id=1214&doi=10.1160/TH08-12-0832

223. Niu Q, Wang W, Li Y, Ruden DM, Wang F, Li Y, et al. Low Molecular Weight Heparin Ablates Lung Cancer Cisplatin-Resistance by Inducing Proteasome-Mediated ABCG2 Protein Degradation. Viglietto G, editor. PLoS ONE. 2012 Jul 23;7(7):e41035.

224. Pfankuchen DB, Stölting DP, Schlesinger M, Royer H-D, Bendas G. Low molecular weight heparin tinzaparin antagonizes cisplatin resistance of ovarian cancer cells. Biochem Pharmacol. 2015 Sep 15;97(2):147–57.

225. Phillips PG, Yalcin M, Cui H, Abdel-Nabi H, Sajjad M, Bernacki R, et al. Increased tumor uptake of chemotherapeutics and improved chemoresponse by novel non-anticoagulant low molecular weight heparin. Anticancer Res. 2011 Feb;31(2):411–9.

226. Schlesinger M, Schmitz P, Zeisig R, Naggi A, Torri G, Casu B, et al. The inhibition of the integrin VLA-4 in MV3 melanoma cell binding by non-anticoagulant heparin derivatives. Thromb Res. 2012;129(5):603–10.

227. Schlesinger M, Roblek M, Ortmann K, Naggi A, Torri G, Borsig L, et al. The role of VLA-4 binding for experimental melanoma metastasis and its inhibition by heparin. Thromb Res. 2014 May;133(5):855–62.

228. Pfankuchen DB, Baltes F, Batool T, Li J-P, Schlesinger M, Bendas G. Heparin antagonizes cisplatin resistance of A2780 ovarian cancer cells by affecting the Wnt signaling pathway. Oncotarget. 2017 Jun 28;

229. Streuli CH. Integrins and cell-fate determination. J Cell Sci. 2009 Jan 15;122:171–7.

230. Hynes RO. Integrins: bidirectional, allosteric signaling machines. Cell. 2002 Sep 20;110(6):673–87.

231. Huang C, Springer TA. Folding of the beta-propeller domain of the integrin alphaL subunit is independent of the I domain and dependent on the beta2 subunit. Proc Natl Acad Sci U S A. 1997 Apr 1;94:3162–7.

232. Lu C, Oxvig C, Springer TA. The Structure of the β-Propeller Domain and C-terminal Region of the Integrin αM Subunit. Dependence On B Subunit Association And Prediction Of Domains. J Biol Chem. 1998 Dec 6;273(24):15138–47.

233. Cai X, Thinn AMM, Wang Z, Shan H, Zhu J. The importance of N-glycosylation on β3 integrin ligand binding and conformational regulation. Sci Rep. 2017 05;7(1):4656.

234. Zheng M, Fang H, Hakomori S. Functional role of N-glycosylation in alpha 5 beta 1 integrin receptor. De-N-glycosylation induces dissociation or altered association of alpha 5 and beta 1 subunits and concomitant loss of fibronectin binding activity. J Biol Chem. 1994 Apr 22;269(16):12325–31.

235. Gu J, Taniguchi N. Regulation of integrin functions by N-glycans. Glycoconj J. 2004;21(1–2):9–15.

236. Pocheć E, Bubka M, Rydlewska M, Janik M, Pokrywka M, Lityńska A. Aberrant Glycosylation of αvβ3 Integrin is Associated with Melanoma Progression. Anticancer Res. 2015 Jan 4;35(4):2093–103.

237. Pocheć E, Janik M, Hoja-Łukowicz D, Link-Lenczowski P, Przybyło M, Lityńska A. Expression of integrins α3β1 and α5β1 and GlcNAc β1,6 glycan branching influences metastatic melanoma cell migration on fibronectin. Eur J Cell Biol. 2013 Dec;92(12):355–62.

238. Yu S, Fan J, Liu L, Zhang L, Wang S, Zhang J. Caveolin-1 up-regulates integrin α2,6-sialylation to promote integrin α5β1-dependent hepatocarcinoma cell adhesion. FEBS Lett. 2013 Mar 18;587(6):782–7.

239. Yuan Y, Wu L, Shen S, Wu S, Burdick MM. Effect of alpha 2,6 sialylation on integrin-mediated adhesion of breast cancer cells to fibronectin and collagen IV. Life Sci. 2016 Mar 15;149:138–45.

240. Alberts B, editor. Molecular biology of the cell. 5th ed. New York: Garland Science; 2008. 1 p.

241. Tiwari S, Askari JA, Humphries MJ, Bulleid NJ. Divalent cations regulate the folding and activation status of integrins during their intracellular trafficking. J Cell Sci. 2011 May 15;124:1672–80.

242. A. S, Graf R, G. D. Neuroblastoma Integrins. In: Shimada H, editor. Neuroblastoma [Internet]. InTech; 2013 [cited 2016 Jun 19]. Available from: http://www.intechopen.com/books/neuroblastoma/neuroblastoma-integrins

243. Kinashi T. Intracellular signalling controlling integrin activation in lymphocytes. Nat Rev Immunol. 2005;5(7):546–59.

244. Lilja J, Ivaska J. Integrin activity in neuronal connectivity. J Cell Sci. 2018 Jun 15;131(12):jcs212803.

245. Humphries JD, Chastney MR, Askari JA, Humphries MJ. Signal transduction via integrin adhesion complexes. Current Opinion in Cell Biology. 2019 Feb;56:14–21.

246. Morgan MR, Humphries MJ, Bass MD. Synergistic control of cell adhesion by integrins and syndecans. Nat Rev Mol Cell Biol. 2007 Dec;8:957–69.

247. Xian X, Gopal S, Couchman JR. Syndecans as receptors and organizers of the extracellular matrix. Cell Tissue Res. 2010 Jan;339:31–46.

248. Huveneers S, Danen EH. Adhesion signaling - crosstalk between integrins, Src and Rho. J Cell Sci. 2009 Apr 15;122:1059–69.

249. Lau T-L, Kim C, Ginsberg MH, Ulmer TS. The structure of the integrin aIIbb3 transmembrane complex explains integrin transmembrane signalling. The EMBO Journal. 2009;28:1351–61.

250. Desgrosellier JS, Cheresh DA. Integrins in cancer: biological implications and therapeutic opportunities. Nat Rev Cancer. 2010 Jan;10(1):9–22.

251. Mizejewski GJ. Role of integrins in cancer: survey of expression patterns. Proc Soc Exp Biol Med. 1999 Nov;222:124–38.

252. Pan B, Guo J, Liao Q, Zhao Y. β1 and β3 integrins in breast, prostate and pancreatic cancer: A novel implication (Review). Oncology Letters [Internet]. 2018 Feb 16 [cited 2018 Oct 18]; Available from: http://www.spandidos-publications.com/10.3892/ol.2018.8076

253. Danen EHJ, Berge PJMT, Muijen GNPV, Hof-Grootenboer AEV, Bröcker EB, Ruiter DJ. Emergence of α5β1 fibronectin- and αvβ3 vitronectin-receptor expression in melanocytic tumour progression. Histopathology. 1994 Mar 1;24(3):249–56.

254. Lydolph MC, Morgan-Fisher M, Høye AM, Couchman JR, Wewer UM, Yoneda A. Alpha9beta1 integrin in melanoma cells can signal different adhesion states for migration and anchorage. Exp Cell Res. 2009 Nov 15;315(19):3312–24.

255. Friedl P, Maaser K, Klein CE, Niggemann B, Krohne G, Zänker KS. Migration of highly aggressive MV3 melanoma cells in 3-dimensional collagen lattices results in local matrix reorganization and shedding of alpha2 and beta1 integrins and CD44. Cancer Res. 1997 May 15;57(10):2061–70.

256. Maaser K, Wolf K, Klein CE, Niggemann B, Zänker KS, Bröcker EB, et al. Functional hierarchy of simultaneously expressed adhesion receptors: integrin alpha2beta1 but not CD44 mediates MV3 melanoma cell migration and matrix reorganization within three-dimensional hyaluronan-containing collagen matrices. Mol Biol Cell. 1999 Oct;10(10):3067–79.

257. Danen EH, van Muijen GN, van de Wiel-van Kemenade E, Jansen KF, Ruiter DJ, Figdor CG. Regulation of integrin-mediated adhesion to laminin and

collagen in human melanocytes and in non-metastatic and highly metastatic human melanoma cells. Int J Cancer. 1993 May 8;54(2):315–21.

258. Aoudjit F, Vuori K. Integrin signaling inhibits paclitaxel-induced apoptosis in breast cancer cells. Oncogene. 2001 Aug;20(36):4995–5004.

259. Truong HH, Xiong J, Ghotra VPS, Nirmala E, Haazen L, Le Dévédec SE, et al. β1 integrin inhibition elicits a prometastatic switch through the TGFβ-miR-200-ZEB network in E-cadherin-positive triple-negative breast cancer. Sci Signal. 2014 Feb 11;7(312):ra15.

260. Parvani JG, Galliher-Beckley AJ, Schiemann BJ, Schiemann WP. Targeted inactivation of β1 integrin induces β3 integrin switching, which drives breast cancer metastasis by TGF-β. Mol Biol Cell. 2013 Nov 1;24(21):3449–59.

261. Desgrosellier JS, Barnes LA, Shields DJ, Huang M, Lau SK, Prévost N, et al. Integrin αvβ3/c-src "Oncogenic Unit" Promotes Anchorage-independence and Tumor Progression. Nat Med. 2009 Oct;15(10):1163–9.

262. Danen EH, Ten Berge PJ, Van Muijen GN, Van 't Hof-Grootenboer AE, Bröcker EB, Ruiter DJ. Emergence of alpha 5 beta 1 fibronectin- and alpha v beta 3 vitronectin-receptor expression in melanocytic tumour progression. Histopathology. 1994 Mar;24(3):249–56.

263. Seftor RE, Seftor EA, Gehlsen KR, Stetler-Stevenson WG, Brown PD, Ruoslahti E, et al. Role of the alpha v beta 3 integrin in human melanoma cell invasion. Proc Natl Acad Sci U S A. 1992 Mar 1;89(5):1557–61.

264. Zheng DQ, Woodard AS, Fornaro M, Tallini G, Languino LR. Prostatic carcinoma cell migration via alpha(v)beta3 integrin is modulated by a focal adhesion kinase pathway. Cancer Res. 1999 Apr 1;59(7):1655–64.

265. Keselowsky BG, Collard DM, García AJ. Surface chemistry modulates fibronectin conformation and directs integrin binding and specificity to control cell adhesion. J Biomed Mater Res A. 2003 Aug 1;66(2):247–59.

266. Keselowsky BG, Collard DM, García AJ. Integrin binding specificity regulates biomaterial surface chemistry effects on cell differentiation. Proc Natl Acad Sci U S A. 2005 Apr 26;102(17):5953–7.

267. García AJ, Vega MD, Boettiger D. Modulation of cell proliferation and differentiation through substrate-dependent changes in fibronectin conformation. Mol Biol Cell. 1999 Mar;10(3):785–98.

268. Vaillant F, Asselin-Labat M-L, Shackleton M, Forrest NC, Lindeman GJ, Visvader JE. The mammary progenitor marker CD61/beta3 integrin identifies cancer stem cells in mouse models of mammary tumorigenesis. Cancer Res. 2008 Oct 1;68(19):7711–7.

269. Seguin L, Desgrosellier JS, Weis SM, Cheresh DA. Integrins and cancer: regulators of cancer stemness, metastasis, and drug resistance. Trends Cell Biol. 2015 Apr;25(4):234–40.

270. Couchman JR, Gopal S, Lim HC, Nørgaard S, Multhaupt HAB. Syndecans: from peripheral coreceptors to mainstream regulators of cell behaviour. Int J Exp Pathol. 2015 Feb;96(1):1–10.

271. Mahalingam Y, Gallagher JT, Couchman JR. Cellular adhesion responses to the heparin-binding (HepII) domain of fibronectin require heparan sulfate with specific properties. J Biol Chem. 2007 Feb 2;282(5):3221–30.

272. Fuster MM, Wang L, Castagnola J, Sikora L, Reddi K, Lee PHA, et al. Genetic alteration of endothelial heparan sulfate selectively inhibits tumor angiogenesis. The Journal of Cell Biology. 2007 May 7;177(3):539–49.

273. McQuade KJ. Syndecan-1 regulates αvβ5 integrin activity in B82L fibroblasts. Journal of Cell Science. 2006 Jun 15;119(12):2445–56.

274. Beauvais DM, Burbach BJ, Rapraeger AC. The syndecan-1 ectodomain regulates αvβ3 integrin activity in human mammary carcinoma cells. The Journal of Cell Biology. 2004 Oct 11;167(1):171–81.

275. Whiteford JR, Couchman JR. A Conserved NXIP Motif Is Required for Cell Adhesion Properties of the Syndecan-4 Ectodomain. Journal of Biological Chemistry. 2006 Oct 27;281(43):32156–63.

276. Couchman JR. Transmembrane signaling proteoglycans. Annu Rev Cell Dev Biol. 2010;26:89–114.

277. Manon-Jensen T, Itoh Y, Couchman JR. Proteoglycans in health and disease: the multiple roles of syndecan shedding. FEBS J. 2010 Aug;277:3876–89.

278. Beauvais DM, Rapraeger AC. Syndecans in tumor cell adhesion and signaling. Reprod Biol Endocrinol. 2004 Jan 7;2:3.

279. Woods A, Longley RL, Tumova S, Couchman JR. Syndecan-4 binding to the high affinity heparin-binding domain of fibronectin drives focal adhesion formation in fibroblasts. Arch Biochem Biophys. 2000 Feb 1;374:66–72.

280. Woods A, Couchman JR. Syndecan-4 and focal adhesion function. Curr Opin Cell Biol. 2001 Oct;13:578–83.

281. Hozumi K, Suzuki N, Nielsen PK, Nomizu M, Yamada Y. Laminin α1 Chain LG4 Module Promotes Cell Attachment through Syndecans and Cell Spreading through Integrin α2β1. Journal of Biological Chemistry. 2006 Oct 27;281(43):32929–40.

282. Ogawa T, Tsubota Y, Hashimoto J, Kariya Y, Miyazaki K. The Short Arm of Laminin γ2 Chain of Laminin-5 (Laminin-332) Binds Syndecan-1 and Regulates Cellular Adhesion and Migration by Suppressing Phosphorylation of Integrin β4 Chain. Ginsberg M, editor. Molecular Biology of the Cell. 2007 May;18(5):1621–33.

283. Frisco-Cabanos HL, Watanabe M, Okumura N, Kusamori K, Takemoto N, Takaya J, et al. Synthetic Molecules that Protect Cells from Anoikis and Their

Use in Cell Transplantation. Angewandte Chemie International Edition. 2014 Oct 13;53(42):11208–13.

284. Koo B-K, Jung YS, Shin J, Han I, Mortier E, Zimmermann P, et al. Structural Basis of Syndecan-4 Phosphorylation as a Molecular Switch to Regulate Signaling. Journal of Molecular Biology. 2006 Jan 27;355(4):651–63.

285. Ng T, Shima D, Squire A, Bastiaens PI, Gschmeissner S, Humphries MJ, et al. PKCalpha regulates beta1 integrin-dependent cell motility through association and control of integrin traffic. EMBO J. 1999;18(14):3909–23.

286. Keum E, Kim Y, Kim J, Kwon S, Lim Y, Han I, et al. Syndecan-4 regulates localization, activity and stability of protein kinase C-alpha. Biochem J. 2004;378(Pt 3):1007–14.

287. Partovian C, Ju R, Zhuang ZW, Martin KA, Simons M. Syndecan-4 regulates subcellular localization of mTOR Complex2 and Akt activation in a PKCalpha-dependent manner in endothelial cells. Mol Cell. 2008 Oct 10;32(1):140–9.

288. Ju R, Simons M. Syndecan 4 regulation of PDK1-dependent Akt activation. Cellular Signalling. 2013 Jan;25(1):101–5.

289. Sulzmaier FJ, Jean C, Schlaepfer DD. FAK in cancer: mechanistic findings and clinical applications. Nature Reviews Cancer. 2014 Aug 7;14(9):598–610.

290. Corsi JM. Autophosphorylation-independent and -dependent functions of focal adhesion kinase during development. J Biol Chem. 2009;284:34769–76.

291. Cance WG, Golubovskaya VM. Focal adhesion kinase versus p53: apoptosis or survival? Sci Signal. 2008;1:e22.

292. Zhao J, Guan JL. Signal transduction by focal adhesion kinase in cancer. Cancer Metastasis Rev. 2009;28:35–49.

293. Parsons JT. Focal adhesion kinase: the first ten years. J Cell Sci. 2003;116:1409–16.

294. Schaller MD. Cellular functions of FAK kinases: insight into molecular mechanisms and novel functions. J Cell Sci. 2010;123:1007–13.

295. Eke I. [beta]1 Integrin/FAK/cortactin signaling is essential for human head and neck cancer resistance to radiotherapy. J Clin Invest. 2012;122:1529–40.

296. Lane D, Goncharenko-Khaider N, Rancourt C, Piche A. Ovarian cancer ascites protects from TRAIL-induced cell death through alphavbeta5 integrin-mediated focal adhesion kinase and Akt activation. Oncogene. 2010;29:3519–31.

297. Kang Y. Role of focal adhesion kinase in regulating YB 1 mediated paclitaxel resistance in ovarian cancer. J Natl Cancer Inst. 2013;105:1485–95.

298. Halder J. Therapeutic efficacy of a novel focal adhesion kinase inhibitor TAE226 in ovarian carcinoma. Cancer Res. 2007;67:10976–83.

299. Goni GM, Epifano C, Boskovic J, Camacho-Artacho M, Zhou J, Bronowska A, et al. Phosphatidylinositol 4,5-bisphosphate triggers activation of focal adhesion kinase by inducing clustering and conformational changes. Proceedings of the National Academy of Sciences. 2014 Aug 5;111(31):E3177–86.

300. Frame MC, Patel H, Serrels B, Lietha D, Eck MJ. The FERM domain: organizing the structure and function of FAK. Nature Rev Mol Cell Biol. 2010;11:802–14.

301. Choi CH, Webb BA, Chimenti MS, Jacobson MP, Barber DL. pH sensing by FAK His58 regulates focal adhesion remodeling. J Cell Biol. 2013;202:849–59.

302. Levental KR. Matrix crosslinking forces tumor progression by enhancing integrin signaling. Cell. 2009;139:891–906.

303. Cutaneous Melanoma - TCGA [Internet]. [cited 2016 May 15]. Available from: http://cancergenome.nih.gov/cancersselected/melanoma

304. Engelman JA. Targeting PI3K signalling in cancer: opportunities, challenges and limitations. Nat Rev Cancer. 2009 Aug;9(8):550–62.

305. Vanhaesebroeck B, Guillermet-Guibert J, Graupera M, Bilanges B. The emerging mechanisms of isoform-specific PI3K signalling. Nature Reviews Molecular Cell Biology. 2010 May;11(5):329–41.

306. Bewick M, Lafrenie R. Adhesion Dependent Signalling in the Tumour Microenvironment: The Future of Drug Targetting. Current Pharmaceutical Design. 2006 Aug 1;12(22):2833–48.

307. Ruan G-X, Kazlauskas A. Focus on Molecules: Akt (PKB). Experimental Eye Research. 2011 Nov;93(5):570–1.

308. Maira S-M, Stauffer F, Brueggen J, Furet P, Schnell C, Fritsch C, et al. Identification and characterization of NVP-BEZ235, a new orally available dual phosphatidylinositol 3-kinase/mammalian target of rapamycin inhibitor with potent in vivo antitumor activity. Molecular Cancer Therapeutics. 2008 Jul 1;7(7):1851–63.

309. Sarbassov DD. Phosphorylation and Regulation of Akt/PKB by the Rictor-mTOR Complex. Science. 2005 Feb 18;307(5712):1098–101.

310. van Muijen GN, Jansen KF, Cornelissen IM, Smeets DF, Beck JL, Ruiter DJ. Establishment and characterization of a human melanoma cell line (MV3) which is highly metastatic in nude mice. Int J Cancer. 1991 Apr 22;48(1):85–91.

311. Van Muijen GN, Cornelissen LM, Jansen CF, Figdor CG, Johnson JP, Bröcker EB, et al. Antigen expression of metastasizing and non-metastasizing human melanoma cells xenografted into nude mice. Clin Exp Metastasis. 1991 Jun;9(3):259–72.

312. Danen EH, Van Muijen GN, Ruiter DJ. Role of integrins as signal transducing cell adhesion molecules in human cutaneous melanoma. Cancer Surv. 1995;24:43–65.

313. van Muijen GN, Danen EH, de Vries TJ, Quax PH, Verheijen JH, Ruiter DJ. Properties of metastasizing and nonmetastasizing human melanoma cells. Recent Results Cancer Res. 1995;139:105–22.

314. Schmitz P. Der Einfluss von Cyr61 auf die Adhäsionsfunktion von Integrinen und dessen Hemmung durch Heparin als Beitrag für eine antimetastatische Wirkung. Bonn: Universitäts- und Landesbibliothek Bonn; 2013.

315. Gerber U, Hoß SG, Shteingauz A, Jüngel E, Jakubzig B, Ilan N, et al. Latent heparanase facilitates VLA-4-mediated melanoma cell binding and emerges as a relevant target of heparin in the interference with metastatic progression. Semin Thromb Hemost. 2015 Mar;41(2):244–54.

316. Green MR, Sambrook J, Sambrook J. Molecular cloning: a laboratory manual. 4th ed. Cold Spring Harbor, N.Y: Cold Spring Harbor Laboratory Press; 2012. 3 p.

317. Manjunath N, Haoquan W, Sandesh S, Premlata S. Lentiviral delivery of short hairpin RNAs. Adv Drug Deliv Rev. 2009 Jul 25;61(9):732–45.

318. Cojocari Dan,. Lentiviral delivery of shRNA expression construct for stable integration and expresion of shRNA. shRNA processing and inhibitory mechanisms. (10.12.2009). http://commons.wikimedia.org/wiki/File:ShRNA_Lentivirus.svg. 2009;Zugriff am 15.11.2012.

319. Pérez-González JA, Vara J, Jiménez A. The mechanism of resistance to puromycin and to the puromycin-precursor O-demethyl-puromycin in Streptomyces alboniger. J Gen Microbiol. 1985 Nov;131(11):2877–83.

320. Duval K, Grover H, Han L-H, Mou Y, Pegoraro AF, Fredberg J, et al. Modeling Physiological Events in 2D vs. 3D Cell Culture. Physiology (Bethesda). 2017;32(4):266–77.

321. Ravi M, Paramesh V, Kaviya SR, Anuradha E, Solomon FDP. 3D cell culture systems: advantages and applications. J Cell Physiol. 2015 Jan;230(1):16–26.

322. Breslin S, O'Driscoll L. The relevance of using 3D cell cultures, in addition to 2D monolayer cultures, when evaluating breast cancer drug sensitivity and resistance. Oncotarget. 2016 Jun 10;7(29):45745–56.

323. Riss TL, Moravec RA, Niles AL, Duellman S, Benink HA, Worzella TJ, et al. Cell Viability Assays. In: Sittampalam GS, Coussens NP, Brimacombe K, Grossman A, Arkin M, Auld D, et al., editors. Assay Guidance Manual [Internet]. Bethesda (MD): Eli Lilly & Company and the National Center for Advancing Translational Sciences; 2004 [cited 2017 Jun 19]. Available from: http://www.ncbi.nlm.nih.gov/books/NBK144065/

324. Zhu Y, Tian T, Zou J, Wang Q, Li Z, Li Y, et al. Dual PI3K/mTOR inhibitor BEZ235 exerts extensive antitumor activity in HER2-positive gastric cancer. BMC Cancer [Internet]. 2015 Dec [cited 2016 Apr 5];15(1). Available from: http://www.biomedcentral.com/1471-2407/15/894

325. Jebahi A, Villedieu M, Pétigny-Lechartier C, Brotin E, Louis M-H, Abeilard E, et al. PI3K/mTOR dual inhibitor NVP-BEZ235 decreases Mcl-1 expression and sensitizes ovarian carcinoma cells to Bcl-xL-targeting strategies, provided that Bim expression is induced. Cancer Letters. 2014 Jun;348(1–2):38–49.

326. Montero JC, Chen X, Ocana A, Pandiella A. Predominance of mTORC1 over mTORC2 in the Regulation of Proliferation of Ovarian Cancer Cells: Therapeutic Implications. Molecular Cancer Therapeutics. 2012 Jun 1;11(6):1342–52.

327. Santiskulvong C, Konecny GE, Fekete M, Chen K-YM, Karam A, Mulholland D, et al. Dual Targeting of Phosphoinositide 3-Kinase and Mammalian Target of Rapamycin Using NVP-BEZ235 as a Novel Therapeutic Approach in Human Ovarian Carcinoma. Clinical Cancer Research. 2011 Apr 15;17(8):2373–84.

328. Motulsky HJ, Christopoulos A. Fitting models to biological data using linear and nonlinear regression. A practical guide to curve fitting. GraphPad Software Inc., San Diego CA, www.graphpad.com .; 2003.

329. Sack U, Tárnok A, Rothe G, editors. Cellular diagnostics: basic principles, methods and clinical applications of flow cytometry. Basel ; New York: Karger; 2009. 738 p.

330. Kierano. English: Schematic of a flow cytometer, from sheath focusing to data acquisition. [Internet]. 2012 [cited 2019 Feb 7]. Available from: https://commons.wikimedia.org/wiki/File:Cytometer.svg

331. Thermo Fisher Scientific. Fluorescence SpectraViewer - DE [Internet]. [cited 2019 Feb 9]. Available from: https://www.thermofisher.com/de/de/home/life-science/cell-analysis/labeling-chemistry/fluorescence-spectraviewer.html

332. Barbosa CMV, Bincoletto C, Barros CC, Ferreira AT, Paredes-Gamero EJ. PLCγ2 and PKC Are Important to Myeloid Lineage Commitment Triggered by M-SCF and G-CSF. Journal of Cellular Biochemistry. 2014 Jan;115(1):42–51.

333. Jaeger J, Koczan D, Thiesen H-J, Ibrahim SM, Gross G, Spang R, et al. Gene expression signatures for tumor progression, tumor subtype, and tumor thickness in laser-microdissected melanoma tissues. Clin Cancer Res. 2007 Feb 1;13(3):806–15.

334. Borsotti P, Ghilardi C, Ostano P, Silini A, Dossi R, Pinessi D, et al. Thrombospondin-1 is part of a Slug-independent motility and metastatic program in cutaneous melanoma, in association with VEGFR-1 and FGF-2. Pigment Cell Melanoma Res. 2015 Jan;28(1):73–81.

335. Jayachandran A, Anaka M, Prithviraj P, Hudson C, McKeown SJ, Lo P-H, et al. Thrombospondin 1 promotes an aggressive phenotype through epithelial-to-mesenchymal transition in human melanoma. Oncotarget. 2014 Jul 30;5(14):5782–97.

336. Kunz M, Koczan D, Ibrahim SM, Gillitzer R, Gross G, Thiesen HJ. Differential expression of thrombospondin 2 in primary and metastatic malignant melanoma. Acta Derm Venereol. 2002;82(3):163–9.

337. Li Z, Calzada MJ, Sipes JM, Cashel JA, Krutzsch HC, Annis DS, et al. Interactions of thrombospondins with alpha4beta1 integrin and CD47 differentially modulate T cell behavior. J Cell Biol. 2002 Apr 29;157(3):509–19.

338. Barazi HO, Li Z, Cashel JA, Krutzsch HC, Annis DS, Mosher DF, et al. Regulation of integrin function by CD47 ligands. Differential effects on alpha vbeta 3 and alpha 4beta1 integrin-mediated adhesion. J Biol Chem. 2002 Nov 8;277(45):42859–66.

339. Liao Q, Kleeff J, Xiao Y, Di Cesare PE, Korc M, Zimmermann A, et al. COMP is selectively up-regulated in degenerating acinar cells in chronic pancreatitis and in chronic-pancreatitis-like lesions in pancreatic cancer. Scand J Gastroenterol. 2003 Feb;38(2):207–15.

340. Kim C, Choi J, Park H, Park Y, Park J, Park T, et al. Global analysis of microarray data reveals intrinsic properties in gene expression and tissue selectivity. Bioinformatics. 2010 Jul 15;26(14):1723–30.

341. Chen J, Xi J, Tian Y, Bova GS, Zhang H. Identification, prioritization, and evaluation of glycoproteins for aggressive prostate cancer using quantitative glycoproteomics and antibody-based assays on tissue specimens. Proteomics. 2013 Aug;13(15):2268–77.

342. Klee EW, Bondar OP, Goodmanson MK, Dyer RB, Erdogan S, Bergstralh EJ, et al. Candidate serum biomarkers for prostate adenocarcinoma identified by mRNA differences in prostate tissue and verified with protein measurements in tissue and blood. Clin Chem. 2012 Mar;58(3):599–609.

343. Di Cesare PE, Chen FS, Moergelin M, Carlson CS, Leslie MP, Perris R, et al. Matrix-matrix interaction of cartilage oligomeric matrix protein and fibronectin. Matrix Biol. 2002 Aug;21(5):461–70.

344. Acharya C, Yik JHN, Kishore A, Van Dinh V, Di Cesare PE, Haudenschild DR. Cartilage oligomeric matrix protein and its binding partners in the cartilage extracellular matrix: interaction, regulation and role in chondrogenesis. Matrix Biol. 2014 Jul;37:102–11.

345. Bayless KJ, Meininger GA, Scholtz JM, Davis GE. Osteopontin is a ligand for the alpha4beta1 integrin. J Cell Sci. 1998 May;111 (Pt 9):1165–74.

346. Bayless KJ, Davis GE. Identification of dual alpha 4beta1 integrin binding sites within a 38 amino acid domain in the N-terminal thrombin fragment of human osteopontin. J Biol Chem. 2001 Apr 20;276(16):13483–9.

347. Hu DD, Lin EC, Kovach NL, Hoyer JR, Smith JW. A biochemical characterization of the binding of osteopontin to integrins alpha v beta 1 and alpha v beta 5. J Biol Chem. 1995 Nov 3;270(44):26232–8.

348. Kumar S, Sharma P, Kumar D, Chakraborty G, Gorain M, Kundu GC. Functional characterization of stromal osteopontin in melanoma progression and metastasis. PLoS ONE. 2013;8(7):e69116.

349. Tuck AB, Arsenault DM, O'Malley FP, Hota C, Ling MC, Wilson SM, et al. Osteopontin induces increased invasiveness and plasminogen activator expression of human mammary epithelial cells. Oncogene. 1999 Jul 22;18(29):4237–46.

350. Hui T, Sørensen ES, Rittling SR. Osteopontin binding to the alpha 4 integrin requires highest affinity integrin conformation, but is independent of post-translational modifications of osteopontin. Matrix Biology. 2015 Jan;41:19–25.

351. Amendola RS, Martin ACBM, Selistre-de-Araújo HS, Paula-Neto HA, Saldanha-Gama R, Barja-Fidalgo C. ADAM9 disintegrin domain activates human neutrophils through an autocrine circuit involving integrins and CXCR2. J Leukoc Biol. 2015 Mar 12;

352. Giricz O, Lauer JL, Fields GB. Variability in melanoma metalloproteinase expression profiling. J Biomol Tech. 2010 Dec;21(4):194–204.

353. Zhou M, Graham R, Russell G, Croucher PI. MDC-9 (ADAM-9/Meltrin gamma) functions as an adhesion molecule by binding the alpha(v)beta(5) integrin. Biochem Biophys Res Commun. 2001 Jan 19;280(2):574–80.

354. Zigrino P, Nischt R, Mauch C. The disintegrin-like and cysteine-rich domains of ADAM-9 mediate interactions between melanoma cells and fibroblasts. J Biol Chem. 2011 Feb 25;286(8):6801–7.

355. Kuo P-L, Huang M-S, Cheng D-E, Hung J-Y, Yang C-J, Chou S-H. Lung cancer-derived galectin-1 enhances tumorigenic potentiation of tumor-associated dendritic cells by expressing heparin-binding EGF-like growth factor. J Biol Chem. 2012 Mar 23;287(13):9753–64.

356. Fry JL, Toker A. Secreted and membrane-bound isoforms of protease ADAM9 have opposing effects on breast cancer cell migration. Cancer Res. 2010 Oct 15;70(20):8187–98.

357. Felli N, Felicetti F, Lustri AM, Errico MC, Bottero L, Cannistraci A, et al. miR-126&126* restored expressions play a tumor suppressor role by directly regulating ADAM9 and MMP7 in melanoma. PLoS ONE. 2013;8(2):e56824.

358. Nath D, Slocombe PM, Webster A, Stephens PE, Docherty AJ, Murphy G. Meltrin gamma(ADAM-9) mediates cellular adhesion through alpha(6)beta(1)integrin, leading to a marked induction of fibroblast cell motility. J Cell Sci. 2000 Jun;113 (Pt 12):2319–28.

359. Uen W-C, Hsieh C-H, Tseng T-T, Jiang SS, Tseng J-C, Lee S-C. Anchorage independency promoted tumor malignancy of melanoma cells under reattachment through elevated interleukin-8 and CXC chemokine receptor 1 expression. Melanoma Res. 2015 Feb;25(1):35–46.

360. Jenkins MH, Brinckerhoff CE, Mullins DW. CXCR3 signaling in BRAFWT melanoma increases IL-8 expression and tumorigenicity. PLoS ONE. 2015;10(3):e0121140.

361. Srivastava SK, Bhardwaj A, Arora S, Tyagi N, Singh AP, Carter JE, et al. Interleukin-8 is a key mediator of FKBP51-induced melanoma growth, angiogenesis and metastasis. Br J Cancer. 2015 May 26;112(11):1772–81.

362. Liu F-T, Rabinovich GA. Galectins as modulators of tumour progression. Nature Reviews Cancer. 2005 Jan;5(1):29–41.

363. Braeuer RR, Zigler M, Kamiya T, Dobroff AS, Huang L, Choi W, et al. Galectin-3 Contributes to Melanoma Growth and Metastasis via Regulation of NFAT1 and Autotaxin. Cancer Research. 2012 Nov 15;72(22):5757–66.

364. Markowska AI, Liu F-T, Panjwani N. Galectin-3 is an important mediator of VEGF- and bFGF-mediated angiogenic response. Journal of Experimental Medicine. 2010 Aug 30;207(9):1981–93.

365. Newlaczyl AU, Yu L-G. Galectin-3 – A jack-of-all-trades in cancer. Cancer Letters. 2011 Dec;313(2):123–8.

366. Reticker-Flynn NE, Malta DFB, Winslow MM, Lamar JM, Xu MJ, Underhill GH, et al. A combinatorial extracellular matrix platform identifies cell-extracellular matrix interactions that correlate with metastasis. Nature Communications. 2012 Oct 9;3:1122.

367. Geaquinto DLA, Fernandes RS, Lima LG, Barja-Fidalgo C, Monteiro RQ. Procoagulant properties of human MV3 melanoma cells. Braz J Med Biol Res. 2008 Feb;41(2):99–105.

368. Edward M. Melanoma cell-derived factors stimulate glycosaminoglycan synthesis by fibroblasts cultured as monolayers and within contracted collagen lattices. Br J Dermatol. 2001 Mar;144:465–70.

369. Piva M, Jakubzig B, Bendas G. Integrin Activation Contributes to Lower Cisplatin Sensitivity in MV3 Melanoma Cells by Inducing the Wnt Signalling Pathway. Cancers. 2017 Sep 16;9(9):125.

370. Fuereder T, Wanek T, Pflegerl P, Jaeger-Lansky A, Hoeflmayer D, Strommer S, et al. Gastric Cancer Growth Control by BEZ235 *In Vivo* Does Not Correlate with PI3K/mTOR Target Inhibition but with [^{18} F]FLT Uptake. Clinical Cancer Research. 2011 Aug 15;17(16):5322–32.

371. Kim TK, Eberwine JH. Mammalian cell transfection: the present and the future. Analytical and Bioanalytical Chemistry. 2010 Aug;397(8):3173–8.

372. Schmitz P. Der Einfluss von Cyr61 auf die Adhäsionsfunktion von Integrinen und dessen Hemmung durch Heparin als Beitrag für eine antimetastatische Wirkung [Internet] [Dissertation]. Bonn; 2013 [cited 2014 Dec 9]. Available from: http://hss.ulb.uni-bonn.de/2013/3178/3178.pdf

373. Beauvais DM, Rapraeger AC. Syndecans in tumor cell adhesion and signaling. Reprod Biol Endocrinol. 2004 Jan 7;2:3.

374. Schlesinger M, Schmitz P, Zeisig R, Naggi A, Torri G, Casu B, et al. The inhibition of the integrin VLA-4 in MV3 melanoma cell binding by non-anticoagulant heparin derivatives. Thromb Res. 2012 May;129:603–10.

375. Pfankuchen DB, Stölting DP, Schlesinger M, Royer H-D, Bendas G. Low molecular weight heparin tinzaparin antagonizes cisplatin resistance of ovarian cancer cells. Biochemical Pharmacology. 2015 Sep;97(2):147–57.

376. Pfankuchen DB, Baltes F, Batool T, Li J-P, Schlesinger M, Bendas G. Heparin antagonizes cisplatin resistance of A2780 ovarian cancer cells by affecting the Wnt signaling pathway. Oncotarget. 2017 Sep 15;8(40):67553–66.

Appendix I

Publications

M. B. R. Piva, B. Jakubzig, G. Bendas

Integrin Activation Contributes to Lower Cisplatin Sensitivity in MV3 Melanoma Cells by Inducing the Wnt Signalling Pathway

Cancers. 2017 Sep 16; 9(9):125. doi: 10.3390/cancers9090125

Piva MB, Suarez ER, Melo CM, Cavalheiro RP, Nader HB, Pinhal MA

Glycosaminoglycans affect heparanase location in CHO cell lines

Glycobiology. 2015 Sep; 25(9):976-83. doi: 10.1093/glycob/cwv035

Conference Posters and Presentations

M. B. R. Piva, B. Jakubzig, G. Bendas

Abstract und Poster: The impact of integrins and syndecan-4 on cisplatin resistance of melanoma cells

EACR – FEBS advanced lecture course: Spetses Summer School, Spetses (Greece), August 2017

M. B. R. Piva, M. Schlesinger, G. Bendas

Oral presentation und Poster: Impact of integrins and syndecan-4 in chemoresistance of melanoma

Annual Meeting of the German Society for Matrix Biology, Cologne (Germany), March 2017

M. B. R. Piva, M. Schlesinger, G. Bendas

Oral presentation: Inhibition of integrin signalling pathway to sensitize melanoma cells for chemotherapeutics

CESAR Annual Meeting, Munich (Germany), September 2016

Maria B. R. Piva, M. Schlesinger, G. Bendas

Abstract und Poster: Is chemoresistance of human melanoma induced by integrin-mediated cell adhesion phenomena?

CESAR Annual Meeting, Innsbruck (Austria), September 2015